NMOCD
Fruitland Coalbed Methane Committee
Exhibit #1

A

GO INTERNATIONAL

COMPENSATED DENSITY LOG

FILING NO.

COMPANY AMOCO PRODUCTION COMPANY

WELL SCHNEIDER GAS COM B NO 1

FIELD BLANCO PICTURED CLIFF

COUNTY SAN JUAN STATE NEW MEXICO

Location: 1110'FSL& 1185'FWL

Sec. 28 Twp. 32N Rge. 10W

Other Services: IEL

Permanent Datum: Ground Level ; Elev.: 6059

Log Measured From KB 11 Ft. Above Perm. Datum

Drilling Measured From KB

Elev.: K.B. 6070
D.F. 6069
G.L. 6059

Date	1-8-77
Run No.	One
Type Log	Gamma-Gamma
Depth—Driller	356
Depth—Logger	3053
Bottom logged interval	3052
Top logged interval	2200
Type fluid in hole	Fresh Gel
Salinity, PPM Cl.	3600
Density	10.6
Level	Full
Max rec. temp., deg F.	110
Operating rig time	1 1/2 Hours
Recorded by	Hamilton Villa
Witnessed by	Bloom

RECEIVED
MAR 15 1977
OIL CON. COM.
DIST. 3

Run No.	Bore-Hole Record Bit	From	To	Casing Record Size	Wgt.	From	To
One	7 7/8	257	3050	8 5/8		Surface	257

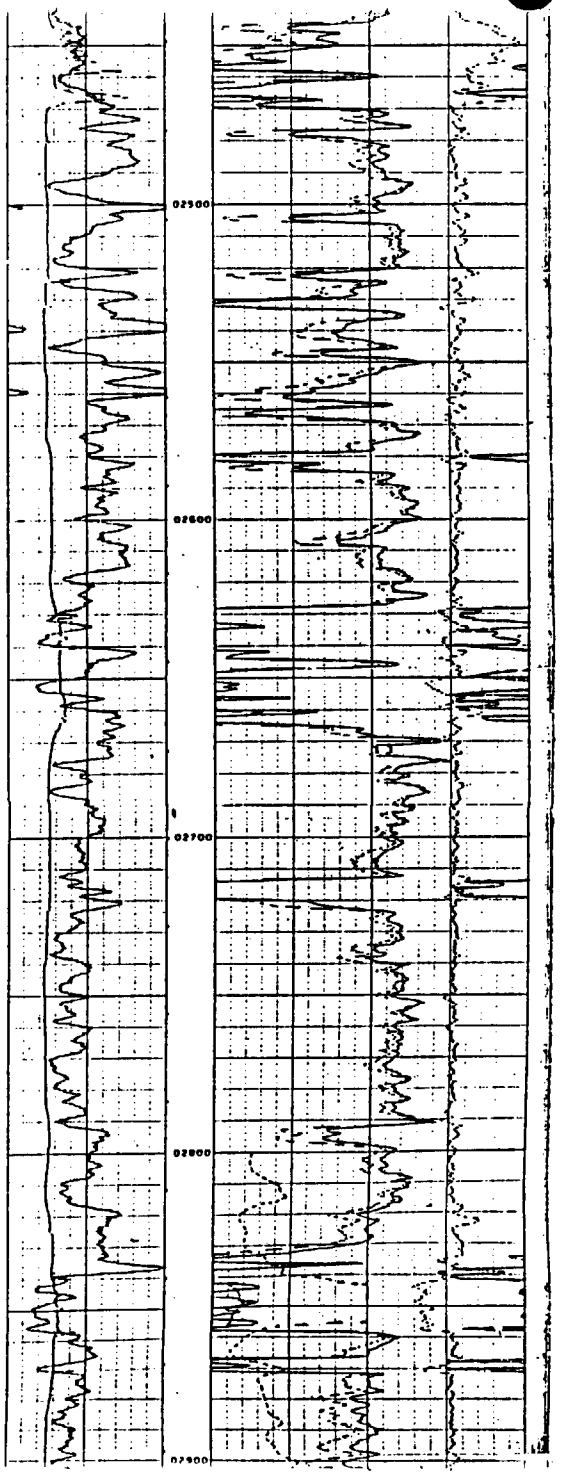

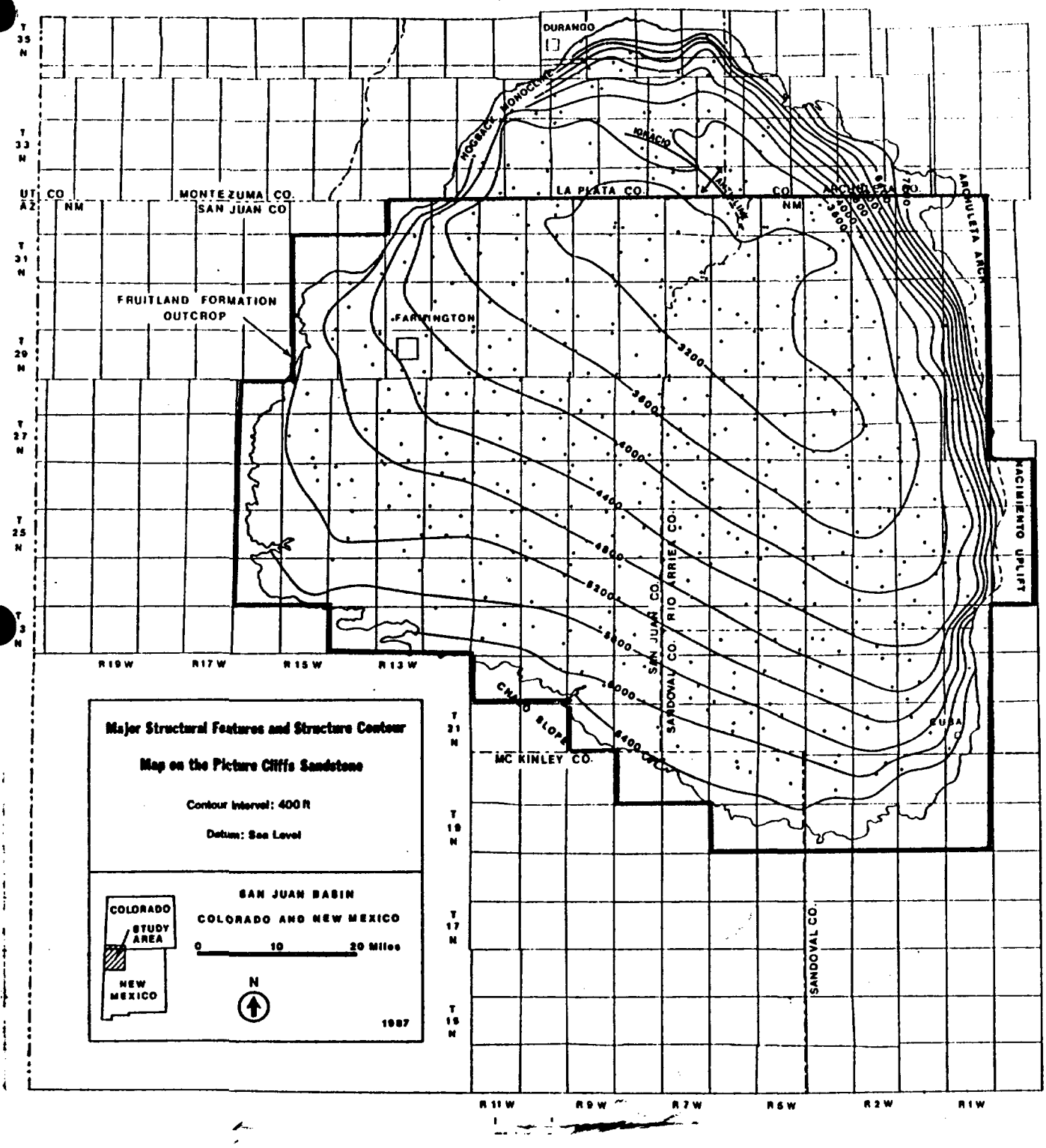
DURANGO
HOGBACK MONOCLINE
NACIMIENTO
UT
CO
AZ
NM
MONTEZUMA CO.
SAN JUAN CO
LA PLATA CO.
CO
NM
ARCHULETA CO.
ARCHULETA ARCH
FRUITLAND FORMATION OUTCROP
FARMINGTON
3200
3600
4000
4400
4800
5200
5600
6000
6400
SAN JUAN CO.
SANDOVAL CO.
RIO ARRIBA CO.
NACIMIENTO UPLIFT
CANADA SLOPE
MC KINLEY CO.
CUBA
SANDOVAL CO.
T 35 N
T 33 N
T 31 N
T 29 N
T 27 N
T 25 N
T 23 N
T 31 N
T 19 N
T 17 N
T 15 N
R19W
R17W
R15W
R13W
R11W
R9W
R7W
R5W
R2W
R1W
Major Structural Features and Structure Contour
Map on the Picture Cliffs Sandstone
Contour Interval: 400 ft
Datum: Sea Level
COLORADO
STUDY AREA
NEW MEXICO
SAN JUAN BASIN
COLORADO AND NEW MEXICO
0 10 20 Miles
N
1987

B 1

IT IS THEREFORE ORDERED:

(A) That, effective _____, a new pool in all or parts of San Juan, Rio Arriba, McKinley and Sandoval Counties, New Mexico, classified as a gas pool for production from the Fruitland Coalbed Seams, is hereby created and designated the San Juan Basin Fruitland Coalbed Methane Gas Pool, with the vertical limits comprising all coal seams within the stratigraphic interval from approximately 2450 feet to 2880 feet on the Gamma Ray/Bulk Density log of the Amoco Production Company Schneider Gas Com "B" Well No. 1, located 1110 feet from the South line and 1185 feet from the West line of Section 28, Township 32 North, Range 10 West, NMPM, San Juan County, New Mexico, which for the purpose of this order shall include all stratigraphically equivalent coal seams which by virtue of intertonguing or other geological events may be found within the upper Pictured Cliffs Formation. The horizontal limits shall consist of the following described lands:

Township 19 North, Ranges 1 West through 6 West, NMPM
Township 20 North, Ranges 1 West through 8 West, NMPM
Township 21 North, Ranges 1 West through 9 West, NMPM
Township 22 North, Ranges 1 West through 11 West, NMPM
Township 23 North, Ranges 1 West through 14 West, NMPM
Township 24 North, Ranges 1 East through 16 West, NMPM
Township 25 North, Ranges 1 East through 16 West, NMPM
Township 26 North, Ranges 1 East through 16 West, NMPM
Township 27 North, Ranges 1 West through 16 West, NMPM
Township 28 North, Ranges 1 West through 16 West, NMPM
Township 29 North, Ranges 1 West through 15 West, NMPM
Township 30 North, Ranges 1 West through 15 West, NMPM
Township 31 North, Ranges 1 West through 15 West, NMPM
Township 32 North, Ranges 1 West through 13 West, NMPM

(B) That for the purpose of this order a San Juan Basin Fruitland Coalbed Methane Gas Well is a well that is producing from the Fruitland Coalbed Seams as demonstrated by a preponderence of data which could include the following data sources:

a) Electric Log Data

b) Drilling Time

c) Drill Cutting or Log Cores

d) Mud Logs

e) Completion Data

f) Gas Analysis

g) Water Analysis

h) Reservoir Performance

i) Other evidence that indicates the production is predominately coalbed methane.

No one characteristic of lithology, performance or sampling will either qualify or disqualify a well from being classified as a Fruitland Coalbed Methane Gas Well.

SPECIAL RULES AND REGULATIONS FOR THE

SAN JUAN BASIN FRUITLAND COALBED METHANE GAS POOL

SAN JUAN, RIO ARRIBA, MCKINLEY AND SANDOVAL COUNTIES, NEW MEXICO

RULE 1. GENERAL

Each well completed or recompleted in the San Juan Fruitland Coalbed Methane Gas Pool shall be spaced, drilled, operated and produced in accordance with the Special Rules and Regulations hereinafter set forth.

RULE 2. POOL ESTABLISHMENT

That the Director may require the operator of a San Juan Basin Fruitland Coalbed Methane Gas Well, a Fruitland Sand Well or Pictured Cliffs Sand Well, which is proposed in the lands described in (A) above, furnish information and data that would demonstrate to the satisfaction of the Director that the existing wells are producing and the proposed well will produce from the appropriate common source of supply.

RULE 3 (a). WELL SPACING & LOCATION

A standard drilling unit for a San Juan Basin Fruitland Coalbed Methane Gas Well shall consist of 320 acres, plus or minus 25%, substantially in the form of a rectangle, consisting of a half section, being a legal subdivision of the U.S. Public Land Surveys, and shall be located no closer than 790 feet to any outer boundary of the tract, nor closer than 130 feet to any interior quarter section line.

In the absence of a standard 320 acre drilling unit, an application for administrative approval of a non-standard unit may be made to the Division Director provided that the acreage to be dedicated to the non-standard unit is contiguous, and the non-standard unit lies wholly within a single governmental half section, and further provided that the operator seeking the non-standard

unit obtains a written waiver from all offset operators of drilled tracts or owners of undrilled tracts adjacent to any point common to the proposed non-standard unit. In lieu of the waiver requirements the applicant may furnish proof of the fact that all of the aforesaid were notified by registered or certified mail (return receipt requested) of the intent to form such non-standard unit. The Director may approve the application if no objection has been received to the formation of such non-standard unit within 20 working days after the Director has received the application.

The drilling unit orientation will be determined by the first well permitted to be drilled in any one particular standard section.

RULE 3 (b). UNORTHODOX WELL LOCATION

The Director shall have authority to grant an exception to the well location requirements of Rule 3 (a) above without notice and hearing when the necessity for such unorthodox location is based upon topographic conditions or the recompletion of a well previously drilled into a deeper horizon, provided said well was drilled at an orthodox or approved unorthodox location for such original horizon.

Applications for administrative approval of unorthodox locations shall be filed in duplicate (original to Santa Fe and one copy to the appropriate District Office) and shall be accompanied by plats showing the ownership of all leases offsetting the spacing unit for which the unorthodox location is sought, and also all wells completed thereon. If the proposed unorthodox location is based on topography, the plat shall also show and describe the existent topographic conditions.

If the proposed location is unorthodox by virtue of being located closer to the outer boundary of the spacing unit than permitted by rule, actual

notice shall be given to any operator of a spacing unit or owner of an undrilled lease toward which the proposed location is being moved.

All such notices shall be given by certified mail (return receipt requested) and the application shall state that such notification has been given. The Director may approve the unorthodox location upon receipt of waivers from all such offset operators or if no offset operator has entered an objection to the unorthodox location within 20 working days after the Director has received the application.

The Director may at his discretion, set any application for administrative approval of an unorthodox location for public hearing.

RULE 4. INCREASED WELL DENSITY

The Director shall have the authority to administratively approve one (1) additional San Juan Basin Fruitland Coalbed Methane Gas Well provided the following conditions are met:

(a) The increased density well must conform to the spacing and boundary footage requirements set forth in Rule 3 (a). and the increased density well cannot be located in the same quarter section as the existing well.

(b) The operator must notify by certified mail (return receipt requested) all: offset operators located in contiguous standup or laydown drilling units; and in the case that the offsetting units are not developed, then notice shall be provided to the owners of contiguous lands.

(c) If no objection is received within 20 working days from receipt of notice, then the application will be administratively approved by the Director. If any objection is received within the time limit, then the Director will set the application for increased well density for public hearing.

RULE 5. HORIZONTALLY DRILLED WELLS

The Director shall have the authority to administratively approve an intentionally deviated well in the San Juan Basin Fruitland Coalbed Methane Gas Pool for the purpose of penetrating the coalbed seams by means of a wellbore drilled horizontally, at any angle deviated from vertical, through such coalbed seams provided the following conditions are met:

(a) The surface location of the well is within the permitted drilling unit area of the proposed well.

(b) The bore hole must not enter or exit the coalbed seams outside of a drilling window which is in accordance with the setback requirements of Rule 3 (a).

If the operator applies for a permit to drill a horizontal well in which the wellbore is intended to cross the interior quarter section line, the operator must notify by certified mail (return receipt requested) all: offset operators located in contiguous standup or laydown developed drilling units; and in the case that the offsetting units are not developed, then notice shall be provided to the owners of contiguous lands.

If no objection is received within 20 working days from receipt of notice, then the application may be administratively approved by the Director. If any objection is received within the time limit, then the Director will set the application for horizontally drilled wells for public hearing.

RULE 6 (a) TESTING.

In lieu of the gas well testing requirements of Order No. R-8170, testing for the San Juan Basin Fruitland Coalbed Methane Gas Pool shall consist of: a

minimum twenty-four (24) hour shut-in period, unless otherwise specified by the Director, and a three (3) hour production test. The following information from this initial production test must be reported:

(1) the surface shut in tubing and/or casing pressure and date these pressures were recorded;

(2) the length of the shut-in period;

(3) the final flowing casing and flowing tubing pressures and the duration and date of the flow period;

(4) the individual fluid flow rate of gas, water and oil which must be determined by use of separator; and

(5) the method of production, e.g. - flowing, pumping, etc., and disposition of gas.

RULE 6 (b). VENTING OR FLARING

Venting or flaring for extended well testing will be permitted for completed San Juan Basin Fruitland Coalbed Methane Gas Wells for a test period of not more than thirty (30) days or a cumulative produced volume of 50 MMCF of vented gas, whichever occurs first, the operator will notify the Director of this testing period.

If an operator has cause to perform further testing of a well, then administrative approval may be made by the Director to permit an additional period time and volume limit, set by the Director after sufficient evidence to justify this request has been submitted. In no case shall a well be administratively authorized to vent for a period greater than twelve (12) months.

RULE 7. EXISTING WELLS

That the operator of an existing Fruitland, Pictured Cliffs or commingled Fruitland/Pictured Cliffs well, which is in conformance with Paragraphs (A) and (B) of this order and is drilling to, completed, or has an approved APD for which the actual or intended completed interval is the San Juan Basin Fruitland Coalbed Methane Gas Pool, may request such well be reclassified as a San Juan Basin Fruitland Coalbed Methane Gas Well by the submittal of a new Form C-102 and C-104 within 90 days of the effective date of this order; this well may be so designated with its original spacing unit size as a non-standard San Juan Basin Fruitland Coalbed Methane Gas Well or may be enlarged to be in conformance with Rule 3 (a).

a location staked as of the effective date of this order

Meridian proposal.

C 1

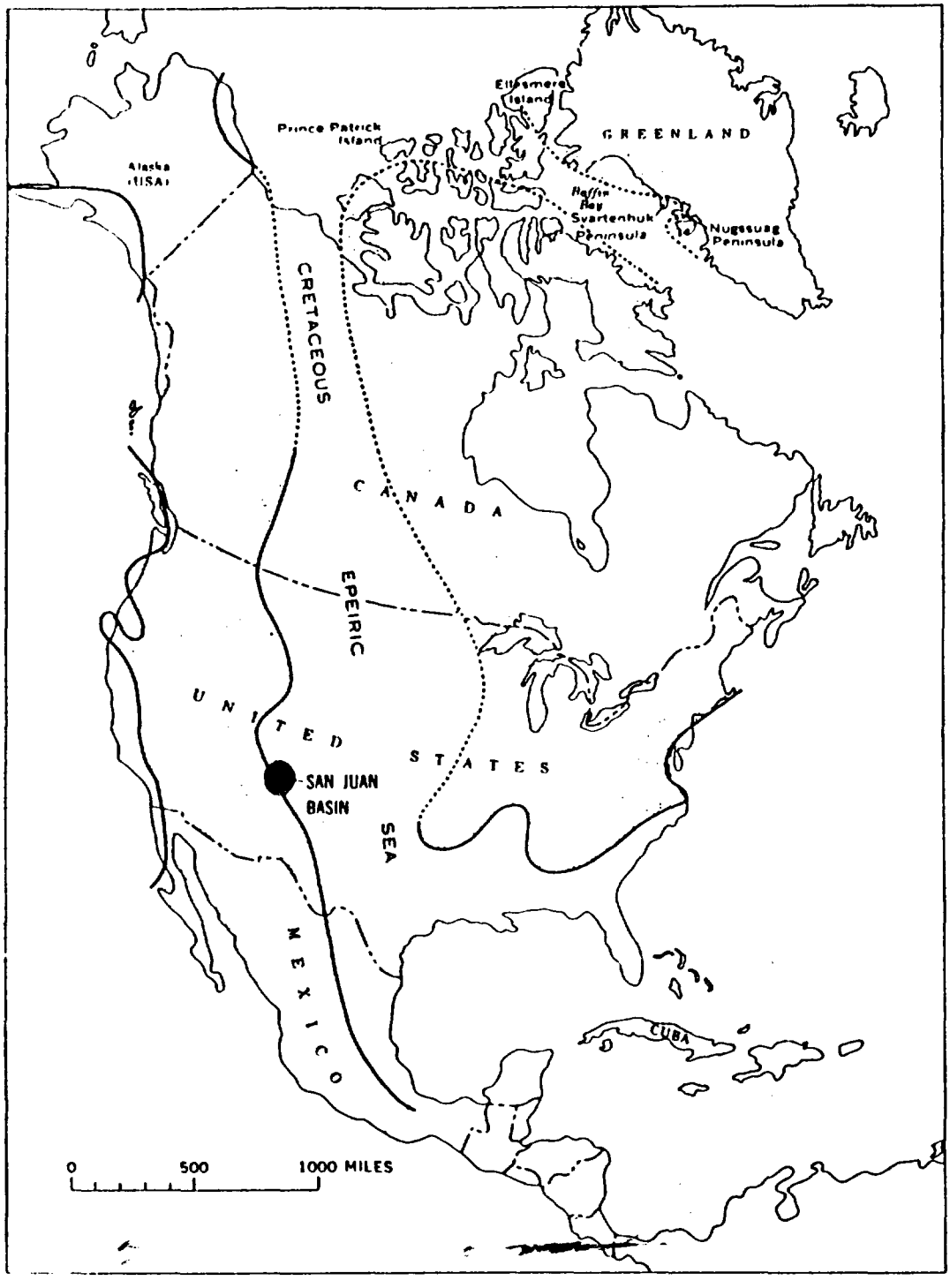

Probable configuration of the North American epeiric seaway at the time that the Upper Cretaceous rocks of the San Juan Basin were being deposited.

A

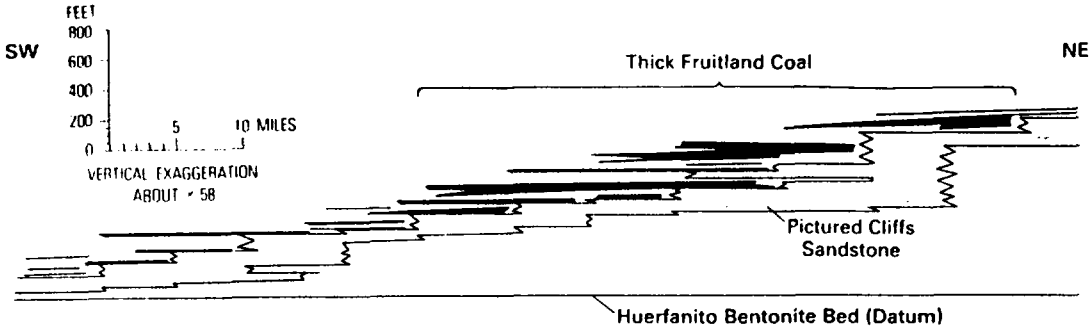

Northeast-trending stratigraphic cross-section showing Fruitland Formation coal beds and underlying Pictured Cliffs Sandstone. This cross section is modified from section B-B' of figure 8; coal bed thicknesses are from plate 3 of Fassett and Hinds (1971)

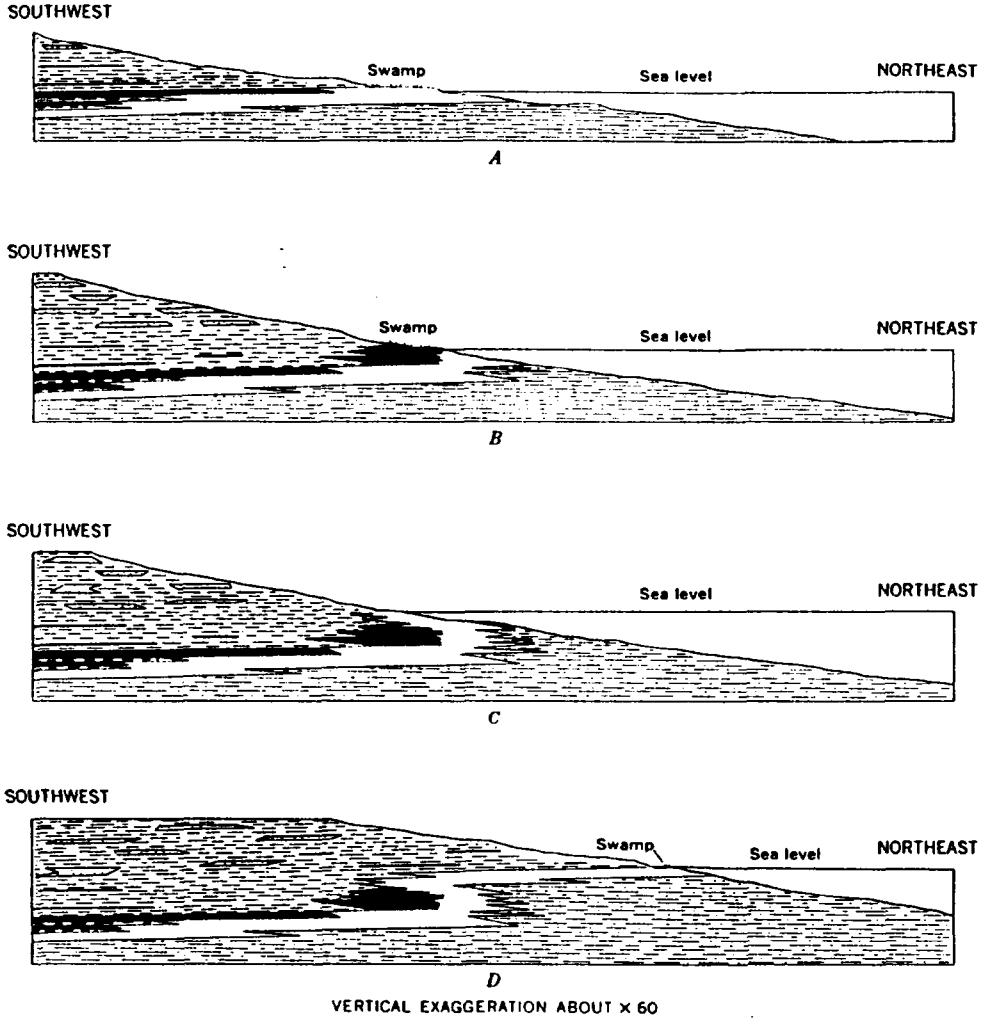

Diagrammatic cross sections showing the relations of the continental, beach, and marine deposits of Pictured Cliffs time after (A) shoreline regression, (B) shoreline stability, (C) shoreline transgression, and (D) shoreline regression.

E 1

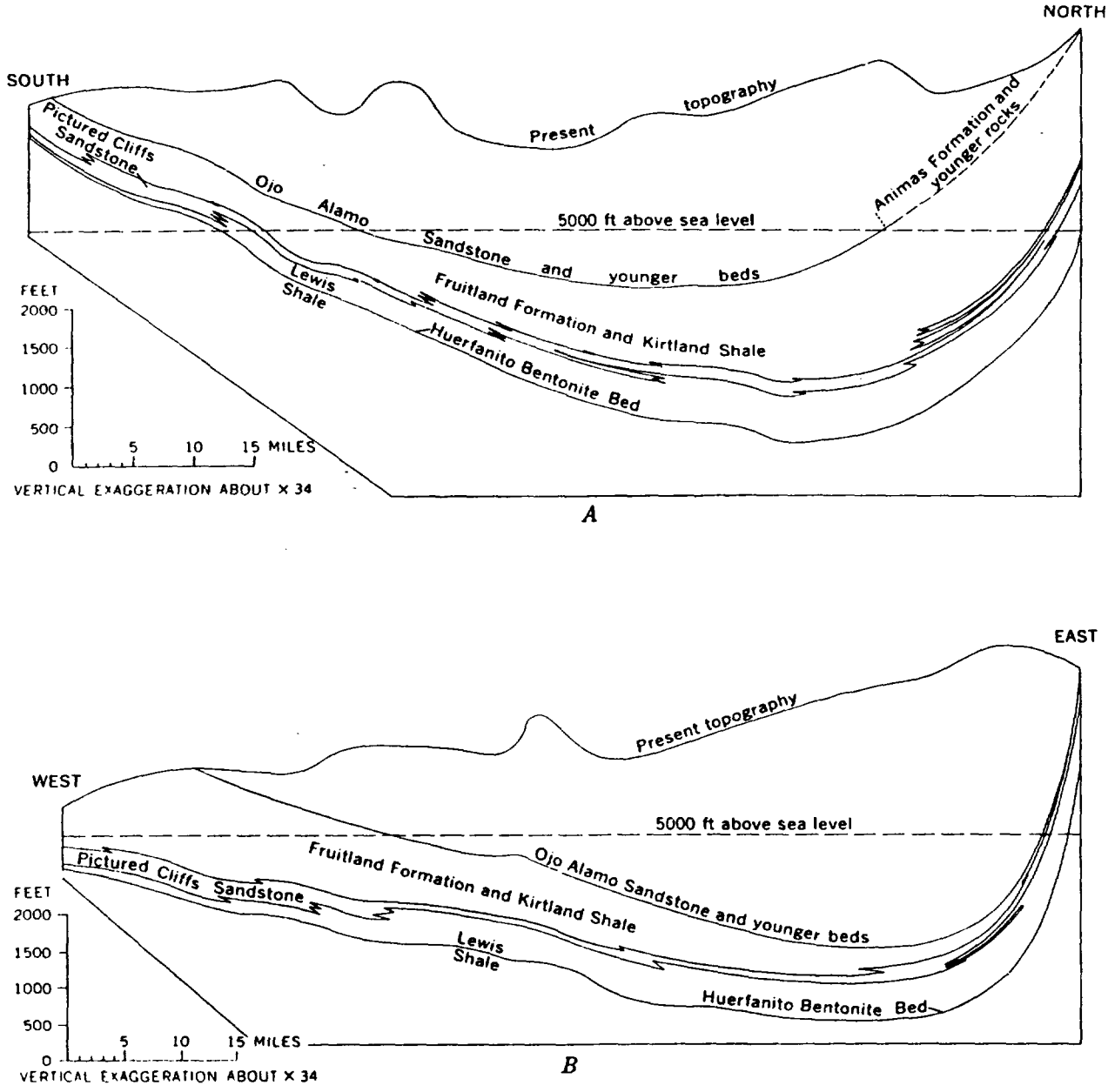

North-trending (A) and east-trending (B) structural cross sections across the San Juan Basin showing the present basin structure. (From Fassett, 1985 [15].

F 1

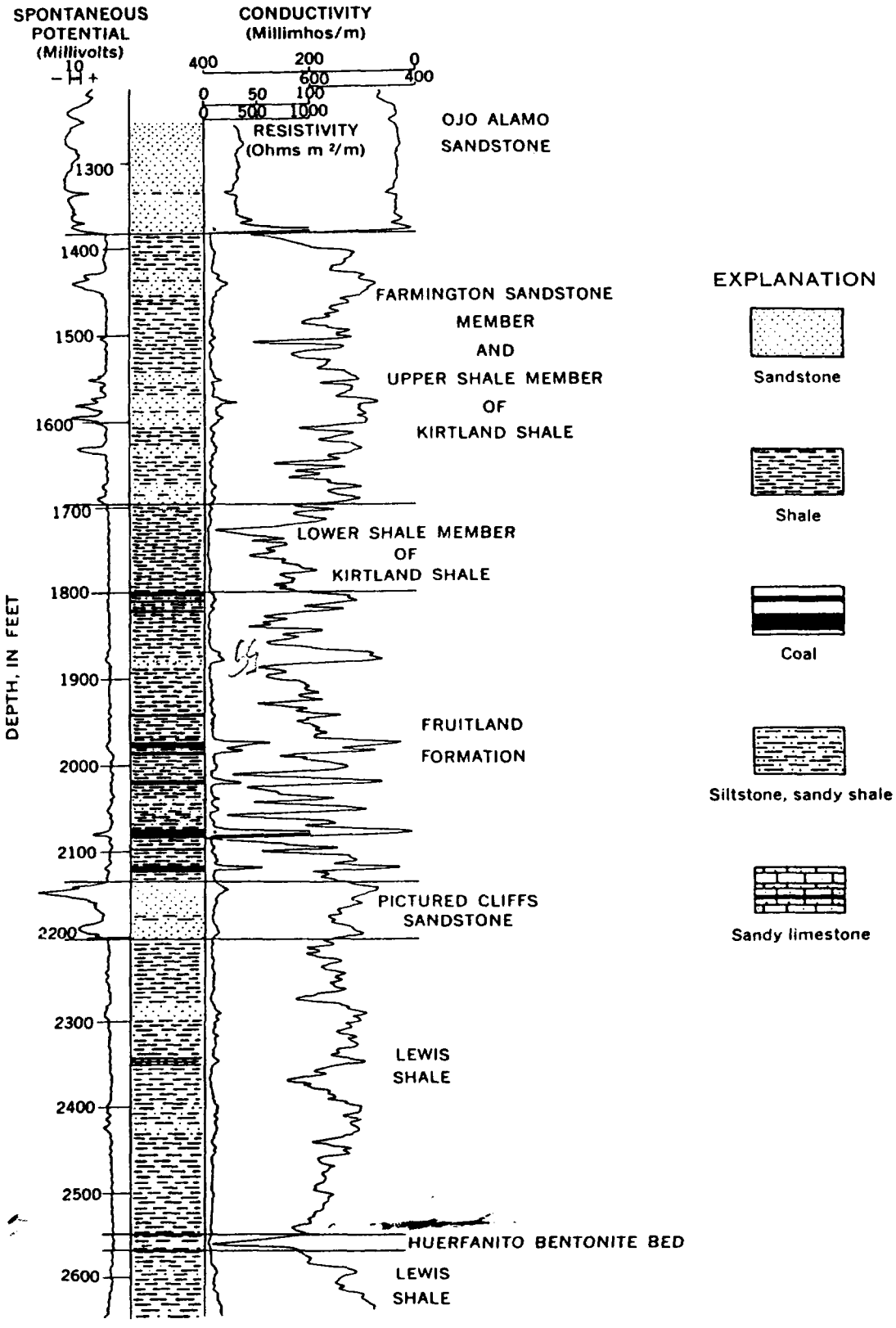

Figure 4 -- Induction-electric log and lithologic column of the type well of the Huerfanito Bentonite Bed of the Lewis Shale showing the interval from below the Huerfanito through the lower part of the Ojo Alamo Sandstone. Lithologies are based on an interpretation of the three geophysical logs shown.

G 1

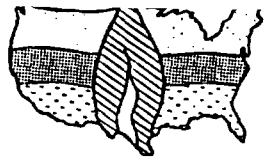

8711 Influence of Coal Composition on the Generation and Retention of Coalbed Natural Gas

J.R. Levine (University of Alabama, School of Mines & Energy Development)

INTRODUCTION

In terms of composition, coal is classified according to three distinct characteristics: 1) "grade", which represents the relative proportion of organic vs. inorganic constituents, 2) "type", which represents the natural variability of the organic constituents initially deposited in the coal, and 3) "rank", which represents the physico-chemical changes imparted to the coal by elevated temperatures and pressures during burial. Grade, type, and rank influence every aspect of coal bed natural gas reservoirs either directly or indirectly. The present paper focuses on two distinct, but related topics:
1) the influence of type and rank on the the composition and quantities of volatile substances formed during coalification, and 2) the influence of grade and type on the retention of gas in the subsurface.

EVOLUTION OF VOLATILE SUBSTANCES DURING COALIFICATION

The most fundamental change taking place in coal during coalification is the progressive enrichment of elemental carbon, accompanied by the elimination and release of large volumes of "volatile" substances relatively rich in hydrogen and oxygen. As these volatile substances are produced, the H/C and O/C atomic ratios of the residual solid coal progressively decrease. The three principal maceral groups, vitrinite, liptinite, and inertinite, differ substantially in their initial H/C - O/C ratios, hence they also differ in the quantity and type of gases formed during coalification.

The coalification process occurs much too slowly to be observed on a human time scale. Consequently, we are constrained to examining the end product and inferring as best we can the processes that led to it. Inasmuch as only a small portion of the volatile substances formed during coalification remain in the coal today, their volume and composition is largely problematical. However, providing a number of reasonable assumptions are made, then the quantities of CH_4, CO_2, and H_2O liberated during coalification can be estimated within a fairly narrow range, based on the major element (C-H-O) composition. The model requires: 1) that the organic microconstituents of coal evolve compositionally along the four generalized maturation pathways depicted in Figure 1 (Tissot and Welte, 1978), 2) that (for the most part) CH_4, CO_2, and H_2O represent the only forms in which carbon, hydrogen, and oxygen can escape from the coal bed, and 3) that once they are formed, CH_4, CO_2, and H_2O cannot recombine with the solid matrix of the coal.

The elemental compositions of coalification "products" and "reactants" can be plotted on a Van Krevelen diagram (Figure 1) which depicts both the rank and type of the organic constituents. Coalification paths for the four principal kerogen types are labeled I, II, III and IV. Kerogen type II is roughly equivalent to the liptinite (a.k.a. exinite) maceral group in coal. Kerogen type III is equivalent to vitrinite, by far the most common microscopic constituent of coal, and kerogen type IV is equivalent to the inertinite maceral group in coal. At low rank the maceral groups differ substantially in composition, but progressively converge upon one another they approach the origin. For example points A and B represent, respectively, the elemental compositions of liptinite and vitrinite macerals coexisting in a coal of vitrinite reflectance 0.5%, but by the time they have been coalified to 2.0% reflectance, they have virtually identical compositions.

A vector connecting any pair of starting and end points can be used to represent the compositional evolution of a particular coal or coal constituent. This vector can be resolved into 1,2, or 3 components, parallel to the dehydration, decarboxylation, and/or demethanation pathways plotted on the diagram. These devolatilization paths represent the change in composition brought about by the progressive removal of H_2O, CO_2, or CH_4 from the coal structure. Applying the constraints of the model, it is possible to reach an end point by a variety of pathways--but only within a limited range--or else condition (3) may be violated. For example, a liptinite maceral of initial composition A on the liptinite curve is coalified to composition C. There are two limiting end member paths to get from point A to point C. In the first, all oxygen is eliminated as CO_2 and none as H_2O while in the second the reverse is true. In the first case, the decarboxylation vector intersects the demethanation path at A', from which point all subsequent compositional

changes can be accounted for by progressively removing CH_4. , plus CH_4 (Path A-A"-C). Any other evolutionary pathways will include both decarboxylation and dehydration components and, con-sequently, and must fall between A-A' and A-A". (Note that the "head-to-tail" construction of the vectors in these examples does not necessarily imply a time sequence in volatile evolution. Volatile evolution occurs concurrently, with either one or the other substance predominating. However, the vectors do imply an explicit quantity of gases evolved.

To quantify this model and determine the precise composition and quantity of gases for each path, a set of equations is formulated whereby the total number of atoms of C, H, and O are equated between reactants (subscript r) and products (subscript p), and the H/C and O/C ratios of the reactants and products are adhered to:

$$Cp = Cr - CH_4 - CO_2 \quad (1)$$
$$Hp = Hr - 4*CH_4 - 2*H_2O \quad (2)$$
$$Op = Or - 2*CO_2 - H_2O \quad (3)$$
$$Hp = Cp * 0.50 \quad (4)$$
$$Op = Cp * 0.06 \quad (5)$$

where Cp, Hp, and Op are the number of atoms or moles of carbon, hydrogen, and oxygen per unit of the product. Cr, Hr, and Or are the number of atoms or moles of carbon, hydrogen, and oxygen in the starting (reactant) mixture; and CH_4, CO_2, and H_2O are the number of molecules or moles of methane, carbon dioxide, and water formed from the reactants during coalification.

The composition of the starting material can be determined by solving the following set of 3 equations with 3 unknowns:

$$Hr/Cr = 1.25 \quad (6)$$
$$Or/Cr = 0.07 \quad (7)$$
$$Cr + Hr + Or = 1000, \quad (8)$$

the solution to which is:

$$Cr = 431 \quad (9)$$
$$Hr = 539 \quad (10)$$
$$Or = 30 \quad (11)$$

The value of 1000 in equation (8) is arbitrary. It can be thought of as representing an imaginary coal "molecule" comprised of 1000 atoms. In subsequent calculations these 1000 atoms shall be partitioned among the various volatile products and coal.

Substituting equations (9-11) into equations (1-5) we are left with 5 equations and 6 unknowns. Hence, in order to derive a unique solution, one additional relationship must be defined. For end member case A-A'-C, $H_2O = 0$; and for case A-A"-C, $CO_2 = 0$. For intermediate paths, some ratio of CO_2 to H_2O must be selected. This needn't be an arbitrary choice, but may be based on knowledge of the functional group composition. For example Van Krevelen (1963) indicates that throughout most of the coal ranks under consideration, approximately half of the oxygen in coal is bound to hydrogen, and about half to carbon. We can propose then that CO_2 an H_2O leave the coal in roughly equal amounts; hence $CO_2 = H_2O$.

Depending on the path chosen, the relative proportions and total weight percentages of the volatile products vary considerably. Table 1 lists the yields of CH_4, CO_2, and H_2O and volatile matter produced along the various maturation pathways depicted in Figure 1. For example, as coal increases from R_o(vit) = 0.5 to R_o = 2.0, vitrinite can evolve anywhere from 24 to 173 cm^3 CH_4(stp)/g coal, depending upon whether B-B'-C or B-B"-C is followed. Assuming a ratio of 1:1 H_2O:CO_2 production, vitrinite will cumulatively generate around 116 cm^3 CH_4(stp)/g. Over this same rank range, and within the constraints of the model, liptinite macerals generate between 421 and 466 cm^3 CH_4(stp)/g; however, in reality, liptinites probably lose a significant proportion of their hydrogen as longer chain hydrocarbons rather than as methane. The devolatilization model can be modified or expanded to accommodate other hydrocarbon gases, however, a new functional relationship must be added for each new unknown.

This method of quantitatively estimating the volatile yield using simultaneous equation.is similar to a widely cited coal devolatilization model proposed by Juntgen and Karweil (1966) but differs in that it does not require that the coal liberate specific quantities of volatile substances. Juntgen and Karweil speculated that the proximate analysis volatile matter content (measured by pyrolysis at 950°C) could be used as an estimate of the total weight of material evolved as volatile products during coalification. However, this assumption is unwarranted and thermodynamically unsound. Moreover, by requiring that their coals produce such a large volume of volatile substances, Juntgen and Karweil's equations yielded negative values for water production--in other words, it was required that water be added to the coal structure to maintain the proper elemental ratios. Thus, the estimates of gas volumes based on this model are exaggerated. A subsequent article by Juntgen and Klein (1975), however, published a lower revised estimate, discussed subsequently, that is in close agreement with the one calculated herein.

Table 2 shows the progressive devolatilization path to Ro(vit) = 2.0% of an hypothetical coal, comprised of 80% vitrinite, 10% liptinite, and 10% inertinite. The total CH_4 production is 107 cm^3/g (Table 1, Path D-D'-C), almost identical to the quantity calculated by Juntgen and Klein (1975) based on experimental pyrolysis. The older estimate by Juntgen and Karweil (1966) for a whole coal was more than 200 cm^3. Unfortunately, the older figure seems to be used more commonly than the more recent one, (e.g. Meissner, 1984)

INFLUENCE OF COAL COMPOSITION ON IN SITU METHANE CONTENTS

With increasing rank coal loses its capacity to retain H_2O; hence, assuming that the beds remain fully water saturated, any water formed during coalification must be produced. Coal has a relatively strong affinity for CO_2 (as opposed to

CH_4, for example), but CO_2 is readily soluble in water; hence, its abundance will tend to diminish over time. Consequently, in comparison with other volatile substances formed during coalification CH_4 tends to become progressively enriched in the coal bed reservoir .

Coal has an attractive affinity for methane that enables it to absorb or adsorb more CH_4 under pressure than would be the case if the methane were a free gas. During the course of coalification coals generate much more methane than they have the capacity to retain (Juntgen and Karweil, 1966), so in a natural setting, most coals should be at or near their maximum methane capacity (at P,T), provided that the coals were not exposed to abnormally low fluid pressures in the past. Bearing this model in mind, the gas content of coal in situ should be proportional to the pressure, temperature, and whatever compositional parameters limit the coal's capacity to sorb gas.

A suite of 57 samples was recently collected from a 3000 ft-deep coal bed methane exploration core hole in the Cahaba basin, central Alabama. The gas contents of the samples were measured using the Bureau of Mines canister desorption test. Then the coals were subjected to a comprehensive suite of analyses, including proximate, ultimate, BTU, and petrography. These data were then normalized and used to develop a multiple linear regression model to predict the gas contents of the samples. The resulting linear model was very successful, explaining 88.5% of the variability in gas content. A large component of the remaining 11.5% variability is probably due to measurement error.

Multiple Linear Regression Model
Gas Contents of Cahaba Core Samples

Gas Content (cm^3/g) = 6.822
+ 0.0025 * Depth (ft)
- 0.0957 * ParrMM
r^2 = .885 + 0.1112 * (%Fusinite + %Semifusinite + %Macrinite)
- 5.449 * H/C (daf)

This regression model indicates that for the suite of coals examined, gas content increases linearly with depth. In laboratory sorption isotherm studies, the gas capacity of coal increases at a less than linear rate, so the anomalously high gas contents at depth may be due to increasing rank (W. Telle, personal communication). There was not, however, enough of a systematic rank variation in the samples to produce a measurable effect in the regression model. The third term, ParrMM, is an estimate of the mineral matter content of the coal using Parr's equation based on ash and sulfur content. Once again the correlation is linear, but with a negative coefficient. The predicted gas content using the model is very close to 0.0 at 100% ParrMM, showing that for these samples, the mineral matter does not participate measurably in the gas sorption process. The fourth term is a indication of the influence of coal petrography on gas sorption capacity. This composite variable, comprised of members of the inertinite maceral group, indicates that while inertinite does not contribute significantly to gas generation, it has a positive influence on the gas content. The fifth term, the hydrogen to carbon ratio (dry, ash-free basis) does not contribute strongly toward the model, but indicates that an increasing H/C ratio has a negative influence on the gas capacity. It is uncertain whether this is related to decreasing rank, or increasing liptinite content. Neither standard rank parameters nor the liptinite percentages showed a significant effect.

It remains to be seen whether this model can be applied to coals in other basins as well. As additional data become available the model will be tested and refined.

REFERENCES CITED

Jüntgen, H. and Karweil, J., 1966, Gasbildung und Gasspeicherung in Steinkohlenflözen, Part I and II: Erdöl u. Kohle, Erdgas, Petrochem, v. 19, p. 251-258 and 339-344.

Jüntgen, H. and Klein, J., 1975, Entstehung von Erdgas aus kohlingen Sedimenten.: Erdöl u. Kohle, Erdgas, Petrochem., Ergänzungsband, I, 74/75, p. 52-69. Industrieverlag v. Hernhausen Leinfelden bei Stuttgart.

Krevelen, D.W. van, 1963, Geochemistry of coal, in Breger, I.A., ed., Organic Geochemistry: Oxford, Pergamon Press, p. 183-247.

Meissner, F.F., 1984, Cretaceous and Lower Tertiary coals as sources for gas accumulations in the Rocky Mountain Area: Hydrocarbon Source Rocks of the Greater Rocky Mountain Region: Rocky Mountain Association of Geologists, Denver, CO, p. 401-432.

Tissot, B.P. and Welte, D.H., 1978, Petroleum Formation and Occurrence: Springer-Verlag, Berlin, 538 p.

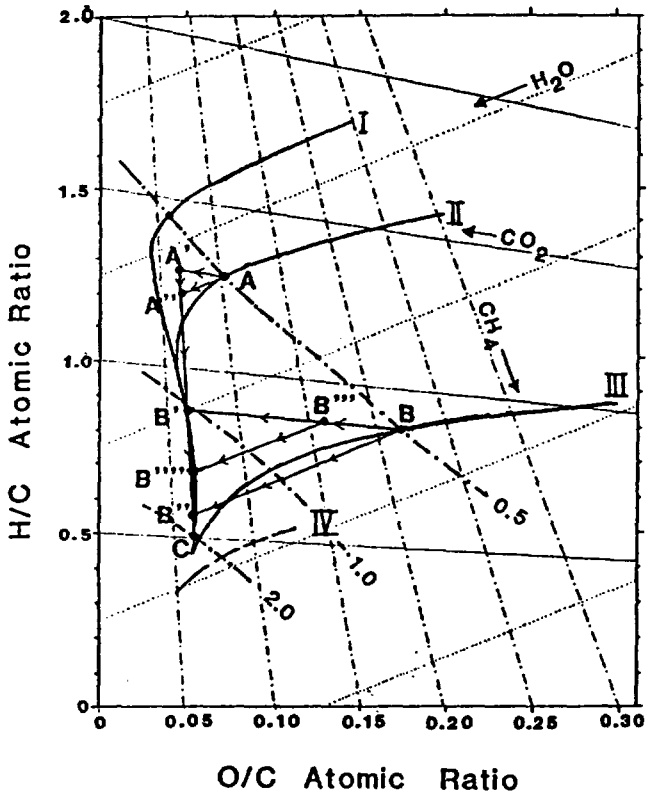

Figure 1 - Van Krevelen diagram depicting evolutionary devolatization paths. Liptinite (A) and vitrinte (B) are situated at the intersections of the Type II and Type III kerogen maturation paths and the 0.5% R_o isoreflectance line. A number of alternate devolatilization paths may be followed for each starting material, each path yielding different quantities of volatile products (see Table 1 for details).

Coalification from R_o(vit) = 0.5 to R_o(vit) = 2.0		Cumulative Grams of Volatiles per Gram of Coal			% of Original Weight Lost as Volatiles	Volume of CH_4 (stp) per Gram of Solid Coal
Path	Description	CH_4	CO_2	H_2O		
A-A'-C	Max. CH_4, Max. CO_2, Min. H_2O	0.333	0.049	0	27.6	466.
A-A"-C	Min. CH_4, Min. CO_2, Max. H_2O	0.301	0	0.036	25.2	421.
B-B'-C	Max. CH_4, Max. CO_2, Min. H_2O	0.124	0.236	0	26.5	173.
B-B"-C	Min. CH_4, Min. CO_2, Max. H_2O	0.017	0	0.156	14.7	24.
B-B"'-B""-C	Intermediate Path: $H_2O \neq CO_2$	0.083	0.146	0.059	22.4	116.
D-D'-C	Intermediate Path: $H_2O \neq CO_2$	0.076	0.110	0.045	18.7	107.

TABLE 1. Volatile Products of Coalification

Step:	C	H	O	H/C	O/C
Starting Material:					
80 % Vitrinite:	4096	3192	712	0.78	0.17
+ 10 % Liptinite:	431	539	30	1.25	0.07
+ 10 % Inertinite:	746	224	30	0.30	0.04
Total:	5273	3955	772	0.75	0.15
Decarboxylation: (79 * CO_2)	-79	0	-158		
	5194	3955	614	0.76	0.12
Dehydration: (315 * H_2O)	0	-630	-315		
	5194	3325	299	0.76	0.06
Demethanation: (208 * CH_4)	-208	-832	0		
	4986	2493	299	0.50	0.06

TABLE 2. Devolatilization Path for Whole Coal (D-D'-C, Table 1.)

王

—

COMPARISON OF GAS ANALYSES

FORMATION	WELL LOCATION	C2	CO2	BTU
Fruitland coal	A-18-32-7	94.84	4.25	976
"	O-08-32-9(CO)	95.92	2.61	997
"	D-11-33-10(CO)	95.53	2.20	1011
"	N-07-31-09	89.67	8.54	949
Fruitland sand	G-08-29-10	83.22	0.65	1235
"	E-22-28-12	85.55	1.45	1138
"	D-34-30-11	82.50	0.33	1223
"	O-28-32-11	83.41	0.42	1224
Pictured Cliffs	J-06-33-10(CO)	79.55	1.66	1234
"	O-26-32-07	85.23	0.58	1188
"	F-13-28-09	91.77	0.48	1102
"	O-18-30-08	88.20	0.94	1157

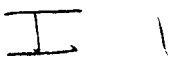

Piper Diagram for Connate Waters from

Piceance Basin,
San Juan Basin,
Warrior Basin

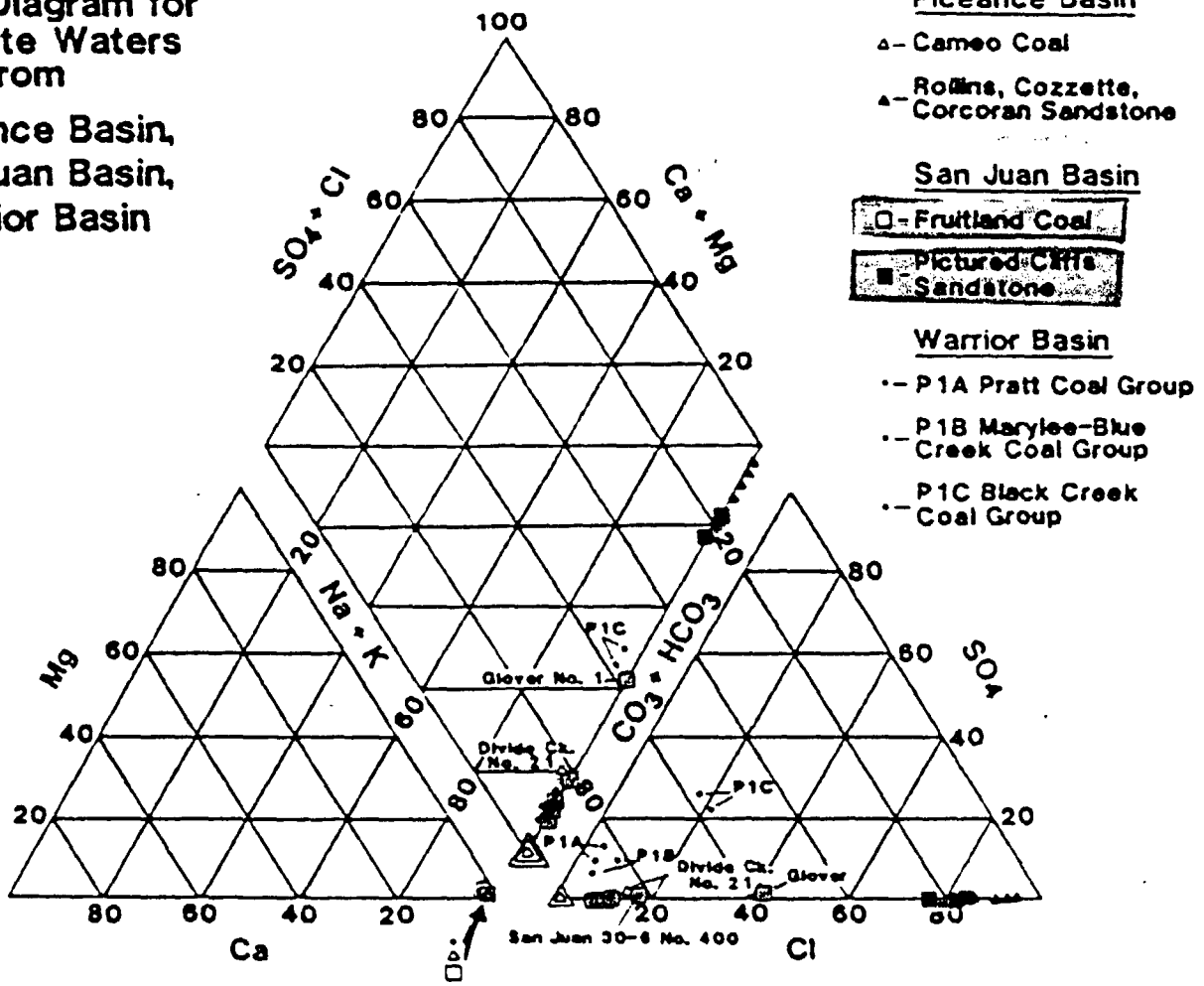

Piceance Basin

- Cameo Coal
- Rollins, Cozzette, Corcoran Sandstone

San Juan Basin

- Fruitland Coal
- Pictured Cliffs Sandstone

Warrior Basin

- P1A Pratt Coal Group
- P1B Marylee-Blue Creek Coal Group
- P1C Black Creek Coal Group

Proceedings of the 1987 Coalbed Methane Symposium, Tuscaloosa, Alabama, Nov. 16-19, 1987

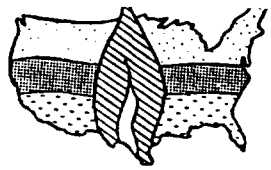

THE 1987 COALBED
METHANE SYMPOSIUM

8714 Origin and Production Implications of Abnormal Coal Reservoir Pressure

A.D. Decker (Resource Enterprises, Inc.); D.M. Horner (Gas Research Institute)

ABSTRACT

The ability to produce low cost, pipeline quality gas from deep coal reservoirs depends largely on thorough integration of exploration methods with appropriate drilling, completion and production strategies. In the extreme case, areas that are not economic with current completion technologies should be avoided with adherence to prudent exploration practices. Therefore, reliable predictive geologic methods to specify coal reservoir conditions need to precede drilling and completion decisions.

Dominant coal reservoir mechanisms include: permeability, saturation, reservoir pressure and gas-in-place. Production characteristics from low permeability coal reservoirs are most sensitive to the interaction between type of saturation and reservoir pressure. The geologic processes responsible for these reservoir conditions have been examined in the Piceance Basin. This basin, known for low permeability reservoirs, was selected for geologic evaluation due to the large coalbed methane resource and large data base. Also located in the basin is the Deep Coal Seam Project, a multi-year, multi-well, field laboratory joint venture by the Gas Research Institute and Resource Enterprises, Inc., providing fully integrated reservoir and geologic engineering data on deep coal reservoirs.

Reservoir diagnostics and modeling suggests that reservoir pressure and type of saturation demonstrate an interaction between catagenesis and permeability. Thick, thermally mature coal deposits actively generate more gas and water than can be adsorbed by the coal or be diffused through a low permeability system. In these regions over-pressuring occurs. Ultimately, pore pressure will exceed in-situ stresses resulting in tensional fractures through the coal bearing sequences. While the coal seams remain in the active gas generation phase, the fractures and pore spaces become gas saturated. Eventual temperature reduction through erosion will halt the gas generating phase, resulting in an under-pressured reservoir. Imbibition of water into these reservoirs is unlikely in areas of low permeability. In contrast, coal seams that have not reached an active gas generation phase may be overpressured and water saturated due to compaction and coal dewatering in a shale bounded situation. Overpressured water saturated coal reservoirs of the Cedar Hills and San Juan 30-6 Unit in the San Juan Basin have, to date, shown the highest production capacity for coalbed methane production.

In summary, geochemical evaluation techniques have been applied to characterize and predict coal reservoir mechanisms in the Piceance and San Juan Basin.

INTRODUCTION

A portion of the extensive gas accumulations found in the San Juan Basin[1], the Green River Basin[2], and the Alberta Basin[3] have been sourced largely by coal. Despite the amount of data collected on coal reservoir characteristics and coal as a source rock, little work has been done integrating the two sciences. A coupled understanding of coal reservoir mechanisms and coal maturation will assist the explorationist in his pursuit of coalbed gas resources. This work was sponsored by the Gas Research Institute under Contract No 5083-214-0844 with Resource Enterprises, Inc.

A geologic model is presented which incorporates coal's resistance to transfer heat with its ability to generate large volumes of gas over a specific temperature and time sequence. In basins where low permeability prohibits cross formational fluid flow, gas generation can exceed the quantity of gas that can migrate through the geologic system. This results in high pore pressure within the coal reservoirs. Conversely, where migration exceeds rate of gas generation, low pore pressure will be observed. These stages of reservoir disequilibrium have been observed in other deep coal basins of the western United States.

The focus of this paper is to describe and quantify these states of pore pressure disequilibrium within some coal reservoirs of the Piceance Basin and San Juan Basin. A sequential approach is undertaken to examine the coal system in each phase of basin evolution, as follows:

1. Determination of the volumes of water and gas produced from coal at specific maturity levels during the coalification process.

2. Relate the maturity levels to specific time periods using thermal maturation models.

3. Determination of the amount of gas that cannot be retained by the coal and, therefore, which must diffuse through the geologic section for specified time interval.

This paper is directed at providing the volumetric calculations of Step 1 and the methodology (using a case study) for Steps 2 and 3.

Included in this paper are geologic observations and interpretations of areas within the Piceance Basin where underpressured and overpressured (less than and greater than hydrostatic pressure, respectively) coal seams have been identified. Also included is a section suggesting a relationship between well deliverability, permeability and reservoir pressure in coal degasification wells in the San Juan Basin. A relationship between material balance, gas/water flow and abnormal coal pore pressure is presented.

THE EVOLUTION OF COAL

In response to burial depth, time and temperature, deposits of terrestrially derived plant tissue evolves physically and chemically into thermally mature coal. Compaction and temperature increases transform the organic material into three primary coal components or macerals. (Macerals are the microscopically recognizable constituents of coal.) The vitrinite maceral represents jellified cell walls or woody material, the exinite maceral is representative of plant resin (cuticles and spores) and the inertinite maceral represents carbonized woody material.

The degree of maturation or coal rank during the coalification process is most accurately measured from the vitrinite maceral. The percentage of vitrinite optical reflectivity (Ro) increases correspondingly with increases in coal rank. The temperature necessary to increase rank as indicated by Ro and derived by Gijzel[4] is shown on Table 1. Systematic chemical and biological degradation of organic material during the coalification process yield varying amounts of water and gas. Examination of such chemical products is important in understanding the water and gas accumulations within present-day coal reservoirs.

The two most significant stages of coal maturation, diagenesis and catagenesis, are defined largely by the products of biological and thermal evolution. Water, biogenic methane and carbon dioxide are the primary coal diagenetic products. Water originates from the depositional system and organic decomposition[5]. All biogenic gas and 98 percent of the coal's water generative capacity occurs during diagenesis at maturity levels of 0.23 to 0.76 Ro[6].

Continued exposure of coal to pressure and temperature allow coal to enter the stage of catagenesis. Juntgen and Klein[7] determined that thermal methane generation commences during catagenesis for coal with a vitrinite reflectance of 0.73 Ro. As shown in Figure 1, active gas generation accelerates at 0.90 Ro and continues through 1.30 Ro, accounting for 76 percent of thermal methane generation. Water produced during catagenesis is from the hydration of inorganic minerals and clays[8]. Water and thermal methane volumetrics as a function of increasing coal maturity is summarized in Figure 2.

Coal's ability to absorb gas decreases with higher temperature[9] and pressure[10], but increases with higher coal rank[11]. Eight to ten times more gas is generated than can be retained, thereby initiating gas migration from the coal into other strata. Therefore, the development of a time framework for the coal generative episodes becomes necessary to understand the possible influence that thermal generation rates have on coal reservoir properties. Deterministic relations between time, temperature and ensuing gas generation episodes are derived from thermal maturity modeling.

Thermal Maturity Modeling

The timing of coal digenetic and catagenetic history may be identified through use of a time-dependent, three-dimensional mathematical model to simulate gas generation dependence on variables such as sedimentary burial rate, paleotemperature, paleopressure, thermal conductivity and heat flow. The simulation initially requires the computation of three-dimensional pore pressure in sediments as a function of time. The system assumes that the inflow-outflow is equal to the net accumulation due to grain and fluid compressibility plus the net accumulation to change in sediment density, rate of sedimentation and change in water depth[12]. The next step of the simulation is evaluation of the simultaneous transfer of heat by conduction and convection[13]. In this step, thermal parameters of the evolving system are particulary sensitive to pressure and temperature. The third step in thermal modeling is relating temperature to specific geologic periods. Lopatin[14] determined for coalification reactions, the reaction rate doubles with each increase of 10°C. He further related time and temperature by specifying a geologic time period with 10°C intervals as follows:

$$TTI = T_1 G_1 + T_2 G_2 + T_n G_n$$

where: TTI = Time Temperature Index
T_1 = Temperature Correction Factor
G_1 = Geologic Heating Time

Next, a correlation between vitrinite reflectance is incorporated as a maturity indicator and the TTI is established. The relationship between vitrinite reflectance (Ro) and the time-temperature index is:

$$R_o\% = 1.301 \lg TTI - 0.5282...$$

The final output of the thermal model reveals the type of depositional basin, tectonic and structural histories, sediment accumulation (or erosion) through time, thermal history of the basin and its effect on coal maturation and compactional history. A comparison of measured vitrinite reflectance and bottomhole temperatures with that predicted by the model indicates the accuracy of modeled events.

ABNORMALLY PRESSURED COAL RESERVOIRS, PICEANCE BASIN

The preceding coal volumetrics and thermal modeling may be used to study the implications of abnormally pressured coal reservoirs within the Piceance Basin of northwestern Colorado. The Basin was selected due to the availability of reservoir and geologic data collected for the Cretaceous coal reservoirs as are dominate in the western U.S. and which contain significant coalbed accumulations.

To date, the thick coal seams of the laterally continuous Cameo Coal Group, (Williams Fork Formation, Mesaverde Group) have been the objective for coalbed gas exploration within the Piceance Basin. A significant coalbed methane resource also exists within the Coal Ridge Coal Group[15], stratigraphically 200 to 400 feet above the top of the Cameo Coal Group, laterally confined to the eastern margin of the basin.

The primary questions to address are: i) what is the origin and implications of abnormally pressured coal reservoirs?, and ii) why stratigraphically equivalent coal seams with similar coal ranks and burial depths have such diverse coal reservoir conditions.

The integration of drill stem test data, bottomhole pressure, buildup tests and drilling mud weights have resulted in identification of a regional northeastern overpressured trend approximately 25 miles in length and eight miles in width (Figure 3). The East Divide Creek Area (which has a reservoir pressure gradient in the Cameo coal seam of 0.59 psi/ft) is located on the southern-most extension of the regional trend. In contrast, the reservoir pressure gradient at the Red Mountain Area is .33 psi/ft. The overpressured region coincides with: i) maximum total coal development in the Basin (Figure 4), ii) thermally mature coals (Figure 5), and iii) northern plunging nose of the Divide Creek Anticline (Figure 3). These coal characteristics are interrelated and result in dynamic reservoir conditions.

The Divide Creek anticline has brought deeply buried, mature coal seams 4,000 - 5,000 feet closer to the surface than laterally equivalent coal seams. The abrupt post-laramide uplift appears to have contributed to the coal disequilibrium state along the axis of the anticline. The timing of coalbed gas and water generative events and material balance calculations may be determined using thermal maturation modeling.

Material Balance

An examination of regional maps (Figure 4 and 5) indicate that up to 100 feet of low-volatile bituminous coal exists in the overpressured region. Following lithification and compaction, 9.18×10^8 barrels of water and 4.27×10^{11} cubic feet of gas are calculated to have been displaced by the coal seams per square mile. To determine the coal's fluid retention capability, earth strain analysis was conducted at the East Divide Creek Site. The upper bound interpretation for coal porosity was calculated to be 6.0 percent[16]. Therefore, if all pore space in the coal was saturated with water, the coal could only contain $.41 \times 10^{-3}$ percent of generated water. If completely gas filled, at equivalent pressure and temperature, the coal could retain roughly 12 percent of the generated gas. Clearly the volumetric difference between the gas and water generated and that which may be stored in the coal system is large and suggests a reason for overpressuring in this region.

Determination of Sequential Thermal Events

The timing of coal generative events at the East Divide Creek Area and Red Mountain Unit was determined by Waples using computer-aided thermal modeling[18]. In order to best match present-day calculated subsurface temperatures of 164°F at Red Mountain and 176°F at East Divide Creek, and to obtain good agreement between measured maturity data and calculated maturity levels, paleo heat flow was varied. This facilitates simultaneous corrections for a nearby late Eocene intrusive event and post-Eocene uplift and erosion. Pre-Eocene heat flows were held constant at 1.5 heat flow units. Based on geologic age dating, the thermal event began 34 million years ago (MYA). A one hundred thousand year heating span was investigated, decaying exponentially. The geologic section was layered to approximate age of deposition and lithology. The thermal conductivities used for pure sandstone was 6.2 watt/meter/Kelvin (w/m/k), for shales 1.5 w/m/k, for dolomites 4.8 w/m/k decline, for siltstone 2.9 w/m/k, and for coal 0.3 w/m/k as reported by Kappelmeyer[18]. The results from the thermal modeling simulation expressed as a function of time and maturity for the volume of water and gas generated by the coals are shown on Figure 6. In both areas, active thermal gas generation from coals occurred approximately 52 MYA when the formations were at their deepest burial and greatest temperature. Active gas generation ceased approximately 25 MYA. Gas generation today is at a much lower rate due to reduced depths resulting from erosion and thermal decay of the igneous event. According to Lopatin's relationship, the current reaction rate is .001 percent as compared to peak gas generation approximately 40 MYA.

A typical geothermal gradient semi-log plot of depth and vitrinite reflectance yields a straight line[14]. A vitrinite profile has been measured at the 1 Deep Seam 32-2 well (Red

Mountain Unit), at the 1 Cameo 20-4 (East Divide Creek Area) , and other areas of the Piceance Basin as reported by Law[19]. All wells examined displayed an increased maturation profile occurring at approximately 0.90 Ro. The unusual vitrinite reflectance profiles measured at the 1 Deep Seam 32-2 and 1 Cameo 20-4 were closely matched by Waples[18] maturation modeling (Figure 7) indicating that maturity modeling in coal-bearing basins must take heat transfer through coalbeds into consideration. Poor thermal conductors, such as coal, result in a heat buildup under the low conductive section. This phenomenon is well documented by a static, cased hole temperature log from the East Divide Creek Area, Mamm Creek and Rullison Field (Figure 8). Note the repeated thermal anomalies at the base of the Cameo and Coal Ridge groups.

Yukler[20] first described the temperature and pressure interrelationship with abnormally pressured reservoirs. He observed a sharp increase in the temperature gradient on top of a high-pressure medium and a sharp decrease in the temperature gradient on top of a low-pressure medium (Figure 9). These findings are consistent with temperature profiles for overpressured coal sections as shown in Figure 8. The abnormally high-pressured sedimentary unit resulted from an insulation effect caused by a zone of low thermal conductivity. A barrier to heat flow is created in the areas of thick, laterally continuous coal seams found in the overpressured region of the Piceance Basin due to the low thermal conductivity of coal. This results in high temperatures and pressures which accelerate coal maturation as noted in vitrinite profiles from wells at the Red Mountain Area and East Divide Creek (Figure 7). The sequential results of thermal maturation events in the Piceance Basin may be summarized as follows:

1. The coal's insulating property which exists from deposition results in heat buildup and accelerates both the initiation and degree of coal maturation. Therefore, increasing temperature initiates increasing gas generation.

2. The rapid decay of the gas generative system is caused by reduced temperatures resulting from erosion of the stratigraphic section.

3. Once in the passive gas generation stage, the migration of gas from the coal seam to achieve equilibrium will result in decreasing pore pressure.

From the perspective of the Piceance Basin evolution, the coal seams underlying the Red Mountain and East Divide Creek Unit have similar thermal histories and generally evolved as a single system. However, thermal maturation and gas generation events alone fail to explain the different reservoir pressure gradients measured within the coal seams at the two areas. (e.g. Red Mountain Area = 0.33 psi/ft, East Divide Creek Area = 0.59 psi/ft). Distinguishing factors between the two areas include the post-laramide uplift paralleling the overpressured, East Divide Creek region, and absent at the Red Mountain Area and nearly twice the gas generation in the overpressured area due to increased coal thickness (Table 2).

The following thermal maturation events are presented as mechanisms for high coal pore pressure. During active gas generation, coal seams in the overpressured region were located in the deepest portion of the basin. Therefore, coalbed gas adsorption reached peak levels due to high formation pressures and temperatures from burial. The gas retention capacity was reduced during rapid post-laramide uplift and erosion. As a result of the uplift, the coal seams are currently at elevated maturation and temperature levels relative to laterally equivalent coal sections (Table 2). High pore pressure may then be related to coalbed gas retention in excess of equilibrium temperatures and pressures. Disequilibrium may have been accentuated by the large concentration of coal volume in the overpressured area (Figure 4).

OVERPRESSURED COAL RESERVOIRS

Gas is produced from overpressured, water saturated Fruitland coal reservoirs at the Cedar Hill Field and San Juan 30-6 Unit in the San Juan Basin. The two fields have been examined in detail[21] in an effort to: (i) determine geologic processes responsible for reservoir characteristics, and (ii) establish reservoir parameters controlling production.

The fields were selected because of their high productivity. The Cedar Hill Field has produced a cumulative of 7.1 Bcf from 7 wells since 1979 and is still producing at a rate of 1.3 Bcf/year. The Fruitland coal discovery was made in the San Juan Unit 30-6 during 1985. Three wells in that field have produced 2.3 Bcf during the first 15 months of production and continue to flow at a rate of 2.2 Bcf/year.

A detailed geologic study of both fields failed to detect significant geologic anomalies that might explain favorable production characteristics. Similarly investigation of drilling and completion techniques failed to yield technological reasons for high productivity. The only obvious factor that both fields share which is lacking in approximately 200 less successful coalbed completions in the San Juan Basin is overpressured coal reservoir conditions over a large lateral area. From the stand point of decreasing formation pressure below gas desorption pressure, over pressure, water saturated coals should have negative production implications. However, the overpressuring condition maybe indicative of a permeability enhancement process resulting in highly permeable coal reservoirs.

Based on regional isoreflectance maps, coal reservoirs in both fields fall in the maturation range of .80 - .90 Ro. According to Figure 2 this maturity level falls below peak gas generation phase. Therefore, sufficient volumes of gas have not been generated to cause high pore pressure. However, coal rank and age are appropriate for relict overpressuring conditions during the coal dewatering phase. Overpressuring during shale compaction and dewatering has been

well documented[22] in detrital sequences. Coal seams bounded by impermeable shales would similarly develop high pore pressure due to the inhibited ability to expel water during compaction. Produced waters from both field contain 12,000 to 14,000 ppm sodium bicarbonate type coal water which is suggestive of sluggish or isolated reservoirs conditions. Coal derived should be a sodium bicarbonate water[23], however, the high levels measured at the Cedar Hill and San Juan 30-6 Unit indicates little dilution of connate water over time, supporting bounded reservoir conditions. In theory, incompressible water under high pressure could be acting as a hydraulic proping mechanisms in coal cleats limiting porosity and permeability reduction effects from lithostatic loading.

Overpressured coal reservoirs are a product of shale bounded coal seams during diagenetic compaction during water expulsion. The process is similar to the origin of overpressured shales and sandstone in the Gulf Coast region. To date, coalbed methane wells producing from deeply buried coal seams with high permeability and deliverability occurring in overpressured, water saturated areas of the San Juan and Piceance Basins. The simultaneous occurrence of overpressuring, water saturation and high permeability in coal seams is not thought to be coincidental but rather suggestive of a common relationship. That relationship could be quantified through integration of geologic and reservoir modelling using data collected from laboratory core measurements in conjunction with field level reservoir tests.

SUMMARY

Recognition of the geologic and resulting reservoir processes controlling gas production from deeply buried coals is the first steps in the formulation of an exploration strategy for coalbed gas. The dominant coal reservoir mechanisms affecting production include: permeability, reservoir pressure, saturation and gas-in-place[24]. The relationship between decreasing coal permeability with increasing depth has been described by McKee[25]. In order to overcome the inherent low coal permeability at depth, permeability enhancement through structural deformation should be sought. Utilizing fundamental relationships including Darcy's Law and equation of state, at a given permeability, overpressured coal reservoirs will have better deliverabilities and, therefore, are a preferred exploration target over underpressured and normally pressured coal seams.

Based on observations resulting from drill stem tests, blowouts from intercepted coal seams, gas flares while drilling through coal seams and coalbed gas production, inferences may be made regarding areas in the Piceance Basin that are either water productive or predominantly flow gas with little or no mobile water (reference Figure 10). The pattern shown in Figure 10 coincides with : (i) an area within an vitrinite isoreflectance contour of 1.1 Ro (Figure 5), and (ii) proximity to the basin outcrop. A relationship is suggested where active gas generation has occurred in coals at depths greater than 4500 feet from the surface and isolated from the outcrop will result in little or no mobile water from coal reservoirs. Large volumes of gas generated from the coals and redistributed laterally and vertically throughout the geologic section is a possible mechanism for relocation of water from the coal reservoirs. Imbibition of water back into the system may be precluded by the absence of cross-formational fluid flow in low permeability basins.

Thermal modeling of geologic evolution has been used to describe and quantify existing reservoir conditions for deep coal seams within the Piceance Basin. Various conclusions and observations regarding coal reservoir conditions as a function of time, temperature and cross-formational fluid migration include:

1. Gas occluded in coal seams with maturities less than .73 Ro vitrinite reflectance may have largely originated from a deeper source or are a biogenic origin.

2. The unusual vitrinite reflectance profile observed in the Piceance Basin (and other deep coal basins) is caused by the low thermal conductivity of the coal.

3. Simplistic and commonly used geothermal gradient maturation models that do not account for heat transfer will fail to predict the accelerated phase of coal maturation and resulting hydrocarbon generation.

4. Active gas generation from coal seams in the Piceance Basin discontinued approximately twenty-five million years ago.

5. In the Piceance Basin, underpressured and overpressured coal reservoirs are part of a single hydrocarbon generation cycle, differing by the volume of hydrocarbons generated and a post-laramide uplift.

6. To date, overpressured coal reservoirs in the San Juan Basin are water saturated and highly permeable. These reservoir conditions may be related to coal water generative cycle under shale bounded conditions.

7. Water and gas generated during the coalification process may have fractured overlying sediments during expulsive cycles.

8. High permeability overpressured coals with high gas-in-place represent attractive coal reservoir conditions. For low permeability basins (such as the Piceance Basin), these reservoir parameters are most likely to occur along positive structural features that overlap thick, thermally mature coal seams.

REFERENCES

1. Meissner, F.E., 1984, Cretaceous and Lower Tertiary Coals as Sources for Gas Accumulations in the Rocky Mountain Area: Hydrocarbon Source Rocks of the Greater Rocky Mountain Region: Rocky Mountain Association of Geologists, Denver, Colorado, p. 401-432.

2. McPeek, L.A., 1981, Eastern Green River Basin: A Developing Giant Gas Supply from Deep, Overpressured Upper Cretaceous Sandstones: AAPG Bull., Vol. 65, p. 1078-1098.

3. Wyman, R.E., Gas Resources in Elmworth Coal Seams: Elmworth - Case Study of a Deep Basin Gas Field, AAPG Memoir 38, p. 173-189.

4. van Gijzel, P., 1982, Characterization and Identification of Kerogen and Bitumen and Determination of Thermal Maturation by Means of Qualitative Microscopical Techniques, in How to Assess Maturation and Paleotemperatures: SEPM Short Courses No. 7, p. 159-216.

5. Law, B.E. et al., 1983, Geologic Implications of Coal Dewatering: AAPG Bull., Vol. 67, p. 2255-2260.

6. Allardice, D.J., and D.G. Evans, 1971, The Brown Coal/Water System: Part 2; Water Sorption Isotherms on Bed Moist Yallourn Brown Coal: Fuel, V. 50, p. 236-253.

7. Juntgen, H. and J. Klein, 1975, Enstehung Von Erdgas Aus Kohligen Sedimenten: Erdol und Kohle, Erdgas, Petrochemie, Erganzungsband, V. 1, p. 52-69.

8. Allardice, D.J. and D.G. Evans, 1978, Moisture in Coal, in C. Karr, Jr., ed., Analytical Methods for Coal and Coal Products, V. 1: New York. Academic Press.

9. Kim, A.G., 1977, Estimating Methane Content of Bituminous Coalbeds From Adsorption Data: U.S. Bureau of Mines Report of Investigations 8245, p. 22.

10. Kissev, F.N., C.M. McCulloch, and C.H. Elder, 1973, The Direct Method of Determining Methane Content of Coalbeds for Ventilation Design: U.S. Bureau of Mines Report.

11. Eddy, G.E., Rightmire, C.T., and C. Byrer, 1982, Relationship of Methane Content of Coal, Rank and Depth: Proceedings of the SPE/DOE Unconventional Gas Recovery Symposium, Pittsburgh, Penn., SPE/DOE 10800, p. 117-122.

12. Welte, D.H., et al., 1981, Application of Organic Geochemistry and Quantitative Analysis to Petroleum Origin and Accumulation - An approach for a Quantitative Basin Study, in G. Atkinson and J.J. Zuckerman, eds., Origin and Chemistry of Petroleum: Elmsford, NY, Pergamon Press, p. 67-88.

13. Stallman, R.W., 1963, Computation of Ground-Water Velocity from Temperature Data, in Methods of Collecting and Interpreting Ground-Water Data: U.S. Geological Survey Water - Supply Paper 1544-H. p.36-46.

14. Lopatin, N.V., 1971, Temperature and Geologic Time as Factors in Coalification: Akademiya Nauk, Uzb. SSSR, Ser. geologicheskaya, Izvestiya, No. 3, p. 95-106. (Translation by N.H. Bostick, Illinois State Geological Survey, February 1972).

15. Decker, D., 1985, Appropriate Stratigraphic Nomenclature for Coal Reservoirs in the Piceance Basin, Abstract Presented at the Rocky Mountain AAPG Convention, Denver, Colorado (June 1985).

16. Hanson, J.M., 1987, Evaluation and analysis of the response of "Cameo" and "Hoffmeister-Rogers" wells to solid earth tides and barometric pressure. Unpublished paper submitted to Resource Enterprises, Inc. under contract to GRI #5083-214-0844.

17. Waples, D.W., 1987, Maturity Modeling of the 1 Cameo 20-4 Well, Unpublished report submitted to Resource Enterprises, Inc.

18. Kappelmeyer, O., Haenel, R.: Geothermics--with Special Reference to Application. Berline-Stuttgart: Borntraeger, 1974.

19. Law, B.E., and V.F. Nuccio, "Segmented Vitrinite Reflectance Profile from the Deep Seam Project, Piceance Basin, Colorado--Evidence of Previous High Pore Pressure". Abstract presented at the Rocky Mountain AAPG Convention, Casper, Wyoming (Sept. 1986).

20. Yukler, M.A., 1976, Analysis of Groundwater Flow Systems and an Application to a Real Case, in D. Gill and D.F. Merriam, eds., Geomathematical and Petrophysical Studies in Sedimentology, Computery and Geology, V. 3: Elmsford, NY, Pergamon Press, p. 33-49.

21. Kelso, B.S. and A.D. Decker, et al., 1987, GRI Geologic Appraisal of Coalbed Methane in the San Juan Basin. The 1987 Coalbed Methane Symposium Proceedings, held at the University of Alabama, Tuscaloosa, Alabama, November 16-19, 1987.

22. Hays, J.B., 1979, Sandstone diagenesis- The hole truth. In: Aspects of Diagenesis. P.A. Scholle adn P.R. Schluger, eds., Soc. Econ. Paleontologists and Mineralogists, Spec. Publ. No. 26, pp. 127-139.

23. Decker, A.D., et al., 1987, Geochemical Technqiues Applied to the Identification and Disposal of Connate Coal Water. The 1987 Coalbed Methane Symposium Proceedings, held at the University of Alabama, Tuscaloosa, Alabama, November 16-19, 1987.

21. Decker, A.D. and J.C. Seccombe, 1986, Geologic Parameters Controlling Natural Gas Production from a Single Deeply Buried Coal Reservoir in the Piceance Basin, Mesa County, Colorado: SPE Paper #15221, presented at Unconventional Gas Technology Symposium, May 1986.

22. McKee, C.R. et al., 1986, Using permeability-vs-depth correlations to assess the potential for producing gas from coal seam: Quarterly Review of Methane from Coal Seams Technology, vol, 4, no. 1, p. 15-26.

TABLE 1

COAL VOLUMETRICS

Ro%	% F	COAL RANK	THERMAL METHANE (Bcf/Mi^2)	WATER (10^6 bbl/mi^2)	THICKNESS (FEET)	
		EARLY PEAT	-	42.0	7.0	DIAGENESIS
		PEAT	-	14.0	3.5	
.23	95	LIGNITE	-	6.8	2.4	
.36	122	SUB-C	-	3.6	1.8	
.43		SUB-B	-	2.3	1.4	
.47		SUB-A	-	1.6	1.4	
.51	158	HvBb	-	.58	1.2	
.76	196	HvAb	.37	.50	1.2	CATAGENESIS
.90		HbAb	2.14			
1.11	248	Mvb	2.16	.45	1.0	
1.30		Mvb	.47			
1.50	302	Lvb	.49	.34	1.0	
2.04	356	Sa	-	.25	1.0	META-GENESIS
2.7	392	TOTAL	5.63	72.42		

AFTER LAW, 1983

TABLE 2

COAL RESERVOIR AND GEOLOGIC PROPERTIES

RED MOUNTAIN UNIT AND EAST DIVIDE CREEK

	COAL THICKNESS (FT)	RANK (Ro)	GAS GENERATED (BCF/mi^2)	IN PLACE (BCF/mi^2)	EXPELLED (BCF/mi^2)	DEPTH (FT)	TEMP ° F	PRESSURE GRADIENT (PSI/ft)	PERMEABILITY (md)
RED MOUNTAIN 1 DEEP SEAM 32-2	61'	.90-1.27	238	18	220	5600'	164'	.33	<.01
EAST DIVIDE CK. 1 CAMEO 20-4	100'	.90-1.27	467	35	432	4450'	176'	.59	>10.0

FIGURE 1

METHANE GENERATION

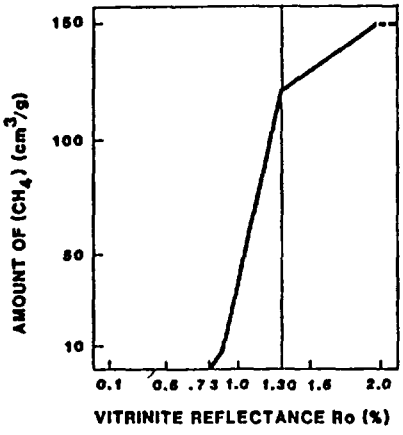

(AFTER WELTE, 1984)

FIGURE 2

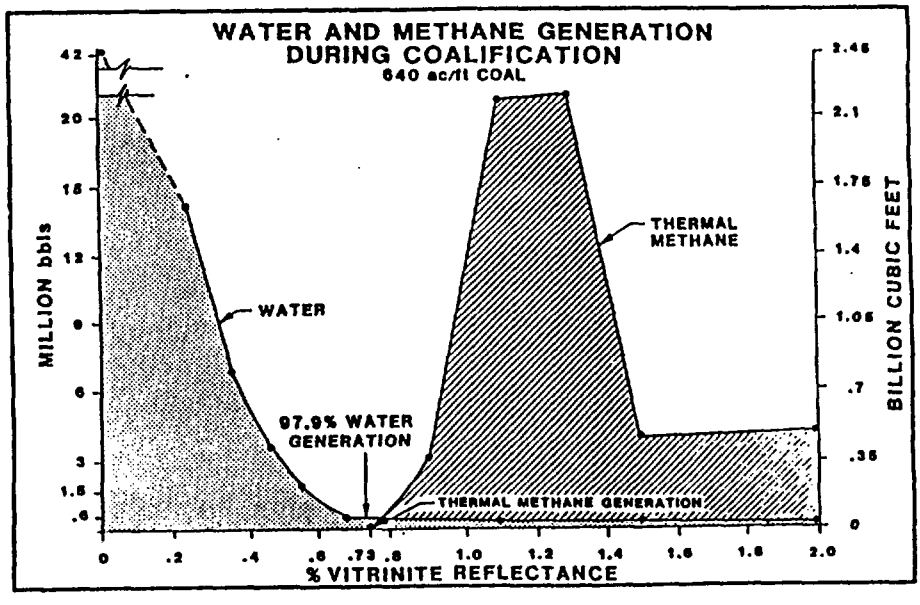

FIGURE 3

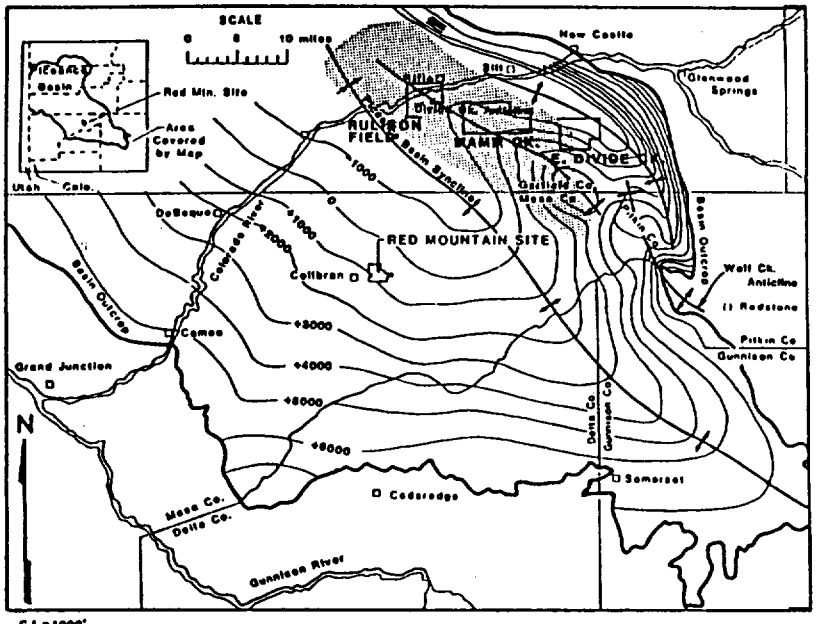

C.I. = 1000'
SUBSEA ELEVATIONS

STRUCTURE CONTOUR MAP
TOP OF ROLLINS SANDSTONE
PICEANCE BASIN, COLORADO

OVERPRESSURED AREA

FIGURE 4

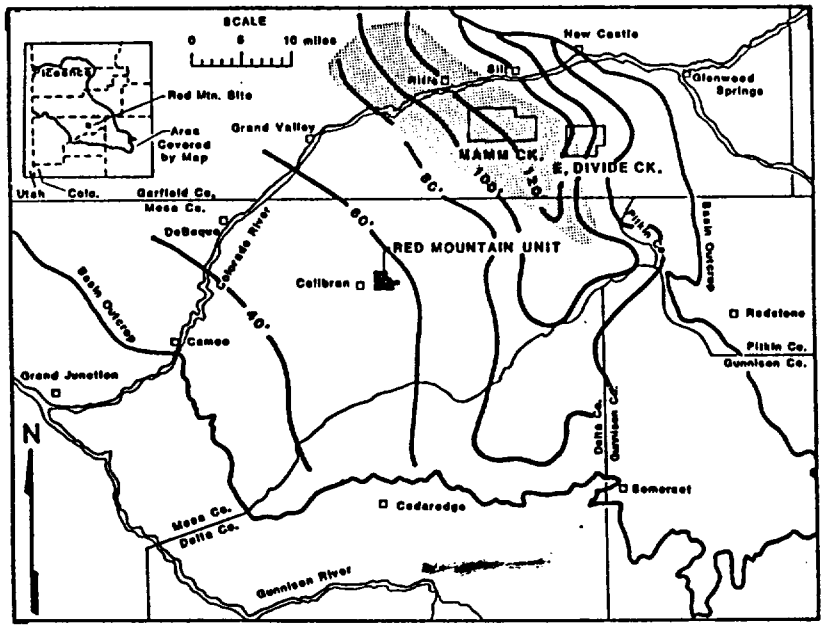

TOTAL COAL ISOPACH TREND MAP

OVERPRESSURED AREA

FIGURE 5

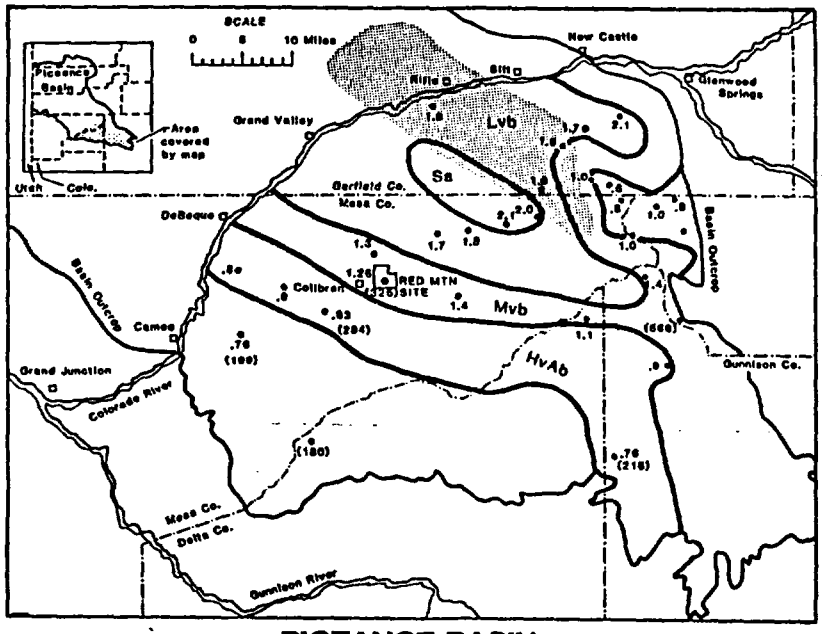

PICEANCE BASIN

• ISOREFLECTANCE CONTOURS

OVERPRESSURED AREA

FIGURE 6

WATER AND THERMAL METHANE GENERATION
AS A FUNCTION OF TIME AND COAL MATURATION

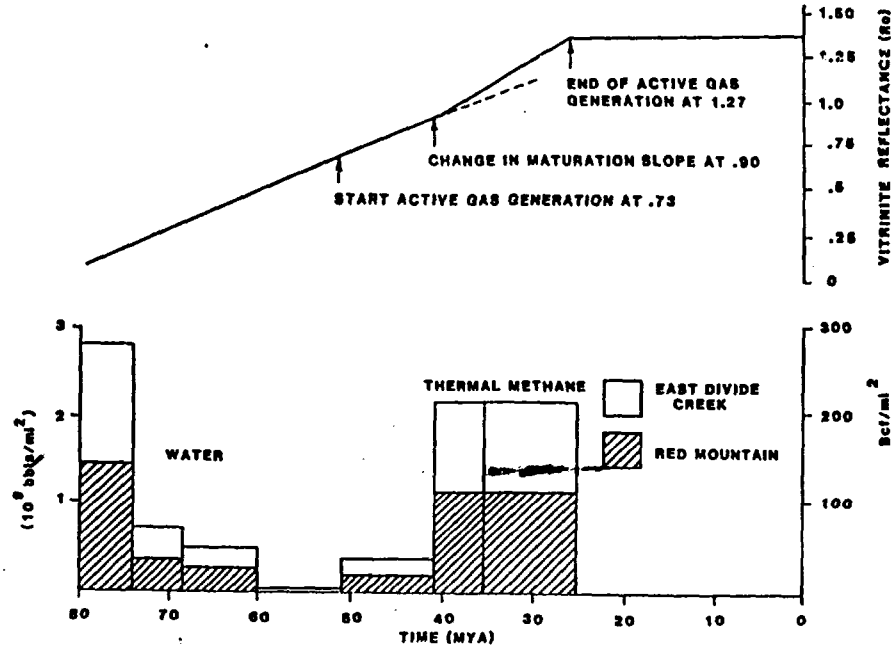

FIGURE 7

MATURITY vs. DEPTH

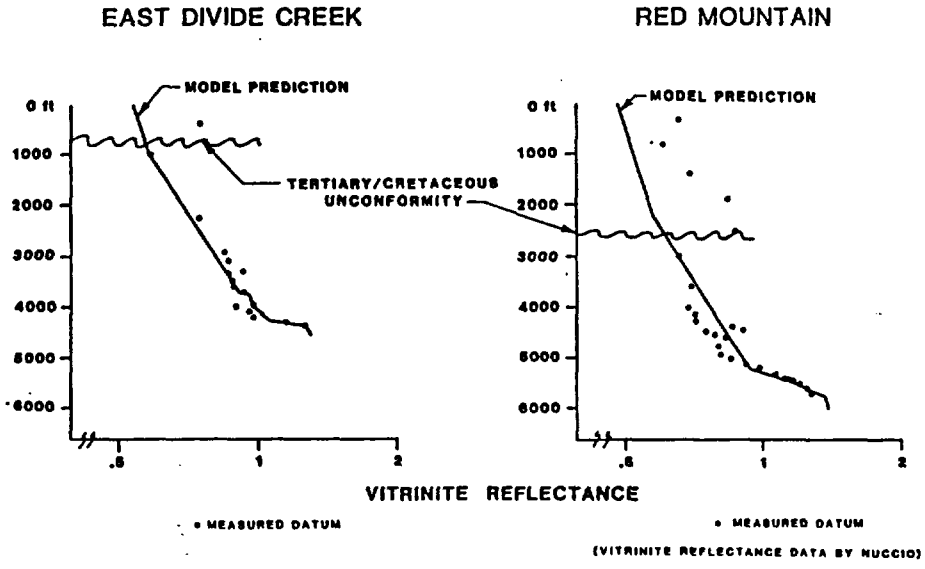

FIGURE 8

STATIC TEMPERATURE LOGS

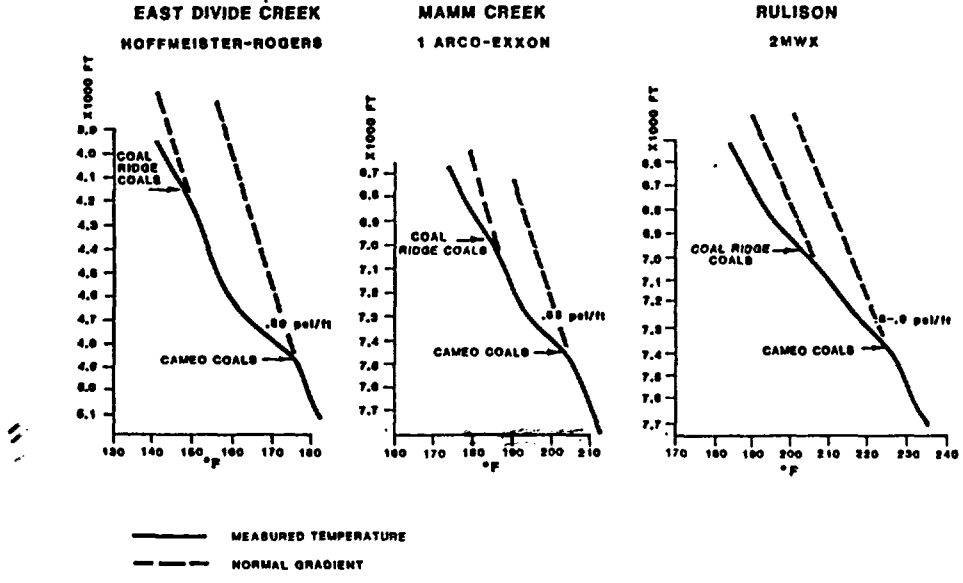

FIGURE 9

PRESSURE - TEMPERATURE RELATIONSHIP

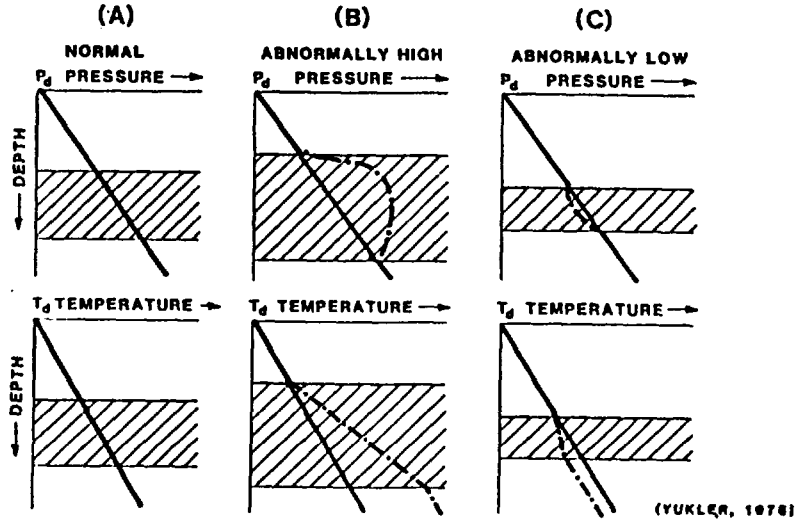

FIGURE 10

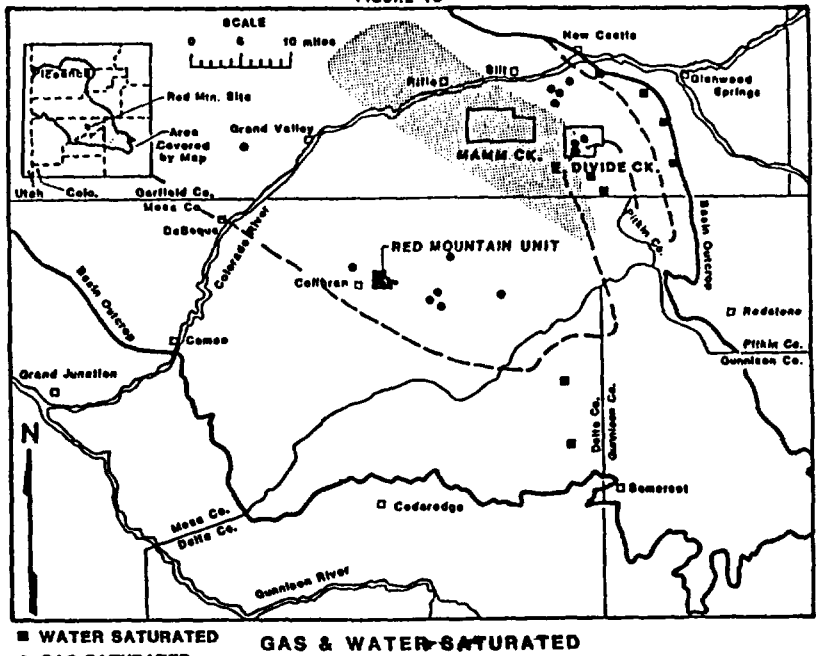

不一

Proceedings of the 1987 Coalbed Methane Symposium, Tuscaloosa, Alabama, Nov. 16-19, 1987

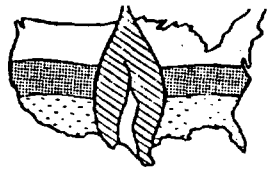

THE 1987 COALBED
METHANE SYMPOSIUM

8731 GRI Geologic and Economic Appraisal of Coalbed Methane in the San Juan Basin

B.S. Kelso (Colorado Geological Survey); A.D. Decker (Resource Enterprises, Inc.); D.E. Wicks (Lewin & Associates, Inc.); D.M. Horner (Gas Research Institute)

ABSTRACT

A regional geologic assessment of the Fruitland Formation coals in the San Juan Basin indicates that this formation has a high potential for natural gas production from coal seams. This study, sponsored by the Gas Research Institute, includes subsurface structure, depth, thickness, and geometry interpretations. Coal ranks were assessed using vitrinite reflectance data and gas contents were compiled from public databases.

In addition to the regional geologic investigation, four sites were chosen for detailed field-level geologic and reservoir analyses. The geologic assessment employed cross-sections, net coal isopachs, and structure maps. Reservoir analyses included pressure, temperature, and permeability, in conjunction with coalbed methane well completion and production histories.

The regional geologic analysis concluded that the Fruitland Formation coals have an estimated in-place methane resource of 56 trillion cubic feet (TCF) - nearly double the previous estimate of 31 (TCF). Field-level investigations concluded that no single completion practice provided better production results than any other and overpressured reservoirs are significant contributing factors in the better producing wells.

An economic evaluation of the coalbed methane resource is due to be completed in early 1988.

INTRODUCTION

Activity of coalbed methane development is greater in the San Juan Basin than in other western coal basins. Production of the vast coalbed methane resource of the Fruitland Formation dates back to 1953, with the Phillips Petroleum Co., No. 6-17, San Juan 32-7 Unit well. More recent activity, specifically directed at resource development, started in the mid-1970's. To date, more than 200 wells have been documented as Fruitland Formation coalbed methane tests. Several pools or fields have been designated in the basin reporting Fruitland coal seams, or the "basal" Fruitland as the producing horizons.

The geologic analysis of the Fruitland Formation coalbed methane resource is part of a larger economic evaluation to determine recoverable coalbed methane in the San Juan and other U.S. coal basins. The San Juan Basin evaluation is divided into three phases: 1) a geologic appraisal of the Fruitland Formation coals, concluding with a gas-in-place resource estimate; 2) case history studies and history matching of Fruitland coalbed methane wells; and 3) an economic appraisal of the resource, using various technology cases. At this time, the regional geologic appraisal and four detailed field investigations have been completed. History matching of wells is underway and the economic evaluation has not been initiated. All three phases of the project will be completed by early 1988.

GEOLOGIC SETTING OF THE SAN JUAN BASIN

Regional Setting

The San Juan Basin is located in northwestern New Mexico and southwestern Colorado, with the study area of this project defined by the Pictured Cliffs Sandstone outcrop (Figure 1). It is approximately 90 miles wide, west to east, and 100 miles long, north to south and covers 7500 square miles.

Stratigraphy and Depositional Environments

The coals of the San Juan Basin are Cretaceous age and located in the Dakota, Mesaverde, and Fruitland formations (Figure 2). The Fruitland, the youngest of these, contains the largest coal resource. Deposition of the Fruitland coals occurred predominantly in lagoons, landward of the Pictured Cliffs barrier strandline. The thickest and most continuous seams are located in the lowermost 70 feet of the formation and are often associated with stratigraphic rises in the Pictured Cliffs. A detailed discussion of the Fruitland-Pictured Cliffs depositional environment is presented in Fassett, 1987 [1] and in the Fassett paper in this proceeding.

The Fruitland Formation is a coastal plain deposit of paludal carbonaceous shales, siltstones, sandstones and coals deposited behind the regressing Pictured Cliffs strandline. Formation thickness ranges from less than 100 to greater than 600 feet and contains evidence of fresh and brackish water environments. The sandstones are soft to hard and grey-white to brown in color. The shales are firm and grey to black in color. The coals were deposited in

lagoons, marshes, swamps and abandoned channels and are overlain by fluvial shales and sandstones. The coals are the most correlative units of the fluvial Fruitland sediments.

The underlying Pictured Cliffs is a regressive, coastal-barrier sandstone. Formation thickness varies from 125 to 400 feet due to minor transgressive episodes, which locally intertongue the Fruitland and Pictured Cliffs. The lower portion of the Pictured Cliffs is primarily interbedded sandstone and shales, with the upper unit a quartzitic, fine-to-medium grained sandstone.

Structure

The San Juan Basin's arcuate structural axis lies just south of the Colorado-New Mexico state line. The U-shaped Hogback Monocline forms the western and northern rims of the basin. To the east, the Nacimiento Uplift and Archuleta Arch bound the basin. The south and southwestern boundaries of the basin are not structurally defined and sediments gently dip northward from the Chaco Slope (Figure 3).

There are few major structural elements within the San Juan Basin and most are of Laramide age. The Ignacio Anticline, located in the north central portion of the basin, is the largest and best documented structure. Minor northwest trending en echelon folds and northeast-trending, high angle, low displacement faults are found on the eastern and southeastern edges of the basin. Radial folds, which plunge toward the basin's center, can be found around the perimeter. Minor structures resulting from Tertiary intrusive activity are located in the basin. Kelly, 1951 [2] and Woodward and Callender, 1977, [3] provide complete structural and tectonic descriptions of the San Juan Basin.

Detailed Field Investigation Settings

The four field investigation sites are located in the northern end of the basin where operator activity levels have been concentrated (Figure 4). The sites selected provide wells with production histories over extensive time periods and all four sites lack major structural features. Two sites are located in the Colorado Ignacio Blanco Field and one each in the New Mexico Cedar Hill and Undesignated Fruitland Fields. Site 1 of the Ignacio Blanco Field and the Undesignated Fruitland Field are in areas of a Pictured Cliffs stratigraphic rise, that is, an area of intertonguing with the Fruitland. The other two sites are stratigraphically less complex.

METHODOLOGY

The geologic evaluation of coal bearing formations is a key element in an economic appraisal of any coalbed methane resource. The San Juan Basin provided an opportunity for detailed geologic field investigations as well as a regional scale study, because of the large number of exploration control points and Fruitland coalbed methane tests. The purpose of the regional geologic investigation was to determine a gas-in-place resource estimate for the Fruitland Formation coals. The detailed geologic field studies were performed to analyze the geology and reservoir properties associated with producing coalbed methane wells, and for use in the regional economic evaluation of the basin.

The regional geologic evaluation consisted of the construction of two geologic cross-sections and the interpretation of several thousand geophysical logs for subsurface geologic data. The cross-sections provided insight into the lateral and vertical distribution of the Fruitland coals. The subsurface geophysical log data were used to construct structure, overburden, and net coal thickness maps associated with the Fruitland Formation and underlying Pictured Cliffs Sandstone.

The geology and coal resources of the Fruitland Formation have previously been documented [4] and other coalbed methane resource estimates have been based upon this work [5,6]. In order to independently evaluate the Fruitland coalbed methane resource, an original investigation of Fruitland coal resources was conducted.

After the resource and distribution of Fruitland coals was determined, an emperical formula was derived using measured gas contents, depth, and coal rank. The formula allowed projection of gas contents into areas lacking measured data. Gas-in- place estimates were then calculated on a township and range basis using the following equation.

$$GIP = GC * h * A * p \quad \ldots\ldots\ldots\ldots\ldots\ldots \quad (1)$$

Where: GIP = Gas in-place (trillion cubic feet)
GC = Gas content (cubic feet/ton)
h = Net coal thickness (feet)
A = Drillable area (acres)
p = Coal density (tons/acre-foot)

The gas-in-place values for 210 townships with sufficient coal thickness and depth of cover were summed to derive the Fruitland Formation gas-in-place resource estimate.

Four detailed field investigation sites in three producing fields were chosen in areas with sufficient coalbed methane well populations for analysis. Detailed geologic cross-sections and subsurface structure and net coal thickness maps were prepared for each area. In addition to the geologic data, reservoir data including pressure, temperature, permeability (very little data), and cleat spacing were collected. Drilling, completion and production history data for each coalbed methane well in the four areas were also compiled. An analysis of the geologic, reservoir and completion data is being performed in an attempt to establish trends between the reservoir data and production histories.

REGIONAL GEOLOGIC ANALYSIS

The primary products of the regional geological analysis are two cross-sections, a net coal isopach map, an overburden map of the Fruitland-Pictured Cliffs contact, and a thermal maturity rank map. All of the products were used to evaluate the geology and properties of the coals necessary to determine a gas-in-place estimate.

Stratigraphic Cross-Sections

Two regional, basin-wide, geologic cross-sections were constructed with density-porosity or gamma-density geophysical logs. (Figure 4). Both were segmented due to the length of the sections and the number of logs used. Section A-A", trending northwest to southeast, is parallel to the depositional strike of the Pictured Cliffs strandline. Section B-B" is constructed perpendicular to depositional strike, or southwest to northeast. Orientation of the cross-sections was designed to support the concept that coals parallel to depositional strike can be followed for greater distances than those perpendicular to strike. Interpretations of the cross-sections were used to understand the lateral continuity of the Fruitland coals and to determine if the Fruitland Formation could be divided into zones, based on vertical coal distribution.

In cross-section A-A", the Fruitland Formation thins from the northwest to the southeast. Maximum thickness is greater than 450 feet. Thinning of the Fruitland in the southeast to less than 100 feet is the result of erosion and a stratigraphic rise of the Pictured Cliffs [4], as seen on the cross-section. Coals are found at depths ranging from 2400 to 4200 feet, with the deeper coals along the southeast extension of A-A". Maximum net coal thickness and thicker individual seams are located on the northwest extension of this cross-section with net coal thickness ranging from 4 to 95 feet, and frequent 20 foot individual seams. The spacing between control points averages 5 miles and correlation of individual beds was not possible at this scale. No grouping or zone determination was established due to the lack of traceable markers.

The cross-section B-B" trends southwest to northeast and shows minor thickness variations in the Fruitland ranging from 200 to 350 feet. A stratigraphic rise is present to the northeast, approximately 10 miles south of the Colorado-New Mexico state line. Coals on the southeast end of the cross-section are located at 1100 foot depths and gradually deepen towards the basin's center, with the deepest coals found at 4000 feet. Net coal thickness ranges from 19 to 67 feet with a single seam of 40 feet found near the northeast limit of the cross-section. Most wells used in this cross-section have a well developed coal in close proximity to the Pictured Cliffs. These basal coals range from 8 to 40 feet in thickness and are sometimes correlative over many miles. The average spacing between wells on section B-B" is 5 miles and no correlation of individual beds was attempted. As with A-A", no division of the Fruitland Formation into coal groups or zones was made.

Net Coal Thickness and Overburden

A Fruitland Formation net coal isopach map was constructed using data from gamma-density, density-porosity, and a limited number of gamma ray-neutron geophysical logs (Figure 5). Net coal values do not include coals thinner than 2 feet with efforts made to exclude partings and shaley units within individual coals. Net coal thickness values ranged from 0 to greater than 100 feet. An eastern area of the basin exhibits 0 net coal values which are the results of non-desposition and erosion of the Fruitland. The maximum net coal values are found in the northwest part of the basin with net thickness exceeding 100 feet. An approximate 10 mile wide, northwest trend is observed in the north central portion of the basin. This trend is parallel to the structural axis of the basin with average net coal thicknesses of 70 to 80 feet. It can be generally stated that the southern end of the basin has less than 30 feet of net coal, with the exception of a small area in the southwest. Net coal values and the geologic cross-sections were used to determine the lateral and vertical distribution of coals in the Fruitland.

The overburden map or depth parameter of the Fruitland coals in the regional geologic analysis was utilized as part of the gas content and containment evaluation. Depths of coals range from 0 feet at the basin's outcrop to more than 4200 feet along the basin's structural axis. Depths change rapidly along the north, northeastern, and northwestern margins of the basin due to the structural monoclines. In the southern part of the basin, coal depths gradually increase as the structural slope increases to the northeast. The deepest coals are found in the northeastern quarter of the basin.

Coal Rank

Fassett and Hinds, 1971 [4] reported the coals of the Fruitland Formation as subbituminous. Support for their conclusion comes from an observation of the weathering nature of the coals when mined and stockpiled. Viewing the coals as a reservoir for natural gas requires a different approach to rank assessment. The approach used in this study was based on the thermal maturity of the coals, which is measured by the vitrinite reflectance. This approach is applicable to all coal basins. Rank generally increases from south to north, with the highest ranks found in the north central portion of the basin. A vitrinite reflectance rank map of the San Juan Basin (Rice, 1983) [7] was modified with additional data and used to establish the various Fruitland coal ranks, ranging from high volatile C bituminous to low volatile bituminous with 0.46 to 1.51 reflectance values.

GAS CONTENTS OF FRUITLAND COALS

A moderately small public domain database of measured gas contents exists for the Fruitland Formation coals. The primary source of the data was the U.S. Bureau of Mines (USBM) gas content measurement database for samples from around the United States. A description of the desorption process and a partial list of samples is found in Diamond and Levine, 1981 [8]. Additional desorption data were acquired from the Colorado Geological Survey.

Twenty-eight data points were standardized for ash content, temperature, and pressure. The data was sorted by coal rank and sample depth to develop correlations relating gas content to depth and rank. Curves were established for high volatile A bituminous and high volatile B and C bituminous coals combined. Insufficient data was available for medium and low volatile coals and

analog curves were founded on the results of similar analyses in a Piceance Basin study [9]. The mathematical relationship that resulted from the analysis is:

$$GC = m * (\ln d) + b \quad \ldots\ldots\ldots\ldots\ldots\ldots 2$$

Where: GC = Gas content (cubic feet/ton)
m = Scaling coefficient
ln d = Natural log of depth (feet)
b = y intercept

GAS IN-PLACE OF THE FRUITLAND COALS

The regional geologic evaluation of the Fruitland Formation coals, San Juan Basin, concluded with a gas-in-place resource estimate. The unit of analysis is a township and range and a gas-in-place value was calculated for each of the 210 units in the study area. Elements of the gas-in-place calculation are gas content, net coal thickness, drillable area, and coal density.

Each of the 210 units was assigned an estimated gas content value using the mathematical relationship discussed previously. Depths used in the calculation were average maximum overburden on the Pictured Cliffs Sandstone. Analysis of the vertical distribution of Fruitland coals showed more than 85 percent of the net coal thickness is within 200 feet of the Pictured Cliffs. Insignificant differences result in gas content values when depth values are varied within this 200 foot range.

Net coal thickness and coal density are factors in the coal resource portion of the gas-in-place calculation. An average net coal thickness was determined for each unit from the coal isopach map constructed in the geologic evaluation. The coal rank map was used to assign coal density to the unit. Densities increase with rank as documented by Averitt, 1975 [10]. The following table shows the variation of coal density with rank used in this study.

Rank	Density (Tons/acre-foot)
High Volatile Bituminous (A, B, and C)	1800
Medium Volatile Bituminous	1850
Low Volatile Bituminous	1900

The drillable area of a unit is determined by totaling the number of acres in the unit and subtracting undevelopable acreage. Undevelopable acreage includes areas with urban development; abandoned, active or permitted coal mining operations; acreage already containing coalbed methane wells; and areas of insufficient coal overburden (gas containment) or coal thickness.

Gas-In-Place Estimate

The total gas-in-place resource estimate for the Fruitland Formation coals is 56 trillion cubic feet (TCF). This is only a resource estimate, not a reserve estimate and no recovery factor has been applied. It must be pointed out that up to this point, we have only been discussing gas in the micro-pore system of the coals and not dealt with "free" gas or gas in the cleat system of the coals. Calculation of the gas in the cleat system will be based on the results from history matching work and is expected to increase the current gas-in-place estimate by 2 to 3 percent. Figure 6 is a gas-in-place contour map for the Fruitland Formation coals.

The 56 TCF gas-in-place estimate is nearly twice the estimate previously reported by Choate and others, 1984 [5]. A comparison of the two estimates revealed that coal resource values used for each were within 10 percent. The conclusion was drawn that gas content data in the two studies were drastically different. Analysis of the data set used by Choate showed the use of fewer core desorption data and a large percentage of chip desorption samples. This explains the increase in the gas-in-place estimate resulting from this study.

DETAILED FIELD INVESTIGATIONS

Four sites located in three coalbed methane production fields were selected for detailed geologic and reservoir analysis. The number of completed wells in each area and their production histories aided in site selection. Figure 4 shows the location of the four sites studied. They are the Cedar Hill Field, New Mexico; an Undesignated Fruitland Field, New Mexico; and two sub-areas of the Ignacio Blanco Field, Colorado. The primary purpose of the field site investigations was to validate the regional geologic study at a field level. In addition, the field investigations incorporated production data into the geologic analysis and established the stratigraphic intervals contributing to the Fruitland coalbed methane production.

Cedar Hill Field

The Cedar Hill Field is located in portions of Townships 31 and 32 North, Range 10 West. Development of the coalbed methane resource in this area was initiated more than ten years ago and presently, the field contains 12 coalbed methane wells. A structure map on the Pictured Cliffs Sandstone for the area shows a maximum of 100 feet structural relief with a series of subtle northeast-southwest trends. Most of the structures in these trends exhibit relief of 20 feet or less. Net coal thickness across the area ranges from 9 to 55 feet. A coal in the basal section of the Fruitland Formation has been the primary production target and thickness ranges from 5 to 27 feet. This seam thins and splits to the southeast. The coal rank in the area is high volatile A bituminous and gas contents average 358 to 521 cubic feet/ton from four samples.

The reservoir parameters assessed in this evaluation are pressure, temperature, saturation, permeability and a gas-in-place estimate. Three bottom hole pressures were available from public records. They range from 1362 psi to 1590 psi or 0.49 to 0.56 psi/foot and indicate an overpressured coal reservoir. Reservoir temperatures of the basal coal ranged from 95 to 114 degrees Fahrenheit. Reservoir saturation status for this area is unknown and based on production histories of the earliest wells, 100 percent water saturation was assumed. Wells drilled at later dates were probably less than 100 percent water saturated and were partially dewatered by the

initial wells. No permeability data was available for any of the coal seams in the field. A gas-in-place estimate of 5 to 35 billion cubic /section (BCF/sec.) was calculated for the ar Hill Field.

Analysis of the completion histories of eight Amoco Production Company wells in the field showed that five were completed open-hole and three were completed through pipe with stimulation. Both completion techniques have proven successful and a conclusion can not be drawn on the best method of completion. Five of the eight wells are completed in a single seam and the remaining three are multiple seam completions. One conclusion drawn from this geologic and reservoir study is that the Cedar Hill Field area is overpressured.

Undesignated Fruitland Field

The Undesignated Fruitland Field is located in Township 30 North, Range 7 West. The field contains four coalbed methane wells with production histories dating from early 1986. This field, much like the Cedar Hill Field, shows very little structural relief on the Pictured Cliffs Sandstone. Structural relief does not exceed 80 feet across the area and a northwest-southeast structural trend is present. Structural closures of small magnitude exist along the trend. Net coal thickness ranges from 36 to 75 feet and approximately 95 percent of the coal occurs within 100 feet of the Pictured Cliffs. The thickest single seam in the area is 30 feet and the coal is ranked high volatile A bituminous. There are no measured gas contents in the study area. Therefore, data from the Cedar Hill Field, based on similar coal rank and depths, were used for this parameter.

Reservoir pressure data in the area range from 1332 to 1521 psi which converts to gradients of 0.45 to 0.50 psi/foot. Based on this data, the area is overpressured. Reservoir temperatures range from 93 to 112 degrees Fahrenheit in the lower Fruitland interval. This field appears to contain both gas and water saturated coal seams. One well in the area exhibits a predominantly gas-saturated coal seam, as shown by recent decreases in gas production and unchanged water production rates. There is no permeability data available for the coal reservoirs in the study area. The gas-in-place resource estimate for the Undesignated Fruitland Field, assuming similar gas content data for the Cedar Hill Field, ranges from 16 to 38 BCF/sec.

The four coalbed methane wells in the field were drilled by Meridian Oil Company. Two are completed open-hole with production liners and two are completed through casing. Three of the four wells have been stimulated. All of the wells have multiple coal seam completions and net coal thickness ranges from 43 to 63 feet per well. One of the open-hole completion wells has had tremendous gas production rates, at times exceeding 4 million cubic feet per day (MMCF/d). The worst well in the field only averages 150 thousand cubic feet per day (MCF/d). The remaining two wells have production rates ranging between 1 and 2 MMCF/day.

Ignacio Blanco Field

The Ignacio Blanco Field encompasses most of the Colorado portion of the basin. Two areas within the field were selected for detailed site investigations. It should be noted that the majority of the coalbed methane wells in the two areas were initially drilled and completed by William Perlman between 1982 and 1984. Amoco Production Company recently took over the Perlman acreage and recompleted a number of the wells in 1986 and 1987. Preliminary production statistics from recompleted wells indicate improvement over past production.

Area 1 - Township 34 North, Range 8 West. Area 1 contains 18 Fruitland coalbed methane wells with erratic production histories dating back to 1982. There is 1100 feet of structural relief across the area with structural lows and possible closures located in the southern half. A stratigraphic rise of the Pictured Cliffs Sandstone and intertonguing with the Fruitland Formation is located in the north and west portions of the study area. Net coal thickness throughout the area ranges from 26 to 76 feet with the thickest individual seam being 35 feet. The coal is ranked medium and low volatile bituminous and gas contents from five samples average 315 cubic feet/ton.

This area contains the two Southern Ute Indian, Oxford wells in section 25, which were part of a Department of Energy (DOE) coalbed methane research project. The coring of these wells revealed 1/4 to 1/2 inch cleat spacing. The Oxford #2 well was used in 1985 by In-situ, Inc., a GRI contractor, for reservoir data analysis. In-situ, Inc. determined a static reservoir pressure of 1490 psi or a gradient of 0.52 psi/ft and a calculated permeability of 5 md [11]. Reservoir temperature data across the area, for the lower Fruitland Formation ranges from 100 to 128 degrees Fahrenheit. The pressure data from In-situ's research and from additional Fruitland Formation drill-stem test data indicate that the southern region of the study area is overpressured. All of the coalbed methane wells produced significant volumes of water in the field. A gas-in-place estimate of 18 to 52 BCF/section is estimated for this area.

Completion methods of the 18 wells in the area included cased and open-hole, with stimulated and unstimulated examples of each. No one method has proven more successful than another and erratic production histories from the wells make it difficult to draw a completion/production history conclusion. As noted before, Amoco has recompleted 6 of the 18 wells in the area with small to moderate size sand/water stimulations. Production data from the recompleted wells is not yet available, but will be valuable for additional analysis.

Area 2 - Township 32 and 33 North, Range 6 West. Area 2 of the Ignacio Blanco Field contains 28 coalbed methane wells. A maximum of 350 feet of structural relief is found in the area and a structural nose is located in the northwest portion of the area. A north-south trend of structural depressions is located along the western edge of the area. Net coal thickness

ranges from 20 to 68 feet, with the thickest individual coal seam being 42 feet. Coal rank is medium volatile bituminous and the area has an average measured gas content of 380 cubic feet/ton.

A research project was conducted at the Tiffany Gas, Glover #1 well in section 2, T32N, R9W, by [illegible] under GRI contract. The purpose of the project was to identify the resource potential and characteristics at a site, and provide the operator with a completion technique that would lead to economical production of Fruitland coalbed methane. Extensive work on reservoir characteristics was conducted and reported by Jones, 1985 [12]. A static reservoir pressure of 1483 psi or gradient of 0.48 psi/foot was measured at the site by In-Situ, Inc. This indicates an overpressured reservoir, at least in the southeastern corner of the study area. A measured permeability value of 3.5 md was obtained from coal samples and 1/4 inch cleat spacing was measured on recovered coal cores. As in Area 1 of the Ignacio Blanco Field, most of the wells in Area 2 produce significant volumes of water. Gas-in-place estimates for this area range from 14 to 45 BCF/section.

Completions of the 28 wells in this area are similar to those discussed in Area 1 of the Ignacio Blanco Field. Amoco has attempted recompletion on a number of the Perlman wells, but production data is not yet available. A variety of completion and stimulation methods have been applied to wells in this area and no single method provides better results than another.

CONCLUSION

The following conclusions have been drawn from the regional geologic analysis and detailed field site investigations of this coalbed methane resource study:

- This extensive subsurface geologic analysis provides a foundation for additional research and development of the Fruitland Formation coalbed methane resource.
- Additional measured gas content data is needed for assessment of the resource.
- It is estimated that the Fruitland Formation coals contain 56 trillion cubic feet of natural gas.
- Lower Fruitland coals at the four field investigation sites are overpressured.
- Permeability measurements at two locations in the Ignacio Blanco Field are low and measurements are not available for the Cedar Hill and the Undesignated Fruitland Fields. Structural enhancement of permeability may exist within all four fields. Fracture and lineament studies are needed for possible identification of enhanced areas.
- Numerous well completion and stimulation methods have been utilized with varying degrees of success.

ACKNOWLEDGEMENTS

The Gas Research Institute (GRI) has sponsored a geologic and economic analysis of the Fruitland Formation coalbed methane resource under its Natural Gas Supply Program. This effort is part of a much larger economic evaluation of recoverable coalbed methane in the San Juan Basin and other U.S. coal basins. The scope of the program is in support of GRI's goal of adding low cost gas to the United States gas supply reserves through research and development. The authors of this paper wish to thank the Gas Research Institute for their support of this project and for their permission to publish the findings.

References

1. Fassett, J., "The non-transferability of a Cretaceous coal model in the San Juan Basin of New Mexico and Colorado", in Paleoenvironmental and Tectonic Control of Coal-Forming Basins of the United States, Geological Society of America Special Paper 210, (1986), p. 155-171.
2. Kelly, V.C., "Tectonics of the San Juan Basin", in Guidebook of the south and west sides of the San Juan Basin, New Mexico and Arizona, New Mexico Geological Society, 2nd Field Conference, (1951), p. 124-131.
3. Woodward, L. and Callender J., "Tectonic framework of the San Juan Basin", in Guidebook to the San Juan Basin III, New Mexico Geological Society, 28th Field Conference, (1977), p. 209-212.
4. Fassett, J.E. and Hinds, J.S., "Geology and fuel resources of the Fruitland Formation and Kirtland Shale, of the San Juan Basin, New Mexico and Colorado", U.S. Geological Survey Professional Paper 676, (1971), 76 p.
5. Choate, R., Lent, J., and Rightmire, C.T., "Upper Cretaceous geology, coal, and the potential for methane recovery from coalbeds in the San Juan Basin-Colorado and New Mexico", in Coalbed Methane Resources of the United States, Am. Assoc. of Petroleum Geologist Studies in Geology Series #17, (1984), p. 185-222.
6. Kelso, B., Goolsby, S., and Tremain, C., "Deep coalbed methane potential of the San Juan River Region, southwestern Colorado", Colorado Geological Survey Open-File Report 80-2, (1980), 56 p.
7. Rice, D., "Relation of natural gas composition to thermal maturity and source rock type in San Juan Basin, northwestern New Mexico and southwestern Colorado", Am. Assoc. Petroleum Geologists Bull., v. 67 no. 8, (August 1983), p. 1199-1218.
8. Diamond, W.P. and Levine, J.R., "Direct method determination of the gas content of coal: Procedures and results", U.S. Bureau of Mines, Report of Investigation No. 8515, (1981), 36 p.

9. McFall, K., Wicks, D., Kelso, B., Sedwick, K., and Brandenburg, C., "An analysis of the coal and coalbed methane resources of the Piceance Basin, Colorado", SPE/DOE Paper 16418, in Proceedings of the 1987 SPE/DOE Low Permeability Symposium, Denver, May 18-19, p. 283-295.

10. Averitt, P., "Coal resources of the United States, January 1, 1974", U.S. Geological Survey, Bulletin 1412, (1975), 131 p.

11. Koenig, Robert, In-situ, Inc., (1987) personal communication.

12. Jones, A.H., "Methane production characteristics of deeply buried coalbed reservoirs", Gas Research Institute Topical Report No. 85/0033, (March 1985), 176 p.

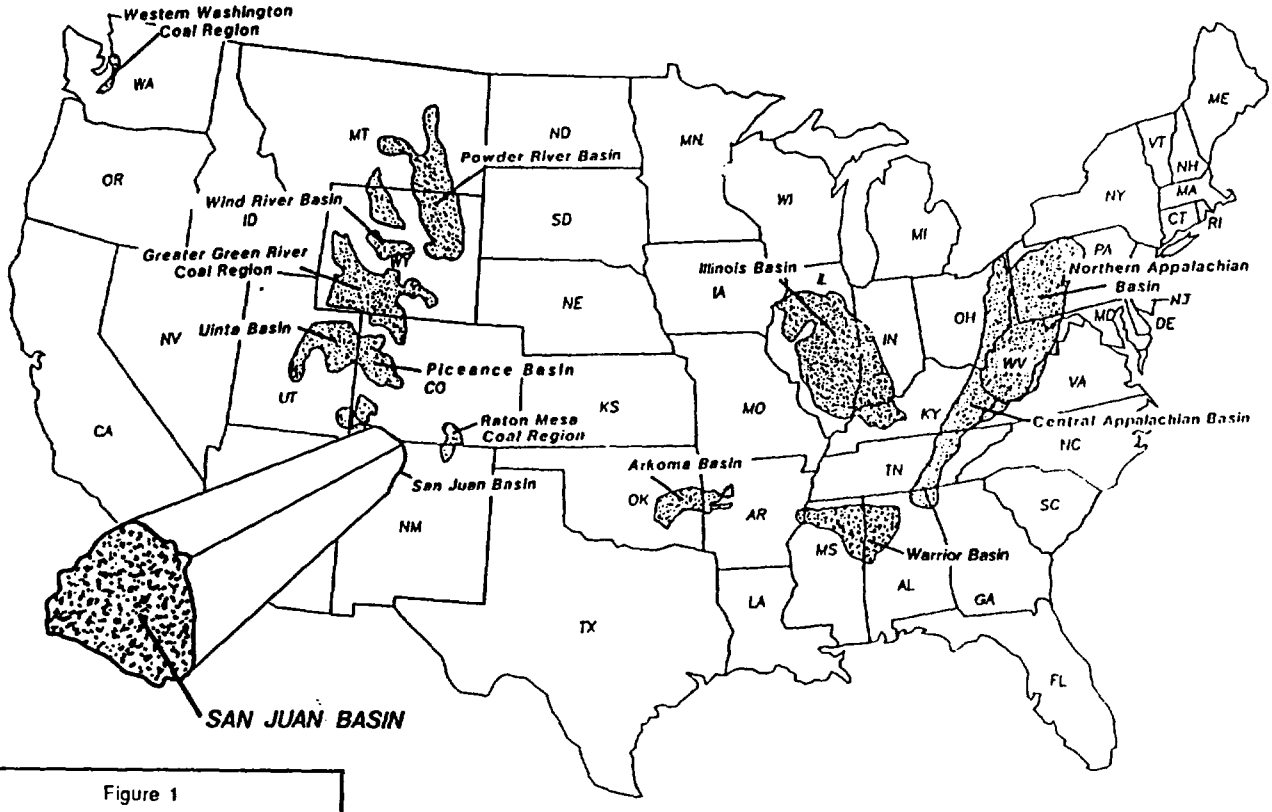

Figure 1

MAJOR COAL BASINS OF THE UNITED STATES

0 100 300
Miles

N

After: Rightmire, 1984.

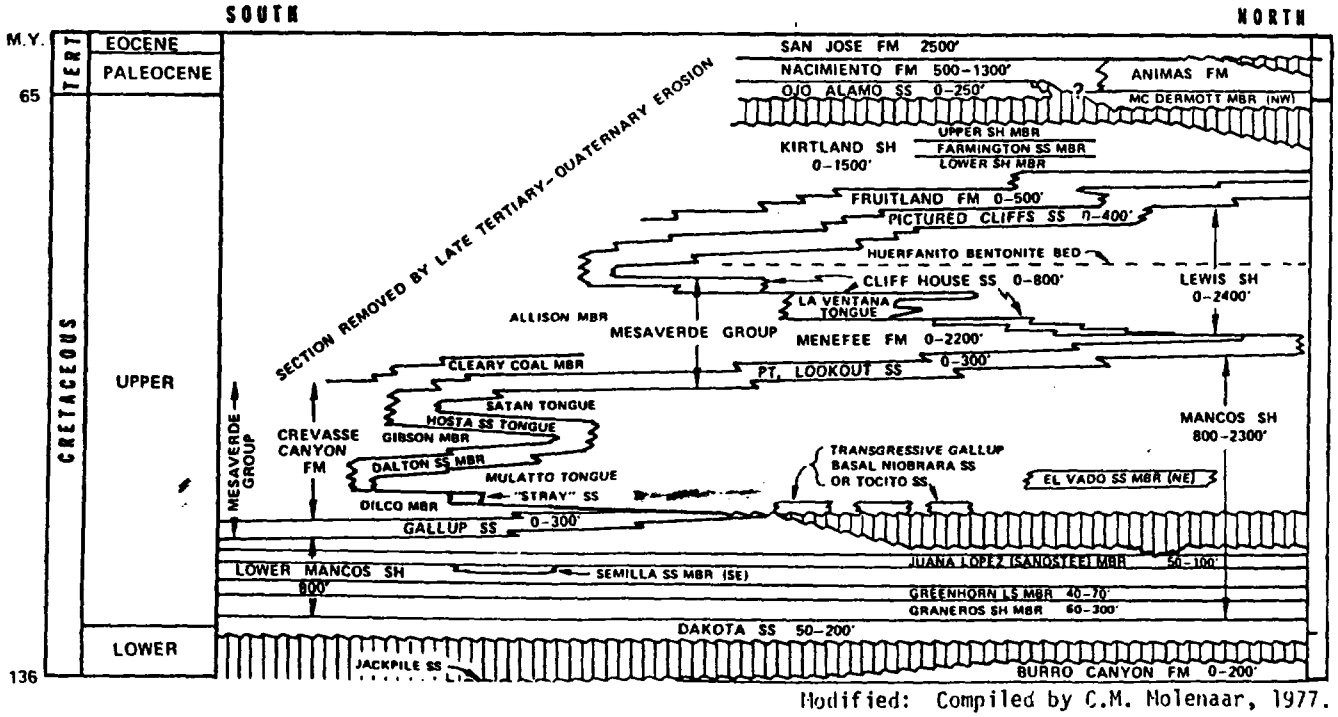

Modified: Compiled by C.M. Molenaar, 1977.

Figure 2. San Juan Basin time - stratigraphic nomenclature chart.

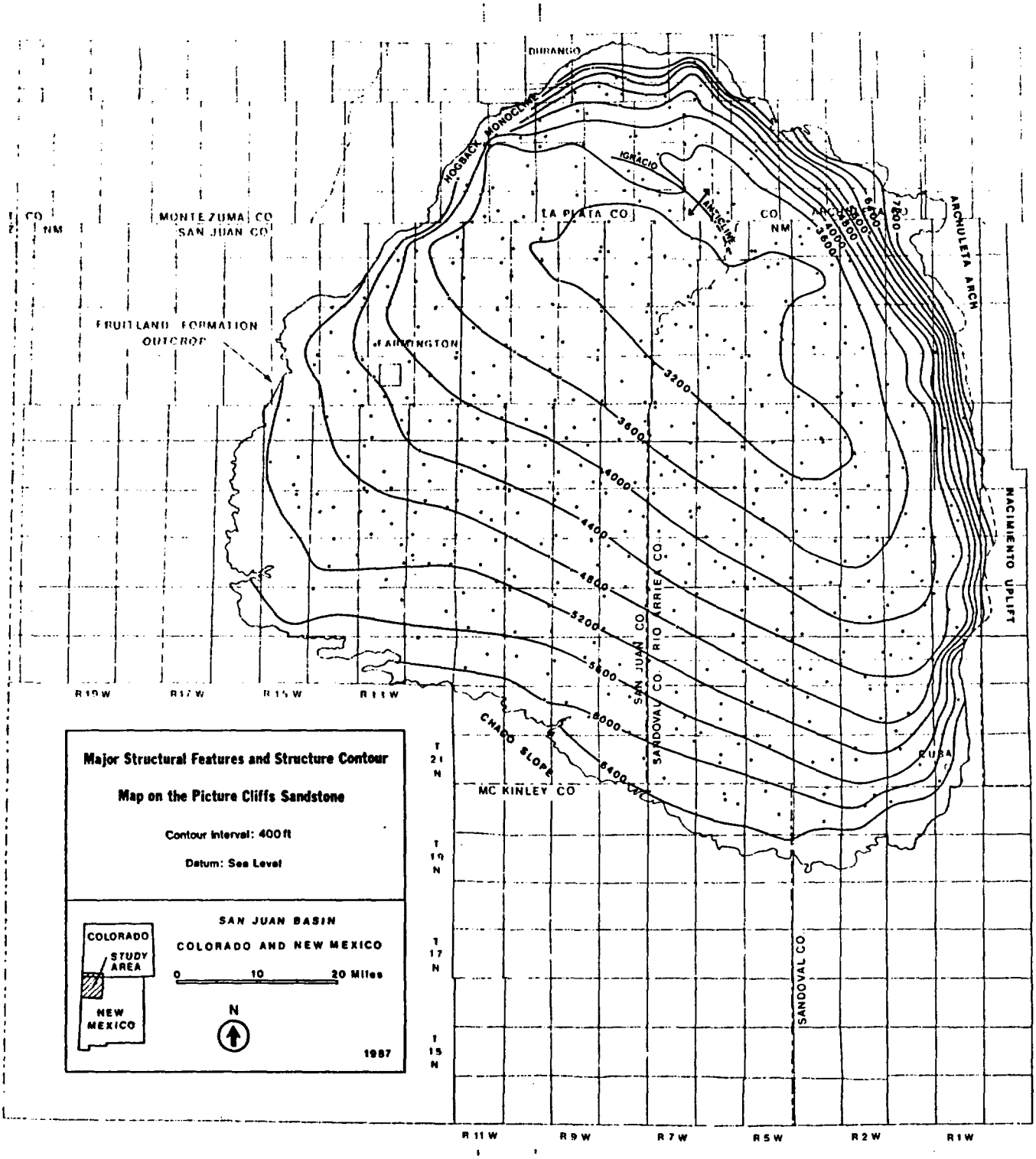
DURANGO
HOGBACK MONOCLINE
IGNACIO
LA PLATA CO
MONTEZUMA CO
SAN JUAN CO
FRUITLAND FORMATION OUTCROP
FARMINGTON
ARCHULETA ARCH
NACIMIENTO UPLIFT
3200
3600
4000
4400
4800
5200
5600
6000
6400
6800
7200
SAN JUAN CO
RIO ARRIBA CO
SANDOVAL CO
RUBA
CHACO SLOPE
MC KINLEY CO
R10W
R7W
R5W
R11W
R9W
R2W
R1W
T 21 N
T 19 N
T 17 N
T 15 N
Major Structural Features and Structure Contour
Map on the Picture Cliffs Sandstone
Contour Interval: 400 ft
Datum: Sea Level
SAN JUAN BASIN
COLORADO AND NEW MEXICO
COLORADO
STUDY AREA
NEW MEXICO
0 10 20 Miles
N
1987

Figure 3.

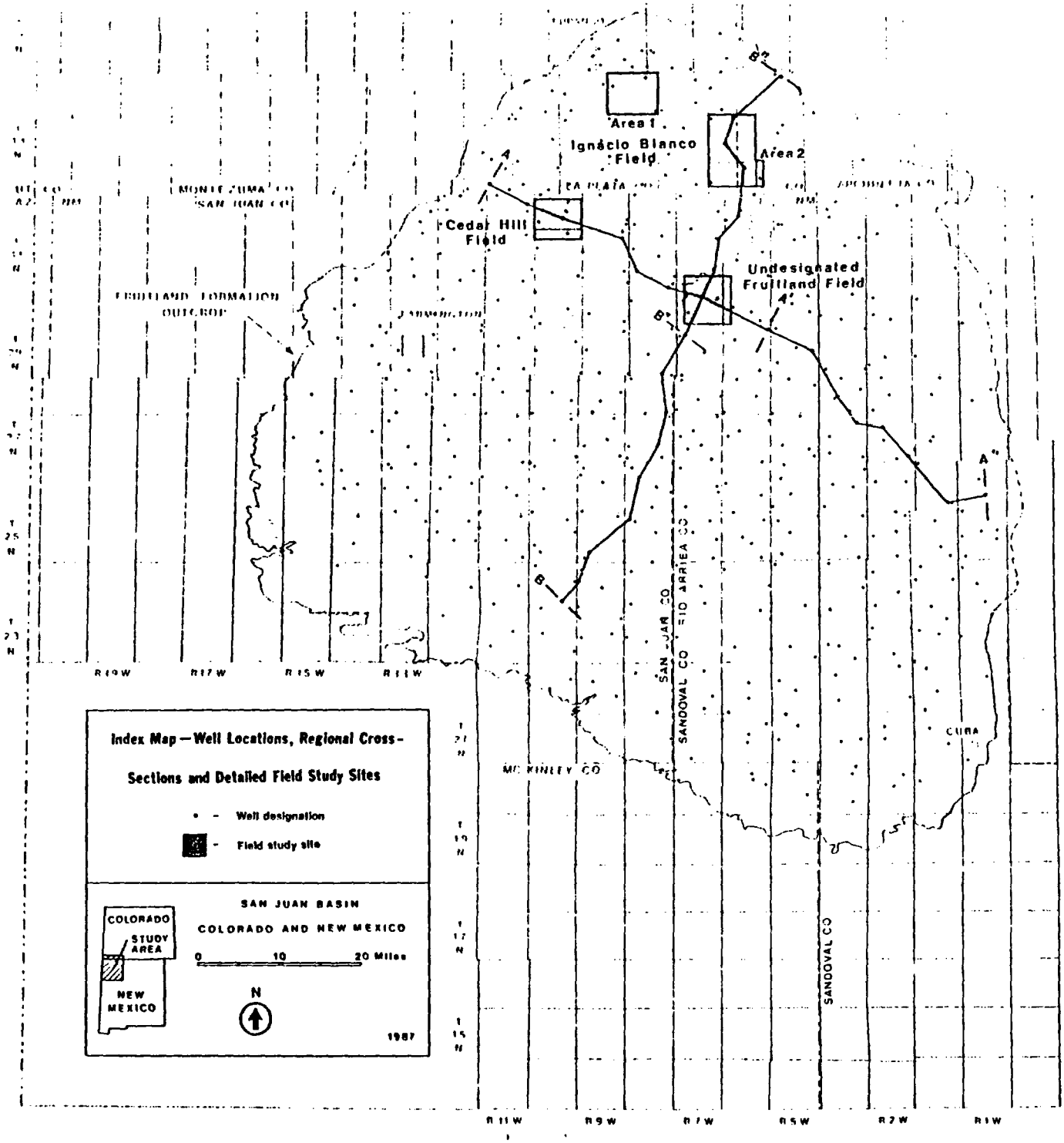
Area 1
Ignacio Blanco Field
Area 2
Cedar Hill Field
Undesignated Fruitland Field
FRUITLAND FORMATION OUTCROP
SAN JUAN CO
SANDOVAL CO
RIO ARRIBA CO
MCKINLEY CO
CUBA
R10W
R11W
R9W
R7W
R5W
R2W
R1W
Index Map—Well Locations, Regional Cross-Sections and Detailed Field Study Sites
Well designation
Field study site
COLORADO
STUDY AREA
NEW MEXICO
SAN JUAN BASIN
COLORADO AND NEW MEXICO
0 10 20 Miles
N
1987

Figure 4.

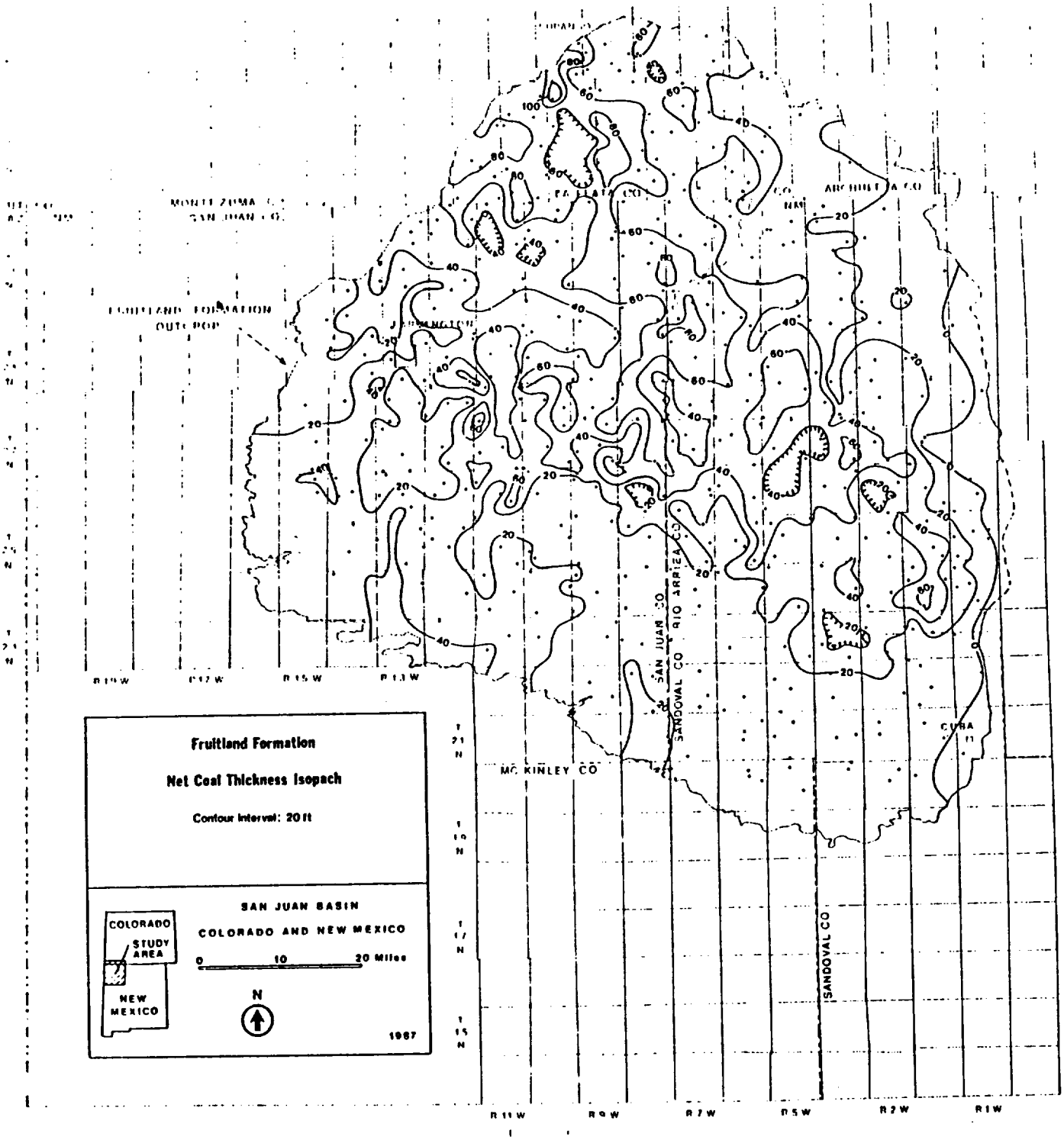
Fruitland Formation
Net Coal Thickness Isopach
Contour Interval: 20 ft
SAN JUAN BASIN
COLORADO AND NEW MEXICO
0 10 20 Miles
COLORADO
STUDY AREA
NEW MEXICO
N
1987
MONTEZUMA CO
SAN JUAN CO
ARCHULETA CO
RIO ARRIBA CO
SANDOVAL CO
MC KINLEY CO
CUBA
R17W
R15W
R13W
R11W
R9W
R7W
R5W
R2W
R1W

Figure 5.

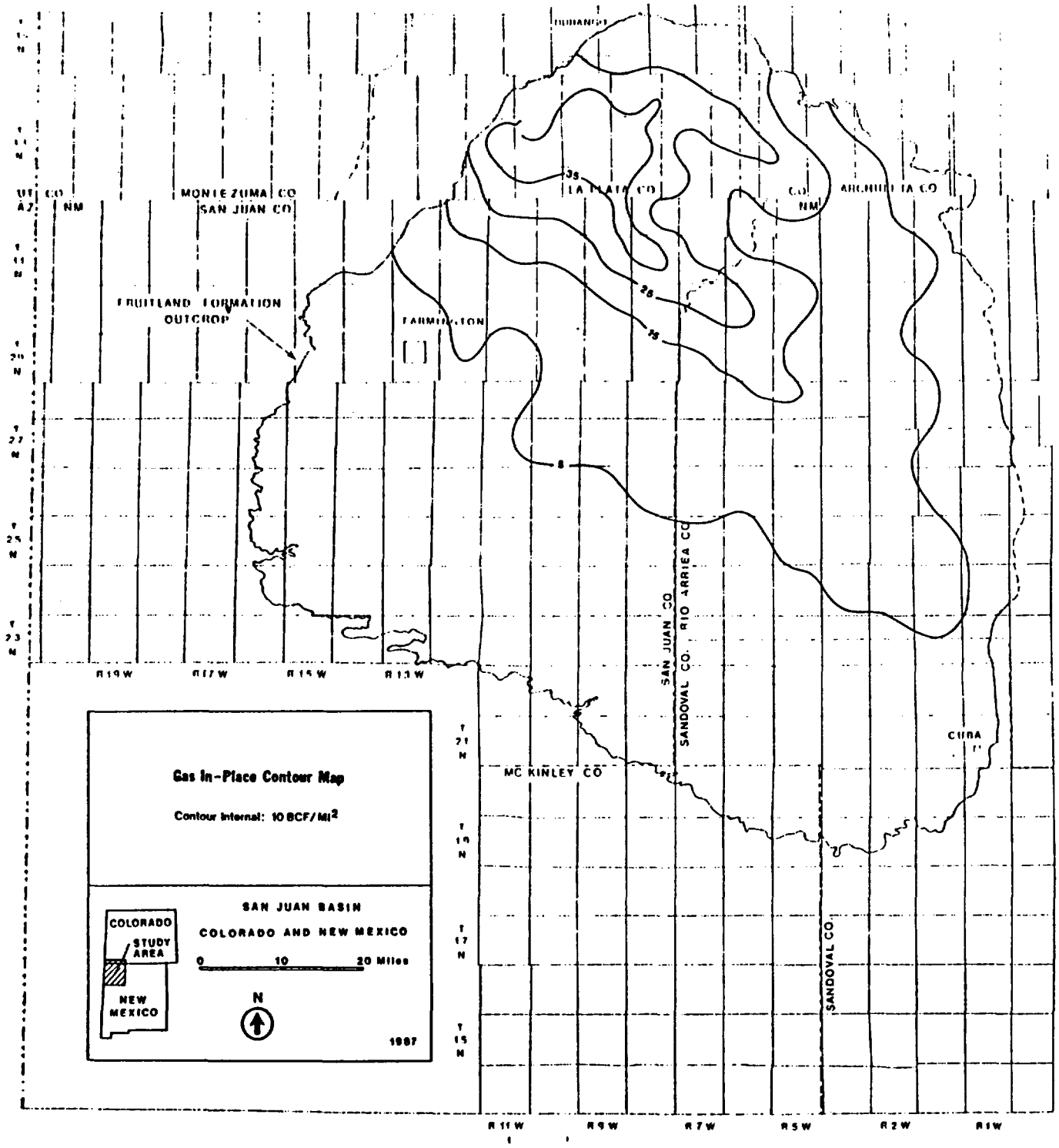
MONTEZUMA CO
SAN JUAN CO
LA PLATA CO
FRUITLAND FORMATION OUTCROP
FARMINGTON
28
25
8
SAN JUAN CO
SANDOVAL CO.
RIO ARRIBA CO
MC KINLEY CO
SANDOVAL CO.
CUBA
R19W
R17W
R15W
R13W
R11W
R9W
R7W
R5W
R2W
R1W
T 21 N
T 19 N
T 17 N
T 15 N
Gas In-Place Contour Map
Contour Internal: 10 BCF/Mi²
SAN JUAN BASIN
COLORADO AND NEW MEXICO
COLORADO
STUDY AREA
NEW MEXICO
0 10 20 Miles
N
1987

Figure 6.

GO INTERNATIONAL

COMPENSATED DENSITY LOG

FILING NO.

COMPANY AMOCO PRODUCTION COMPANY

WELL SCHNEIDER GAS COM B NO 1

FIELD BLANCO PICTURED CLIFF

COUNTY SAN JUAN STATE NEW MEXICO

Location: 1110'FSL & 1185'FWL

Sec. 28 Twp. 32N Rge. 10W

Other Services: IEL

Permanent Datum: Ground Level : Elev.: 6059

Log Measured From KB 11 Ft. Above Perm. Datum

Drilling Measured From KB

Elev.: K.B. 6070
D.F. 6069
G.L. 6059

Date	1-8-77		
Run No.	One		
Type Log	Gamma-Gamma		
Depth—Driller	3050		
Depth—Logger	3053		
Bottom logged interval	3052		
Top logged interval	2200		
Type fluid in hole	Fresh Gel		
Salinity, PPM Cl.	3600		
Density	10.6		
Level	Full		
Max rec. temp., deg F.	110		
Operating rig time	1 1/2 Hours		
Recorded by	Hamilton, Villa		
Witnessed by	Bloom		

RECEIVED
MAR 15 1977
OIL CON. COM.
DIST. 3

Run No.	Bore-Hole Record Bit	From	To	Casing Record Size	Wgt.	From	To
One	7 7/8	257	3050	8 5/8		Surface	257

Cedar Hills
1- 1538

3633

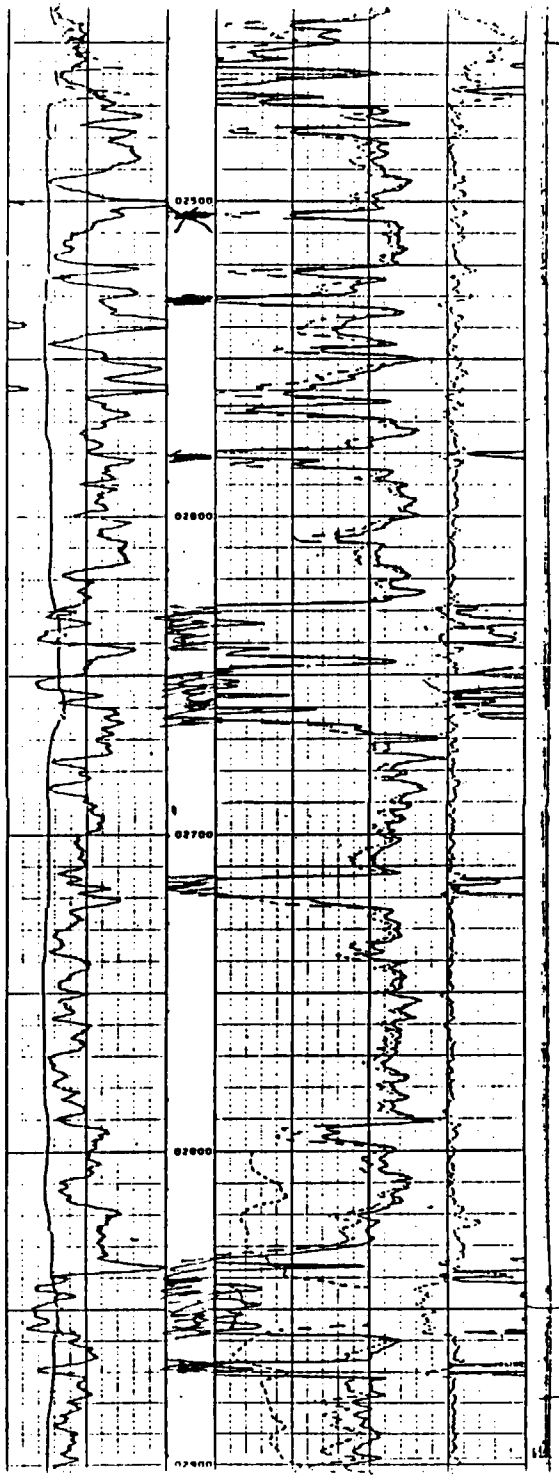

Kirtland

Fruitland

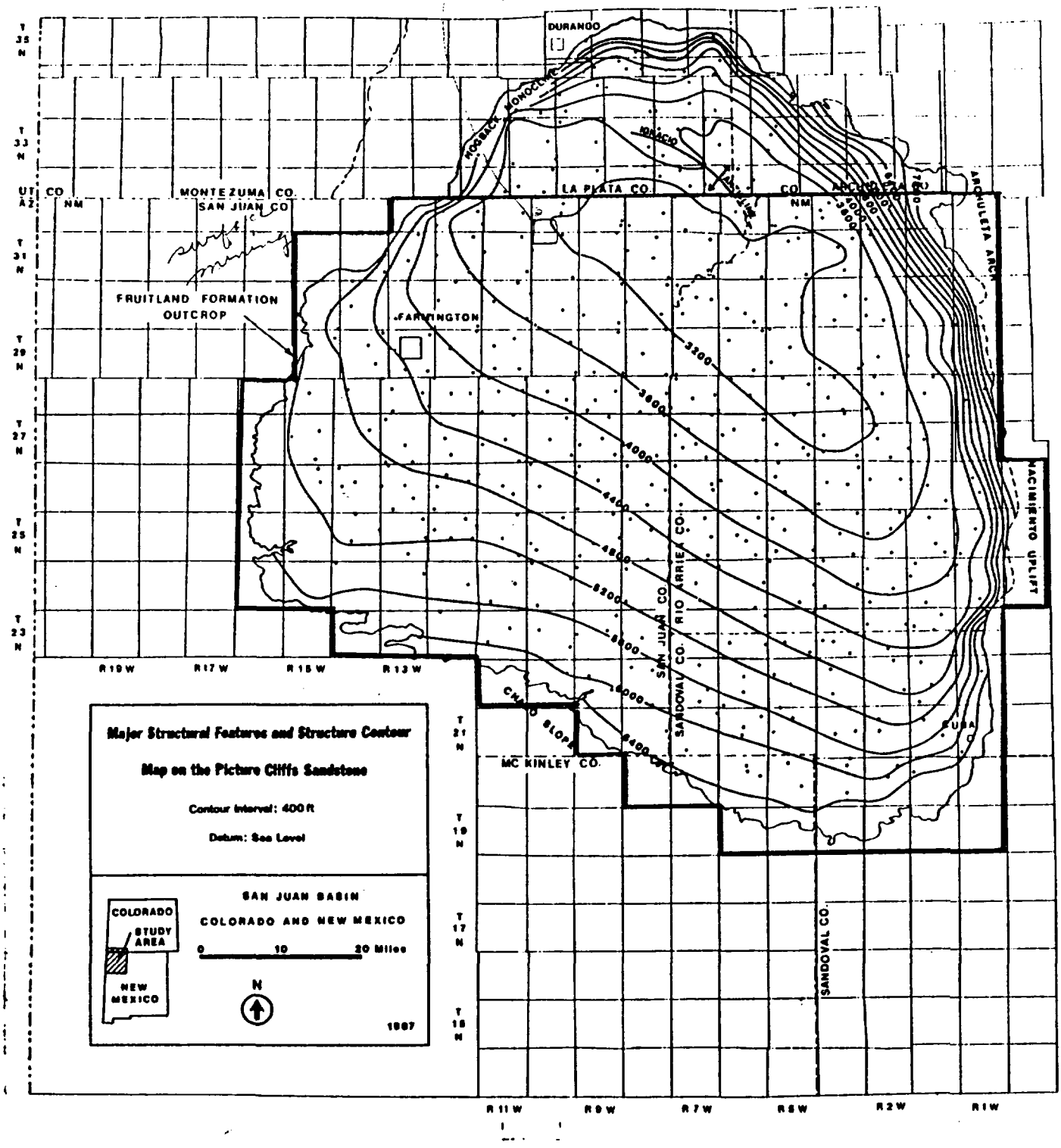
DURANGO
HOGBACK MONOCLINE
NACIMIENTO UPLIFT
ARCHULETA ARCH
MONTEZUMA CO.
SAN JUAN CO.
LA PLATA CO.
UT
CO
AZ
NM
FRUITLAND FORMATION OUTCROP
FARMINGTON
3200
3600
4000
4400
4800
5200
5600
6000
6400
SAN JUAN CO.
RIO ARRIBA CO.
SANDOVAL CO.
CHACO SLOPE
MC KINLEY CO.
SUBA
T 35 N
T 33 N
T 31 N
T 29 N
T 27 N
T 25 N
T 23 N
T 21 N
T 19 N
T 17 N
T 15 N
R 19 W
R 17 W
R 15 W
R 13 W
R 11 W
R 9 W
R 7 W
R 5 W
R 3 W
R 1 W
Major Structural Features and Structure Contour
Map on the Picture Cliffs Sandstone
Contour Interval: 400 ft
Datum: Sea Level
COLORADO
STUDY AREA
NEW MEXICO
SAN JUAN BASIN
COLORADO AND NEW MEXICO
0 10 20 Miles
N
1987

Proceedings of the 1987 Coalbed Methane Symposium, Tuscaloosa, Alabama, Nov. 16-19, 1987

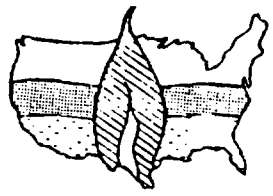

THE 1987 COALBED METHANE SYMPOSIUM

8731 GRI Geologic and Economic Appraisal of Coalbed Methane in the San Juan Basin

B.S. Kelso (Colorado Geological Survey); A.D. Decker (Resource Enterprises, Inc.); D.E. Wicks (Lewin & Associates, Inc.); D.M. Horner (Gas Research Institute)

ABSTRACT

A regional geologic assessment of the Fruitland Formation coals in the San Juan Basin indicates that this formation has a high potential for natural gas production from coal seams. This study, sponsored by the Gas Research Institute, includes subsurface structure, depth, thickness, and geometry interpretations. Coal ranks were assessed using vitrinite reflectance data and gas contents were compiled from public databases.

In addition to the regional geologic investigation, four sites were chosen for detailed field-level geologic and reservoir analyses. The geologic assessment employed cross-sections, net coal isopachs, and structure maps. Reservoir analyses included pressure, temperature, and permeability, in conjunction with coalbed methane well completion and production histories.

The regional geologic analysis concluded that the Fruitland Formation coals have an estimated in-place methane resource of 56 trillion cubic feet (TCF) - nearly double the previous estimate of 31 (TCF). Field-level investigations concluded that no single completion practice provided better production results than any other and overpressured reservoirs are significant contributing factors in the better producing wells.

An economic evaluation of the coalbed methane resource is due to be completed in early 1988.

INTRODUCTION

Activity of coalbed methane development is greater in the San Juan Basin than in other western coal basins. Production of the vast coalbed methane resource of the Fruitland Formation dates back to 1953, with the Phillips Petroleum Co., No. 6-17, San Juan 32-7 Unit well. More recent activity, specifically directed at resource development, started in the mid-1970's. To date, more than 200 wells have been documented as Fruitland Formation coalbed methane tests. Several pools or fields have been designated in the basin reporting Fruitland coal seams, or the "basal" Fruitland as the producing horizons.

The geologic analysis of the Fruitland Formation coalbed methane resource is part of a larger economic evaluation to determine recoverable coalbed methane in the San Juan and other U.S. coal basins. The San Juan Basin evaluation is divided into three phases: 1) a geologic appraisal of the Fruitland Formation coals, concluding with a gas-in-place resource estimate; 2) case history studies and history matching of Fruitland coalbed methane wells; and 3) an economic appraisal of the resource, using various technology cases. At this time, the regional geologic appraisal and four detailed field investigations have been completed. History matching of wells is underway and the economic evaluation has not been initiated. All three phases of the project will be completed by early 1988.

GEOLOGIC SETTING OF THE SAN JUAN BASIN

Regional Setting

The San Juan Basin is located in northwestern New Mexico and southwestern Colorado, with the study area of this project defined by the Pictured Cliffs Sandstone outcrop (Figure 1). It is approximately 90 miles wide, west to east, and 100 miles long, north to south and covers 7500 square miles.

Stratigraphy and Depositional Environments

The coals of the San Juan Basin are Cretaceous age and located in the Dakota, Mesaverde, and Fruitland formations (Figure 2). The Fruitland, the youngest of these, contains the largest coal resource. Deposition of the Fruitland coals occurred predominantly in lagoons, landward of the Pictured Cliffs barrier strandline. The thickest and most continuous seams are located in the lowermost 70 feet of the formation and are often associated with stratigraphic rises in the Pictured Cliffs. A detailed discussion of the Fruitland-Pictured Cliffs depositional environment is presented in Fassett, 1987 [1] and in the Fassett paper in this proceeding.

The Fruitland Formation is a coastal plain deposit of paludal carbonaceous shales, siltstones, sandstones and coals deposited behind the regressing Pictured Cliffs strandline. Formation thickness ranges from less than 100 to greater than 600 feet and contains evidence of fresh and brackish water environments. The sandstones are soft to hard and grey-white to brown in color. The shales are firm and grey to black in color. The coals were deposited in

lagoons, marshes, swamps and abandoned channels and are overlain by fluvial shales and sandstones. The coals are the most correlative units of the fluvial Fruitland sediments.

The underlying Pictured Cliffs is a regressive, coastal-barrier sandstone. Formation thickness varies from 125 to 400 feet due to minor transgressive episodes, which locally intertongue the Fruitland and Pictured Cliffs. The lower portion of the Pictured Cliffs is primarily interbedded sandstone and shales, with the upper unit a quartzitic, fine-to-medium grained sandstone.

Structure

The San Juan Basin's arcuate structural axis lies just south of the Colorado-New Mexico state line. The U-shaped Hogback Monocline forms the western and northern rims of the basin. To the east, the Nacimiento Uplift and Archuleta Arch bound the basin. The south and southwestern boundaries of the basin are not structurally defined and sediments gently dip northward from the Chaco Slope (Figure 3).

There are few major structural elements within the San Juan Basin and most are of Laramide age. The Ignacio Anticline, located in the north central portion of the basin, is the largest and best documented structure. Minor northwest trending en echelon folds and northeast-trending, high angle, low displacement faults are found on the eastern and southeastern edges of the basin. Radial folds, which plunge toward the basin's center, can be found around the perimeter. Minor structures resulting from Tertiary intrusive activity are located in the basin. Kelly, 1951 [2] and Woodward and Callender, 1977, [3] provide complete structural and tectonic descriptions of the San Juan Basin.

Detailed Field Investigation Settings

The four field investigation sites are located in the northern end of the basin where operator activity levels have been concentrated (Figure 4). The sites selected provide wells with production histories over extensive time periods and all four sites lack major structural features. Two sites are located in the Colorado Ignacio Blanco Field and one each in the New Mexico Cedar Hill and Undesignated Fruitland Fields. Site 1 of the Ignacio Blanco Field and the Undesignated Fruitland Field are in areas of a Pictured Cliffs stratigraphic rise, that is, an area of intertonguing with the Fruitland. The other two sites are stratigraphically less complex.

METHODOLOGY

The geologic evaluation of coal bearing formations is a key element in an economic appraisal of any coalbed methane resource. The San Juan Basin provided an opportunity for detailed geologic field investigations as well as a regional scale study, because of the large number of exploration control points and Fruitland coalbed methane tests. The purpose of the regional geologic investigation was to determine a gas-in-place resource estimate for the Fruitland Formation coals. The detailed geologic field studies were performed to analyze the geology and reservoir properties associated with producing coalbed methane wells, and for use in the regional economic evaluation of the basin.

The regional geologic evaluation consisted of the construction of two geologic cross-sections and the interpretation of several thousand geophysical logs for subsurface geologic data. The cross-sections provided insight into the lateral and vertical distribution of the Fruitland coals. The subsurface geophysical log data were used to construct structure, overburden, and net coal thickness maps associated with the Fruitland Formation and underlying Pictured Cliffs Sandstone.

The geology and coal resources of the Fruitland Formation have previously been documented [4] and other coalbed methane resource estimates have been based upon this work [5,6]. In order to independently evaluate the Fruitland coalbed methane resource, an original investigation of Fruitland coal resources was conducted.

After the resource and distribution of Fruitland coals was determined, an emperical formula was derived using measured gas contents, depth, and coal rank. The formula allowed projection of gas contents into areas lacking measured data. Gas-in- place estimates were then calculated on a township and range basis using the following equation.

$$GIP = GC * h * A * p \quad \ldots\ldots\ldots\ldots\ldots\ldots \quad (1)$$

Where: GIP = Gas in-place (trillion cubic feet)
GC = Gas content (cubic feet/ton)
h = Net coal thickness (feet)
A = Drillable area (acres)
p = Coal density (tons/acre-foot)

The gas-in-place values for 210 townships with sufficient coal thickness and depth of cover were summed to derive the Fruitland Formation gas-in-place resource estimate.

Four detailed field investigation sites in three producing fields were chosen in areas with sufficient coalbed methane well populations for analysis. Detailed geologic cross-sections and subsurface structure and net coal thickness maps were prepared for each area. In addition to the geologic data, reservoir data including pressure, temperature, permeability (very little data), and cleat spacing were collected. Drilling, completion and production history data for each coalbed methane well in the four areas were also compiled. An analysis of the geologic, reservoir and completion data is being performed in an attempt to establish trends between the reservoir data and production histories.

REGIONAL GEOLOGIC ANALYSIS

The primary products of the regional geological analysis are two cross-sections, a net coal isopach map, an overburden map of the Fruitland-Pictured Cliffs contact, and a thermal maturity rank map. All of the products were used to evaluate the geology and properties of the coals necessary to determine a gas-in-place estimate.

Stratigraphic Cross-Sections

Two regional, basin-wide, geologic cross-sections were constructed with density-porosity or gamma-density geophysical logs. (Figure 4). Both were segmented due to the length of the sections and the number of logs used. Section A-A", trending northwest to southeast, is parallel to the depositional strike of the Pictured Cliffs strandline. Section B-B" is constructed perpendicular to depositional strike, or southwest to northeast. Orientation of the cross-sections was designed to support the concept that coals parallel to depositional strike can be followed for greater distances than those perpendicular to strike. Interpretations of the cross-sections were used to understand the lateral continuity of the Fruitland coals and to determine if the Fruitland Formation could be divided into zones, based on vertical coal distribution.

In cross-section A-A", the Fruitland Formation thins from the northwest to the southeast. Maximum thickness is greater than 450 feet. Thinning of the Fruitland in the southeast to less than 100 feet is the result of erosion and a stratigraphic rise of the Pictured Cliffs [4], as seen on the cross-section. Coals are found at depths ranging from 2400 to 4200 feet, with the deeper coals along the southeast extension of A-A". Maximum net coal thickness and thicker individual seams are located on the northwest extension of this cross-section with net coal thickness ranging from 4 to 95 feet, and frequent 20 foot individual seams. The spacing between control points averages 5 miles and correlation of individual beds was not possible at this scale. No grouping or zone determination was established due to the lack of traceable markers.

The cross-section B-B" trends southwest to northeast and shows minor thickness variations in the Fruitland ranging from 200 to 350 feet. A stratigraphic rise is present to the northeast, approximately 10 miles south of the Colorado-New Mexico state line. Coals on the southeast end of the cross-section are located at 1100 foot depths and gradually deepen towards the basin's center, with the deepest coals found at 4000 feet. Net coal thickness ranges from 19 to 67 feet with a single seam of 40 feet found near the northeast limit of the cross-section. Most wells used in this cross-section have a well developed coal in close proximity to the Pictured Cliffs. These basal coals range from 8 to 40 feet in thickness and are sometimes correlative over many miles. The average spacing between wells on section B-B" is 5 miles and no correlation of individual beds was attempted. As with A-A", no division of the Fruitland Formation into coal groups or zones was made.

Net Coal Thickness and Overburden

A Fruitland Formation net coal isopach map was constructed using data from gamma-density, density-porosity, and a limited number of gamma ray-neutron geophysical logs (Figure 5). Net coal values do not include coals thinner than 2 feet with efforts made to exclude partings and shaley units within individual coals. Net coal thickness values ranged from 0 to greater than 100 feet. An eastern area of the basin exhibits 0 net coal values which are the results of non-desposition and erosion of the Fruitland. The maximum net coal values are found in the northwest part of the basin with net thickness exceeding 100 feet. An approximate 10 mile wide, northwest trend is observed in the north central portion of the basin. This trend is parallel to the structural axis of the basin with average net coal thicknesses of 70 to 80 feet. It can be generally stated that the southern end of the basin has less than 30 feet of net coal, with the exception of a small area in the southwest. Net coal values and the geologic cross-sections were used to determine the lateral and vertical distribution of coals in the Fruitland.

The overburden map or depth parameter of the Fruitland coals in the regional geologic analysis was utilized as part of the gas content and containment evaluation. Depths of coals range from 0 feet at the basin's outcrop to more than 4200 feet along the basin's structural axis. Depths change rapidly along the north, northeastern, and northwestern margins of the basin due to the structural monoclines. In the southern part of the basin, coal depths gradually increase as the structural slope increases to the northeast. The deepest coals are found in the northeastern quarter of the basin.

Coal Rank

Fassett and Hinds, 1971 [4] reported the coals of the Fruitland Formation as subbituminous. Support for their conclusion comes from an observation of the weathering nature of the coals when mined and stockpiled. Viewing the coals as a reservoir for natural gas requires a different approach to rank assessment. The approach used in this study was based on the thermal maturity of the coals, which is measured by the vitrinite reflectance. This approach is applicable to all coal basins. Rank generally increases from south to north, with the highest ranks found in the north central portion of the basin. A vitrinite reflectance rank map of the San Juan Basin (Rice, 1983) [7] was modified with additional data and used to establish the various Fruitland coal ranks, ranging from high volatile C bituminous to low volatile bituminous with 0.46 to 1.51 reflectance values.

GAS CONTENTS OF FRUITLAND COALS

A moderately small public domain database of measured gas contents exists for the Fruitland Formation coals. The primary source of the data was the U.S. Bureau of Mines (USBM) gas content measurement database for samples from around the United States. A description of the desorption process and a partial list of samples is found in Diamond and Levine, 1981 [8]. Additional desorption data were acquired from the Colorado Geological Survey.

Twenty-eight data points were standardized for ash content, temperature, and pressure. The data was sorted by coal rank and sample depth to develop correlations relating gas content to depth and rank. Curves were established for high volatile A bituminous and high volatile B and C bituminous coals combined. Insufficient data was available for medium and low volatile coals and

analog curves were founded on the results of similar analyses in a Piceance Basin study [9]. The mathematical relationship that resulted from the analysis is:

$$GC = m * (\ln d) + b \quad \ldots\ldots\ldots\ldots\ldots\ldots 2$$

Where: GC = Gas content (cubic feet/ton)
m = Scaling coefficient
ln d = Natural log of depth (feet)
b = y intercept

GAS IN-PLACE OF THE FRUITLAND COALS

The regional geologic evaluation of the Fruitland Formation coals, San Juan Basin, concluded with a gas-in-place resource estimate. The unit of analysis is a township and range and a gas-in-place value was calculated for each of the 210 units in the study area. Elements of the gas-in-place calculation are gas content, net coal thickness, drillable area, and coal density.

Each of the 210 units was assigned an estimated gas content value using the mathematical relationship discussed previously. Depths used in the calculation were average maximum overburden on the Pictured Cliffs Sandstone. Analysis of the vertical distribution of Fruitland coals showed more than 85 percent of the net coal thickness is within 200 feet of the Pictured Cliffs. Insignificant differences result in gas content values when depth values are varied within this 200 foot range.

Net coal thickness and coal density are factors in the coal resource portion of the gas-in-place calculation. An average net coal thickness was determined for each unit from the coal isopach map constructed in the geologic evaluation. The coal rank map was used to assign coal density to the unit. Densities increase with rank as documented by Averitt, 1975 [10]. The following table shows the variation of coal density with rank used in this study.

Rank	Density (Tons/acre-foot)
High Volatile Bituminous (A, B, and C)	1800
Medium Volatile Bituminous	1850
Low Volatile Bituminous	1900

The drillable area of a unit is determined by totaling the number of acres in the unit and subtracting undevelopable acreage. Undevelopable acreage includes areas with urban development; abandoned, active or permitted coal mining operations; acreage already containing coalbed methane wells; and areas of insufficient coal overburden (gas containment) or coal thickness.

Gas-In-Place Estimate

The total gas-in-place resource estimate for the Fruitland Formation coals is 56 trillion cubic feet (TCF). This is only a resource estimate, not a reserve estimate and no recovery factor has been applied. It must be pointed out that up to this point, we have only been discussing gas in the micro-pore system of the coals and not dealt with "free" gas or gas in the cleat system of the coals. Calculation of the gas in the cleat system will be based on the results from history matching work and is expected to increase the current gas-in-place estimate by 2 to 3 percent. Figure 6 is a gas-in-place contour map for the Fruitland Formation coals.

The 56 TCF gas-in-place estimate is nearly twice the estimate previously reported by Choate and others, 1984 [5]. A comparison of the two estimates revealed that coal resource values used for each were within 10 percent. The conclusion was drawn that gas content data in the two studies were drastically different. Analysis of the data set used by Choate showed the use of fewer core desorption data and a large percentage of chip desorption samples. This explains the increase in the gas-in-place estimate resulting from this study.

DETAILED FIELD INVESTIGATIONS

Four sites located in three coalbed methane production fields were selected for detailed geologic and reservoir analysis. The number of completed wells in each area and their production histories aided in site selection. Figure 4 shows the location of the four sites studied. They are the Cedar Hill Field, New Mexico; an Undesignated Fruitland Field, New Mexico; and two sub-areas of the Ignacio Blanco Field, Colorado. The primary purpose of the field site investigations was to validate the regional geologic study at a field level. In addition, the field investigations incorporated production data into the geologic analysis and established the stratigraphic intervals contributing to the Fruitland coalbed methane production.

Cedar Hill Field

The Cedar Hill Field is located in portions of Townships 31 and 32 North, Range 10 West. Development of the coalbed methane resource in this area was initiated more than ten years ago and presently, the field contains 12 coalbed methane wells. A structure map on the Pictured Cliffs Sandstone for the area shows a maximum of 100 feet structural relief with a series of subtle northeast-southwest trends. Most of the structures in these trends exhibit relief of 20 feet or less. Net coal thickness across the area ranges from 9 to 55 feet. A coal in the basal section of the Fruitland Formation has been the primary production target and thickness ranges from 5 to 27 feet. This seam thins and splits to the southeast. The coal rank in the area is high volatile A bituminous and gas contents average 358 to 521 cubic feet/ton from four samples.

The reservoir parameters assessed in this evaluation are pressure, temperature, saturation, permeability and a gas-in-place estimate. Three bottom hole pressures were available from public records. They range from 1362 psi to 1590 psi or 0.49 to 0.56 psi/foot and indicate an overpressured coal reservoir. Reservoir temperatures of the basal coal ranged from 95 to 114 degrees Fahrenheit. Reservoir saturation status for this area is unknown and based on production histories of the earliest wells, 100 percent water saturation was assumed. Wells drilled at later dates were probably less than 100 percent water saturated and were partially dewatered by the

initial wells. No permeability data was available for any of the coal seams in the field. A gas-in-place estimate of 5 to 35 billion cubic feet/section (BCF/sec.) was calculated for the Cedar Hill Field.

Analysis of the completion histories of eight Amoco Production Company wells in the field showed that five were completed open-hole and three were completed through pipe with stimulation. Both completion techniques have proven successful and a conclusion can not be drawn on the best method of completion. Five of the eight wells are completed in a single seam and the remaining three are multiple seam completions. One conclusion drawn from this geologic and reservoir study is that the Cedar Hill Field area is overpressured.

Undesignated Fruitland Field

The Undesignated Fruitland Field is located in Township 30 North, Range 7 West. The field contains four coalbed methane wells with production histories dating from early 1986. This field, much like the Cedar Hill Field, shows very little structural relief on the Pictured Cliffs Sandstone. Structural relief does not exceed 80 feet across the area and a northwest-southeast structural trend is present. Structural closures of small magnitude exist along the trend. Net coal thickness ranges from 36 to 75 feet and approximately 95 percent of the coal occurs within 100 feet of the Pictured Cliffs. The thickest single seam in the area is 30 feet and the coal is ranked high volatile A bituminous. There are no measured gas contents in the study area. Therefore, data from the Cedar Hill Field, based on similar coal rank and depths, were used for this parameter.

Reservoir pressure data in the area range from 1332 to 1521 psi which converts to gradients of 0.45 to 0.50 psi/foot. Based on this data, the area is overpressured. Reservoir temperatures range from 93 to 112 degrees Fahrenheit in the lower Fruitland interval. This field appears to contain both gas and water saturated coal seams. One well in the area exhibits a predominantly gas-saturated coal seam, as shown by recent decreases in gas production and unchanged water production rates. There is no permeability data available for the coal reservoirs in the study area. The gas-in-place resource estimate for the Undesignated Fruitland Field, assuming similar gas content data for the Cedar Hill Field, ranges from 16 to 38 BCF/sec.

The four coalbed methane wells in the field were drilled by Meridian Oil Company. Two are completed open-hole with production liners and two are completed through casing. Three of the four wells have been stimulated. All of the wells have multiple coal seam completions and net coal thickness ranges from 43 to 63 feet per well. One of the open-hole completion wells has had tremendous gas production rates, at times exceeding 4 million cubic feet per day (MMCF/d). The worst well in the field only averages 150 thousand cubic feet per day (MCF/d). The remaining two wells have production rates ranging between 1 and 2 MMCF/day.

Ignacio Blanco Field

The Ignacio Blanco Field encompasses most of the Colorado portion of the basin. Two areas within the field were selected for detailed site investigations. It should be noted that the majority of the coalbed methane wells in the two areas were initially drilled and completed by William Perlman between 1982 and 1984. Amoco Production Company recently took over the Perlman acreage and recompleted a number of the wells in 1986 and 1987. Preliminary production statistics from recompleted wells indicate improvement over past production.

Area 1 - Township 34 North, Range 8 West. Area 1 contains 18 Fruitland coalbed methane wells with erratic production histories dating back to 1982. There is 1100 feet of structural relief across the area with structural lows and possible closures located in the southern half. A stratigraphic rise of the Pictured Cliffs Sandstone and intertonguing with the Fruitland Formation is located in the north and west portions of the study area. Net coal thickness throughout the area ranges from 26 to 76 feet with the thickest individual seam being 35 feet. The coal is ranked medium and low volatile bituminous and gas contents from five samples average 315 cubic feet/ton.

This area contains the two Southern Ute Indian, Oxford wells in section 25, which were part of a Department of Energy (DOE) coalbed methane research project. The coring of these wells revealed 1/4 to 1/2 inch cleat spacing. The Oxford #2 well was used in 1985 by In-situ, Inc., a GRI contractor, for reservoir data analysis. In-situ, Inc. determined a static reservoir pressure of 1490 psi or a gradient of 0.52 psi/ft and a calculated permeability of 5 md [11]. Reservoir temperature data across the area, for the lower Fruitland Formation ranges from 100 to 128 degrees Fahrenheit. The pressure data from In-situ's research and from additional Fruitland Formation drill-stem test data indicate that the southern region of the study area is overpressured. All of the coalbed methane wells produced significant volumes of water in the field. A gas-in-place estimate of 18 to 52 BCF/section is estimated for this area.

Completion methods of the 18 wells in the area included cased and open-hole, with stimulated and unstimulated examples of each. No one method has proven more successful than another and erratic production histories from the wells make it difficult to draw a completion/production history conclusion. As noted before, Amoco has recompleted 6 of the 18 wells in the area with small to moderate size sand/water stimulations. Production data from the recompleted wells is not yet available, but will be valuable for additional analysis.

Area 2 - Township 32 and 33 North, Range 6 West. Area 2 of the Ignacio Blanco Field contains 28 coalbed methane wells. A maximum of 350 feet of structural relief is found in the area and a structural nose is located in the northwest portion of the area. A north-south trend of structural depressions is located along the western edge of the area. Net coal thickness

ranges from 20 to 68 feet, with the thickest individual coal seam being 42 feet. Coal rank is medium volatile bituminous and the area has an average measured gas content of 380 cubic feet/ton.

A research project was conducted at the Tiffany Gas, Glover #1 well in section 2, T32N, R6W, by Terra Tek, Inc., under GRI contract. The purpose of the project was to identify the resource potential and characteristics at a site, and provide the operator with a completion technique that would lead to economical production of Fruitland coalbed methane. Extensive work on reservoir characteristics was conducted and reported by Jones, 1985 [12]. A static reservoir pressure of 1483 psi or gradient of 0.48 psi/foot was measured at the site by In-Situ, Inc. This indicates an overpressured reservoir, at least in the southeastern corner of the study area. A measured permeability value of 3.5 md was obtained from coal samples and 1/4 inch cleat spacing was measured on recovered coal cores. As in Area 1 of the Ignacio Blanco Field, most of the wells in Area 2 produce significant volumes of water. Gas-in-place estimates for this area range from 14 to 45 BCF/section.

Completions of the 28 wells in this area are similar to those discussed in Area 1 of the Ignacio Blanco Field. Amoco has attempted recompletion on a number of the Perlman wells, but production data is not yet available. A variety of completion and stimulation methods have been applied to wells in this area and no single method provides better results than another.

CONCLUSION

The following conclusions have been drawn from the regional geologic analysis and detailed field site investigations of this coalbed methane resource study:

- This extensive subsurface geologic analysis provides a foundation for additional research and development of the Fruitland Formation coalbed methane resource.
- Additional measured gas content data is needed for assessment of the resource.
- It is estimated that the Fruitland Formation coals contain 56 trillion cubic feet of natural gas.
- Lower Fruitland coals at the four field investigation sites are overpressured.
- Permeability measurements at two locations in the Ignacio Blanco Field are low and measurements are not available for the Cedar Hill and the Undesignated Fruitland Fields. Structural enhancement of permeability may exist within all four fields. Fracture and lineament studies are needed for possible identification of enhanced areas.
- Numerous well completion and stimulation methods have been utilized with varying degrees of success.

ACKNOWLEDGEMENTS

The Gas Research Institute (GRI) has sponsored a geologic and economic analysis of the Fruitland Formation coalbed methane resource under its Natural Gas Supply Program. This effort is part of a much larger economic evaluation of recoverable coalbed methane in the San Juan Basin and other U.S. coal basins. The scope of the program is in support of GRI's goal of adding low cost gas to the United States gas supply reserves through research and development. The authors of this paper wish to thank the Gas Research Institute for their support of this project and for their permission to publish the findings.

References

1. Fassett, J., "The non-transferability of a Cretaceous coal model in the San Juan Basin of New Mexico and Colorado", in Paleoenvironmental and Tectonic Control of Coal-Forming Basins of the United States, Geological Society of America Special Paper 210, (1986), p. 155-171.

2. Kelly, V.C., "Tectonics of the San Juan Basin", in Guidebook of the south and west sides of the San Juan Basin, New Mexico and Arizona, New Mexico Geological Society, 2nd Field Conference, (1951), p. 124-131.

3. Woodward, L. and Callender J., "Tectonic framework of the San Juan Basin", in Guidebook to the San Juan Basin III, New Mexico Geological Society, 28th Field Conference, (1977), p. 209-212.

4. Fassett, J.E. and Hinds, J.S., "Geology and fuel resources of the Fruitland Formation and Kirtland Shale, of the San Juan Basin, New Mexico and Colorado", U.S. Geological Survey Professional Paper 676, (1971), 76 p.

5. Choate, R., Lent, J., and Rightmire, C.T., "Upper Cretaceous geology, coal, and the potential for methane recovery from coalbeds in the San Juan Basin-Colorado and New Mexico", in Coalbed Methane Resources of the United States, Am. Assoc. of Petroleum Geologist Studies in Geology Series #17, (1984), p. 185-222.

6. Kelso, B., Goolsby, S., and Tremain, C., "Deep coalbed methane potential of the San Juan River Region, southwestern Colorado", Colorado Geological Survey Open-File Report 80-2, (1980), 56 p.

7. Rice, D., "Relation of natural gas composition to thermal maturity and source rock type in San Juan Basin, northwestern New Mexico and southwestern Colorado", Am. Assoc. Petroleum Geologists Bull., v. 67 no. 8, (August 1983), p. 1199-1218.

8. Diamond, W.P. and Levine, J.R., "Direct method determination of the gas content of coal: Procedures and results", U.S. Bureau of Mines, Report of Investigation No. 8515, (1981), 36 p.

9. McFall, K., Wicks, D., Kelso, B., Sedwick, K., and Brandenburg, C., "An analysis of the coal and coalbed methane resources of the Piceance Basin, Colorado", SPE/DOE Paper 16418, in Proceedings of the 1987 SPE/DOE Low Permeability Symposium, Denver, May 18-19, p. 283-295.

10. Averitt, P., "Coal resources of the United States, January 1, 1974", U.S. Geological Survey, Bulletin 1412, (1975), 131 p.

11. Koenig, Robert, In-situ, Inc., (1987) personal communication.

12. Jones, A.H., "Methane production characteristics of deeply buried coalbed reservoirs", Gas Research Institute Topical Report No. 85/0033, (March 1985), 176 p.

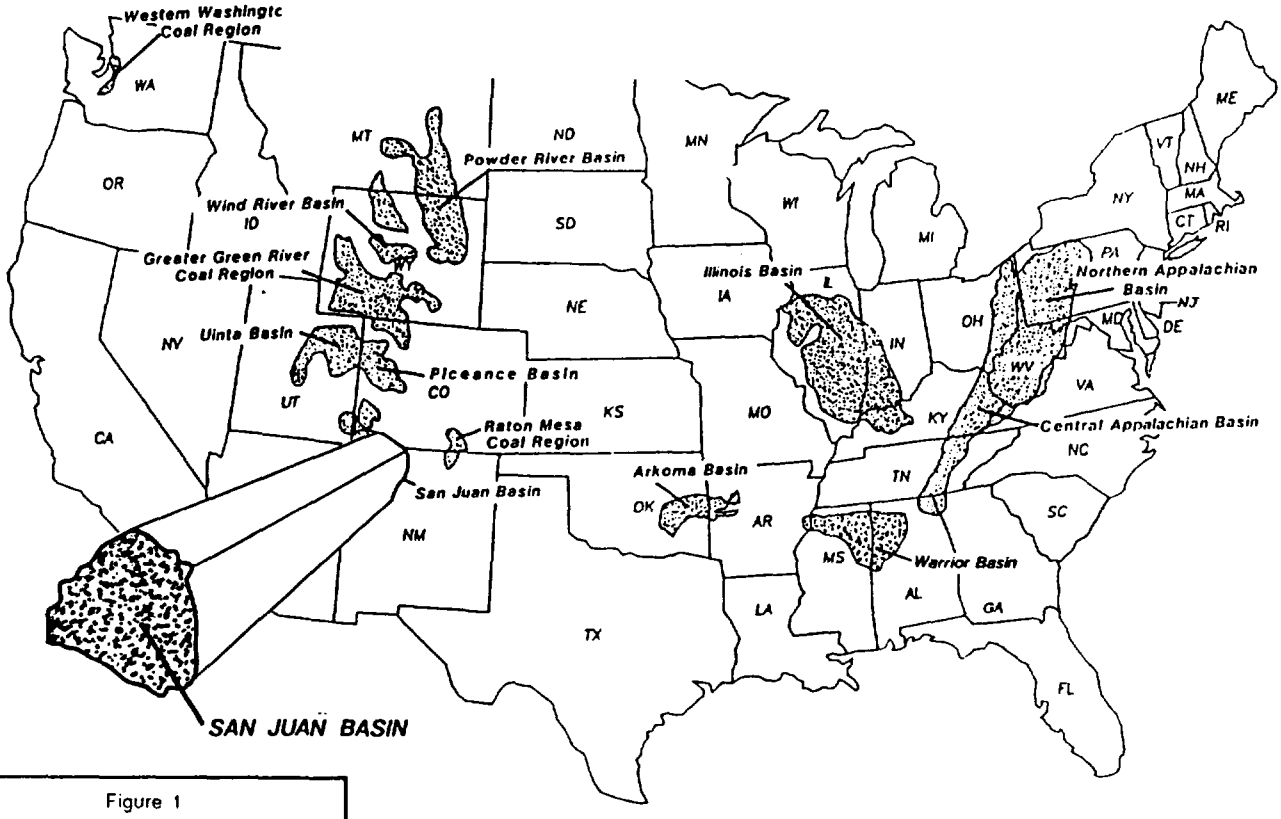

Figure 1

MAJOR COAL BASINS OF THE UNITED STATES

0 100 300
Miles

N

After Rightmire, 1984

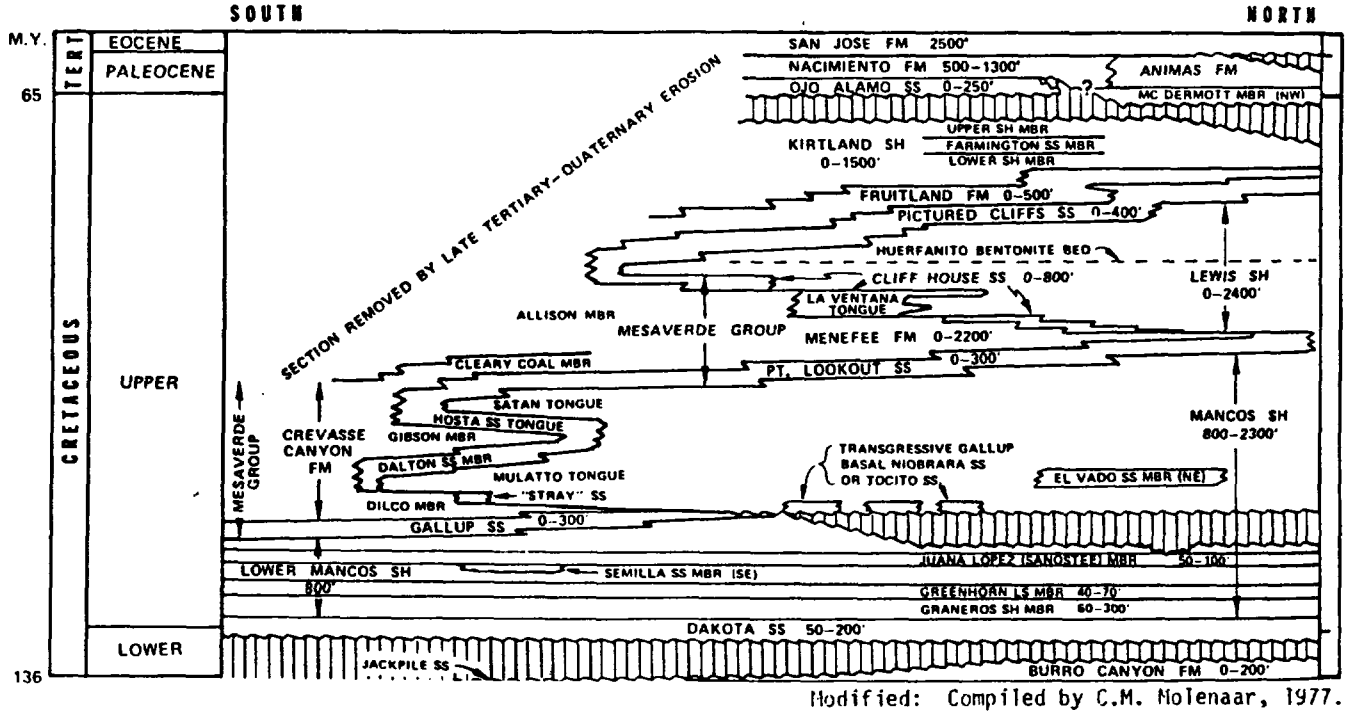

Modified: Compiled by C.M. Molenaar, 1977.

Figure 2. San Juan Basin time - stratigraphic nomenclature chart.

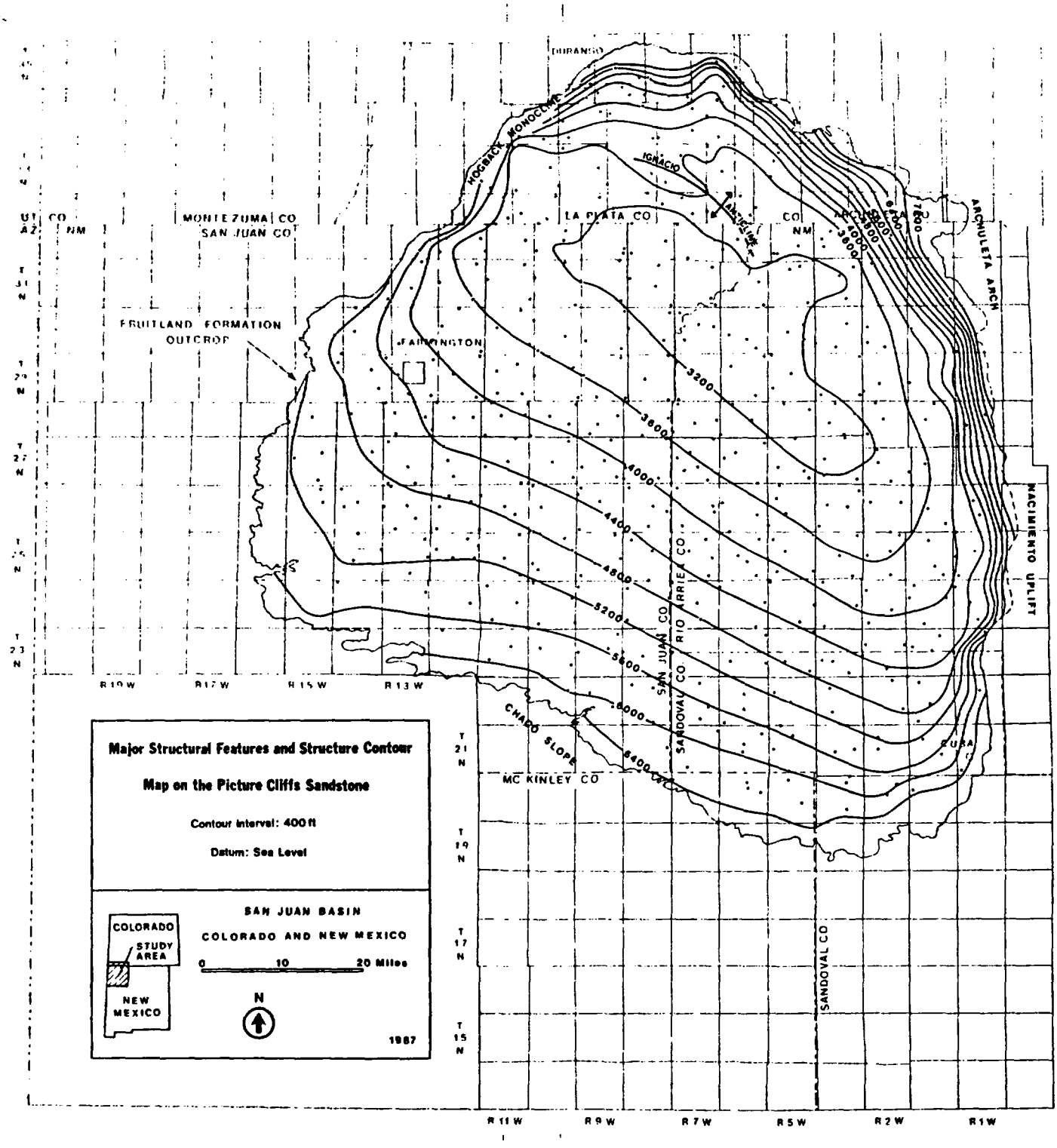
DURANGO
HOGBACK MONOCLINE
IGNACIO
MONTEZUMA CO
SAN JUAN CO
LA PLATA CO
FRUITLAND FORMATION OUTCROP
FARMINGTON
ARCHULETA ARCH
NACIMIENTO UPLIFT
3200
3600
4000
4400
4800
5200
5600
6000
6400
SAN JUAN CO
RIO ARRIBA CO
SANDOVAL CO
MC KINLEY CO
CUBA
R19W
R17W
R15W
R13W
R11W
R9W
R7W
R5W
R2W
R1W
T 21 N
T 19 N
T 17 N
T 15 N
Major Structural Features and Structure Contour
Map on the Picture Cliffs Sandstone
Contour interval: 400 ft
Datum: Sea Level
COLORADO
STUDY AREA
NEW MEXICO
SAN JUAN BASIN
COLORADO AND NEW MEXICO
0 10 20 Miles
N
1987

Figure 3.

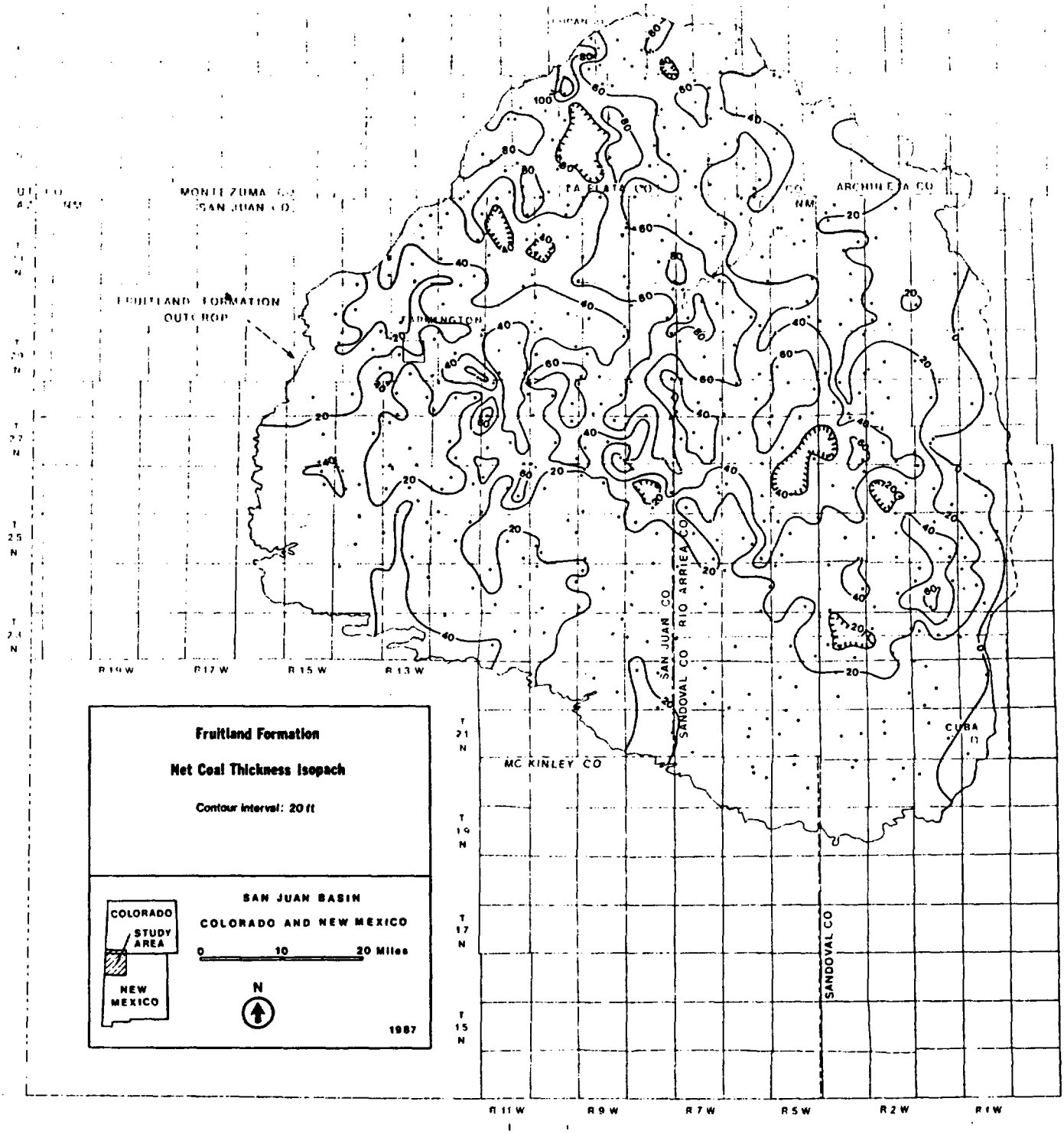
Fruitland Formation
Net Coal Thickness Isopach
Contour interval: 20 ft
SAN JUAN BASIN
COLORADO AND NEW MEXICO
COLORADO
STUDY AREA
NEW MEXICO
0 10 20 Miles
N
1987
FRUITLAND FORMATION OUTCROP
FARMINGTON
MONTEZUMA CO
SAN JUAN CO
RIO ARRIBA CO
SANDOVAL CO
MC KINLEY CO
CUBA
R19W
R17W
R15W
R13W
R11W
R9W
R7W
R5W
R2W
R1W
T25N
T23N
T21N
T19N
T17N
T15N

Figure 5.

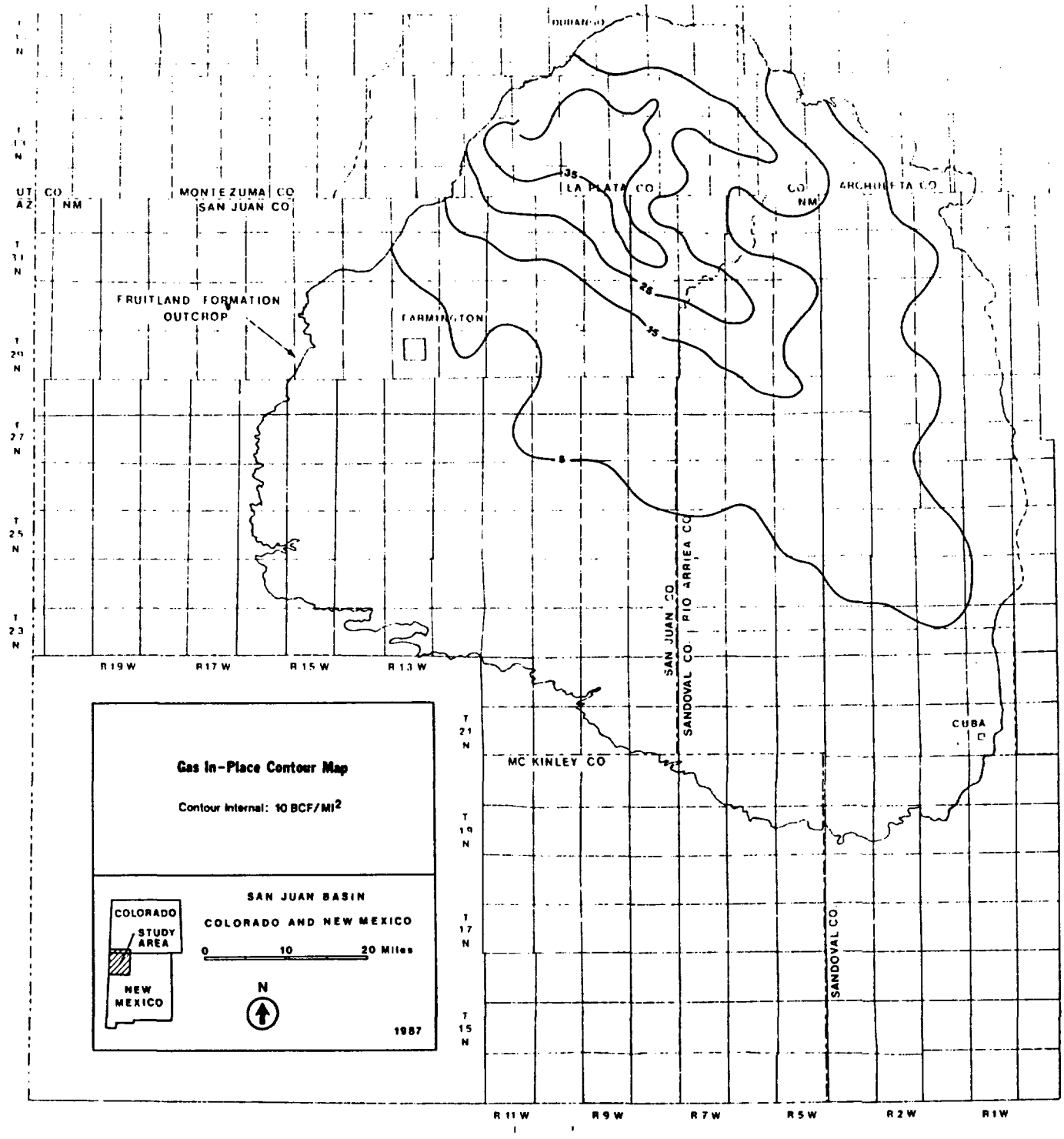
UT
AZ
CO
NM
MONTEZUMA CO
SAN JUAN CO
LA PLATA CO
ARCHULETA CO
FRUITLAND FORMATION
OUTCROP
FARMINGTON
35
25
15
5
T 31 N
T 29 N
T 27 N
T 25 N
T 23 N
T 21 N
T 19 N
T 17 N
T 15 N
R 19 W
R 17 W
R 15 W
R 13 W
R 11 W
R 9 W
R 7 W
R 5 W
R 2 W
R 1 W
SAN JUAN CO
SANDOVAL CO
RIO ARRIBA CO
MC KINLEY CO
SANDOVAL CO
CUBA
Gas In-Place Contour Map
Contour Interval: 10 BCF/MI2
COLORADO
STUDY AREA
NEW MEXICO
SAN JUAN BASIN
COLORADO AND NEW MEXICO
0
10
20 Miles
N
1987

Figure 6.

Proceedings of the 1987 Coalbed Methane Symposium, Tuscaloosa, Alabama, Nov. 16-19, 1987

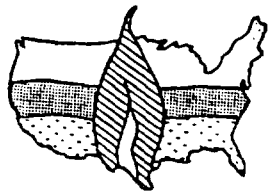

THE 1987 COALBED
METHANE SYMPOSIUM

8714 Origin and Production Implications of Abnormal Coal Reservoir Pressure

A.D. Decker (Resource Enterprises, Inc.); D.M. Horner (Gas Research Institute)

ABSTRACT

The ability to produce low cost, pipeline quality gas from deep coal reservoirs depends largely on thorough integration of exploration methods with appropriate drilling, completion and production strategies. In the extreme case, areas that are not economic with current completion technologies should be avoided with adherence to prudent exploration practices. Therefore, reliable predictive geologic methods to specify coal reservoir conditions need to precede drilling and completion decisions.

Dominant coal reservoir mechanisms include: permeability, saturation, reservoir pressure and gas-in-place. Production characteristics from low permeability coal reservoirs are most sensitive to the interaction between type of saturation and reservoir pressure. The geologic processes responsible for these reservoir conditions have been examined in the Piceance Basin. This basin, known for low permeability reservoirs, was selected for geologic evaluation due to the large coalbed methane resource and large data base. Also located in the basin is the Deep Coal Seam Project, a multi-year, multi-well, field laboratory joint venture by the Gas Research Institute and Resource Enterprises, Inc., providing fully integrated reservoir and geologic engineering data on deep coal reservoirs.

Reservoir diagnostics and modeling suggests that reservoir pressure and type of saturation demonstrate an interaction between catagenesis and permeability. Thick, thermally mature coal deposits actively generate more gas and water than can be adsorbed by the coal or be diffused through a low permeability system. In these regions over-pressuring occurs. Ultimately, pore pressure will exceed in-situ stresses resulting in tensional fractures through the coal bearing sequences. While the coal seams remain in the active gas generation phase, the fractures and pore spaces become gas saturated. Eventual temperature reduction through erosion will halt the gas generating phase, resulting in an under-pressured reservoir. Imbibition of water into these reservoirs is unlikely in areas of low permeability. In contrast, coal seams that have not reached an active gas generation phase may be overpressured and water saturated due to compaction and coal dewatering in a shale bounded situation. Overpressured water saturated coal reservoirs of the Cedar Hills and San Juan 30-6 Unit in the San Juan Basin have, to date, shown the highest production capacity for coalbed methane production.

In summary, geochemical evaluation techniques have been applied to characterize and predict coal reservoir mechanisms in the Piceance and San Juan Basin.

INTRODUCTION

A portion of the extensive gas accumulations found in the San Juan Basin[1], the Green River Basin[2], and the Alberta Basin[3] have been sourced largely by coal. Despite the amount of data collected on coal reservoir characteristics and coal as a source rock, little work has been done integrating the two sciences. A coupled understanding of coal reservoir mechanisms and coal maturation will assist the explorationist in his pursuit of coalbed gas resources. This work was sponsored by the Gas Research Institute under Contract No 5083-214-0844 with Resource Enterprises, Inc.

A geologic model is presented which incorporates coal's resistance to transfer heat with its ability to generate large volumes of gas over a specific temperature and time sequence. In basins where low permeability prohibits cross formational fluid flow, gas generation can exceed the quantity of gas that can migrate through the geologic system. This results in high pore pressure within the coal reservoirs. Conversely, where migration exceeds rate of gas generation, low pore pressure will be observed. These stages of reservoir disequilibrium have been observed in other deep coal basins of the western United States.

The focus of this paper is to describe and quantify these states of pore pressure disequilibrium within some coal reservoirs of the Piceance Basin and San Juan Basin. A sequential approach is undertaken to examine the coal system in each phase of basin evolution, as follows:

1. Determination of the volumes of water and gas produced from coal at specific maturity levels during the coalification process.

2. Relate the maturity levels to specific time periods using thermal maturation models.

3. Determination of the amount of gas that cannot be retained by the coal and, therefore, which must diffuse through the geologic section for specified time interval.

This paper is directed at providing the volumetric calculations of Step 1 and the methodology (using a case study) for Steps 2 and 3.

Included in this paper are geologic observations and interpretations of areas within the Piceance Basin where underpressured and overpressured (less than and greater than hydrostatic pressure, respectively) coal seams have been identified. Also included is a section suggesting a relationship between well deliverability, permeability and reservoir pressure in coal degasification wells in the San Juan Basin. A relationship between material balance, gas/water flow and abnormal coal pore pressure is presented.

THE EVOLUTION OF COAL

In response to burial depth, time and temperature, deposits of terrestrially derived plant tissue evolves physically and chemically into thermally mature coal. Compaction and temperature increases transform the organic material into three primary coal components or macerals. (Macerals are the microscopically recognizable constituents of coal.) The vitrinite maceral represents jellified cell walls or woody material, the exinite maceral is representative of plant resin (cuticles and spores) and the inertinite maceral represents carbonized woody material.

The degree of maturation or coal rank during the coalification process is most accurately measured from the vitrinite maceral. The percentage of vitrinite optical reflectivity (Ro) increases correspondingly with increases in coal rank. The temperature necessary to increase rank as indicated by Ro and derived by Gijzel[4] is shown on Table 1. Systematic chemical and biological degradation of organic material during the coalification process yield varying amounts of water and gas. Examination of such chemical products is important in understanding the water and gas accumulations within present-day coal reservoirs.

The two most significant stages of coal maturation, diagenesis and catagenesis, are defined largely by the products of biological and thermal evolution. Water, biogenic methane and carbon dioxide are the primary coal diagenetic products. Water originates from the depositional system and organic decomposition[5]. All biogenic gas and 98 percent of the coal's water generative capacity occurs during diagenesis at maturity levels of 0.23 to 0.76 Ro[6].

Continued exposure of coal to pressure and temperature allow coal to enter the stage of catagenesis. Juntgen and Klein[7] determined that thermal methane generation commences during catagenesis for coal with a vitrinite reflectance of 0.73 Ro. As shown in Figure 1, active gas generation accelerates at 0.90 Ro and continues through 1.30 Ro, accounting for 76 percent of thermal methane generation. Water produced during catagenesis is from the hydration of inorganic minerals and clays[8]. Water and thermal methane volumetrics as a function of increasing coal maturity is summarized in Figure 2.

Coal's ability to absorb gas decreases with higher temperature[9] and pressure[10], but increases with higher coal rank[11]. Eight to ten times more gas is generated than can be retained, thereby initiating gas migration from the coal into other strata. Therefore, the development of a time framework for the coal generative episodes becomes necessary to understand the possible influence that thermal generation rates have on coal reservoir properties. Deterministic relations between time, temperature and ensuing gas generation episodes are derived from thermal maturity modeling.

Thermal Maturity Modeling

The timing of coal digenetic and catagenetic history may be identified through use of a time-dependent, three-dimensional mathematical model to simulate gas generation dependence on variables such as sedimentary burial rate, paleotemperature, paleopressure, thermal conductivity and heat flow. The simulation initially requires the computation of three-dimensional pore pressure in sediments as a function of time. The system assumes that the inflow-outflow is equal to the net accumulation due to grain and fluid compressibility plus the net accumulation to change in sediment density, rate of sedimentation and change in water depth[12]. The next step of the simulation is evaluation of the simultaneous transfer of heat by conduction and convection[13]. In this step, thermal parameters of the evolving system are particulary sensitive to pressure and temperature. The third step in thermal modeling is relating temperature to specific geologic periods. Lopatin[14] determined for coalification reactions, the reaction rate doubles with each increase of 10°C. He further related time and temperature by specifying a geologic time period with 10°C intervals as follows:

$$TTI = T_1 G_1 + T_2 G_2 + T_n G_n$$

where: TTI = Time Temperature Index
T_1 = Temperature Correction Factor
G_1 = Geologic Heating Time

Next, a correlation between vitrinite reflectance is incorporated as a maturity indicator and the TTI is established. The relationship between vitrinite reflectance (Ro) and the time-temperature index is:

$$R_o\% = 1.301 \lg TTI - 0.5282...$$

The final output of the thermal model reveals the type of depositional basin, tectonic and structural histories, sediment accumulation (or erosion) through time, thermal history of the basin and its effect on coal maturation and compactional history. A comparison of measured vitrinite reflectance and bottomhole temperatures with that predicted by the model indicates the accuracy of modeled events.

ABNORMALLY PRESSURED COAL RESERVOIRS, PICEANCE BASIN

The preceding coal volumetrics and thermal modeling may be used to study the implications of abnormally pressured coal reservoirs within the Piceance Basin of northwestern Colorado. The Basin was selected due to the availability of reservoir and geologic data collected for the Cretaceous coal reservoirs as are dominate in the western U.S. and which contain significant coalbed accumulations.

To date, the thick coal seams of the laterally continuous Cameo Coal Group, (Williams Fork Formation, Mesaverde Group) have been the objective for coalbed gas exploration within the Piceance Basin. A significant coalbed methane resource also exists within the Coal Ridge Coal Group[15], stratigraphically 200 to 400 feet above the top of the Cameo Coal Group, laterally confined to the eastern margin of the basin.

The primary questions to address are: i) what is the origin and implications of abnormally pressured coal reservoirs?, and ii) why stratigraphically equivalent coal seams with similar coal ranks and burial depths have such diverse coal reservoir conditions.

The integration of drill stem test data, bottomhole pressure, buildup tests and drilling mud weights have resulted in identification of a regional northeastern overpressured trend approximately 25 miles in length and eight miles in width (Figure 3). The East Divide Creek Area (which has a reservoir pressure gradient in the Cameo coal seam of 0.59 psi/ft) is located on the southern-most extension of the regional trend. In contrast, the reservoir pressure gradient at the Red Mountain Area is .33 psi/ft. The overpressured region coincides with: i) maximum total coal development in the Basin (Figure 4), ii) thermally mature coals (Figure 5), and iii) northern plunging nose of the Divide Creek Anticline (Figure 3). These coal characteristics are interrelated and result in dynamic reservoir conditions.

The Divide Creek anticline has brought deeply buried, mature coal seams 4,000 - 5,000 feet closer to the surface than laterally equivalent coal seams. The abrupt post-laramide uplift appears to have contributed to the coal disequilibrium state along the axis of the anticline. The timing of coalbed gas and water generative events and material balance calculations may be determined using thermal maturation modeling.

Material Balance

An examination of regional maps (Figure 4 and 5) indicate that up to 100 feet of low-volatile bituminous coal exists in the overpressured region. Following lithification and compaction, 9.18×10^8 barrels of water and 4.27×10^{11} cubic feet of gas are calculated to have been displaced by the coal seams per square mile. To determine the coal's fluid retention capability, earth strain analysis was conducted at the East Divide Creek Site. The upper bound interpretation for coal porosity was calculated to be 6.0 percent[16]. Therefore, if all pore space in the coal was saturated with water, the coal could only contain $.41 \times 10^{-3}$ percent of generated water. If completely gas filled, at equivalent pressure and temperature, the coal could retain roughly 12 percent of the generated gas. Clearly the volumetric difference between the gas and water generated and that which may be stored in the coal system is large and suggests a reason for overpressuring in this region.

Determination of Sequential Thermal Events

The timing of coal generative events at the East Divide Creek Area and Red Mountain Unit was determined by Waples using computer-aided thermal modeling[18]. In order to best match present-day calculated subsurface temperatures of 164°F at Red Mountain and 176°F at East Divide Creek, and to obtain good agreement between measured maturity data and calculated maturity levels, paleo heat flow was varied. This facilitates simultaneous corrections for a nearby late Eocene intrusive event and post-Eocene uplift and erosion. Pre-Eocene heat flows were held constant at 1.5 heat flow units. Based on geologic age dating, the thermal event began 34 million years ago (MYA). A one hundred thousand year heating span was investigated, decaying exponentially. The geologic section was layered to approximate age of deposition and lithology. The thermal conductivities used for pure sandstone was 6.2 watt/meter/Kelvin (w/m/k), for shales 1.5 w/m/k, for dolomites 4.8 w/m/k decline, for siltstone 2.9 w/m/k, and for coal 0.3 w/m/k as reported by Kappelmeyer[18]. The results from the thermal modeling simulation expressed as a function of time and maturity for the volume of water and gas generated by the coals are shown on Figure 6. In both areas, active thermal gas generation from coals occurred approximately 52 MYA when the formations were at their deepest burial and greatest temperature. Active gas generation ceased approximately 25 MYA. Gas generation today is at a much lower rate due to reduced depths resulting from erosion and thermal decay of the igneous event. According to Lopatin's relationship, the current reaction rate is .001 percent as compared to peak gas generation approximately 40 MYA.

A typical geothermal gradient semi-log plot of depth and vitrinite reflectance yields a straight line[14]. A vitrinite profile has been measured at the 1 Deep Seam 32-2 well (Red

Mountain Unit), at the 1 Cameo 20-4 (East Divide Creek Area) , and other areas of the Piceance Basin as reported by Law[19]. All wells examined displayed an increased maturation profile occurring at approximately 0.90 Ro. The unusual vitrinite reflectance profiles measured at the 1 Deep Seam 32-2 and 1 Cameo 20-4 were closely matched by Waples[18] maturation modeling (Figure 7) indicating that maturity modeling in coal-bearing basins must take heat transfer through coalbeds into consideration. Poor thermal conductors, such as coal, result in a heat buildup under the low conductive section. This phenomenon is well documented by a static, cased hole temperature log from the East Divide Creek Area, Mamm Creek and Rullison Field (Figure 8). Note the repeated thermal anomalies at the base of the Cameo and Coal Ridge groups.

Yukler[20] first described the temperature and pressure interrelationship with abnormally pressured reservoirs. He observed a sharp increase in the temperature gradient on top of a high-pressure medium and a sharp decrease in the temperature gradient on top of a low-pressure medium (Figure 9). These findings are consistent with temperature profiles for overpressured coal sections as shown in Figure 8. The abnormally high-pressured sedimentary unit resulted from an insulation effect caused by a zone of low thermal conductivity. A barrier to heat flow is created in the areas of thick, laterally continuous coal seams found in the overpressured region of the Piceance Basin due to the low thermal conductivity of coal. This results in high temperatures and pressures which accelerate coal maturation as noted in vitrinite profiles from wells at the Red Mountain Area and East Divide Creek (Figure 7). The sequential results of thermal maturation events in the Piceance Basin may be summarized as follows:

1. The coal's insulating property which exists from deposition results in heat buildup and accelerates both the initiation and degree of coal maturation. Therefore, increasing temperature initiates increasing gas generation.

2. The rapid decay of the gas generative system is caused by reduced temperatures resulting from erosion of the stratigraphic section.

3. Once in the passive gas generation stage, the migration of gas from the coal seam to achieve equilibrium will result in decreasing pore pressure.

From the perspective of the Piceance Basin evolution, the coal seams underlying the Red Mountain and East Divide Creek Unit have similar thermal histories and generally evolved as a single system. However, thermal maturation and gas generation events alone fail to explain the different reservoir pressure gradients measured within the coal seams at the two areas. (e.g. Red Mountain Area = 0.33 psi/ft, East Divide Creek Area = 0.59 psi/ft). Distinguishing factors between the two areas include the post-laramide uplift paralleling the overpressured, East Divide Creek region, and absent at the Red Mountain Area and nearly twice the gas generation in the overpressured area due to increased coal thickness (Table 2).

The following thermal maturation events are presented as mechanisms for high coal pore pressure. During active gas generation, coal seams in the overpressured region were located in the deepest portion of the basin. Therefore, coalbed gas adsorption reached peak levels due to high formation pressures and temperatures from burial. The gas retention capacity was reduced during rapid post-laramide uplift and erosion. As a result of the uplift, the coal seams are currently at elevated maturation and temperature levels relative to laterally equivalent coal sections (Table 2). High pore pressure may then be related to coalbed gas retention in excess of equilibrium temperatures and pressures. Disequilibrium may have been accentuated by the large concentration of coal volume in the overpressured area (Figure 4).

OVERPRESSURED COAL RESERVOIRS

Gas is produced from overpressured, water saturated Fruitland coal reservoirs at the Cedar Hill Field and San Juan 30-6 Unit in the San Juan Basin. The two fields have been examined in detail[21] in an effort to: (i) determine geologic processes responsible for reservoir characteristics, and (ii) establish reservoir parameters controlling production.

The fields were selected because of their high productivity. The Cedar Hill Field has produced a cumulative of 7.1 Bcf from 7 wells since 1979 and is still producing at a rate of 1.3 Bcf/year. The Fruitland coal discovery was made in the San Juan Unit 30-6 during 1985. Three wells in that field have produced 2.3 Bcf during the first 15 months of production and continue to flow at a rate of 2.2 Bcf/year.

A detailed geologic study of both fields failed to detect significant geologic anomalies that might explain favorable production characteristics. Similarly investigation of drilling and completion techniques failed to yield technological reasons for high productivity. The only obvious factor that both fields share which is lacking in approximately 200 less successful coalbed completions in the San Juan Basin is overpressured coal reservoir conditions over a large lateral area. From the stand point of decreasing formation pressure below gas desorption pressure, over pressure, water saturated coals should have negative production implications. However, the overpressuring condition maybe indicative of a permeability enhancement process resulting in highly permeable coal reservoirs.

Based on regional isoreflectance maps, coal reservoirs in both fields fall in the maturation range of .80 - .90 Ro. According to Figure 2 this maturity level falls below peak gas generation phase. Therefore, sufficient volumes of gas have not been generated to cause high pore pressure. However, coal rank and age are appropriate for relict overpressuring conditions during the coal dewatering phase. Overpressuring during shale compaction and dewatering has been

well documented[22] in detrital sequences. Coal seams bounded by impermeable shales would similarly develop high pore pressure due to the inhibited ability to expel water during compaction. Produced waters from both field contain 12,000 to 14,000 ppm sodium bicarbonate type coal water which is suggestive of sluggish or isolated reservoirs conditions. Coal derived should be a sodium bicarbonate water[23], however, the high levels measured at the Cedar Hill and San Juan 30-6 Unit indicates little dilution of connate water over time, supporting bounded reservoir conditions. In theory, incompressible water under high pressure could be acting as a hydraulic proping mechanisms in coal cleats limiting porosity and permeability reduction effects from lithostatic loading.

Overpressured coal reservoirs are a product of shale bounded coal seams during diagenetic compaction during water expulsion. The process is similar to the origin of overpressured shales and sandstone in the Gulf Coast region. To date, coalbed methane wells producing from deeply buried coal seams with high permeability and deliverability occurring in overpressured, water saturated areas of the San Juan and Piceance Basins. The simultaneous occurrence of overpressuring, water saturation and high permeability in coal seams is not thought to be coincidental but rather suggestive of a common relationship. That relationship could be quantified through integration of geologic and reservoir modelling using data collected from laboratory core measurements in conjunction with field level reservoir tests.

SUMMARY

Recognition of the geologic and resulting reservoir processes controlling gas production from deeply buried coals is the first steps in the formulation of an exploration strategy for coalbed gas. The dominant coal reservoir mechanisms affecting production include: permeability, reservoir pressure, saturation and gas-in-place[24]. The relationship between decreasing coal permeability with increasing depth has been described by McKee[25]. In order to overcome the inherent low coal permeability at depth, permeability enhancement through structural deformation should be sought. Utilizing fundamental relationships including Darcy's Law and equation of state, at a given permeability, overpressured coal reservoirs will have better deliverabilities and, therefore, are a preferred exploration target over underpressured and normally pressured coal seams.

Based on observations resulting from drill stem tests, blowouts from intercepted coal seams, gas flares while drilling through coal seams and coalbed gas production, inferences may be made regarding areas in the Piceance Basin that are either water productive or predominantly flow gas with little or no mobile water (reference Figure 10). The pattern shown in Figure 10 coincides with : (i) an area within an vitrinite isoreflectance contour of 1.1 Ro (Figure 5), and (ii) proximity to the basin outcrop. A relationship is suggested where active gas generation has occurred in coals at depths greater than 4500 feet from the surface and isolated from the outcrop will result in little or no mobile water from coal reservoirs. Large volumes of gas generated from the coals and redistributed laterally and vertically throughout the geologic section is a possible mechanism for relocation of water from the coal reservoirs. Imbibition of water back into the system may be precluded by the absence of cross-formational fluid flow in low permeability basins.

Thermal modeling of geologic evolution has been used to describe and quantify existing reservoir conditions for deep coal seams within the Piceance Basin. Various conclusions and observations regarding coal reservoir conditions as a function of time, temperature and cross-formational fluid migration include:

1. Gas occluded in coal seams with maturities less than .73 Ro vitrinite reflectance may have largely originated from a deeper source or are a biogenic origin.

2. The unusual vitrinite reflectance profile observed in the Piceance Basin (and other deep coal basins) is caused by the low thermal conductivity of the coal.

3. Simplistic and commonly used geothermal gradient maturation models that do not account for heat transfer will fail to predict the accelerated phase of coal maturation and resulting hydrocarbon generation.

4. Active gas generation from coal seams in the Piceance Basin discontinued approximately twenty-five million years ago.

5. In the Piceance Basin, underpressured and overpressured coal reservoirs are part of a single hydrocarbon generation cycle, differing by the volume of hydrocarbons generated and a post-laramide uplift.

6. To date, overpressured coal reservoirs in the San Juan Basin are water saturated and highly permeable. These reservoir conditions may be related to coal water generative cycle under shale bounded conditions.

7. Water and gas generated during the coalification process may have fractured overlying sediments during expulsive cycles.

8. High permeability overpressured coals with high gas-in-place represent attractive coal reservoir conditions. For low permeability basins (such as the Piceance Basin), these reservoir parameters are most likely to occur along positive structural features that overlap thick, thermally mature coal seams.

REFERENCES

1. Meissner, F.E., 1984, Cretaceous and Lower Tertiary Coals as Sources for Gas Accumulations in the Rocky Mountain Area: Hydrocarbon Source Rocks of the Greater Rocky Mountain Region: Rocky Mountain Association of Geologists, Denver, Colorado, p. 401-432.

2. McPeek, L.A., 1981, Eastern Green River Basin: A Developing Giant Gas Supply from Deep, Overpressured Upper Cretaceous Sandstones: AAPG Bull., Vol. 65, p. 1078-1098.

3. Wyman, R.E., Gas Resources in Elmworth Coal Seams: Elmworth - Case Study of a Deep Basin Gas Field, AAPG Memoir 38, p. 173-189.

4. van Gijzel, P., 1982, Characterization and Identification of Kerogen and Bitumen and Determination of Thermal Maturation by Means of Qualitative Microscopical Techniques, in How to Assess Maturation and Paleotemperatures: SEPM Short Courses No. 7, p. 159-216.

5. Law, B.E. et al., 1983, Geologic Implications of Coal Dewatering: AAPG Bull., Vol. 67, p. 2255-2260.

6. Allardice, D.J., and D.G. Evans, 1971, The Brown Coal/Water System: Part 2; Water Sorption Isotherms on Bed Moist Yallourn Brown Coal: Fuel, V. 50, p. 236-253.

7. Juntgen, H. and J. Klein, 1975, Enstehung Von Erdgas Aus Kohligen Sedimenten: Erdol und Kohle, Erdgas, Petrochemie, Erganzungsband, V. 1, p. 52-69.

8. Allardice, D.J. and D.G. Evans, 1978, Moisture in Coal, in C. Karr, Jr., ed., Analytical Methods for Coal and Coal Products, V. 1: New York. Academic Press.

9. Kim, A.G., 1977, Estimating Methane Content of Bituminous Coalbeds From Adsorption Data: U.S. Bureau of Mines Report of Investigations 8245, p. 22.

10. Kissev, F.N., C.M. McCulloch, and C.H. Elder, 1973, The Direct Method of Determining Methane Content of Coalbeds for Ventilation Design: U.S. Bureau of Mines Report.

11. Eddy, G.E., Rightmire, C.T., and C. Byrer, 1982, Relationship of Methane Content of Coal, Rank and Depth: Proceedings of the SPE/DOE Unconventional Gas Recovery Symposium, Pittsburgh, Penn., SPE/DOE 10800, p. 117-122.

12. Welte, D.H., et al., 1981, Application of Organic Geochemistry and Quantitative Analysis to Petroleum Origin and Accumulation - An approach for a Quantitative Basin Study, in G. Atkinson and J.J. Zuckerman, eds., Origin and Chemistry of Petroleum: Elmsford, NY, Pergamon Press, p. 67-88.

13. Stallman, R.W., 1963, Computation of Ground-Water Velocity from Temperature Data, in Methods of Collecting and Interpreting Ground-Water Data: U.S. Geological Survey Water - Supply Paper 1544-H. p.36-46.

14. Lopatin, N.V., 1971, Temperature and Geologic Time as Factors in Coalification: Akademiya Nauk, Uzb. SSSR, Ser. geologicheskaya, Izvestiya, No. 3, p. 95-106. (Translation by N.H. Bostick, Illinois State Geological Survey, February 1972).

15. Decker, D., 1985, Appropriate Stratigraphic Nomenclature for Coal Reservoirs in the Piceance Basin, Abstract Presented at the Rocky Mountain AAPG Convention, Denver, Colorado (June 1985).

16. Hanson, J.M., 1987, Evaluation and analysis of the response of "Cameo" and "Hoffmeister-Rogers" wells to solid earth tides and barometric pressure. Unpublished paper submitted to Resource Enterprises, Inc. under contract to GRI #5083-214-0844.

17. Waples, D.W., 1987, Maturity Modeling of the 1 Cameo 20-4 Well, Unpublished report submitted to Resource Enterprises, Inc.

18. Kappelmeyer, O., Haenel, R.: Geothermics--with Special Reference to Application. Berline-Stuttgart: Borntraeger, 1974.

19. Law, B.E., and V.F. Nuccio, "Segmented Vitrinite Reflectance Profile from the Deep Seam Project, Piceance Basin, Colorado--Evidence of Previous High Pore Pressure". Abstract presented at the Rocky Mountain AAPG Convention, Casper, Wyoming (Sept. 1986).

20. Yukler, M.A., 1976, Analysis of Groundwater Flow Systems and an Application to a Real Case, in D. Gill and D.F. Merriam, eds., Geomathematical and Petrophysical Studies in Sedimentology, Computery and Geology, V. 3: Elmsford, NY, Pergamon Press, p. 33-49.

21. Kelso, B.S. and A.D. Decker, et al., 1987, GRI Geologic Appraisal of Coalbed Methane in the San Juan Basin. The 1987 Coalbed Methane Symposium Proceedings, held at the University of Alabama, Tuscaloosa, Alabama, November 16-19, 1987.

22. Hays, J.B., 1979, Sandstone diagenesis- The hole truth. In: Aspects of Diagenesis. P.A. Scholle adn P.R. Schluger, eds., Soc. Econ. Paleontologists and Mineralogists, Spec. Publ. No. 26, pp. 127-139.

23. Decker, A.D., et al., 1987, Geochemical Technqiues Applied to the Identification and Disposal of Connate Coal Water. The 1987 Coalbed Methane Symposium Proceedings, held at the University of Alabama, Tuscaloosa, Alabama, November 16-19, 1987.

21. Decker, A.D. and J.C. Seccombe, 1986, Geologic Parameters Controlling Natural Gas Production from a Single Deeply Buried Coal Reservoir in the Piceance Basin, Mesa County, Colorado: SPE Paper #15221, presented at Unconventional Gas Technology Symposium, May 1986.

22. McKee, C.R. et al., 1986, Using permeability-vs-depth correlations to assess the potential for producing gas from coal seam: Quarterly Review of Methane from Coal Seams Technology, vol, 4, no. 1, p. 15-26.

TABLE 1

COAL VOLUMETRICS

Ro%	% F	COAL RANK	THERMAL METHANE (Bcf/Mi^2)	WATER (10^6 bbl/mi^2)	THICKNESS (FEET)	
		EARLY PEAT	-	42.0	7.0	DIAGENESIS
		PEAT	-	14.0	3.5	
.23	95	LIGNITE	-	6.8	2.4	
.36	122	SUB-C	-	3.6	1.8	
.43		SUB-B	-	2.3	1.4	
.47		SUB-A	-	1.6	1.4	
.51	158	HvBb	-	.58	1.2	
.76	196	HvAb	.37	.50	1.2	CATAGENESIS
.90		HbAb	2.14			
1.11	248	Mvb	2.16	.45	1.0	
1.30		Mvb	.47			
1.50	302	Lvb	.49	.34	1.0	
2.04	356	Sa	-	.25	1.0	METAGENESIS
2.7	392	TOTAL	5.63	72.42		

AFTER LAW, 1983

TABLE 2

COAL RESERVOIR AND GEOLOGIC PROPERTIES

RED MOUNTAIN UNIT AND EAST DIVIDE CREEK

	COAL THICKNESS (FT)	RANK (Ro)	GAS GENERATED (BCF/mi^2)	IN PLACE (BCF/mi^2)	EXPELLED (BCF/mi^2)	DEPTH (FT)	TEMP ° F	PRESSURE GRADIENT (PSI/ft)	PERMEABILITY (md)
RED MOUNTAIN 1 DEEP SEAM 32-2	51'	.90-1.27	238	18	220	6600'	164'	.33	<.01
EAST DIVIDE CK. 1 CAMEO 20-4	100'	.90-1.27	467	35	432	4450'	176'	.58	>10.0

FIGURE 1

METHANE GENERATION

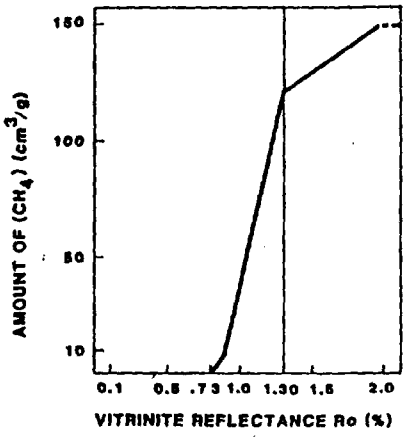

(AFTER WELTE, 1984)

FIGURE 2

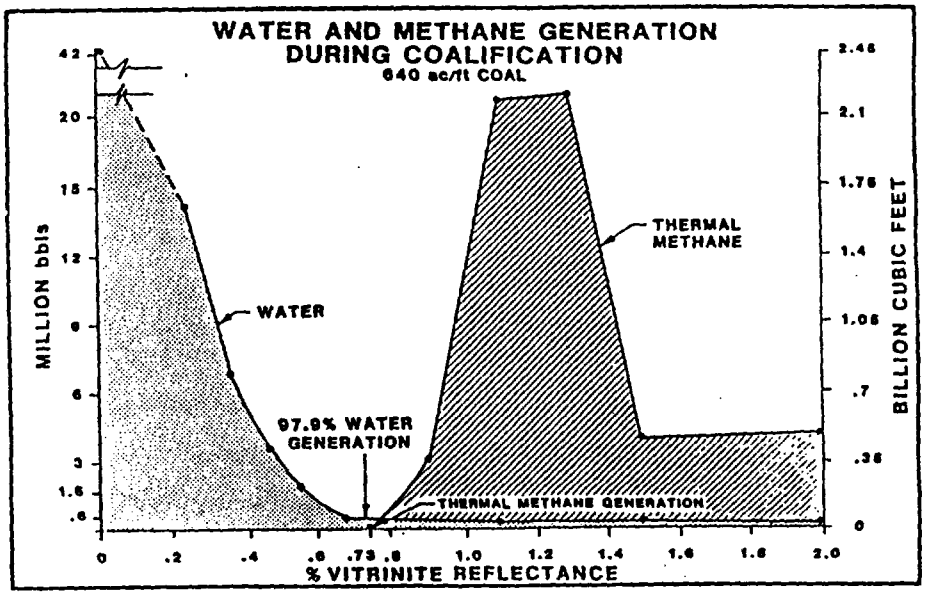

FIGURE 3

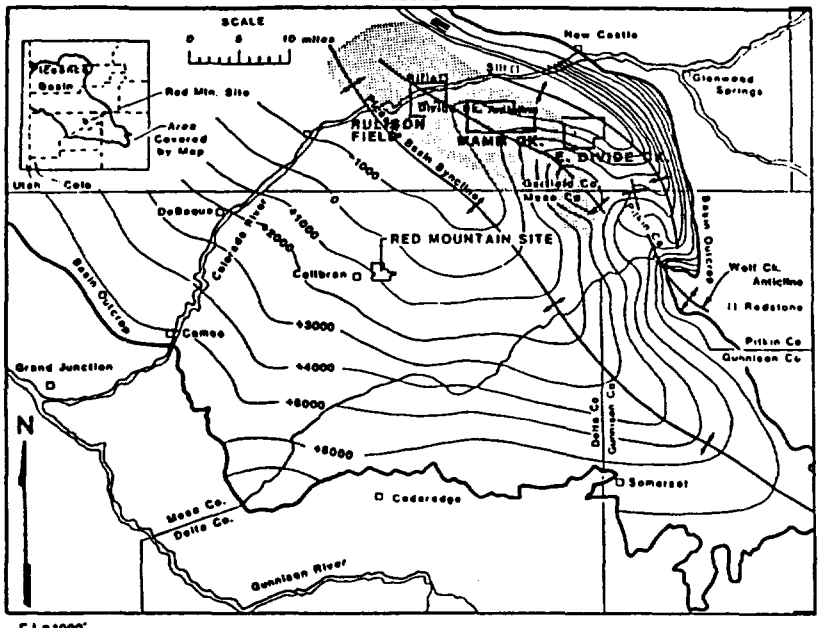

C.I. = 1000'
SUBSEA ELEVATIONS

STRUCTURE CONTOUR MAP
TOP OF ROLLINS SANDSTONE
PICEANCE BASIN, COLORADO

OVERPRESSURED AREA

FIGURE 4

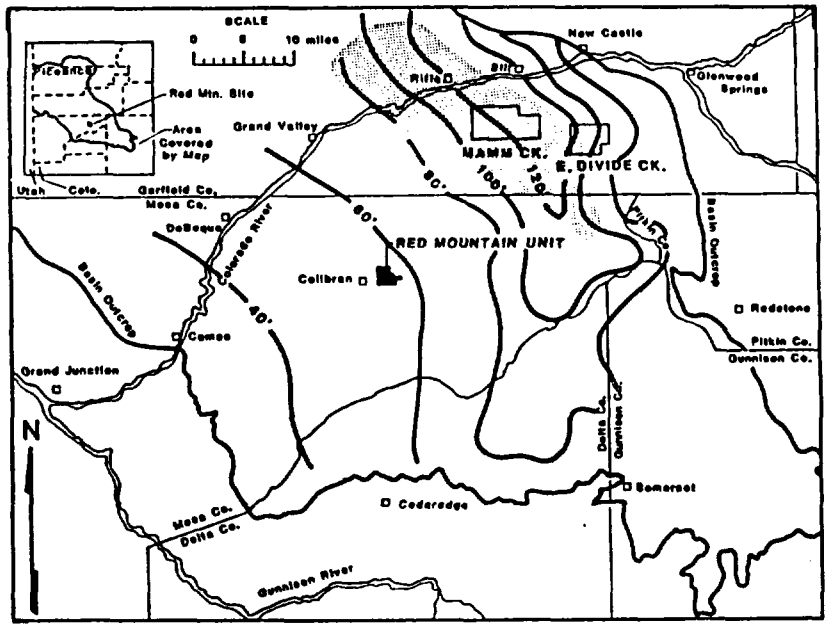

TOTAL COAL ISOPACH TREND MAP

OVERPRESSURED AREA

FIGURE 5

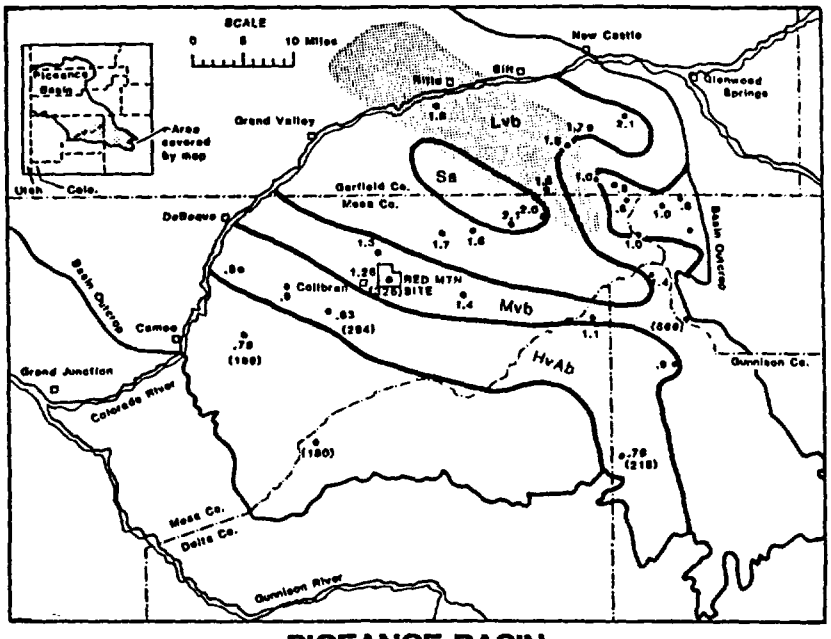

FIGURE 6

WATER AND THERMAL METHANE GENERATION
AS A FUNCTION OF TIME AND COAL MATURATION

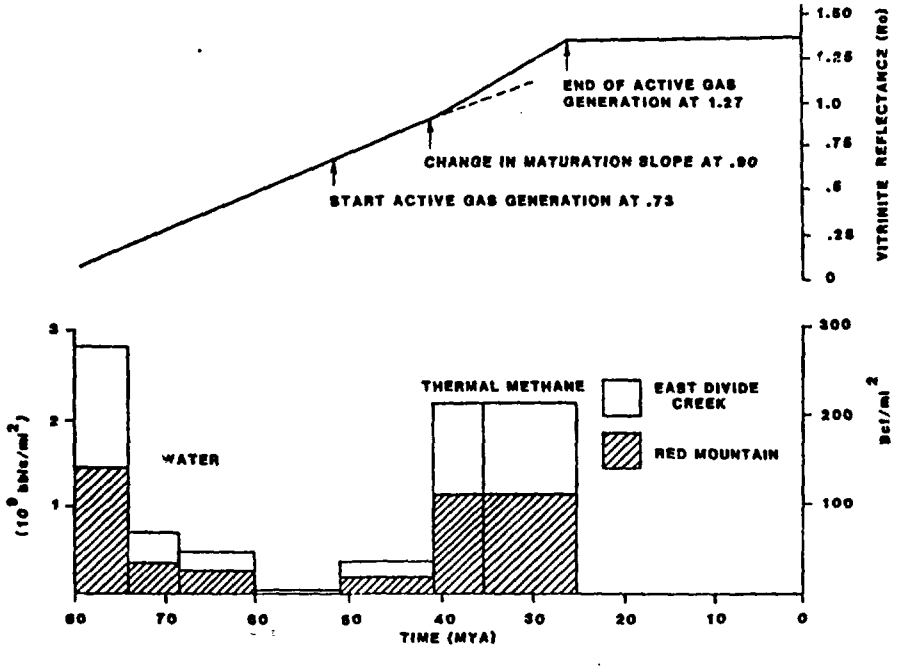

FIGURE 7

MATURITY vs. DEPTH

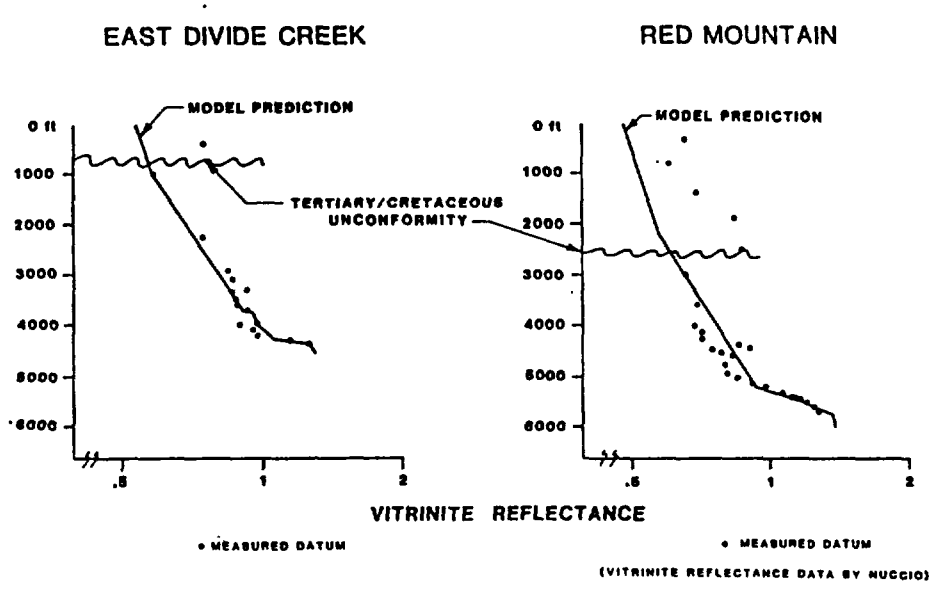

FIGURE 8

STATIC TEMPERATURE LOGS

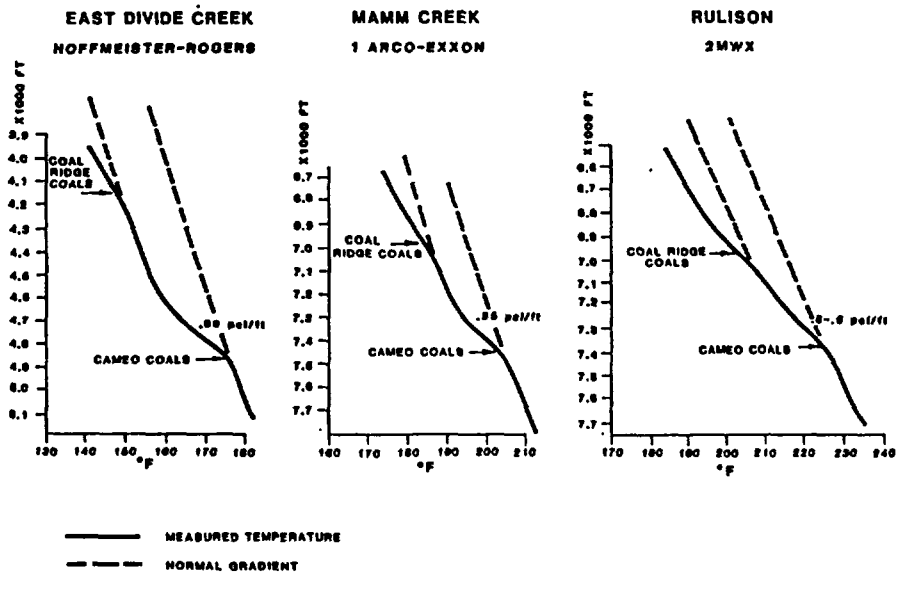

FIGURE 9

PRESSURE - TEMPERATURE RELATIONSHIP

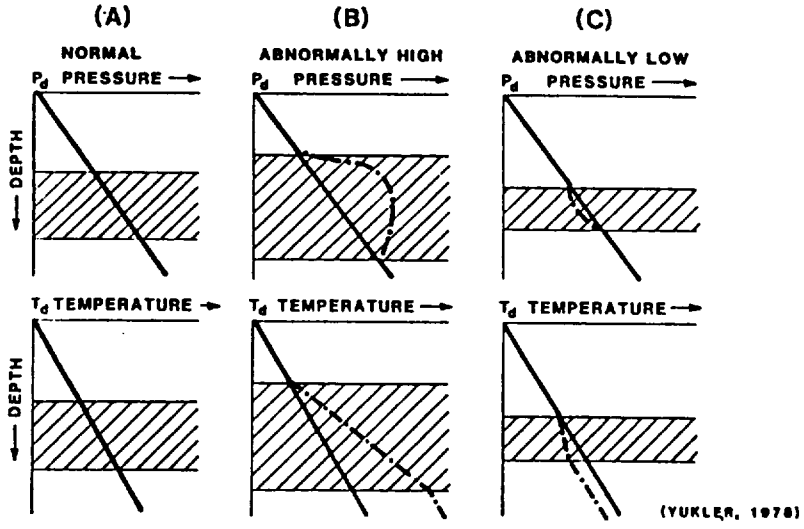

FIGURE 10

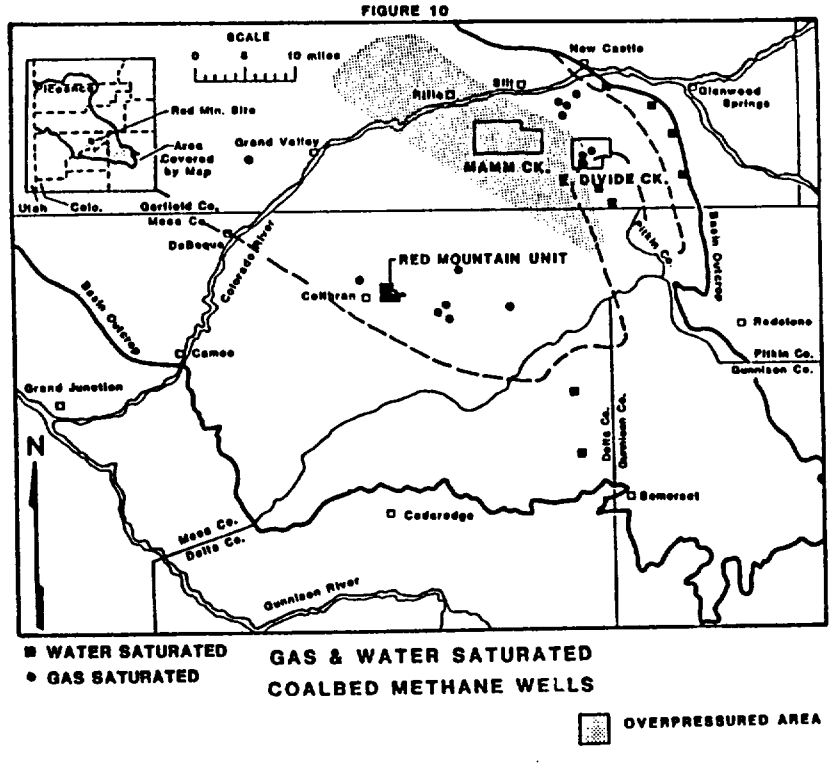

Piper Diagram for Connate Waters from

Piceance Basin, San Juan Basin, Warrior Basin

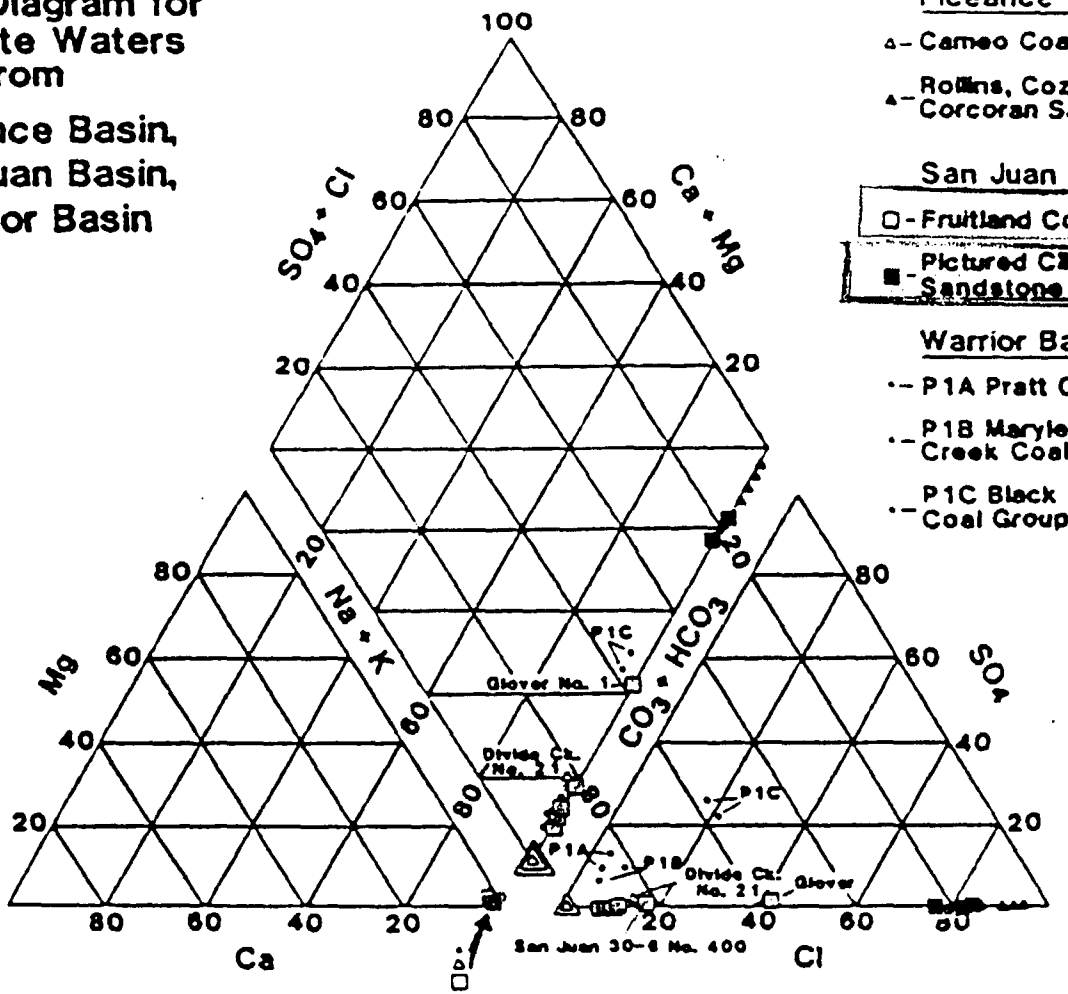

Piceance Basin

- Cameo Coal
- Rollins, Cozzette, Corcoran Sandstone

San Juan Basin

- Fruitland Coal
- Pictured Cliffs Sandstone

Warrior Basin

- P1A Pratt Coal Group
- P1B Marylee–Blue Creek Coal Group
- P1C Black Creek Coal Group

COMPARISON OF GAS ANALYSES

FORMATION	WELL LOCATION	C2+	CO2	BTU
Fruitland coal	A-18-32-7	94.84	4.25	976
"	O-08-32-9(CO)	95.92	2.61	997
"	D-11-33-10(CO)	95.53	2.20	1011
"	N-07-31-09	89.67	8.54	949
Fruitland sand	G-08-29-10	83.22	0.65	1235
"	E-22-28-12	85.55	1.45	1138
"	D-34-30-11	82.50	0.33	1223
"	O-28-32-11	83.41	0.42	1224
Pictured Cliffs	J-06-33-10(CO)	79.55	1.66	1234
"	O-26-32-07	85.23	0.58	1188
"	F-13-28-09	91.77	0.48	1102
"	O-18-30-08	88.20	0.94	1157

Proceedings of the 1987 Coalbed Methane Symposium Tuscaloosa, Alabama, Nov. 16-19, 1987

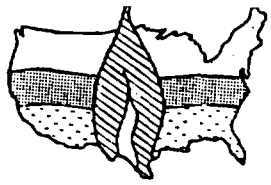

THE 1987 COALBED METHANE SYMPOSIUM

8711 Influence of Coal Composition on the Generation and Retention of Coalbed Natural Gas

J.R. Levine (University of Alabama, School of Mines & Energy Development)

INTRODUCTION

In terms of composition, coal is classified according to three distinct characteristics: 1) "grade", which represents the relative proportion of organic vs. inorganic constituents, 2) "type", which represents the natural variability of the organic constituents initially deposited in the coal, and 3) "rank", which represents the physico-chemical changes imparted to the coal by elevated temperatures and pressures during burial. Grade, type, and rank influence every aspect of coal bed natural gas reservoirs either directly or indirectly. The present paper focuses on two distinct, but related topics:
1) the influence of type and rank on the the composition and quantities of volatile substances formed during coalification, and 2) the influence of grade and type on the retention of gas in the subsurface.

EVOLUTION OF VOLATILE SUBSTANCES DURING COALIFICATION

The most fundamental change taking place in coal during coalification is the progressive enrichment of elemental carbon, accompanied by the elimination and release of large volumes of "volatile" substances relatively rich in hydrogen and oxygen. As these volatile substances are produced, the H/C and O/C atomic ratios of the residual solid coal progressively decrease. The three principal maceral groups, vitrinite, liptinite, and inertinite, differ substantially in their initial H/C - O/C ratios, hence they also differ in the quantity and type of gases formed during coalification.

The coalification process occurs much too slowly to be observed on a human time scale. Consequently, we are constrained to examining the end product and inferring as best we can the processes that led to it. Inasmuch as only a small portion of the volatile substances formed during coalification remain in the coal today, their volume and composition is largely problematical. However, providing a number of reasonable assumptions are made, then the quantities of CH_4, CO_2, and H_2O liberated during coalification can be estimated within a fairly narrow range, based on the major element (C-H-O) composition. The model requires: 1) that the organic microconstituents of coal evolve compositionally along the four generalized maturation pathways depicted in Figure 1 (Tissot and Welte, 1978), 2) that (for the most part) CH_4, CO_2, and H_2O represent the only forms in which carbon, hydrogen, and oxygen can escape from the coal bed, and 3) that once they are formed, CH_4, CO_2, and H_2O cannot recombine with the solid matrix of the coal.

The elemental compositions of coalification "products" and "reactants" can be plotted on a Van Krevelen diagram (Figure 1) which depicts both the rank and type of the organic constituents. Coalification paths for the four principal kerogen types are labeled I, II, III and IV. Kerogen type II is roughly equivalent to the liptinite (a.k.a. exinite) maceral group in coal. Kerogen type III is equivalent to vitrinite, by far the most common microscopic constituent of coal, and kerogen type IV is equivalent to the inertinite maceral group in coal. At low rank the maceral groups differ substantially in composition, but progressively converge upon one another they approach the origin. For example points A and B represent, respectively, the elemental compositions of liptinite and vitrinite macerals coexisting in a coal of vitrinite reflectance 0.5%, but by the time they have been coalified to 2.0% reflectance, they have virtually identical compositions.

A vector connecting any pair of starting and end points can be used to represent the compositional evolution of a particular coal or coal constituent. This vector can be resolved into 1,2, or 3 components, parallel to the dehydration, decarboxylation, and/or demethanation pathways plotted on the diagram. These devolatilization paths represent the change in composition brought about by the progressive removal of H_2O, CO_2, or CH_4 from the coal structure. Applying the constraints of the model, it is possible to reach an end point by a variety of pathways--but only within a limited range--or else condition (3) may be violated. For example, a liptinite maceral of initial composition A on the liptinite curve is coalified to composition C. There are two limiting end member paths to get from point A to point C. In the first, all oxygen is eliminated as CO_2 and none as H_2O while in the second the reverse is true. In the first case, the decarboxylation vector intersects the demethanation path at A', from which point all subsequent compositional

changes can be accounted for by progressively removing CH_4. , plus CH_4 (Path A-A"-C). Any other evolutionary pathways will include both decarboxylation and dehydration components and, con-sequently, and must fall between A-A' and A-A". (Note that the "head-to-tail" construction of the vectors in these examples does not necessarily imply a time sequence in volatile evolution. Volatile evolution occurs concurrently, with either one or the other substance predominating. However, the vectors do imply an explicit quantity of gases evolved.

To quantify this model and determine the precise composition and quantity of gases for each path, a set of equations is formulated whereby the total number of atoms of C, H, and O are equated between reactants (subscript r) and products (subscript p), and the H/C and O/C ratios of the reactants and products are adhered to:

$$Cp = Cr - CH_4 - CO_2 \quad (1)$$
$$Hp = Hr - 4*CH_4 - 2*H_2O \quad (2)$$
$$Op = Or - 2*CO_2 - H_2O \quad (3)$$
$$Hp = Cp * 0.50 \quad (4)$$
$$Op = Cp * 0.06 \quad (5)$$

where Cp, Hp, and Op are the number of atoms or moles of carbon, hydrogen, and oxygen per unit of the product. Cr, Hr, and Or are the number of atoms or moles of carbon, hydrogen, and oxygen in the starting (reactant) mixture; and CH_4, CO_2, and H_2O are the number of molecules or moles of methane, carbon dioxide, and water formed from the reactants during coalification.

The composition of the starting material can be determined by solving the following set of 3 equations with 3 unknowns:

$$Hr/Cr = 1.25 \quad (6)$$
$$Or/Cr = 0.07 \quad (7)$$
$$Cr + Hr + Or = 1000, \quad (8)$$

the solution to which is:

$$Cr = 431 \quad (9)$$
$$Hr = 539 \quad (10)$$
$$Or = 30 \quad (11)$$

The value of 1000 in equation (8) is arbitrary. It can be thought of as representing an imaginary coal "molecule" comprised of 1000 atoms. In subsequent calculations these 1000 atoms shall be partitioned among the various volatile products and coal.

Substituting equations (9-11) into equations (1-5) we are left with 5 equations and 6 unknowns. Hence, in order to derive a unique solution, one additional relationship must be defined. For end member case A-A'-C, $H_2O = 0$; and for case A-A"-C, $CO_2 = 0$. For intermediate paths, some ratio of CO_2 to H_2O must be selected. This needn't be an arbitrary choice, but may be based on knowledge of the functional group composition. For example Van Krevelen (1963) indicates that throughout most of the coal ranks under consideration, approximately half of the oxygen in coal is bound to hydrogen, and about half to carbon. We can propose then that CO_2 an H_2O leave the coal in roughly equal amounts; hence $CO_2 = H_2O$.

Depending on the path chosen, the relative proportions and total weight percentages of the volatile products vary considerably. Table 1 lists the yields of CH_4, CO_2, and H_2O and volatile matter produced along the various maturation pathways depicted in Figure 1. For example, as coal increases from R_o(vit) = 0.5 to R_o = 2.0, vitrinite can evolve anywhere from 24 to 173 cm^3 CH_4(stp)/g coal, depending upon whether B-B'-C or B-B"-C is followed. Assuming a ratio of 1:1 H_2O:CO_2 production, vitrinite will cumulatively generate around 116 cm^3 CH_4(stp)/g. Over this same rank range, and within the constraints of the model, liptinite macerals generate between 421 and 466 cm^3 CH_4(stp)/g; however, in reality, liptinites probably lose a significant proportion of their hydrogen as longer chain hydrocarbons rather than as methane. The devolatilization model can be modified or expanded to accommodate other hydrocarbon gases, however, a new functional relationship must be added for each new unknown.

This method of quantitatively estimating the volatile yield using simultaneous equation.is similar to a widely cited coal devolatilization model proposed by Juntgen and Karweil (1966) but differs in that it does not require that the coal liberate specific quantities of volatile substances. Juntgen and Karweil speculated that the proximate analysis volatile matter content (measured by pyrolysis at 950°C) could be used as an estimate of the total weight of material evolved as volatile products during coalification. However, this assumption is unwarranted and thermodynamically unsound. Moreover, by requiring that their coals produce such a large volume of volatile substances, Juntgen and Karweil's equations yielded negative values for water production--in other words, it was required that water be added to the coal structure to maintain the proper elemental ratios. Thus, the estimates of gas volumes based on this model are exaggerated. A subsequent article by Juntgen and Klein (1975), however, published a lower revised estimate, discussed subsequently, that is in close agreement with the one calculated herein.

Table 2 shows the progressive devolatilization path to Ro(vit) = 2.0% of an hypothetical coal, comprised of 80% vitrinite, 10% liptinite, and 10% inertinite. The total CH_4 production is 107 cm^3/g (Table 1, Path D-D'-C), almost identical to the quantity calculated by Juntgen and Klein (1975) based on experimental pyrolysis. The older estimate by Juntgen and Karweil (1966) for a whole coal was more than 200 cm^3. Unfortunately, the older figure seems to be used more commonly than the more recent one, (e.g. Meissner, 1984)

INFLUENCE OF COAL COMPOSITION ON IN SITU METHANE CONTENTS

With increasing rank coal loses its capacity to retain H_2O; hence, assuming that the beds remain fully water saturated, any water formed during coalification must be produced. Coal has a relatively strong affinity for CO_2 (as opposed to

CH_4 for example), but CO_2 is readily soluble in water; hence, its abundance will tend to diminish over time. Consequently, in comparison with other volatile substances formed during coalification CH_4 tends to become progressively enriched in the coal bed reservoir .

Coal has an attractive affinity for methane that enables it to absorb or adsorb more CH_4 under pressure than would be the case if the methane were a free gas. During the course of coalification coals generate much more methane than they have the capacity to retain (Juntgen and Karweil, 1966), so in a natural setting, most coals should be at or near their maximum methane capacity (at P,T), provided that the coals were not exposed to abnormally low fluid pressures in the past. Bearing this model in mind, the gas content of coal in situ should be proportional to the pressure, temperature, and whatever compositional parameters limit the coal's capacity to sorb gas.

A suite of 57 samples was recently collected from a 3000 ft-deep coal bed methane exploration core hole in the Cahaba basin, central Alabama. The gas contents of the samples were measured using the Bureau of Mines canister desorption test. Then the coals were subjected to a comprehensive suite of analyses, including proximate, ultimate, BTU, and petrography. These data were then normalized and used to develop a multiple linear regression model to predict the gas contents of the samples. The resulting linear model was very successful, explaining 88.5% of the variability in gas content. A large component of the remaining 11.5% variability is probably due to measurement error.

Multiple Linear Regression Model
Gas Contents of Cahaba Core Samples

Gas Content (cm^3/g) = 6.822
+ 0.0025 * Depth (ft)
- 0.0957 * ParrMM
r^2 = .885 + 0.1112 * (%Fusinite + %Semifusinite
- 5.449 * H/C (daf) + %Macrinite)

This regression model indicates that for the suite of coals examined, gas content increases linearly with depth. In laboratory sorption isotherm studies, the gas capacity of coal increases at a less than linear rate, so the anomalously high gas contents at depth may be due to increasing rank (W. Telle, personal communication). There was not, however, enough of a systematic rank variation in the samples to produce a measurable effect in the regression model. The third term, ParrMM, is an estimate of the mineral matter content of the coal using Parr's equation based on ash and sulfur content. Once again the correlation is linear, but with a negative coefficient. The predicted gas content using the model is very close to 0.0 at 100% ParrMM, showing that for these samples, the mineral matter does not participate measurably in the gas sorption process. The fourth term is a indication of the influence of coal petrography on gas sorption capacity. This composite variable, comprised of members of the inertinite maceral group, indicates that while inertinite does not contribute significantly to gas generation, it has a positive influence on the gas content. The fifth term, the hydrogen to carbon ratio (dry, ash-free basis) does not contribute strongly toward the model, but indicates that an increasing H/C ratio has a negative influence on the gas capacity. It is uncertain whether this is related to decreasing rank, or increasing liptinite content. Neither standard rank parameters nor the liptinite percentages showed a significant effect.

It remains to be seen whether this model can be applied to coals in other basins as well. As additional data become available the model will be tested and refined.

REFERENCES CITED

Jüntgen, H. and Karweil, J., 1966, Gasbildung und Gasspeicherung in Steinkohlenflözen, Part I and II: Erdöl u. Kohle, Erdgas, Petrochem, v. 19, p. 251-258 and 339-344.

Jüntgen, H. and Klein, J., 1975, Entstehung von Erdgas aus kohlingen Sedimenten.: Erdöl u. Kohle, Erdgas, Petrochem., Ergänzungsband, I, 74/75, p. 52-69. Industrieverlag v. Hernhausen Leinfelden bei Stuttgart.

Krevelen, D.W. van, 1963, Geochemistry of coal, in Breger, I.A., ed., Organic Geochemistry: Oxford, Pergamon Press, p. 183-247.

Meissner, F.F., 1984, Cretaceous and Lower Tertiary coals as sources for gas accumulations in the Rocky Mountain Area: Hydrocarbon Source Rocks of the Greater Rocky Mountain Region: Rocky Mountain Association of Geologists, Denver, CO, p. 401-432.

Tissot, B.P. and Welte, D.H., 1978, Petroleum Formation and Occurrence: Springer-Verlag, Berlin, 538 p.

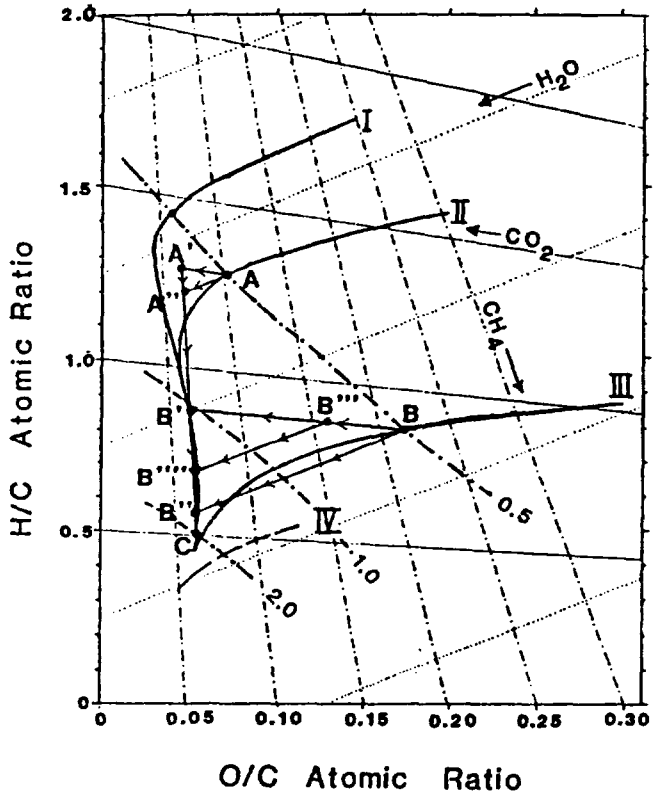

Figure 1 - Van Krevelen diagram depicting evolutionary devolatization paths. Liptinite (A) and vitrinte (B) are situated at the intersections of the Type II and Type III kerogen maturation paths and the 0.5% R_o isoreflectance line. A number of alternate devolatilization paths may be followed for each starting material, each path yielding different quantities of volatile products (see Table 1 for details).

Coalification from R_o(vit) = 0.5 to R_o(vit) = 2.0		Cumulative Grams of Volatiles per Gram of Coal			% of Original Weight Lost as Volatiles	Volume of CH_4 (stp) per Gram of Solid Coal
Path	Description	CH_4	CO_2	H_2O		
A-A'-C	Max. CH_4, Max. CO_2, Min. H_2O	0.333	0.049	0	27.6	466.
A-A''-C	Min. CH_4, Min. CO_2, Max. H_2O	0.301	0	0.036	25.2	421.
B-B'-C	Max. CH_4, Max. CO_2, Min. H_2O	0.124	0.236	0	26.5	173.
B-B''-C	Min. CH_4, Min. CO_2, Max. H_2O	0.017	0	0.156	14.7	24.
B-B'''-B''''-C	Intermediate Path: $H_2O \equiv CO_2$	0.083	0.146	0.059	22.4	116.
D-D'-C	Intermediate Path: $H_2O \equiv CO_2$	0.076	0.110	0.045	18.7	107.

TABLE 1. Volatile Products of Coalification

Step:	C	H	O	H/C	O/C
Starting Material:					
80 % Vitrinite:	4096	3192	712	0.78	0.17
+ 10 % Liptinite:	431	539	30	1.25	0.07
+ 10 % Inertinite:	746	224	30	0.30	0.04
Total:	5273	3955	772	0.75	0.15
Decarboxylation:	-79	0	-158		
(79 ≡ CO_2)	5194	3955	614	0.76	0.12
Dehydration:	0	-630	-315		
(315 ≡ H_2O)	5194	3325	299	0.76	0.06
Demethanation:	-208	-832	0		
(208 ≡ CH_4)	4986	2493	299	0.50	0.06

TABLE 2. Devolatilization Path for Whole Coal (D-D'-C, Table 1.)

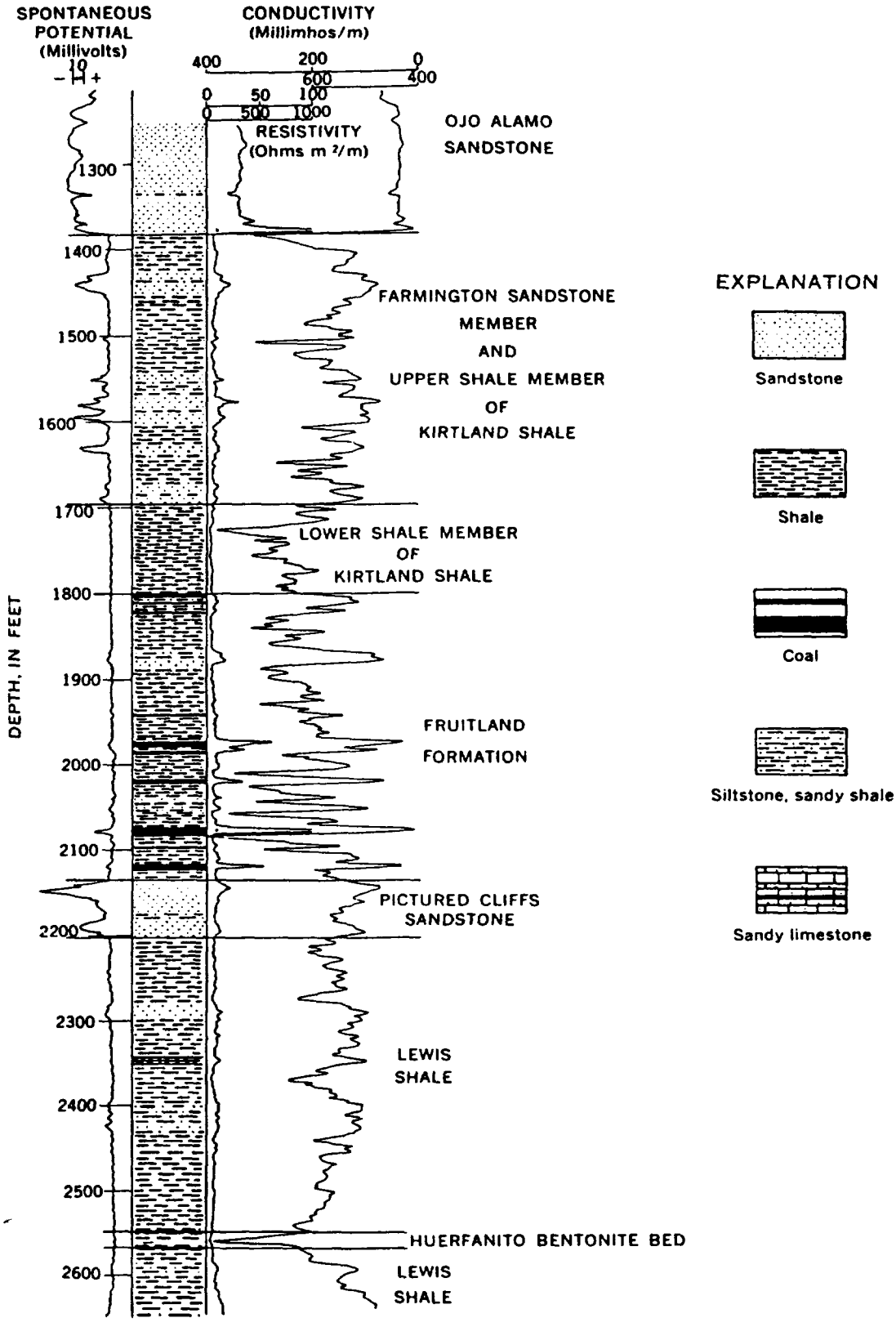

Figure 4 -- Induction-electric log and lithologic column of the type well of the Huerfanito Bentonite Bed of the Lewis Shale showing the interval from below the Huerfanito through the lower part of the Ojo Alamo Sandstone. Lithologies are based on an interpretation of the three geophysical logs shown.

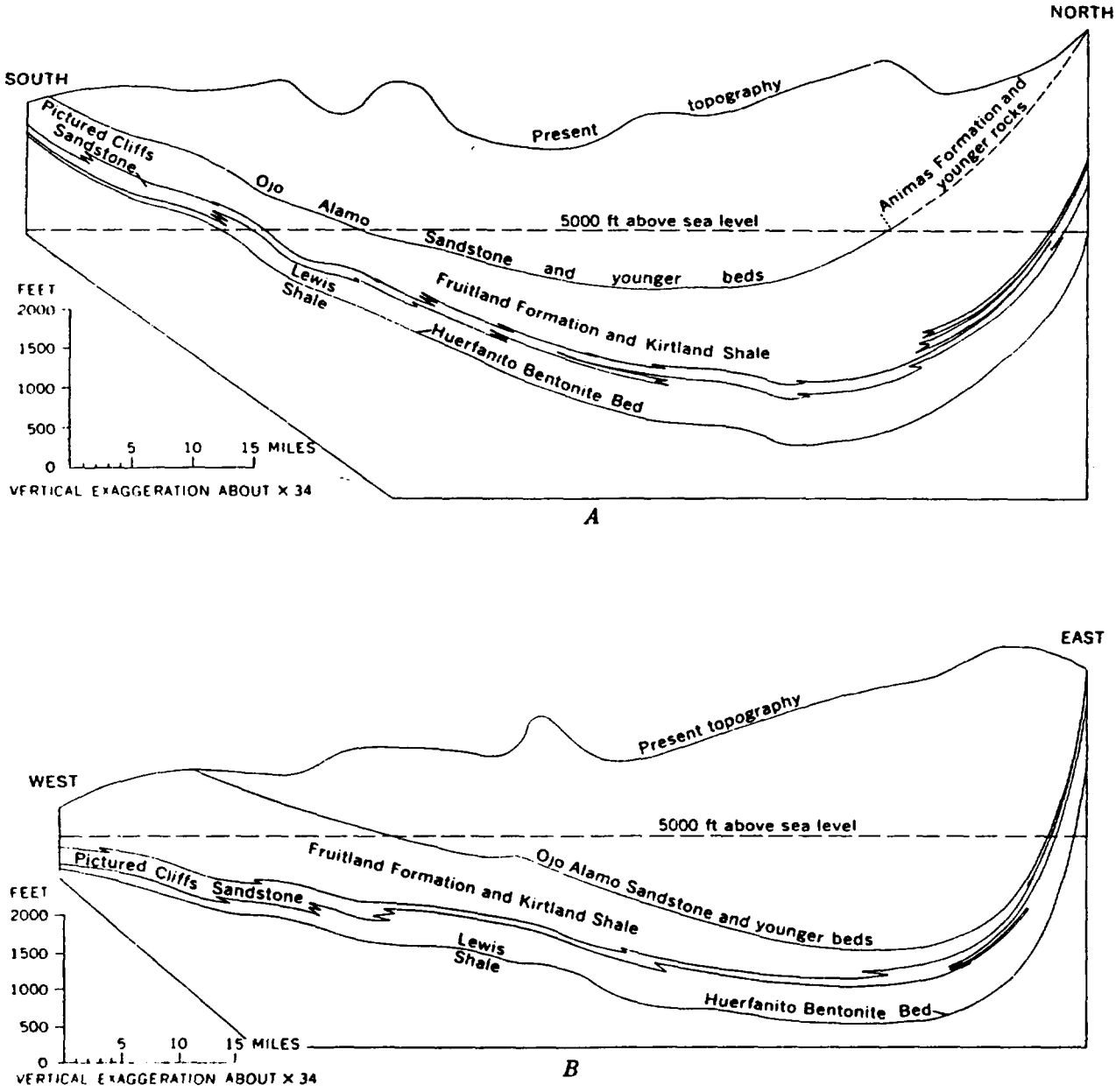

North-trending (A) and east-trending (B) structural cross sections across the San Juan Basin showing the present basin structure. (From Fassett, 1985 [15].

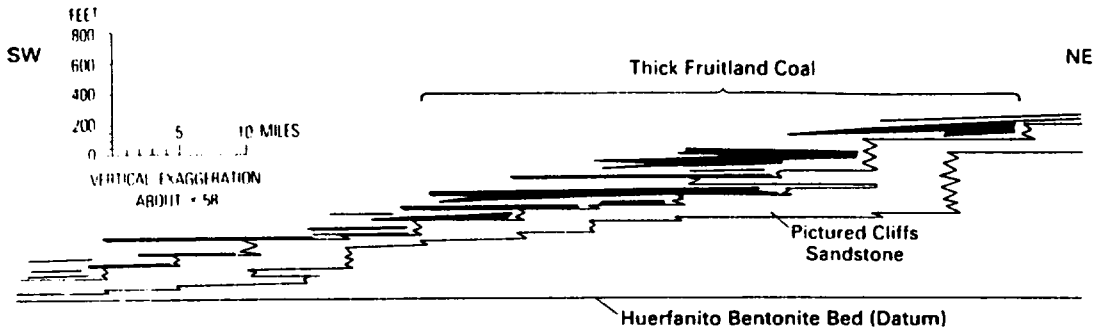

Northeast-trending stratigraphic cross-section showing Fruitland Formation coal beds and underlying Pictured Cliffs Sandstone. This cross section is modified from section B-B' of figure 8; coal bed thicknesses are from plate 3 of Fassett and Hinds (1971)

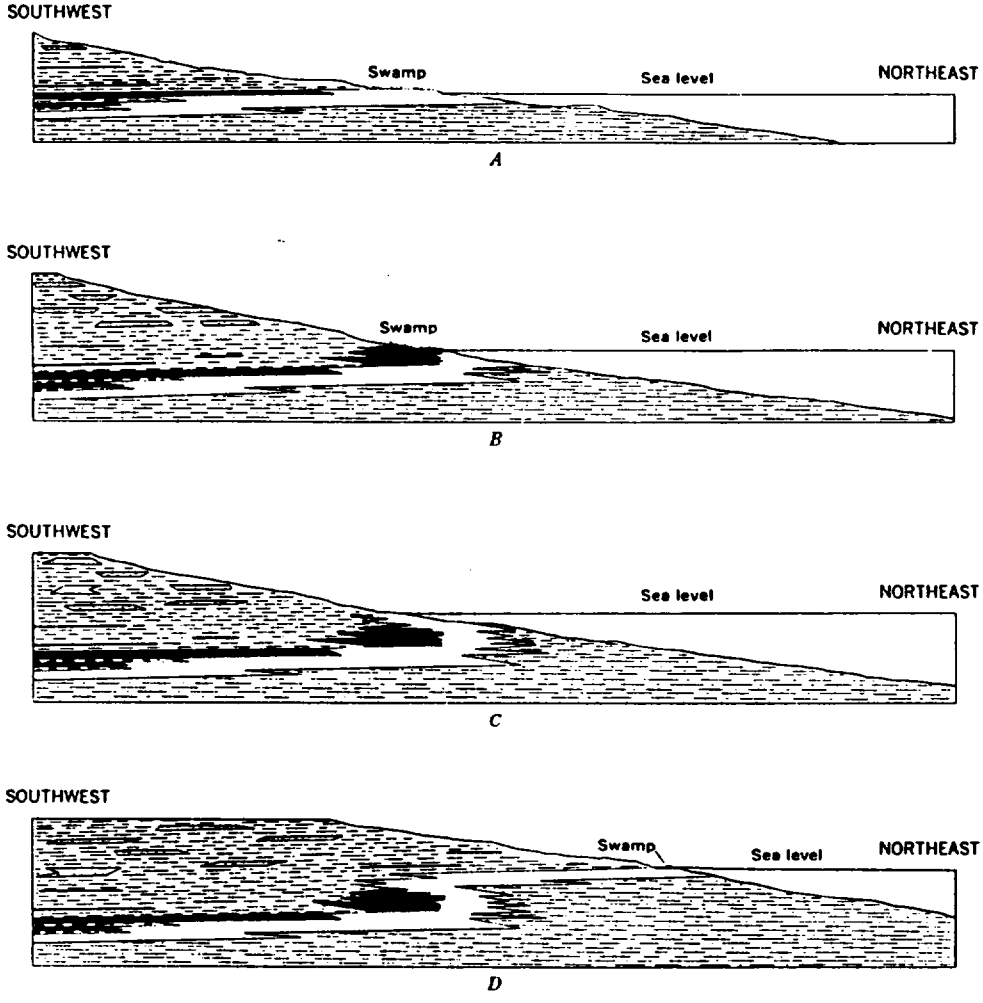

Diagrammatic cross sections showing the relations of the continental, beach, and marine deposits of Pictured Cliffs time after (A) shoreline regression, (B) shoreline stability, (C) shoreline transgression, and (D) shoreline regression.

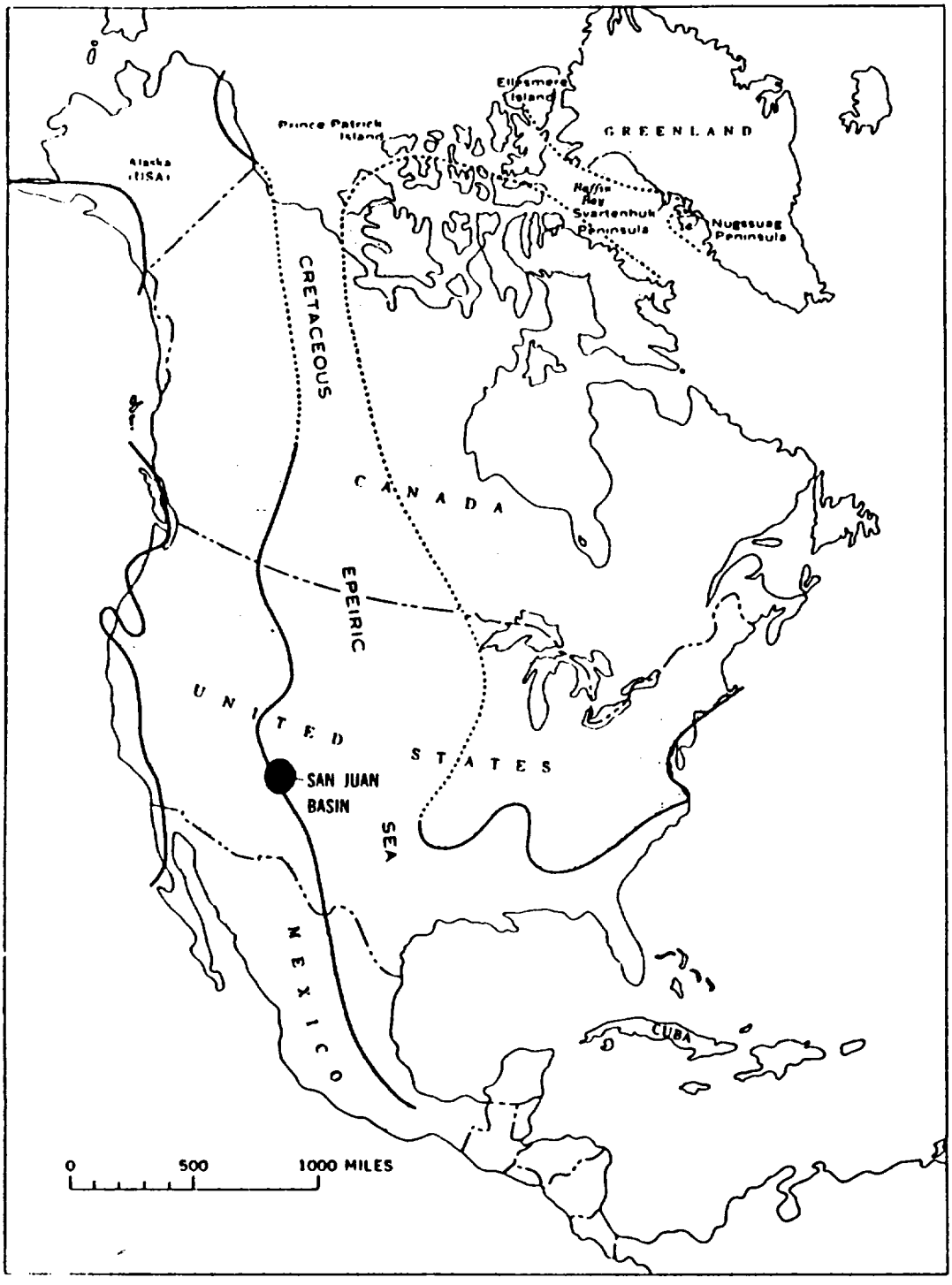

Probable configuration of the North American epeiric seaway at the time that the Upper Cretaceous rocks of the San Juan Basin were being deposited.

(B) That for the purpose of this order a San Juan Basin Fruitland Coalbed Methane Gas Well is a well that is producing from the Fruitland Coalbed Seams as demonstrated by a preponderence of data which could include the following data sources:

a) Electric Log Data

b) Drilling Time

c) Drill Cutting or Log Cores

d) Mud Logs

e) Completion Data

f) Gas Analysis

g) Water Analysis

h) Reservoir Performance

i) Other evidence that indicates the production is predominately coalbed methane.

No one characteristic of lithology, performance or sampling will either qualify or disqualify a well from being classified as a Fruitland Coalbed Methane Gas Well.

IT IS THEREFORE ORDERED:

(A) That, effective _____, a new pool in all or parts of San Juan, Rio Arriba, McKinley and Sandoval Counties, New Mexico, classified as a gas pool for production from the Fruitland Coalbed Seams, is hereby created and designated the San Juan Basin Fruitland Coalbed Methane Gas Pool, with the vertical limits comprising all coal seams within the stratigraphic interval from approximately 2450 feet to 2880 feet on the Gamma Ray/Bulk Density log of the Amoco Production Company Schneider Gas Com "B" Well No. 1, located 1110 feet from the South line and 1185 feet from the West line of Section 28, Township 32 North, Range 10 West, NMPM, San Juan County, New Mexico, which for the purpose of this order shall include all stratigraphically equivalent coal seams which by virtue of intertonguing or other geological events may be found within the upper Pictured Cliffs Formation. The horizontal limits shall consist of the following described lands:

Township 19 North, Ranges 1 West through 6 West, NMPM
Township 20 North, Ranges 1 West through 8 West, NMPM
Township 21 North, Ranges 1 West through 9 West, NMPM
Township 22 North, Ranges 1 West through 11 West, NMPM
Township 23 North, Ranges 1 West through 14 West, NMPM
Township 24 North, Ranges 1 East through 16 West, NMPM
Township 25 North, Ranges 1 East through 16 West, NMPM
Township 26 North, Ranges 1 East through 16 West, NMPM
Township 27 North, Ranges 1 West through 16 West, NMPM
Township 28 North, Ranges 1 West through 16 West, NMPM
Township 29 North, Ranges 1 West through 15 West, NMPM
Township 30 North, Ranges 1 West through 15 West, NMPM
Township 31 North, Ranges 1 West through 15 West, NMPM
Township 32 North, Ranges 1 West through 13 West, NMPM

SPECIAL RULES AND REGULATIONS FOR THE

SAN JUAN BASIN FRUITLAND COALBED METHANE GAS POOL

SAN JUAN, RIO ARRIBA, MCKINLEY AND SANDOVAL COUNTIES, NEW MEXICO

RULE 1. GENERAL

Each well completed or recompleted in the San Juan Fruitland Coalbed Methane Gas Pool shall be spaced, drilled, operated and produced in accordance with the Special Rules and Regulations hereinafter set forth.

RULE 2. POOL ESTABLISHMENT

That the Director may require the operator of a San Juan Basin Fruitland Coalbed Methane Gas Well, a Fruitland Sand Well or Pictured Cliffs Sand Well, which is proposed in the lands described in (A) above, furnish information and data that would demonstrate to the satisfaction of the Director that the existing wells are producing and the proposed well will produce from the appropriate common source of supply.

RULE 3 (a). WELL SPACING & LOCATION

A standard drilling unit for a San Juan Basin Fruitland Coalbed Methane Gas Well shall consist of 320 acres, plus or minus 25%, substantially in the form of a rectangle, consisting of a half section, being a legal subdivision of the U.S. Public Land Surveys, and shall be located no closer than 790 feet to any outer boundary of the tract, nor closer than 130 feet to any interior quarter section line.

In the absence of a standard 320 acre drilling unit, an application for administrative approval of a non-standard unit may be made to the Division Director provided that the acreage to be dedicated to the non-standard unit is contiguous, and the non-standard unit lies wholly within a single governmental half section, and further provided that the operator seeking the non-standard

unit obtains a written waiver from all offset operators of drilled tracts or owners of undrilled tracts adjacent to any point common to the proposed non-standard unit. In lieu of the waiver requirements the applicant may furnish proof of the fact that all of the aforesaid were notified by registered or certified mail (return receipt requested) of the intent to form such non-standard unit. The Director may approve the application if no objection has been received to the formation of such non-standard unit within 20 working days after the Director has received the application.

The drilling unit orientation will be determined by the first well permitted to be drilled in any one particular standard section.

RULE 3 (b). UNORTHODOX WELL LOCATION

The Director shall have authority to grant an exception to the well location requirements of Rule 3 (a) above without notice and hearing when the necessity for such unorthodox location is based upon topographic conditions or the recompletion of a well previously drilled into a deeper horizon, provided said well was drilled at an orthodox or approved unorthodox location for such original horizon.

Applications for administrative approval of unorthodox locations shall be filed in duplicate (original to Santa Fe and one copy to the appropriate District Office) and shall be accompanied by plats showing the ownership of all leases offsetting the spacing unit for which the unorthodox location is sought, and also all wells completed thereon. If the proposed unorthodox location is based on topography, the plat shall also show and describe the existent topographic conditions.

If the proposed location is unorthodox by virtue of being located closer to the outer boundary of the spacing unit than permitted by rule, actual

notice shall be given to any operator of a spacing unit or owner of an undrilled ~~lease~~ acreage tract toward which the proposed location is being moved.

All such notices shall be given by certified mail (return receipt requested) and the application shall state that such notification has been given. The Director may approve the unorthodox location upon receipt of waivers from all such offset operators or if no offset operator has entered an objection to the unorthodox location within 20 working days after the Director has received the application.

The Director may at his discretion, set any application for administrative approval of an unorthodox location for public hearing.

RULE 4. INCREASED WELL DENSITY

The Director shall have the authority to administratively approve one (1) additional San Juan Basin Fruitland Coalbed Methane Gas Well provided the following conditions are met:

(a) The increased density well must conform to the spacing and boundary footage requirements set forth in Rule 3 (a). and the increased density well cannot be located in the same quarter section as the existing well.

(b) The operator must notify by certified mail (return receipt requested) all: offset operators located in contiguous standup or laydown drilling units; and in the case that the offsetting units are not developed, then notice shall be provided to the owners of contiguous lands.

(c) If no objection is received within 20 working days from receipt of notice, then the application will be administratively approved by the Director. If any objection is received within the time limit, then the Director will set the application for increased well density for public hearing.

RULE 5. HORIZONTALLY DRILLED WELLS

The Director shall have the authority to administratively approve an intentionally deviated well in the San Juan Basin Fruitland Coalbed Methane Gas Pool for the purpose of penetrating the coalbed seams by means of a wellbore drilled horizontally, at any angle deviated from vertical, through such coalbed seams provided the following conditions are met:

(a) The surface location of the well is within the permitted drilling unit area of the proposed well.

(b) The bore hole must not enter or exit the coalbed seams outside of a drilling window which is in accordance with the setback requirements of Rule 3 (a).

If the operator applies for a permit to drill a horizontal well in which the wellbore is intended to cross the interior quarter section line, the operator must notify by certified mail (return receipt requested) all: offset operators located in contiguous standup or laydown developed drilling units; and in the case that the offsetting units are not developed, then notice shall be provided to the owners of contiguous lands.

If no objection is received within 20 working days from receipt of notice, then the application may be administratively approved by the Director. If any objection is received within the time limit, then the Director will set the application for horizontally drilled wells for public hearing.

RULE 6 (a) TESTING.

In lieu of the gas well testing requirements of Order No. R-8170, testing for the San Juan Basin Fruitland Coalbed Methane Gas Pool shall consist of: a

minimum twenty-four (24) hour shut-in period, unless otherwise specified by the Director, and a three (3) hour production test. The following information from this initial production test must be reported:

(1) the surface shut in tubing and/or casing pressure and date these pressures were recorded;

(2) the length of the shut-in period;

(3) the final flowing casing and flowing tubing pressures and the duration and date of the flow period;

(4) the individual fluid flow rate of gas, water and oil which must be determined by use of separator; and

(5) the method of production, e.g. - flowing, pumping, etc., and disposition of gas.

RULE 6 (b). VENTING OR FLARING

Venting or flaring for extended well testing will be permitted for completed San Juan Basin Fruitland Coalbed Methane Gas Wells for a test period of not more than thirty (30) days or a cumulative produced volume of 50 MMCF of vented gas, whichever occurs first, the operator will notify the Director of this testing period.

If an operator has cause to perform further testing of a well, then administrative approval may be made by the Director to permit an additional period time and volume limit, set by the Director after sufficient evidence to justify this request has been submitted. In no case shall a well be administratively authorized to vent for a period greater than twelve (12) months.

RULE 7. EXISTING WELLS

That the operator of an existing Fruitland, Pictured Cliffs or commingled Fruitland/Pictured Cliffs well, which is in conformance with Paragraphs (A) and (B) of this order and is drilling to, completed, or has an approved APD for which the actual or intended completed interval is the San Juan Basin Fruitland Coalbed Methane Gas Pool, may request such well be reclassified as a San Juan Basin Fruitland Coalbed Methane Gas Well by the submittal of a new Form C-102 and C-104 within 90 days of the effective date of this order; this well may be so designated with its original spacing unit size as a non-standard San Juan Basin Fruitland Coalbed Methane Gas Well or may be enlarged to be in conformance with Rule 3 (a).

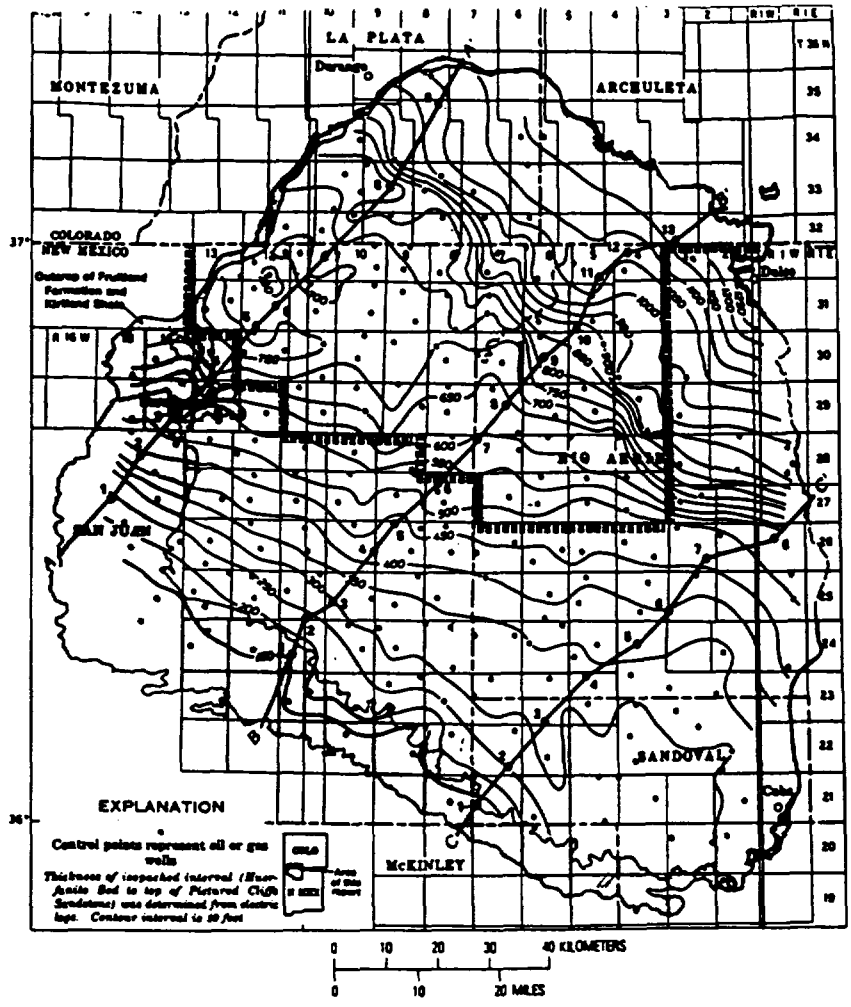

Figure 7. Isopach map of the interval between the Huerfanito Bentonite Bed of the Lewis Shale and the top of the Pictured Cliffs Sandstone. Lines of cross sections A-A', B-B', and C-C' of figure 8 are shown.

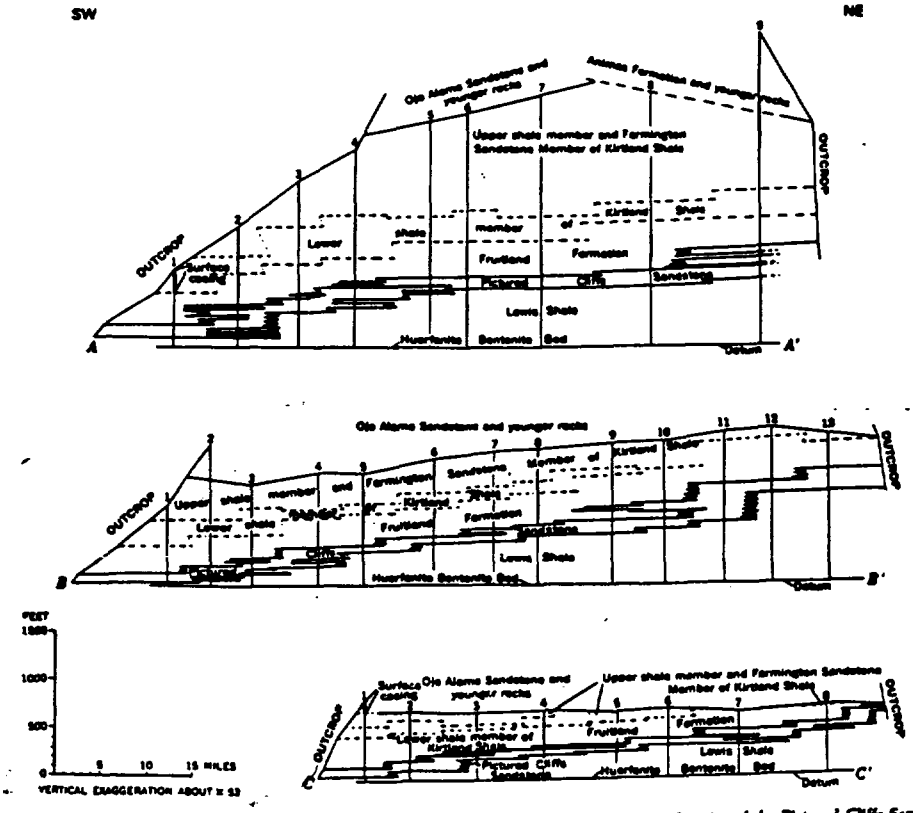

Figure 8. Northeast-trending stratigraphic cross sections showing the northeastward stratigraphic rise of the Pictured Cliffs Sandstone and associated rocks. (Lines of cross sections are shown on figure 7.)

NMOCD Case Nos. 9420 & 9421
July 6, 1988
Dugan Production Corp., et. al.

Map and cross sections from Fassett (1988).

Demarcation line by Dugan et al.

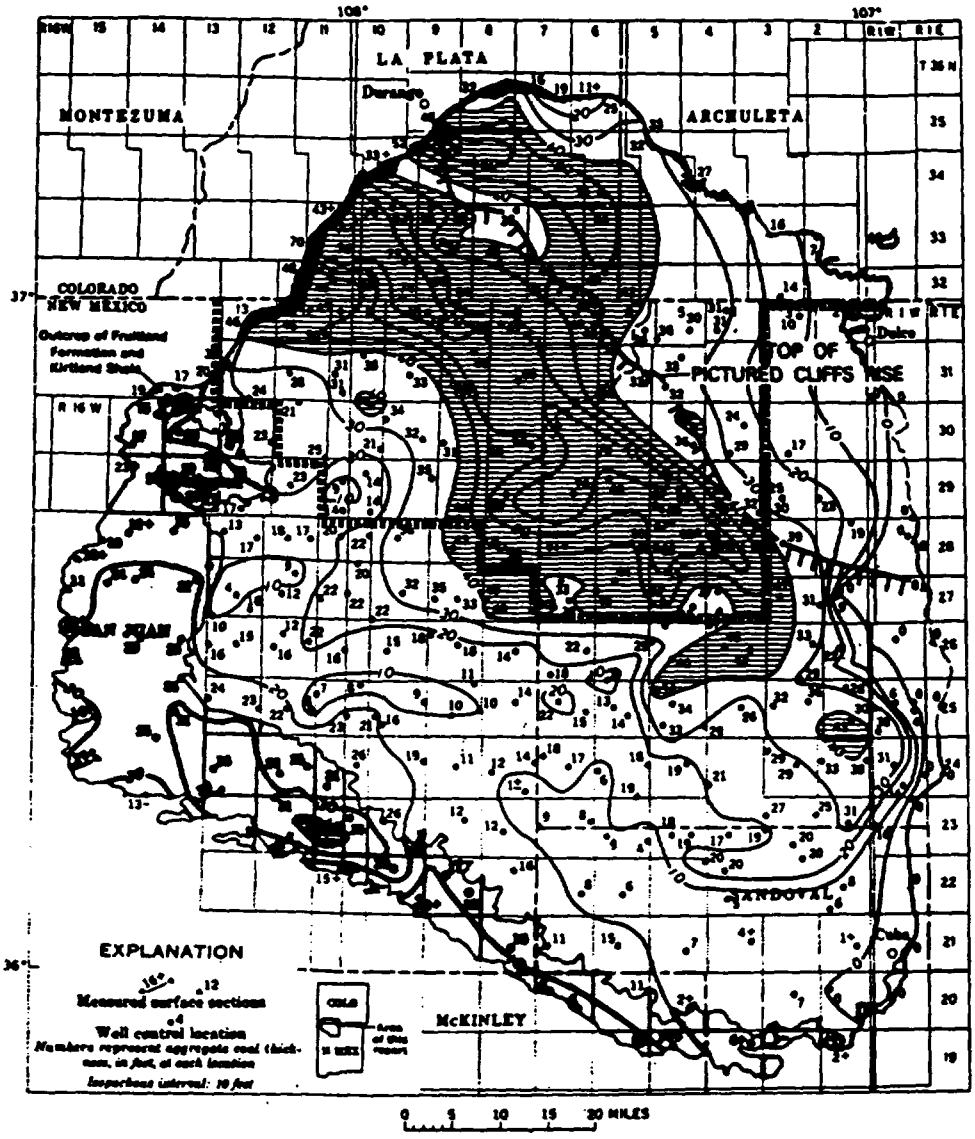

Figure 9. Composite map showing the total-coal-thickness isopachs for Fruitland Formation coal (from figure 6) and the top of the largest stratigraphic rise of the Pictured Cliffs Sandstone in the north-central part of the basin (from figure 7). This composite map shows that the area of thickest Fruitland coal is located southwest of the greatest stratigraphic rise of the Pictured Cliffs. Areas where total-coal thickness is greater than 40 feet are patterned.

Map from Fassett (1988).

Demarcation line by Dugan et al.

NMOCD Case Nos. 9420 & 9421
July 6, 1988
Dugan Production Corp., et. al.
Exhibit No. 2

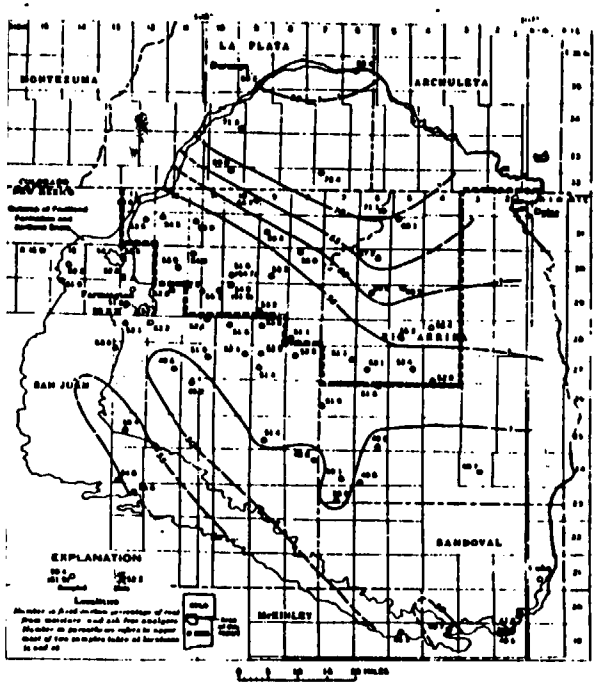

FIGURE 26.—Fixed-carbon percentage of coal samples from the Fruitland Formation. Contour values in percent; interval varies.

Map from Fassett and Hinds (1971).

Demarcation line by Dugan et al.

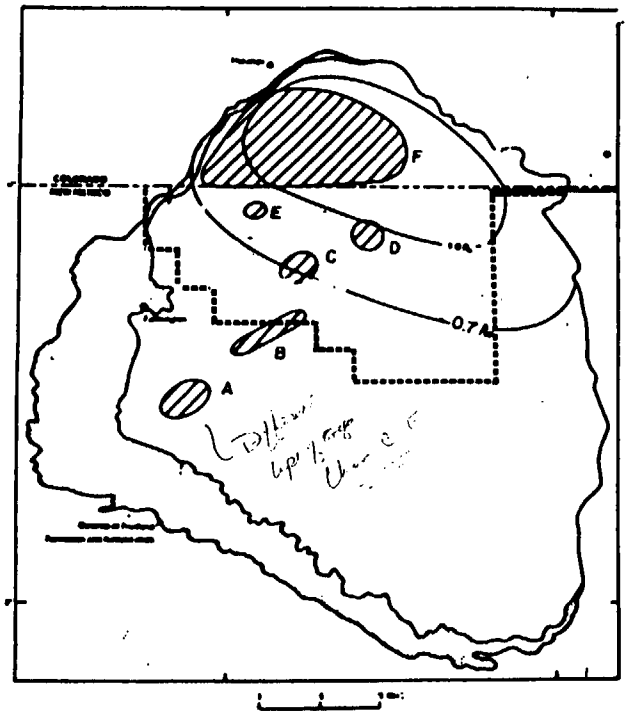

Figure 4. Map of central basin showing isoreflectance (Ro) lines on coals of Fruitland Formation. Study areas are labeled with letters and hachured.

Map from Rice et al (1988).

Demarcation line by Dugan et al.

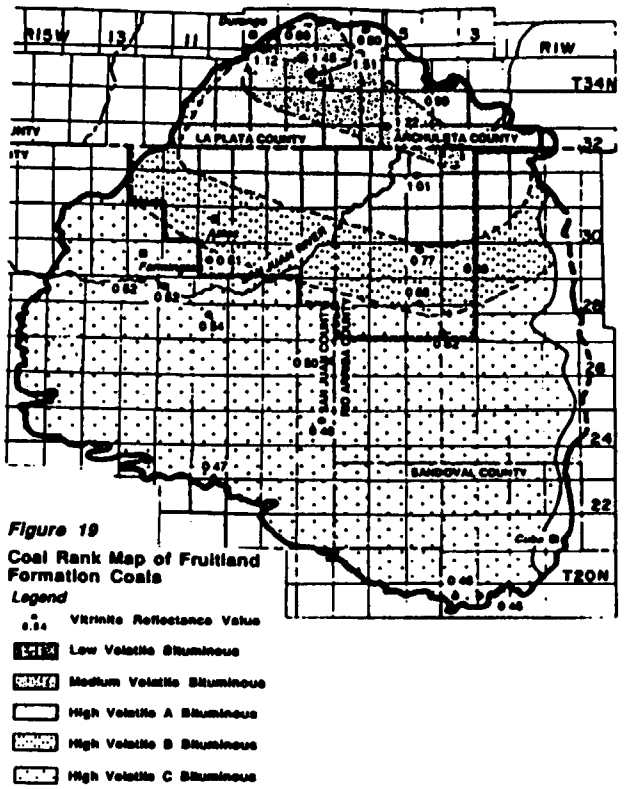

Figure 19
Coal Rank Map of Fruitland Formation Coals

Map from Kelso, Wicks and Kuuskraa (1988) after Rice (1983).

Demarcation line by Dugan et al.

NMOCD Case Nos. 9420 & 9421
July 6, 1988
Dugan Production Corp., et. al.

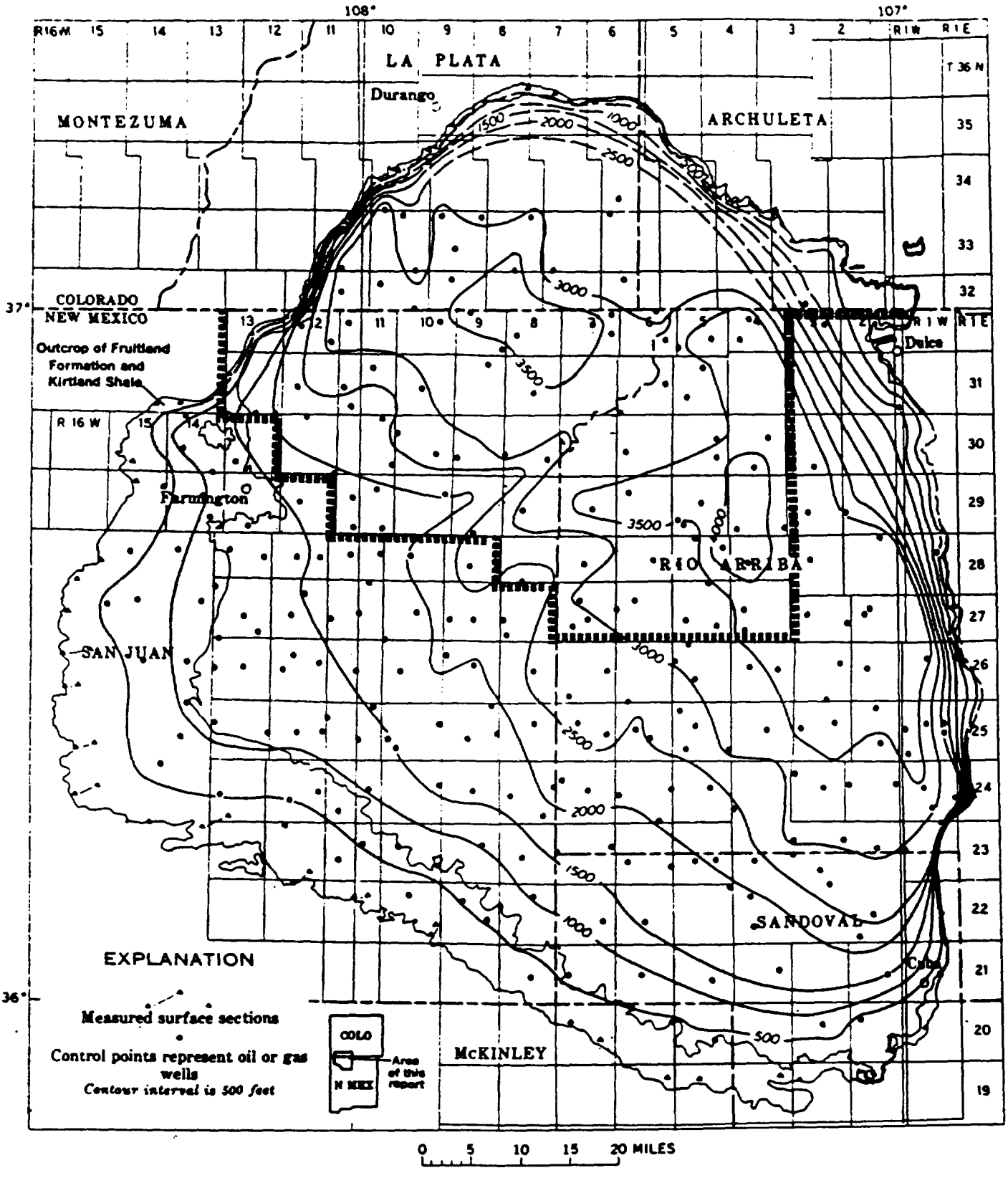

FIGURE 27.—Isopach map showing average thickness of overburden on Fruitland Formation coal deposits.

Map from Fassett and Hinds (1971).

Demarcation line by Dugan et al.

NMOCD Case Nos. 9420 & 9421
July 6, 1988
Dugan Production Corp., et. al.
Exhibit No. 4

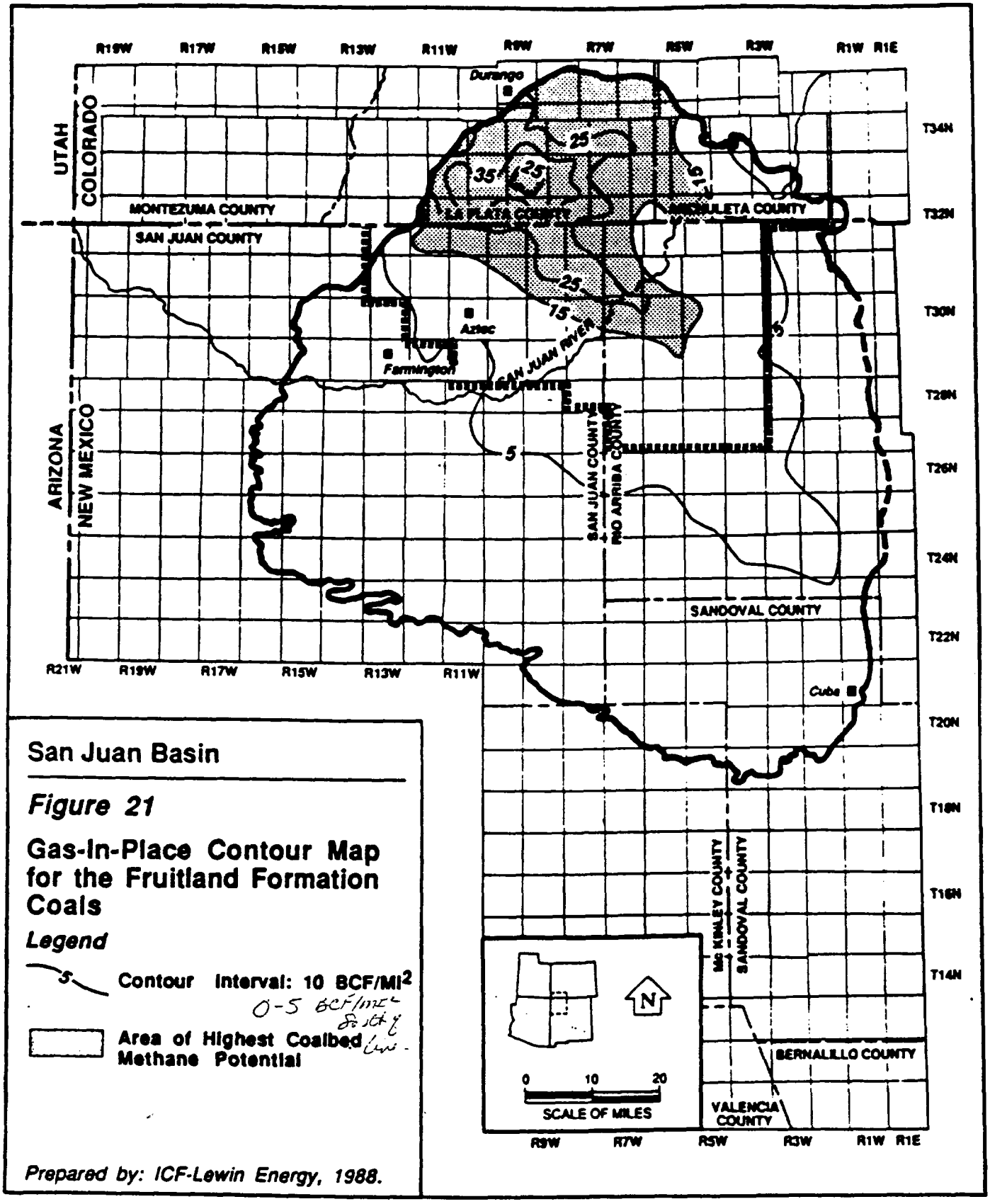

Map from Kelso, Wicks and Kuuskraa (1988).

Demarcation line by Dugan et al.

NMOCD Case Nos. 9420 & 9421
July 6, 1988
Dugan Production Corp., et. al.
Exhibit No. 5

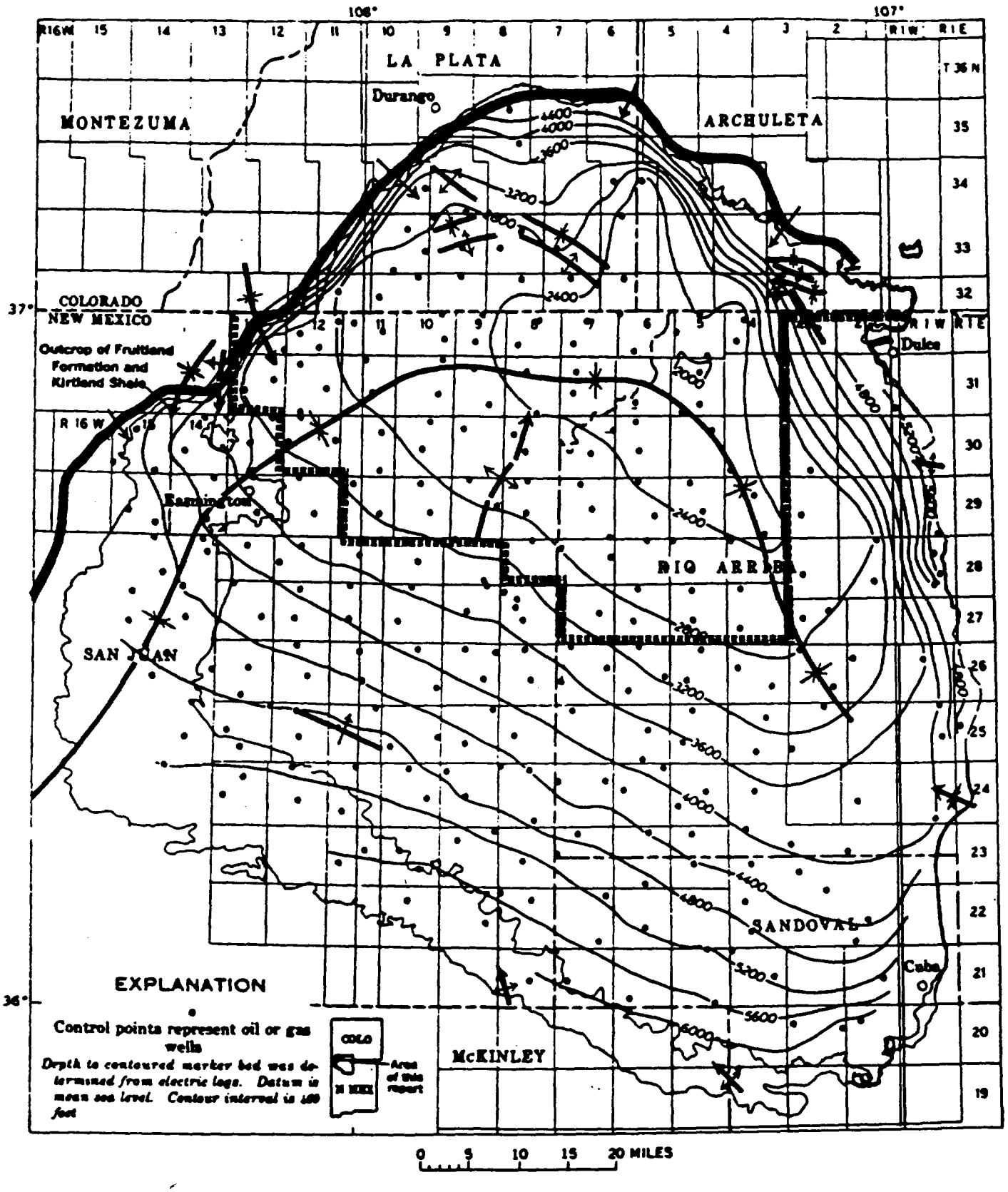

Contour map from Fassett and Hinds (1971).

Tectonic elements from Kelley and Clinton (1960).

Demarcation line by Dugan et al.

EXPLANATION

Crest of anticline, arch, uplift, upwarp, or swell, with direction of plunge

Trough of syncline, basin, or sag, with direction of plunge

Monocline or steep limb of fold, with direction of facing

NMOCD Case Nos. 9420 & 9421
July 6, 1988
Dugan Production Corp., et. al

NMOCD Case Nos. 9420 & 9421
July 6, 1988
Dugan Production Corp., et. al.
Exhibit No. 7

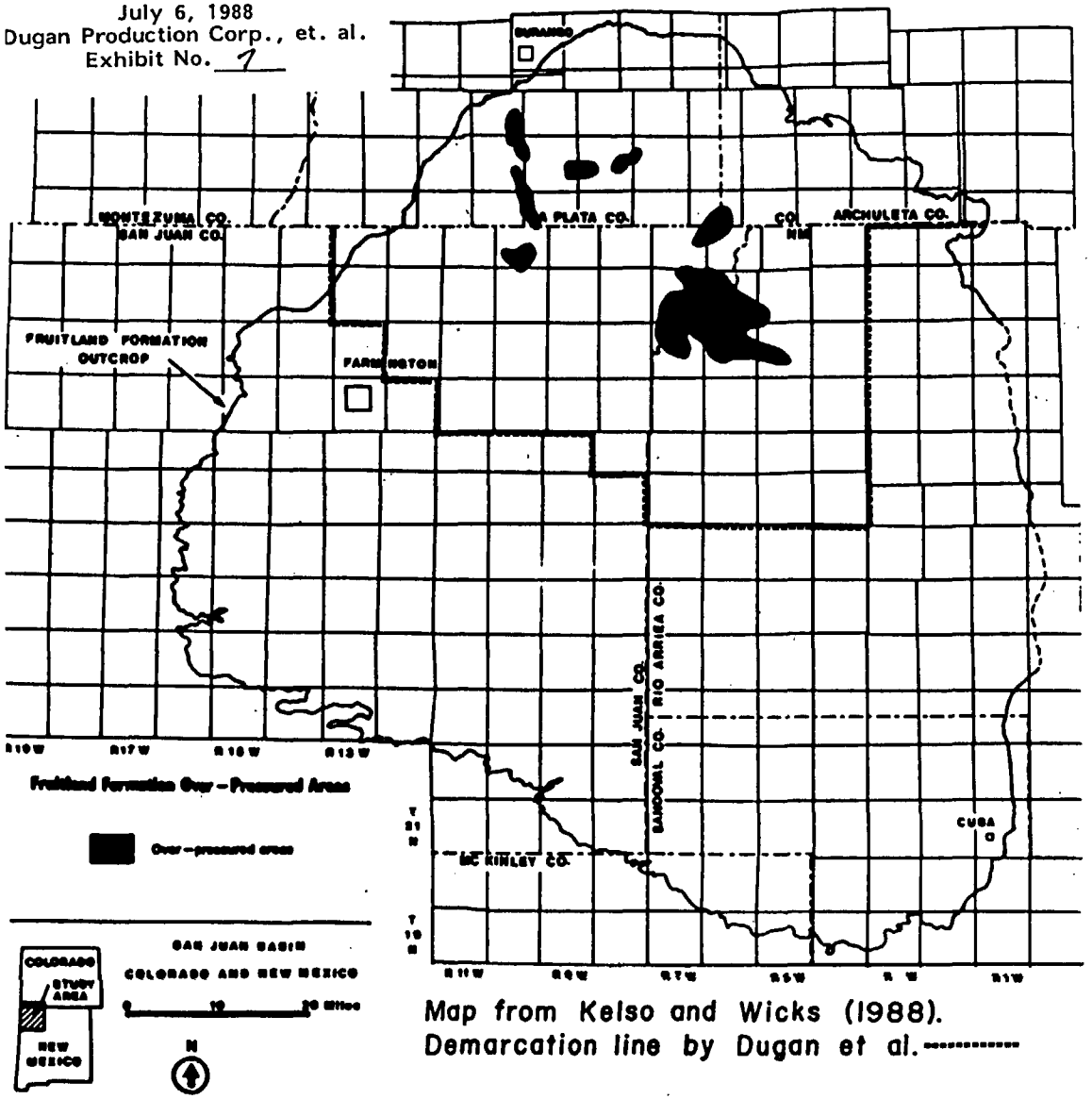

Map from Kelso and Wicks (1988).
Demarcation line by Dugan et al.----------

BUREAU OF ECONOMIC GEOLOGY

DRAFT

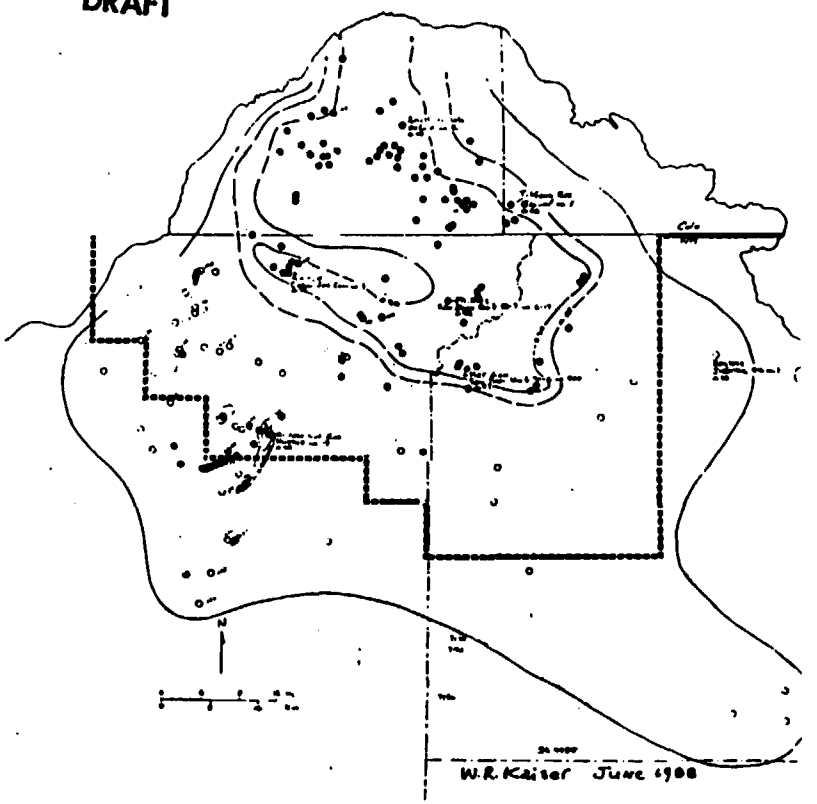

Pressure Gradient (psi/ft)

- > 0.50
- 0.50 - 0.44
- 0.43 - 0.40
- < 0.40

This report was prepared by the University of Texas at Austin as an account of work sponsored by Gas Research Institute ('GRI') under GRI contract No. 5087-214-1544. Neither GRI, members of GRI, nor any person acting on behalf of either;

a. Makes any warranty or representation, express or implied, with respect to the accuracy, completeness, or usefulness of the information contained in this report, or that the use of any information, apparatus, method, or process disclosed in this report may not infringe privately-owned rights, or

b. Assumes any liability with respect to the use of, or for damages resulting from the use of, any information, apparatus, method, or process disclosed in this report.

Demarcation line by Dugan et al.----------

BUREAU OF ECONOMIC GEOLOGY

DRAFT

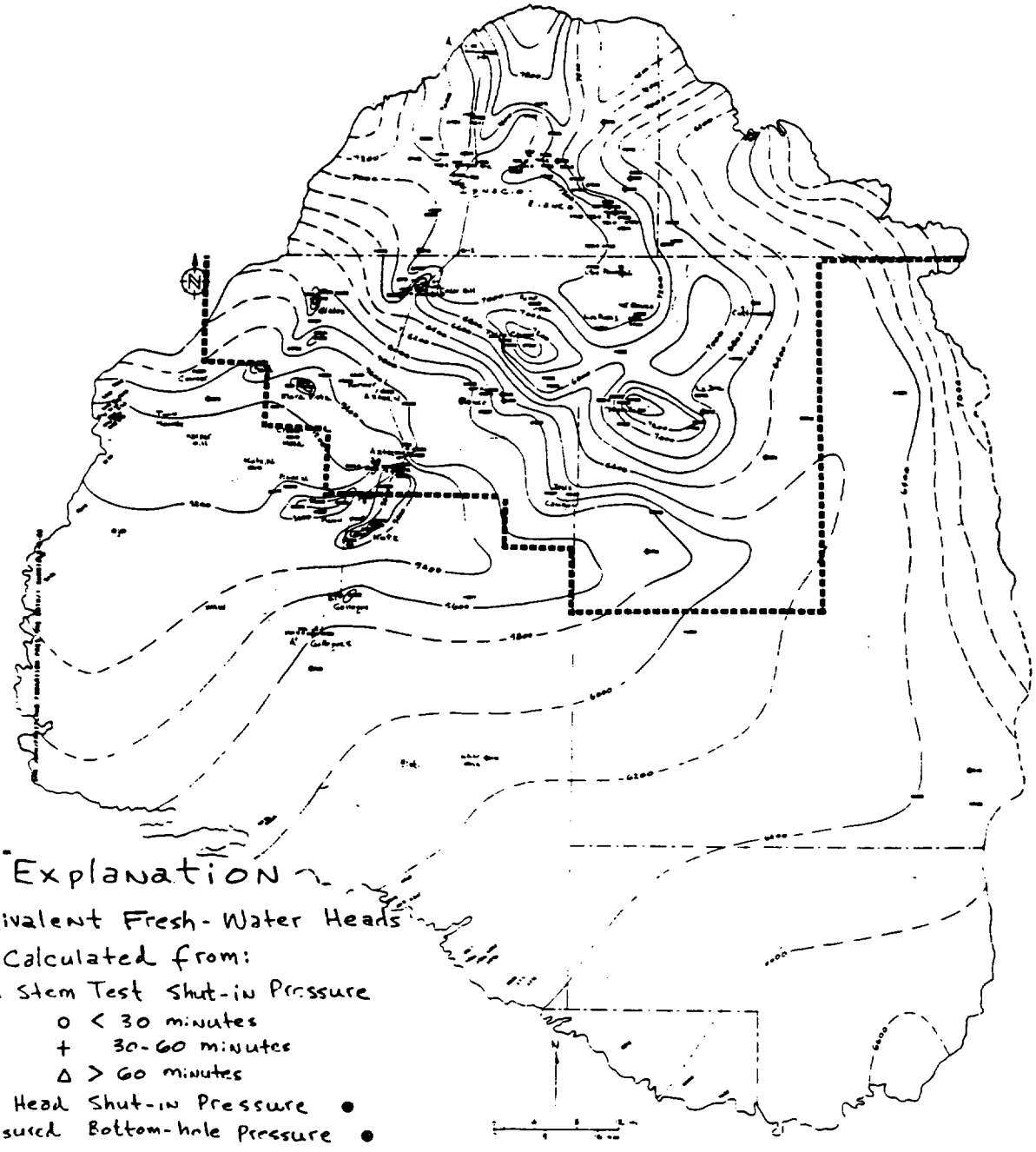

Explanation

Equivalent Fresh-Water Heads
Calculated from:
Drill Stem Test Shut-in Pressure
- o < 30 minutes
- + 30-60 minutes
- Δ > 60 minutes

Well Head Shut-in Pressure ●
Measured Bottom-hole Pressure ●

6565 Static Water Level (location approximate)

◈ Anomalously Low Value not used in Contouring

Aztec : Fruitland Gas Field

W.R. Kaiser June 1988

Demarcation line by Dugan et al. ----------

NMOCD Case Nos. 9420 & 9421
July 6, 1988
Dugan Production Corp., et. al.
Exhibit No. 8

LEGAL DESCRIPTION
OF PROPOSED DIVIDING LINE

Beginning at a point on the New Mexico-Colorado state line, which point is the Northwest corner of Township 32 North, Range 13 West, N.M.P.M., thence South to the Northwest corner of Township 30 North, Range 13 West, N.M.P.M., thence East to the Northwest corner of Township 30 North, Range 12 West, N.M.P.M., thence South to the Northwest corner of Township 29 North, Range 12 West, N.M.P.M., thence East to the Northwest corner of Township 29 North, Range 11 West, N.M.P.M., thence South to the Northwest corner of Township 28 North, Range 11 West, N.M.P.M., thence East to the Northwest corner of Township 28 North, Range 8 West, N.M.P.M., thence South to the Northwest corner of Township 27 North, Range 8 West, N.M.P.M., thence East to the Northwest Corner of Township 27 North, Range 7 West, N.M.P.M., thence South to the Northwest corner of Township 26 North, Range 7 West, N.M.P.M., thence East to the Northwest corner of Township 26 North, Range 3 West, N.M.P.M., thence North along the western boundary of the Jicarilla Apache Tribal Reservation to a point on the New Mexico-Colorado state line, which point is the Northwest corner of Township 32 North, Range 3 West, N.M.P.M., thence East along the New Mexico-Colorado state line to the outcrop of the Fruitland formation.

NMOCD Case Nos. 9420 & 9421
July 6, 1988
Dugan Production Corp., et. al.
Exhibit No. 9

REFERENCES

Fassett, J.E., and Hinds, J.S., 1971, Geology and fuel resources of the Fruitland Formation and Kirtland Shale of the San Juan Basin, New Mexico and Colorado: U.S. Geological Survey Professional paper 676, 76 p.

Fassett, J.E., 1988, Geometry and depositional environment of Fruitland Formation coal beds, San Juan Basin, New Mexico and Colorado: Anatomy of a giant coal-bed methane deposit, in Fassett, J.E., ed., Geology and coal-bed methane resources of the northern San Juan Basin, Colorado and New Mexico: Rocky Mountain Association of Geologists Guidebook.

Kaiser, W.R., June 27, 1988, Personal communication.

Kelso, B.S, and Wicks, D.E., 1988, A geologic analysis of the Fruitland Formation coal and coal-bed methane resources of the San Juan Basin, southwestern Colorado and northwestern New Mexico, in Fassett, J.E. ed., Geology and coal-bed methane resources of the northern San Juan Basin, Colorado and New Mexico: Rocky Mountain Association of Geologists Guidebook.

Kelso, B.S., Wicks, D.E., and Kuuskraa, V.A., 1988, A geologic assessment of natural gas from coal seams in the Fruitland Formation, San Juan Basin: Topical Report (September 1986-September 1987), prepared for Gas Research Institute under contract number 5084-214-1066, 56 p.

Rice, D.D., Threlkeld, C.N., Vuletich, A.K., and Pawlewicz, M.J., 1988, Identification and significance of coal-bed gas, San Juan Basin, northwestern New Mexico and southwestern Colorado, in Fassett, J.E., ed., Geology and coalbed methane resources of the northern San Juan Basin, Colorado and New Mexico: Rocky Mountain Association of Geologists Guidebook.

NMOCD Case Nos. 9420 & 9421
July 6, 1988
Dugan Production Corp., et. al.
Exhibit No. 10

SAN JUAN BASIN FRUITLAND COAL OUTCROP

LOCATION OF GAS SAMPLE ANALYSIS
TESTS USED FOR AVERAGES

(Map from Rice, et al - Map of Central basin showing iso-reflectance (Ro) lines on coals of Fruitland Formation)

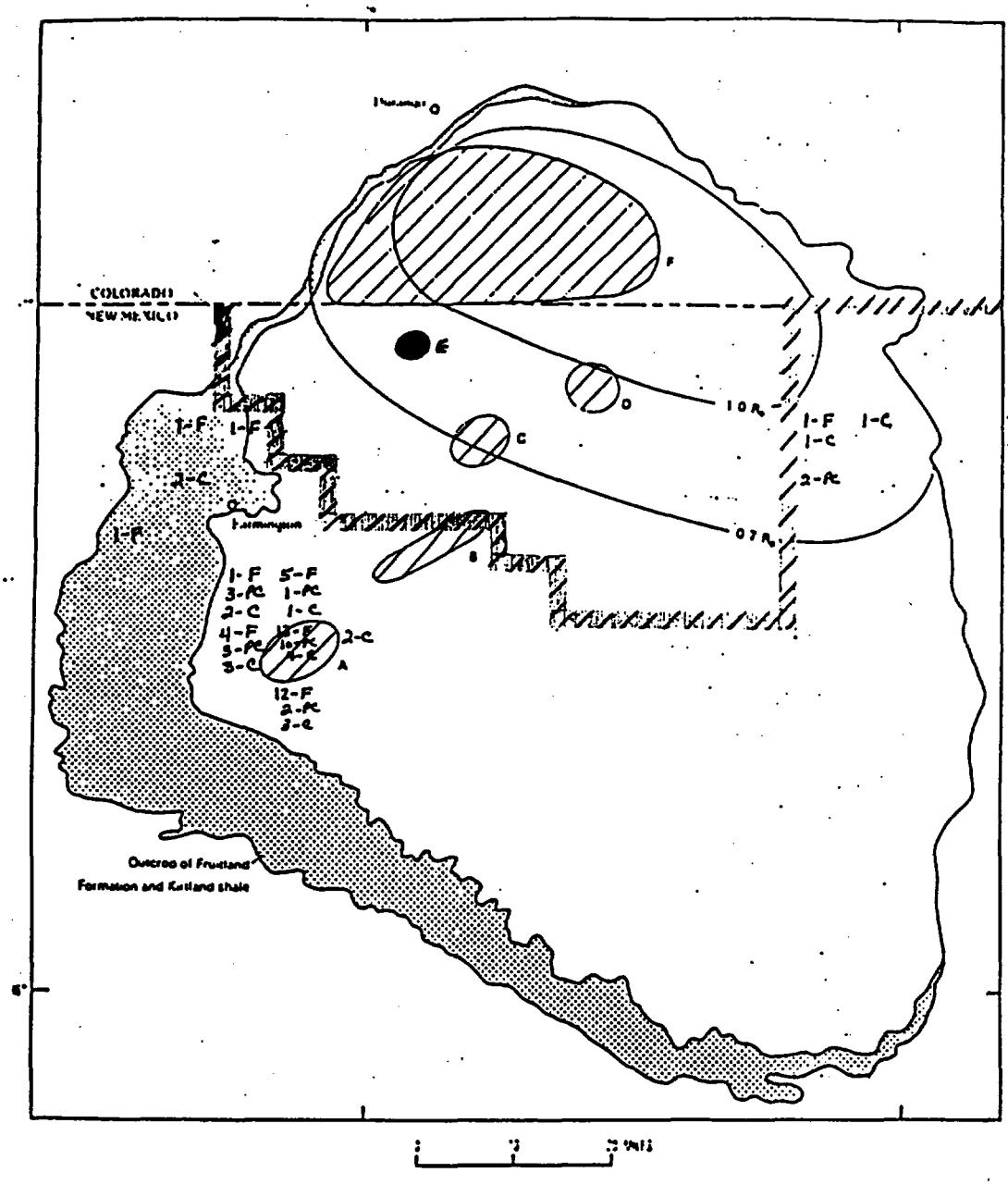

//////// - Demarcation line by Dugan, et al

3 F - Number of Fruitland coal dominated gas analyses used in township

3 PC - Number of Pictured Cliffs coal dominated gas analyses used in township

3 C - Number of combination gas analyses used in township

NMOCD Case Nos. 9420 & 9421
July 6, 1988
Dugan Production Corp., et. al.
Exhibit No. 12

Range 13W

Range 12W

County _____

State _____

Range 11W

Town

Town 27N

Town 26N

Town 25N

WAW

FRLD/PC

F 32,500/a

N.T.B. #1

Sam Jackson #1

Mandana St. #1

Mandana St. #2

NMOCD Case Nos. 9420 & 9421
July 6, 1988
Dugan Production Corp., et. al.
Exhibit No. 14

DECLINE PLOT TO SUPPORT NO DRAINAGE INTERFERENCE ON 160 ACRE SPACING

FRUITLAND - PC FORMATION, SO. GALLEGOS FIELD, SAN JUAN CO, NM

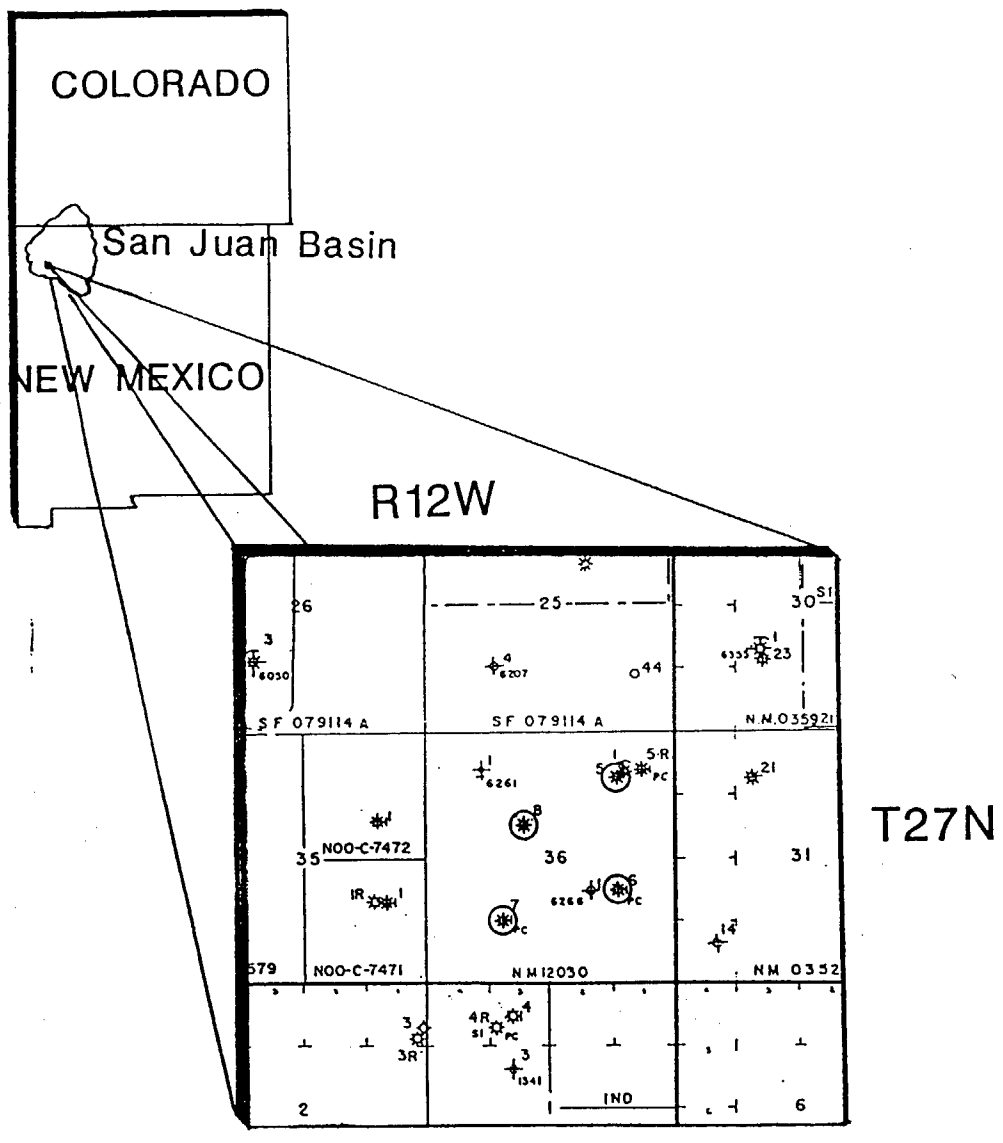

LOCATION MAP

⊛ -Nassau Well Locations

POINT - Nassau No. 5 ESTABLISHED DECLINE TREND is UNAFFECTED BY 3 WELL COMBINED 160 ACRE OFFSET PRODUCTION. THEREFORE NO DRAINAGE INTERFERENCE IS INDICATED.

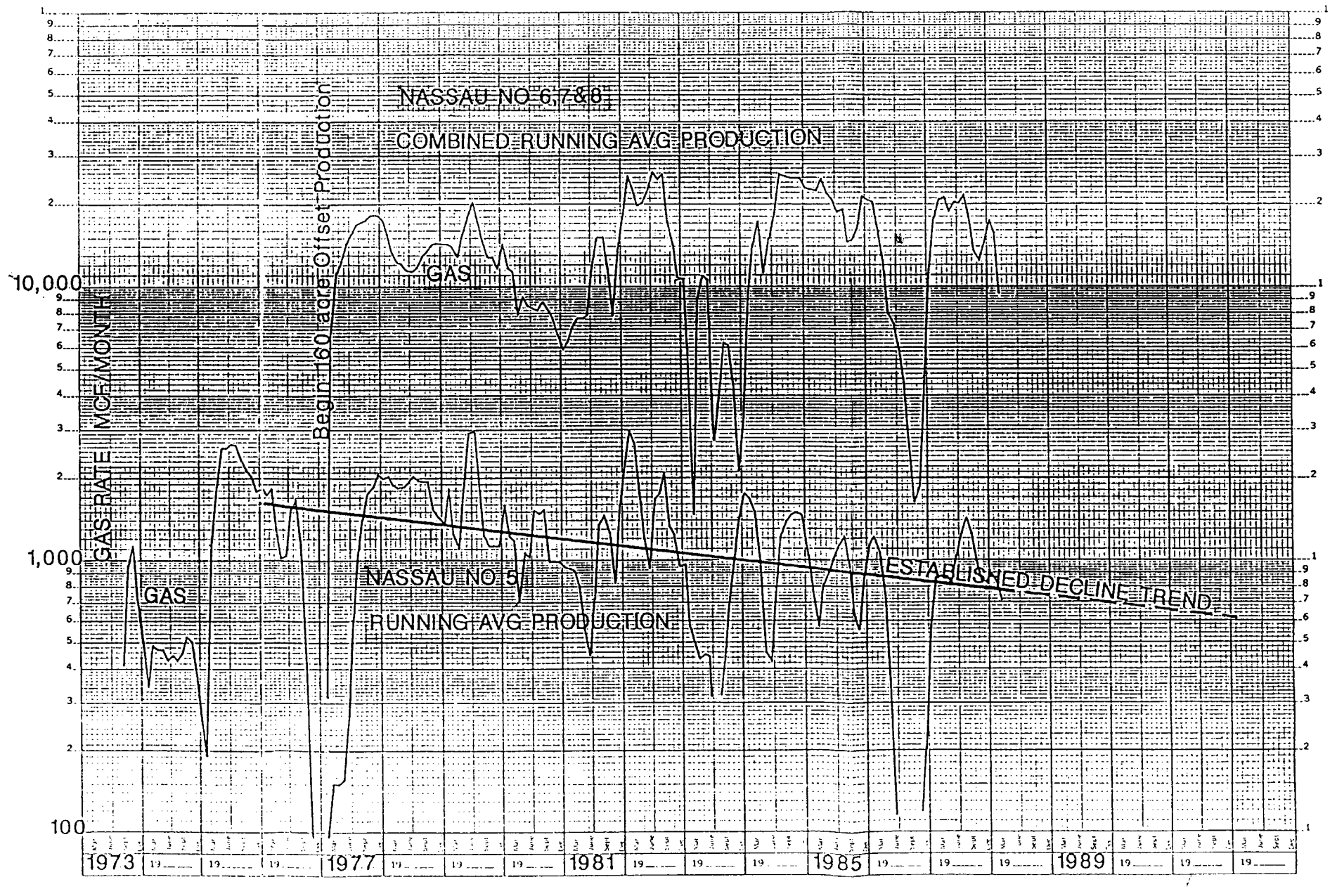

NMOCD Case Nos. 9420 & 9421
July 6, 1988
Dugan Production Corp., et. al.
Exhibit No. 13

JULY 6, 1988

AVERAGE FRUITLAND AND PICTURED CLIFFS GAS ANALYSIS FOR SAN JUAN BASIN WELLS SOUTH OF DEMARCATION LINE PROPOSED BY DUGAN, et al.

	CO2	H2S	N2	METHANE	ETHANE	PROPANE	I-BUTANE	N-BUTANE	I-PENTANE	N-PENTANE	HEXANE PLUS	OXYGEN	TOTAL	SPECIFIC GRAVITY	BTU	C1/C1-5
AVERAGE FRUITLAND DOMINATED GAS	1.270	0.000	0.625	95.368	2.125	0.350	0.060	0.063	0.023	0.017	0.069	0.000	100.000	0.588	1023	0.973
AVERAGE PICTURED CLIFFS DOMINATED GAS	0.525	0.000	0.570	87.747	6.229	2.642	0.488	0.613	0.241	0.157	0.389	0.000	100.000	0.656	1139	0.894
AVERAGE COMBINATION GAS	1.054	0.000	0.744	91.511	4.546	1.262	0.246	0.244	0.112	0.071	0.206	0.000	100.000	0.619	1075	0.934

AVERAGE FRUITLAND GAS ANALYSIS FOR CEDAR HILLS FIELD - NORTH OF DEMARCATION LINE PROPOSED BY DUGAN, et al. (from Decker, et al.)

	CO2	H2S	N2	METHANE	ETHANE	PROPANE	I-BUTANE	N-BUTANE	I-PENTANE	N-PENTANE	HEXANE PLUS	OXYGEN	TOTAL	SPECIFIC GRAVITY	BTU	C1/C1-5
AVERAGE FRUITLAND GAS	6.027	0.000	0.090	93.587	0.153	0.065	0.005	0.005	0.002	0.000	0.017	0.000	99.990	0.614	951	0.957

South of Demarcation Line

NMOCD Case Nos. 9420 & 9421
July 6, 1988
Dugan Production Corp., et. al.
Exhibit No. 11

FRUITLAND - PICTURED CLIFFS GAS ANALYSIS COMARISON

WELL	OPERATOR	LOCATION Q	S	T	R	DATE	POOL	CO2	H2S	N2	METHANE	ETHANE	PROPANE	I-BUTANE	N-BUTANE	I-PENTANE	N-PENTANE	HEXANE PLUS	OXYGEN	TOTAL	SPECIFIC GRAVITY	BTU	C1/C1-5
FRUITLAND DOMINATED GAS																							
VIRG STATE #3	HIXON	M	2	25	12	11/11/81	WAW	1.670	0.000	0.220	95.130	2.890	0.060	0.020	0.010	0.000	0.000	0.000	0.000	100.000	0.587	1019	0.970
RED MAC 2R	DUGAN	A	3	25	12	05/29/88	WAW	2.280	0.000	0.940	91.730	3.440	1.000	0.070	0.330	0.080	0.050	0.080	0.000	100.000	0.618	1039	0.949
RED MAC #1	DUGAN	J	3	25	12	05/29/88	WAW	2.460	0.000	0.290	94.450	2.710	0.070	0.010	0.010	0.000	0.000	0.000	0.000	100.000	0.594	1008	0.971
KA DA PAH 1	HIXON	K	3	25	12	03/10/87	WAW	0.210	0.000	1.160	97.410	0.910	0.200	0.070	0.010	0.000	0.000	0.030	0.000	100.000	0.573	1013	0.988
KA DA PAH #1R	HIXON	N	3	25	12	11/22/86	WAW	2.280	0.000	0.280	94.750	2.530	0.100	0.020	0.010	0.000	0.000	0.030	0.000	100.000	0.593	1011	0.973
IN NI DA PAH #1R	HIXON	I	4	25	12	11/18/85	WAW	3.270	0.000	0.240	91.970	5.050	0.180	0.000	0.030	0.030	0.030	0.200	0.000	100.000	0.611	1041	0.945
KA-DA-PAH #2	HIXON	L	4	25	12	09/23/87	WAW	2.160	0.000	0.290	95.600	1.890	0.040	0.010	0.000	0.000	0.000	0.010	0.000	100.000	0.587	1005	0.980
CHRIS RAY COM #1	HIXON	A	5	25	12	09/23/78	WAW	1.830	0.000	0.240	96.090	1.720	0.070	0.020	0.010	0.000	0.000	0.020	0.000	100.000	0.584	1005	0.981
FEDERAL C #5	HIXON	F	6	25	12	07/23/87	WAW	0.230	0.000	1.770	95.560	1.440	0.680	0.100	0.130	0.020	0.020	0.050	0.000	100.000	0.583	1024	0.976
PHL FEDERAL #1	HIXON	E	9	25	12	10/22/87	WAW	0.710	0.000	1.090	94.630	2.370	0.760	0.140	0.150	0.040	0.030	0.080	0.000	100.000	0.593	1038	0.964
YA-GEE-TAH #1	HIXON	F	10	25	12	08/29/86	WAW	2.260	0.000	0.220	94.920	2.500	0.060	0.010	0.010	0.000	0.000	0.020	0.000	100.000	0.591	1010	0.974
FEDERAL 2	HIXON	A	20	25	12	05/27/87	WAW	0.330	0.000	2.670	96.310	0.450	0.150	0.060	0.010	0.000	0.000	0.020	0.000	100.000	0.574	995	0.993
DAN DEAL #1	DUGAN	D	7	26	12	04/03/85	WAW	1.910	0.000	1.010	93.250	2.800	0.500	0.100	0.110	0.060	0.050	0.210	0.000	100.000	0.607	1031	0.963
ALLEN #1	DUGAN	C	12	26	12	02/03/70	GALLEGOS	0.000	0.000	0.610	99.020	0.260	0.060	0.020	0.000	0.010	0.020	0.000	0.000	100.000	0.560	1013	0.996
DESG. HITTER 1	DUGAN	D	27	26	12	05/29/88	WAW	2.070	0.000	0.960	95.690	1.160	0.070	0.010	0.020	0.000	0.000	0.020	0.000	100.000	0.586	995	0.987
DESG. HITTER 2	DUGAN	M	27	26	12	05/29/88	WAW	2.050	0.000	0.400	95.630	1.610	0.200	0.020	0.060	0.010	0.000	0.010	0.000	100.000	0.588	1007	0.981
S.J. FED COM S#1	CHEVRON	B	32	26	12	04/11/85	WAW	0.960	0.000	0.900	93.280	3.580	0.960	0.180	0.080	0.010	0.000	0.050	0.000	100.000	0.600	1046	0.951
CHACO WASH COM 2	HIXON	I	22	26	12	10/06/84	WAW	0.000	0.000	0.620	98.170	0.910	0.100	0.000	0.000	0.000	0.000	0.000	0.000	100.000	0.564	1014	0.950
OLD HICKORY #2	DUGAN	J	33	26	12	05/25/68	WAW	1.370	0.000	0.260	96.430	1.700	0.180	0.020	0.020	0.000	0.000	0.020	0.000	100.000	0.589	1015	0.980
NAVAJO LB #1	CHEVRON	M	33	26	12	04/11/85	WAW	1.510	0.000	0.330	95.220	2.450	0.190	0.020	0.040	0.010	0.010	0.220	0.000	100.000	0.592	1028	0.972
M. WASHINGTON #1	DUGAN	A	34	26	12	11/19/85	WAW	2.310	0.000	0.270	94.380	2.540	0.330	0.050	0.090	0.000	0.000	0.030	0.000	100.000	0.597	1017	0.969
RACHEL #2	DUGAN	I	34	26	12	05/25/88	WAW	2.590	0.000	0.350	94.410	2.590	0.030	0.010	0.010	0.000	0.000	0.010	0.000	100.000	0.595	1005	0.973
E. WASHINGTON #3	DUGAN	D	35	26	12	11/19/85	WAW	2.060	0.000	0.340	94.280	2.630	0.440	0.040	0.060	0.030	0.020	0.060	0.000	100.000	0.595	1022	0.967
E. WASHINGTON #1	DUGAN	N	35	26	12	11/19/85	WAW	2.370	0.000	0.290	93.400	3.440	0.350	0.030	0.050	0.020	0.020	0.030	0.000	100.000	0.602	1023	0.960
E. WASHINGTON #2	DUGAN	F	35	26	12	11/19/85	WAW	2.350	0.000	0.220	93.140	3.620	0.340	0.050	0.070	0.010	0.010	0.190	0.000	100.000	0.607	1032	0.958
CHACO LMTD #1J	MERRION	K	1	26	13	05/13/85	WAW	0.190	0.000	1.050	96.320	1.000	0.960	0.180	0.130	0.060	0.050	0.040	0.000	100.000	0.583	1036	0.976
CHACO LMTD #1	MERRION	M	1	26	13	11/06/85	WAW	0.260	0.000	1.500	96.500	1.200	0.250	0.040	0.000	0.090	0.110	0.050	0.000	100.000	0.578	1018	0.983
CHACO LMTD #2J	MERRION	E	12	26	13	10/11/84	WAW	0.300	0.000	0.670	95.510	2.250	0.700	0.120	0.170	0.060	0.050	0.160	0.000	100.000	0.589	1049	0.966
CHACO LMTD #3	MERRION	F	12	26	13	10/11/84	WAW	0.300	0.000	0.670	95.510	2.250	0.700	0.120	0.170	0.060	0.050	0.160	0.000	100.000	0.587	1049	0.966
DA-ON-PAH #1	MERRION	H	25	27	12	12/22/87	GALLEGOS	0.240	0.000	0.670	97.690	1.120	0.220	0.050	0.000	0.000	0.000	0.010	0.000	100.000	0.566	1018	0.986
PETE #1R	MERRION	I	35	27	12	10/03/84	GALLEGOS	0.200	0.000	0.530	98.080	0.840	0.190	0.030	0.030	0.010	0.030	0.050	0.000	100.000	0.568	1022	0.989
NASSAU #6	MCHUGH	J	36	27	12	04/06/87	GALLEGOS	0.360	0.000	0.280	96.070	2.060	0.700	0.120	0.150	0.050	0.030	0.180	0.000	100.000	0.586	1047	0.969
NASSAU #7	MCHUGH	K	36	27	12	03/24/88	GALLEGOS	0.300	0.000	0.390	96.020	0.870	0.240	0.050	0.040	0.010	0.010	0.070	0.000	100.000	0.565	1023	0.986
NASSAU #2	MCHUGH	F	36	27	12	03/24/88	GALLEGOS	0.340	0.000	0.230	97.220	1.810	0.290	0.060	0.030	0.010	0.000	0.020	0.000	100.000	0.577	1025	0.978
HI-ROLL #2	MERRION	M	35	27	13	06/01/87	DAK	1.740	0.000	0.790	91.490	5.020	0.500	0.110	0.110	0.040	0.020	0.180	0.000	100.000	0.611	1044	0.940
RAVEN AREA METER	DUGAN		26	28	15	10/25/87	DJD	2.570	0.000	0.250	92.670	3.060	0.800	0.180	0.110	0.070	0.020	0.070	0.000	100.000	0.611	1032	0.956
JIC 456 #1	BAYLESS	N	11	30	3	05/19/88	UNDES	0.797	0.000	0.248	95.221	2.117	0.306	0.052	0.069	0.027	0.022	0.140	0.000	100.000	0.586	1037	0.964
7 OF DIAMONDS #1	DUGAN	I	2	30	15	12/29/84	UNDES	0.700	0.000	0.550	96.370	0.190	0.100	0.020	0.020	0.000	0.000	0.050	0.000	100.000	0.568	1007	0.997
WINIFRED #2 PC	DUGAN	B	35	30	14	10/08/87	HARPER	0.940	0.000	0.370	96.800	0.890	0.560	0.120	0.130	0.050	0.030	0.110	0.000	100.000	0.583	1029	0.982
AVG FRUITLAND DOMINATED GAS								1.270	0.000	0.625	95.398	2.125	0.350	0.060	0.065	0.025	0.017	0.065	0.000	100.000	0.588	1020	0.972

FRUITLAND - PICTURED CLIFFS GAS ANALYSIS COMARISON

WELL	OPERATOR	LOCATION Q	S	T	R	DATE	POOL	CO2	H2S	N2	METHANE	ETHANE	PROPANE	I-BUTANE	N-BUTANE	I-PENTANE	N-PENTANE	HEXANE PLUS	OXYGEN	TOTAL	SPECIFIC GRAVITY	BTU	C1/C1-5
PICTURED CLIFFS DOMINATED GAS																							
NIXON FED #1J	NIXON	B	4	25	12	08/22/85	WAW	1.160	0.000	0.850	87.320	6.310	2.520	0.460	0.620	0.230	0.170	0.360	0.000	100.000	0.658	1132	0.894
BLE-NA-NUF-FAH 1	NIXON	I	5	25	12	04/13/87	WAW	1.410	0.000	1.170	86.300	5.820	2.990	0.570	0.850	0.310	0.210	0.370	0.000	100.000	0.672	1141	0.889
BENGAL 6 #6	DUGAN	P	2	26	12	04/09/87	GALLEGOS	0.690	0.000	0.400	82.320	9.950	4.290	0.600	1.030	0.270	0.220	0.230	0.000	100.000	0.693	1206	0.834
CHACO #4	MERRION	D	7	26	12	11/09/85	WAW	1.000	0.000	0.280	87.640	6.810	2.410	0.480	0.490	0.250	0.140	0.500	0.000	100.000	0.658	1145	0.892
CHACO PLANT 1&2	MERRION		18	26	12	05/07/86	WAW	0.740	0.000	0.260	88.120	6.150	2.500	0.490	0.620	0.260	0.180	0.680	0.000	100.000	0.661	1156	0.896
MIKE #1J	DUGAN	D	20	26	12	05/12/68	WAW	1.160	0.000	0.400	89.570	5.670	1.920	0.440	0.300	0.200	0.060	0.280	0.000	100.000	0.637	1107	0.912
DIETRICH 28 G#1	ALEXANDER	G	28	26	12	03/06/87	WAW	1.100	0.000	1.100	85.480	7.190	3.270	0.570	0.670	0.260	0.130	0.230	0.000	100.000	0.669	1146	0.876
DIETRICH 28 J#2	ALEXANDER	J	28	26	12	03/06/87	WAW	1.190	0.000	0.300	88.540	6.130	2.340	0.480	0.420	0.220	0.090	0.290	0.000	100.000	0.647	1123	0.901
ABO #2	DUGAN	M	28	26	12	05/29/88	WAW	1.140	0.000	0.450	87.120	6.940	2.710	0.490	0.570	0.210	0.130	0.240	0.000	100.000	0.657	1137	0.887
CHACO WASH #1 PC	NIXON	C	32	26	12	09/23/87	WAW	1.220	0.000	0.970	88.960	5.550	1.760	0.510	0.350	0.260	0.230	0.190	0.000	100.000	0.642	1103	0.911
OLD HICKORY #1	DUGAN	F	33	26	12	04/11/83	WAW	1.120	0.000	0.280	89.410	5.490	2.170	0.450	0.440	0.210	0.100	0.330	0.000	100.000	0.642	1118	0.910
RUBY #1	BAYLESS	C	34	26	12	01/06/86	WAW	1.350	0.000	0.310	87.690	6.600	2.230	0.380	0.560	0.200	0.150	0.530	0.000	100.000	0.658	1136	0.897
CHACO #11	MERRION	E	1	26	13	11/07/85	WAW	1.150	0.000	0.970	88.140	5.200	2.650	0.510	0.620	0.240	0.220	0.300	0.000	100.000	0.655	1125	0.903
CHACO #5	MERRION	P	1	26	13	11/08/85	WAW	0.950	0.000	0.800	89.350	5.420	2.020	0.470	0.370	0.230	0.090	0.300	0.000	100.000	0.640	1110	0.912
CHACO #3	MERRION	H	12	26	13	01/10/86	WAW	1.040	0.000	0.410	89.250	5.950	1.920	0.360	0.340	0.140	0.080	0.510	0.000	100.000	0.643	1118	0.910
REX #3J	DUGAN	C	18	27	12	05/25/88	WAW	0.580	0.000	0.280	89.220	6.090	2.670	0.500	0.660	0.240	0.170	0.590	0.000	100.000	0.658	1156	0.895
PINEY #1	DUGAN	N	4	27	13	05/04/85	WAW	0.520	0.000	0.370	88.740	5.780	2.660	0.490	0.620	0.240	0.150	0.430	0.000	100.000	0.651	1145	0.899
PINEY #2	DUGAN	P	9	27	13	06/01/88	WAW	0.560	0.000	0.270	88.730	5.790	2.590	0.200	0.890	0.230	0.160	0.580	0.000	100.000	0.654	1150	0.900
HI-ROLL #4	MERRION	D	35	27	13	08/01/87	WAW	1.280	0.000	2.090	87.790	4.960	2.200	0.440	0.500	0.200	0.120	0.420	0.000	100.000	0.653	1100	0.912
JIC 451 #1	BAYLESS	K	4	29	3	12/04/87	UNDES	0.000	0.000	0.000	85.440	7.235	4.770	0.683	1.094	0.292	0.218	0.268	0.000	100.000	0.677	1202	0.857
JIC 452 #1-Y	BAYLESS	P	6	29	3	11/30/87	UNDES	0.066	0.000	0.000	88.551	5.782	2.686	0.674	0.858	0.363	0.281	0.539	0.000	100.001	0.658	1179	0.891
AVG PICTURED CLIFFS DOMINATED GAS								0.925	0.000	0.570	87.747	6.229	2.642	0.486	0.613	0.241	0.157	0.389	0.000	100.000	0.656	1139	0.894
COMBINATION GAS																							
MD STATE COM #2	NIXON	B	2	25	12	11/19/86	WAW	1.780	0.000	0.800	90.630	4.990	1.060	0.180	0.240	0.090	0.060	0.170	0.000	100.000	0.624	1063	0.932
MD STATE COM #1	NIXON	C	2	25	12	01/05/88	WAW	2.070	0.000	1.010	91.170	3.420	1.290	0.350	0.380	0.140	0.090	0.080	0.000	100.000	0.626	1055	0.941
RED MAC #3	DUGAN	D	3	25	12	05/12/88	WAW	0.270	0.000	0.400	92.160	4.420	1.890	0.190	0.320	0.120	0.070	0.160	0.000	100.000	0.614	1054	0.929
WESTERN FED #9	DUGAN	E	7	26	11	02/04/88	GALLEGOS	0.920	0.000	0.310	91.660	4.460	1.630	0.300	0.370	0.120	0.060	0.150	0.000	100.000	0.620	1058	0.929
WESTERN FED #7	DUGAN	M	7	26	11	04/26/87	GALLEGOS	0.180	0.000	2.530	89.140	4.930	0.620	0.140	0.170	0.070	0.050	0.170	0.000	100.000	0.618	1067	0.918
CHACO PLANT #1J	DUGAN	P	17	26	12	11/05/21	WAW	1.010	0.000	0.450	91.180	5.100	1.480	0.380	0.140	0.160	0.020	0.080	0.000	100.000	0.619	1061	0.926
ABO #1	DUGAN	D	28	26	12	11/07/83	WAW	1.720	0.000	0.360	93.480	2.420	0.580	0.200	0.160	0.060	0.020	0.600	0.000	100.000	0.617	1043	0.961
NMP STATE #1	NIXON	C	32	26	12	03/31/88	WAW	1.640	0.000	0.310	92.050	3.950	1.490	0.270	0.210	0.030	0.020	0.050	0.000	100.000	0.614	1041	0.949
S.J. STATE COM 1	NIXON	N	32	26	12	09/23/87	WAW	1.760	0.000	0.280	90.940	6.060	0.850	0.080	0.010	0.000	0.000	0.020	0.000	100.000	0.612	1056	0.929
CHACO UNIT #20	MERRION	B	1	26	13	11/06/85	WAW	0.220	0.000	1.550	92.630	3.380	1.230	0.280	0.210	0.180	0.160	0.160	0.000	100.000	0.610	1049	0.945
BARTELSVILLE #1	MERRION	C	2	26	13	11/06/85	WAW	0.900	0.000	2.620	90.270	3.810	1.250	0.340	0.240	0.150	0.150	0.290	0.000	100.000	0.627	1061	0.938
SOUTHLAND WELLS	MERRION	F	3	26	12	11/06/85	WAW	1.100	0.000	0.210	90.960	5.150	1.470	0.270	0.260	0.190	0.170	0.220	0.000	100.000	0.626	1095	0.924
KAESAL #5P	MORROW	I	36	27	12	04/06/87	GALLEGOS	0.440	0.000	1.010	93.590	2.250	1.260	0.250	0.340	0.100	0.070	0.090	0.000	100.000	0.604	1063	0.951
MI-ROLL #3	MERRION	E	35	27	13	05/07/85	WAW	2.130	0.000	0.400	90.020	5.620	1.060	0.310	0.140	0.130	0.020	0.170	0.000	100.000	0.629	1069	0.925
MI-ROLL #1R	MERRION	O	35	27	13	05/08/85	WAW	1.530	0.000	0.460	91.460	5.220	0.740	0.200	0.110	0.090	0.020	0.230	0.000	100.000	0.617	1066	0.935
COM #2	DUGAN	A	2	29	14	12/11/87	HARPER	0.550	0.000	0.300	87.400	6.780	2.750	0.480	0.670	0.250	0.190	0.630	0.000	100.000	0.664	1165	0.887
COM #3	DUGAN	J	2	29	14	10/12/87	HARPER	0.560	0.000	0.240	96.080	1.660	0.740	0.140	0.190	0.060	0.050	0.260	0.000	100.000	0.591	1051	0.971
JIC 516 #1	BAYLESS	D	7	30	2	06/06/88	UNDES	0.162	0.000	0.961	93.554	5.654	1.643	0.309	0.351	0.120	0.075	0.172	0.000	100.000	0.620	1092	0.917
JIC 461 #1	BAYLESS	L	14	30	3	11/30/87	UNDES	1.068	0.000	0.000	93.268	4.496	0.571	0.123	0.121	0.077	0.043	0.193	0.000	99.995	0.602	1056	0.945
AVG COMBINATION GAS								1.054	0.000	0.744	91.511	4.546	1.262	0.248	0.244	0.112	0.071	0.206	0.000	100.000	0.619	1075	0.934

We suggest that structural activity contributed to relatively greater stratigraphic rise in this area and, indirectly, to the distribution of thick Fruitland coal seams (Ayers and others, this volume, Fig. 2.20). The Pictured Cliffs shoreline prograded rapidly basinward across the southern half of the basin. After the shoreline crossed the structural hingeline, sporadic structural activity began and the northern part of the basin subsided more rapidly to accommodate a greater thickness of sediment. The changing balance between sediment input and pulsatory subsidence north of the hingeline resulted in oscillation and aggradation of the shoreline, accounting for the most significant stratigraphic rise of the Pictured Cliffs in the basin and allowing time for thick peat accumulation landward of the oscillating shoreline. This model explains why the greatest net thickness of Fruitland coal is in the northern part of the basin, and why coal seams in the Fruitland Formation are thicker than those in subjacent continental strata. Further testing is needed to verify the existence of the structural hingeline; seismic studies would be especially useful. A regional map of structural elements that were identified in regional reflection seismic lines shows northwest-trending faults in the area of this hingeline (Huffman and Taylor, 1991).

Structural controls on producibility of coalbed methane

Earlier studies suggested that Fruitland coal seams have limited extent and that they are bounded on their basinward (northeast) margins by Pictured Cliffs shoreline sandstone and along paleostrike (northwest–southeast) by Fruitland fluvial sandstones (Fassett and Hinds, 1971; Fassett, 1986). However, as we have demonstrated, some Fruitland coal seams may be regionally continuous, overriding and thinning over upper Pictured Cliffs tongues (Figs. 4.16 and 4.18) in the paleodip direction. Updip pinch-out lines of upper Pictured Cliffs tongues may be areas where Fruitland coal seams drape over shoreline sandstones and have a higher fracture density because of compaction-induced fractures. The structural attitude of an upper Fruitland coal bed (Fig. 4.19) differs markedly from the structural attitude of other strata, such as the Huerfanito Bentonite (Fig. 4.2). Along paleostrike, coal seams split and interfinger with fluvial channel-fill sandstone complexes (Fig. 4.17), and many of these coal benches, rather than terminating against the channel sandstones, override or underlie them, forming zigzag splits similar to those described in coal-bearing strata in other basins (Britten and others, 1975; Ayers and Kaiser, 1984). Although these coal seams pinch and swell, they are laterally continuous, which contributes to their effectiveness as aquifers. Fractures related to compactional folding of coal beds are well documented (Donaldson, 1979; Houseknecht and Iannacchione, 1982; Tyler and others, 1991). If such fracture systems are sufficiently developed, areas of interbedded sandstones and coal seams would be good targets for coalbed methane exploration (Fig. 4.20).

This study has shown that Fruitland coal beds are more extensive and complex than previously inferred (Figs. 4.16–4.18). The significance of these findings is threefold. First, coalbed methane reservoirs are larger (more extensive) than previously thought. Second, compaction-induced fractures, and therefore enhanced coalbed permeability, may occur in areas where extensive coal seams drape over shoreline sandstones or form zigzag splits with channel-fill sandstone complexes. Finally, the greater lateral extent of coal seams, inferred from this research, is critical to the interpretation of ground-water flow and abnormal pressure in the Fruitland Formation (Kaiser and others, this volume, Chapter 8).

The viability of the hypothesis of increased fracture density where coal beds are folded is uncertain; additional subsurface and outcrop studies are required. However, given the abundance of folds and the potential for folding-induced fractures to contribute to enhanced coalbed methane production, such studies are warranted.

Coalbed methane activity and reservoir conditions

The Navajo Lake area has a long and noteworthy history of coalbed methane production. The Phillips No. 6–17 well (Figs. 4.2 and 4.3) is often referred to as the discovery well for coalbed methane in the San Juan Basin. This well, which is an open-hole completion in upper Fruitland coal beds and sandstones, is located on the northwest flank of a minor, north-plunging anticline. It has operated for more than 25 yrs with little decline in gas production (averaging 160 to 180 Mcf/d) or pressure (Hale and Firth, 1988). The well produces little or no water, indicating some element of structural and/or stratigraphic trapping. Although Hale and Firth (1988) discount structural trapping, their interpretation was based on a structure map of the Huerfanito Bentonite, which does not accurately reflect the structural attitude of Fruitland coal beds. Since 1985, Meridian Oil and Blackwood and Nichols have completed several coalbed methane wells in the Navajo Lake area, including the most productive coalbed methane wells in the United States. Some Meridian wells in this area (Figs. 4.2, 4.3, and 4.19) have produced at a rate of 300 to 15,000 Mcf/d (see Kaiser and Ayers, this volume, Chapter 10, for discussion of production). Meridian 400 wells are completed in lower Fruitland coal beds on the margin of a syncline and near the updip pinch-out of UP1 (Fig. 4.19).

In the Navajo Lake area, Fruitland coal beds are mostly in the area of regional overpressuring and highest Fruitland bottom-hole pressures; overpressuring is attributed to artesian conditions (Kaiser and others, this volume, Chapter 8). The boundary between overpressured and underpressured strata crosses the southern part of the area (Fig. 4.4); this boundary may be caused by southwestward pinch-out and/or offset of aquifer coal beds across faults that are inferred to make up the structural hingeline (Fig. 4.2). Both gas- and water-saturated coal seams are present in the Navajo Lake area. In this area, Fruitland coal rank increases from high volatile B bituminous at the south to medium volatile bituminous at the north (Scott and others, this volume, Fig. 9.3), and it contains more than 10 Bcf of methane/mi^2 (Ayers and others, this volume, Fig. 2.21). Fruitland coalbed gas is dry (C_1/C_{1-5} >95%), and it contains a high percentage of carbon dioxide (commonly 3–10%) (Scott and others, this volume, Fig. 9.10). Primary fractures (face cleats) in oriented cores from Blackwood and Nichols NEBU No. 403 trend northeastward, consistent with regional cleat trends in the southern part of the basin (Tremain and others, this volume, Fig. 5.1). Highly productive wells in the Navajo Lake area are reported to have fracture-enhanced permeability that may be predicted from lineament analysis. However, a recent study showed no significant relations between methane production and lineament attributes in the northern San Juan Basin (Baumgardner, this volume, Chapter 7). Geologic and hydrologic controls on producibility of coalbed methane in the Navajo Lake area are further discussed by Kaiser and Ayers (this volume, Chapter 10).

Summary and conclusions

In summary, we suggest both depositional and structural controls affect the occurrence and producibility of Fruitland coalbed methane in the Navajo Lake area. The distribution of thick coal seams was controlled by depositional setting, which in turn was structurally controlled; tectonically induced subsidence north of the hingeline temporarily confined the Pictured Cliffs shoreline to a narrow belt, and this

FRUITLAND COAL GAS FOR CEDAR HILL GAS FIELD - NORTH OF DEMARCATION LINE

WELL	OPERATOR	LOCATION S	T	R	DATE	CO2	H2S	N2	METHANE	ETHANE	PROPANE	I-BUTANE	N-BUTANE	I-PENTANE	N-PENTANE	HEXANE PLUS	OXYGEN	TOTAL	SPECIFIC GRAVITY	BTU	C1/C1-5
CAHN #1	AMOCO	33	32	10	08/86	5.380	0.000	0.130	93.910	0.300	0.150	0.030	0.030	0.010	0.000	0.060	0.000	100.000	0.613	957	0.994
EALOM CL	AMOCO	33	32	10	11/85	5.960	0.000	0.020	93.730	0.220	0.040	0.000	0.000	0.000	0.000	0.030	0.000	100.000	0.613	950	0.997
LEEFER	AMOCO	34	32	10	11/85	6.990	0.000	0.020	92.710	0.230	0.040	0.000	0.000	0.000	0.000	0.010	0.000	100.000	0.623	939	0.997
SCHNEIDER B-1S	AMOCO	28	32	10	11/82	4.870	0.000	0.000	94.910	0.170	0.050	0.000	0.000	0.000	0.000	0.000	0.000	100.000	0.602	963	0.998
STATE BW #1	AMOCO	32	32	10	11/82	5.960	0.000	0.360	93.550	0.000	0.070	0.000	0.000	0.000	0.000	0.000	0.000	99.940	0.613	947	0.999
STATE BX	AMOCO	32	32	10	11/85	7.000	0.000	0.010	92.710	0.240	0.040	0.000	0.000	0.000	0.000	0.000	0.000	100.000	0.622	939	0.997
AVERAGE ANALYSIS FOR CEDAR HILL FIELD - NORTH OF DEMARCATION LINE						6.027	0.000	0.090	93.587	0.193	0.065	0.005	0.005	0.002	0.000	0.017	0.000	99.990	0.614	951	0.997

Gas Analysis Data From Decker, et.al.

(Kaiser and others, this volume, Fig. 8.1) and, consequently, such areas are favorable for hydrocarbon accumulation (Tóth, 1980). Available chemical analyses show Na–Cl-type waters. Coal seams may be thicker than 10 ft (>3 m) and they occur primarily in northeast-trending belts (Ayers and others, this volume, Figs. 2.15 and 2.17). A northeast-trending, dip-elongate belt of thick coal extends almost to the southwestern margin of the basin (Ayers and others, this volume, Figs. 2.17 and 2.19) and coincides with a similar trending belt of high gas production (>100 Mcf/d) (Fig. 10.15). This belt includes productive wells (200 to 500 Mcf/d) in the Fulcher and WAW–Gallegos areas (Fig. 10.15) completed in coal seams of subbituminous and high volatile C bituminous rank (Scott and others, this volume, Fig. 9.3), and it flanks a major northeast-trending Fruitland channel-sandstone belt. Sandstone wells of the Aztec, Kutz, and Gallegos fields (Fig. 10.20) are completed in channel-sandstone belts (thin-coal areas) that flank northeast-trending belts of thick coal (Ayers and others, this volume, Fig. 2.15).

Northeast-trending coal seams may have served as pathways that allowed gas to migrate out of the north-central part of the basin, either entrained or dissolved in ground water, or by diffusion in response to the concentration gradient. Carbon dioxide appears to have migrated. Plumes of high carbon dioxide content gases extend updip (southwestward) from the overpressured area, coincident with northeast-trending coal belts (Scott and others, this volume, Fig. 9.10), and terminate at the San Juan River valley, a regional no-flow boundary (Kaiser and others, this volume, Figs. 8.1 and 8.24).

In the west-central part of the basin (area 2), the Fruitland Formation is mainly an aquitard, and gas is produced water free (Kaiser and others, this volume, Chapter 8). Water-free production in this regional discharge area is explained in terms of the low flow, hydrostratigraphy, trapping mechanism, and coal wettability. Limited flow in the basal Fruitland coal and Pictured Cliffs Sandstone accounts for water production from some wells completed in the basal coal. Conventional trapping and low gas permeability relative to water are also important factors. Stratigraphic trapping is postulated to be more important than structural trapping on the basis of gentle, northeast monoclinal dip and associated updip (southwestward) pinch-out of reservoir coal seams (Ayers and others, this volume, Fig. 2.2). Coal seams in the southern part of the basin are lower rank (subbituminous to high volatile C bituminous) and may be water wet; hence, in these low-permeability strata, water is less mobile than gas.

In the west-central, underpressured part of the basin, Fruitland coalbed wells have MAPs ranging from 30 to 300 Mcf/d, similar to productivities of many wells in the north-central, overpressured part of the basin (Ignacio Blanco field) in areas 1B and 1C (Fig. 10.19). Although coalbed methane production is highest from overpressured coal seams, economic production occurs over a wide pressure range. Cumulative production of some wells exceeds 1 Bcf in area 2 (for example, Clay 1, Gallegos area, >1 Bcf in 14 yrs). However, most wells in this area have cumulative productions of a few hundred million cubic feet, and some have produced oil at the rate of 2 or 3 bbls/d. Numerous Fruitland sandstone gas fields occur in the southwestern part of the basin (Fig. 10.20). Several of them, such as Aztec field, are associated with potentiometric mounds (Kaiser and others, this volume, Fig. 8.1). Analysis of production decline has shown that many wells identified as sandstone completions actually have coal-decline behavior and probably are producing coalbed methane indirectly from coal seams (Fig. 10.4). In some cases, sandstone volumetrics require gas production from the associated coal seams. Some wells are dually completed in Fruitland coal seams and Pictured Cliffs Sandstone or Mesaverde sandstones, and the production is commingled. Consequently, the contribution of Fruitland coalbed methane to total gas production in the west-central part of the basin is substantial but unquantifiable.

WAW–Gallegos area—Coalbed methane wells in the WAW–Gallegos area, which is located in area 2 in the southwestern corner of the basin (Figs. 10.15 and 10.20), produce at rates of 30 to more than 300 Mcf/d. Wells completed in 1990 average about 180 Mcf/d. Long-term productivity is demonstrated by the Clay 1 well (sec. 12 T26N R12W), which was completed as a coalbed well in 1976 and had an average production rate of 185 Mcf/d in 1989. The area is underpressured and lies mostly within the regional discharge area. Structural dip is homoclinal to the northeast at less than 1° (~80 ft/mi [~15 m/km]). Strike- and dip-elongate coal seams of subbituminous rank have maximum thicknesses of 10 to 20 ft (3 to 6 m) (Ayers and others, this volume, Fig. 2.17). Stratigraphic and hydrodynamic trapping may account for considerable gas volume beyond that adsorbed at reservoir pressures below or near hydrostatic pressure. Coal seams pinch out updip (southwestward), and ground water flows downdip (northward). Enhanced permeability is inferred for wells producing water from the basal Fruitland coal. Gas may in part come from the underlying Pictured Cliffs Sandstone. Thus, the presence of significant free gas and enhanced permeability are thought to combine to explain relatively high gas productivities in the WAW–Gallegos area.

Area 3: underpressured, eastern area

Little is known about the hydrogeology of the eastern part of the basin. Area 3 (Fig. 10.19) is regionally underpressured, and because of limited data, it appears to be hydrologically featureless. Widely spaced head contours suggest sluggish ground-water flow (Kaiser and others, this volume, Fig. 8.1). Fruitland-produced waters are Na–Cl type that resemble seawater. An area of thick coal, corresponding to coals of belt E (Ayers and others, this volume, Fig. 2.15), trends northwestward across Rio Arriba County, parallel to depositional strike. There are only a few producing Fruitland wells (coal and/or sandstone completions) in the area. After 1 or 2 yrs of production, these wells have average annual productions of less than 1 to 3 MMcf, accompanied by little or no water.

Conclusions

1. Coalbed methane production in the Fruitland Formation is lognormally distributed. Production histograms and probability and scatter plots suggest that coal beds having free gas may be common. Production from overpressured coal seams is greater than that from underpressured seams, although production rates from the two pressure regimes overlap. Initial gas potential is a predictor of long-term productivity. Highly productive wells produce both gas and water, reflecting superior permeability and artesian overpressure. Decline curves of coalbed and sandstone reservoirs differ. Coalbed wells have negative decline early in their production history, followed by exponential decline at less than 5%/yr late in their lives. Sandstone wells that exhibit coal-decline behavior probably are producing coalbed methane indirectly from adjoining coal seams.

2. Approximately 90% of the Fruitland coalbed methane production is from the Meridian 400 area and Cedar Hill and Ignacio Blanco fields in the overpressured part of the basin. Wells in the Meridian 400 area are the most productive (>1,000 Mcf/d), whereas those in Ignacio Blanco field are the least productive (~30 to 300 Mcf/d) and may still be dewatering. Coalbed wells in the west-central (underpres-

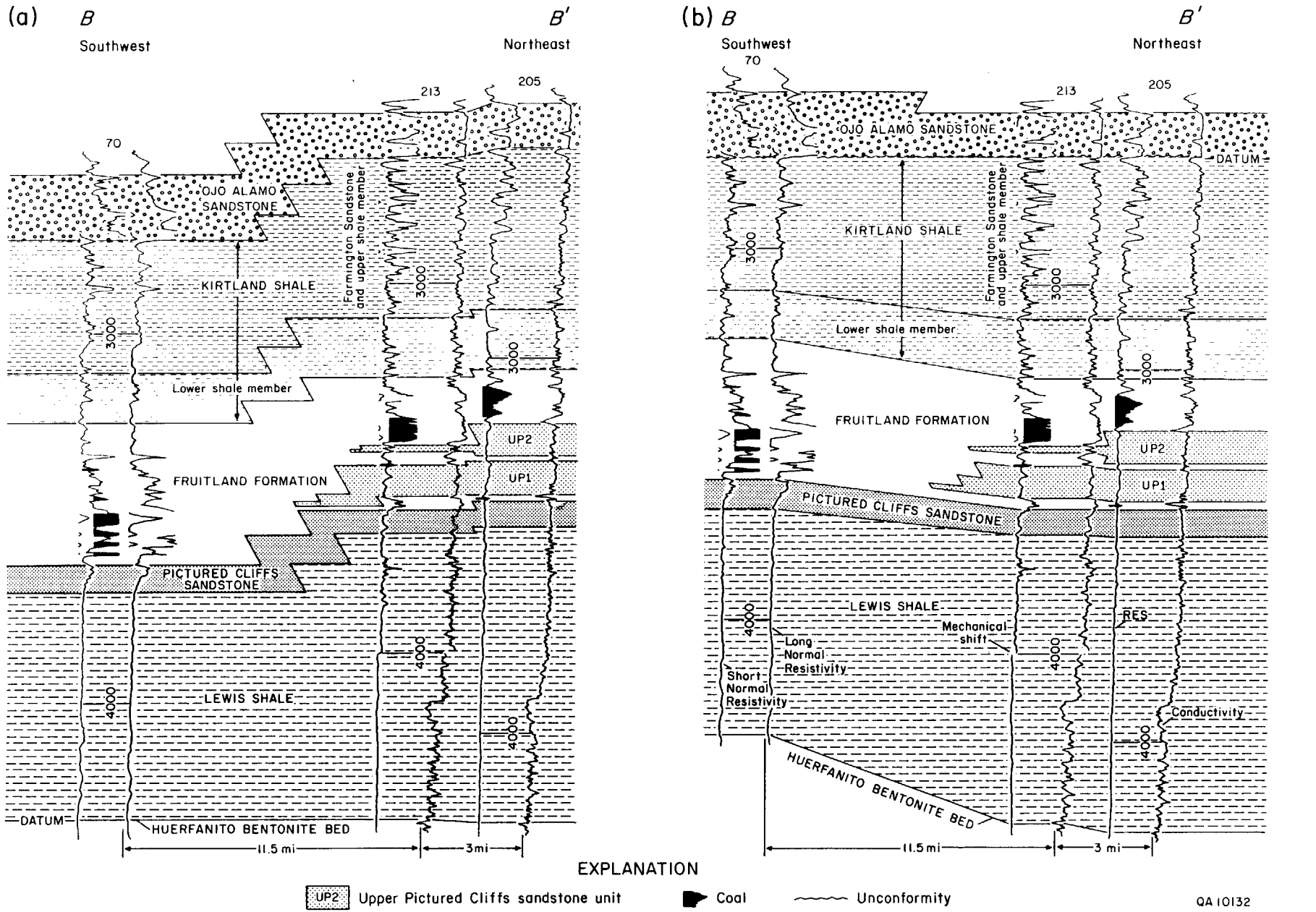

FIGURE 4.18—Cross section B–B'. (a) Datum is the Huerfanito Bentonite. Use of this datum suggests that coal seams terminate abruptly against Pictured Cliffs shoreline sandstones. (b) Datum is base of the Ojo Alamo Sandstone. Use of a datum above the Fruitland Formation suggests that swamp facies (coal seams) migrated over abandoned, foundered Pictured Cliffs shoreline sandstones. See Fig. 4.19 for location.

(Kaiser and others, this volume, Fig. 8.1) and, consequently, such areas are favorable for hydrocarbon accumulation (Tóth, 1980). Available chemical analyses show Na–Cl-type waters. Coal seams may be thicker than 10 ft (>3 m) and they occur primarily in northeast-trending belts (Ayers and others, this volume, Figs. 2.15 and 2.17). A northeast-trending, dip-elongate belt of thick coal extends almost to the southwestern margin of the basin (Ayers and others, this volume, Figs. 2.17 and 2.19) and coincides with a similar trending belt of high gas production (>100 Mcf/d) (Fig. 10.15). This belt includes productive wells (200 to 500 Mcf/d) in the Fulcher and WAW–Gallegos areas (Fig. 10.15) completed in coal seams of subbituminous and high volatile C bituminous rank (Scott and others, this volume, Fig. 9.3), and it flanks a major northeast-trending Fruitland channel-sandstone belt. Sandstone wells of the Aztec, Kutz, and Gallegos fields (Fig. 10.20) are completed in channel-sandstone belts (thin-coal areas) that flank northeast-trending belts of thick coal (Ayers and others, this volume, Fig. 2.15).

Northeast-trending coal seams may have served as pathways that allowed gas to migrate out of the north-central part of the basin, either entrained or dissolved in ground water, or by diffusion in response to the concentration gradient. Carbon dioxide appears to have migrated. Plumes of high carbon dioxide content gases extend updip (southwestward) from the overpressured area, coincident with northeast-trending coal belts (Scott and others, this volume, Fig. 9.10), and terminate at the San Juan River valley, a regional no-flow boundary (Kaiser and others, this volume, Figs. 8.1 and 8.24).

In the west-central part of the basin (area 2), the Fruitland Formation is mainly an aquitard, and gas is produced water free (Kaiser and others, this volume, Chapter 8). Water-free production in this regional discharge area is explained in terms of the low flow, hydrostratigraphy, trapping mechanism, and coal wettability. Limited flow in the basal Fruitland coal and Pictured Cliffs Sandstone accounts for water production from some wells completed in the basal coal. Conventional trapping and low gas permeability relative to water are also important factors. Stratigraphic trapping is postulated to be more important than structural trapping on the basis of gentle, northeast monoclinal dip and associated updip (southwestward) pinch-out of reservoir coal seams (Ayers and others, this volume, Fig. 2.2). Coal seams in the southern part of the basin are lower rank (subbituminous to high volatile C bituminous) and may be water wet; hence, in these low-permeability strata, water is less mobile than gas.

In the west-central, underpressured part of the basin, Fruitland coalbed wells have MAPs ranging from 30 to 300 Mcf/d, similar to productivities of many wells in the north-central, overpressured part of the basin (Ignacio Blanco field) in areas 1B and 1C (Fig. 10.19). Although coalbed methane production is highest from overpressured coal seams, economic production occurs over a wide pressure range. Cumulative production of some wells exceeds 1 Bcf in area 2 (for example, Clay 1, Gallegos area, >1 Bcf in 14 yrs). However, most wells in this area have cumulative productions of a few hundred million cubic feet, and some have produced oil at the rate of 2 or 3 bbls/d. Numerous Fruitland sandstone gas fields occur in the southwestern part of the basin (Fig. 10.20). Several of them, such as Aztec field, are associated with potentiometric mounds (Kaiser and others, this volume, Fig. 8.1). Analysis of production decline has shown that many wells identified as sandstone completions actually have coal-decline behavior and probably are producing coalbed methane indirectly from coal seams (Fig. 10.4). In some cases, sandstone volumetrics require gas production from the associated coal seams. Some wells are dually completed in Fruitland coal seams and Pictured Cliffs Sandstone or Mesaverde sandstones, and the production is commingled. Consequently, the contribution of Fruitland coalbed methane to total gas production in the west-central part of the basin is substantial but unquantifiable.

WAW–Gallegos area—Coalbed methane wells in the WAW–Gallegos area, which is located in area 2 in the southwestern corner of the basin (Figs. 10.15 and 10.20), produce at rates of 30 to more than 300 Mcf/d. Wells completed in 1990 average about 180 Mcf/d. Long-term productivity is demonstrated by the Clay 1 well (sec. 12 T26N R12W), which was completed as a coalbed well in 1976 and had an average production rate of 185 Mcf/d in 1989. The area is underpressured and lies mostly within the regional discharge area. Structural dip is homoclinal to the northeast at less than 1° (~80 ft/mi [~15 m/km]). Strike- and dip-elongate coal seams of subbituminous rank have maximum thicknesses of 10 to 20 ft (3 to 6 m) (Ayers and others, this volume, Fig. 2.17). Stratigraphic and hydrodynamic trapping may account for considerable gas volume beyond that adsorbed at reservoir pressures below or near hydrostatic pressure. Coal seams pinch out updip (southwestward), and ground water flows downdip (northward). Enhanced permeability is inferred for wells producing water from the basal Fruitland coal. Gas may in part come from the underlying Pictured Cliffs Sandstone. Thus, the presence of significant free gas and enhanced permeability are thought to combine to explain relatively high gas productivities in the WAW–Gallegos area.

Area 3: underpressured, eastern area

Little is known about the hydrogeology of the eastern part of the basin. Area 3 (Fig. 10.19) is regionally underpressured, and because of limited data, it appears to be hydrologically featureless. Widely spaced head contours suggest sluggish ground-water flow (Kaiser and others, this volume, Fig. 8.1). Fruitland-produced waters are Na–Cl type that resemble seawater. An area of thick coal, corresponding to coals of belt E (Ayers and others, this volume, Fig. 2.15), trends northwestward across Rio Arriba County, parallel to depositional strike. There are only a few producing Fruitland wells (coal and/or sandstone completions) in the area. After 1 or 2 yrs of production, these wells have average annual productions of less than 1 to 3 MMcf, accompanied by little or no water.

Conclusions

1. Coalbed methane production in the Fruitland Formation is lognormally distributed. Production histograms and probability and scatter plots suggest that coal beds having free gas may be common. Production from overpressured coal seams is greater than that from underpressured seams, although production rates from the two pressure regimes overlap. Initial gas potential is a predictor of long-term productivity. Highly productive wells produce both gas and water, reflecting superior permeability and artesian overpressure. Decline curves of coalbed and sandstone reservoirs differ. Coalbed wells have negative decline early in their production history, followed by exponential decline at less than 5%/yr late in their lives. Sandstone wells that exhibit coal-decline behavior probably are producing coalbed methane indirectly from adjoining coal seams.

2. Approximately 90% of the Fruitland coalbed methane production is from the Meridian 400 area and Cedar Hill and Ignacio Blanco fields in the overpressured part of the basin. Wells in the Meridian 400 area are the most productive (>1,000 Mcf/d), whereas those in Ignacio Blanco field are the least productive (~30 to 300 Mcf/d) and may still be dewatering. Coalbed wells in the west-central (underpres-

We suggest that structural activity contributed to relatively greater stratigraphic rise in this area and, indirectly, to the distribution of thick Fruitland coal seams (Ayers and others, this volume, Fig. 2.20). The Pictured Cliffs shoreline prograded rapidly basinward across the southern half of the basin. After the shoreline crossed the structural hingeline, sporadic structural activity began and the northern part of the basin subsided more rapidly to accommodate a greater thickness of sediment. The changing balance between sediment input and pulsatory subsidence north of the hingeline resulted in oscillation and aggradation of the shoreline, accounting for the most significant stratigraphic rise of the Pictured Cliffs in the basin and allowing time for thick peat accumulation landward of the oscillating shoreline. This model explains why the greatest net thickness of Fruitland coal is in the northern part of the basin, and why coal seams in the Fruitland Formation are thicker than those in subjacent continental strata. Further testing is needed to verify the existence of the structural hingeline; seismic studies would be especially useful. A regional map of structural elements that were identified in regional reflection seismic lines shows northwest-trending faults in the area of this hingeline (Huffman and Taylor, 1991).

Structural controls on producibility of coalbed methane

Earlier studies suggested that Fruitland coal seams have limited extent and that they are bounded on their basinward (northeast) margins by Pictured Cliffs shoreline sandstone and along paleostrike (northwest–southeast) by Fruitland fluvial sandstones (Fassett and Hinds, 1971; Fassett, 1986). However, as we have demonstrated, some Fruitland coal seams may be regionally continuous, overriding and thinning over upper Pictured Cliffs tongues (Figs. 4.16 and 4.18) in the paleodip direction. Updip pinch-out lines of upper Pictured Cliffs tongues may be areas where Fruitland coal seams drape over shoreline sandstones and have a higher fracture density because of compaction-induced fractures. The structural attitude of an upper Fruitland coal bed (Fig. 4.19) differs markedly from the structural attitude of other strata, such as the Huerfanito Bentonite (Fig. 4.2). Along paleostrike, coal seams split and interfinger with fluvial channel-fill sandstone complexes (Fig. 4.17), and many of these coal benches, rather than terminating against the channel sandstones, override or underlie them, forming zigzag splits similar to those described in coal-bearing strata in other basins (Britten and others, 1975; Ayers and Kaiser, 1984). Although these coal seams pinch and swell, they are laterally continuous, which contributes to their effectiveness as aquifers. Fractures related to compactional folding of coal beds are well documented (Donaldson, 1979; Houseknecht and Iannacchione, 1982; Tyler and others, 1991). If such fracture systems are sufficiently developed, areas of interbedded sandstones and coal seams would be good targets for coalbed methane exploration (Fig. 4.20).

This study has shown that Fruitland coal beds are more extensive and complex than previously inferred (Figs. 4.16–4.18). The significance of these findings is threefold. First, coalbed methane reservoirs are larger (more extensive) than previously thought. Second, compaction-induced fractures, and therefore enhanced coalbed permeability, may occur in areas where extensive coal seams drape over shoreline sandstones or form zigzag splits with channel-fill sandstone complexes. Finally, the greater lateral extent of coal seams, inferred from this research, is critical to the interpretation of ground-water flow and abnormal pressure in the Fruitland Formation (Kaiser and others, this volume, Chapter 8).

The viability of the hypothesis of increased fracture density where coal beds are folded is uncertain; additional subsurface and outcrop studies are required. However, given the abundance of folds and the potential for folding-induced fractures to contribute to enhanced coalbed methane production, such studies are warranted.

Coalbed methane activity and reservoir conditions

The Navajo Lake area has a long and noteworthy history of coalbed methane production. The Phillips No. 6–17 well (Figs. 4.2 and 4.3) is often referred to as the discovery well for coalbed methane in the San Juan Basin. This well, which is an open-hole completion in upper Fruitland coal beds and sandstones, is located on the northwest flank of a minor, north-plunging anticline. It has operated for more than 25 yrs with little decline in gas production (averaging 160 to 180 Mcf/d) or pressure (Hale and Firth, 1988). The well produces little or no water, indicating some element of structural and/or stratigraphic trapping. Although Hale and Firth (1988) discount structural trapping, their interpretation was based on a structure map of the Huerfanito Bentonite, which does not accurately reflect the structural attitude of Fruitland coal beds. Since 1985, Meridian Oil and Blackwood and Nichols have completed several coalbed methane wells in the Navajo Lake area, including the most productive coalbed methane wells in the United States. Some Meridian wells in this area (Figs. 4.2, 4.3, and 4.19) have produced at a rate of 300 to 15,000 Mcf/d (see Kaiser and Ayers, this volume, Chapter 10, for discussion of production). Meridian 400 wells are completed in lower Fruitland coal beds on the margin of a syncline and near the updip pinch-out of UP1 (Fig. 4.19).

In the Navajo Lake area, Fruitland coal beds are mostly in the area of regional overpressuring and highest Fruitland bottom-hole pressures; overpressuring is attributed to artesian conditions (Kaiser and others, this volume, Chapter 8). The boundary between overpressured and underpressured strata crosses the southern part of the area (Fig. 4.4); this boundary may be caused by southwestward pinch-out and/or offset of aquifer coal beds across faults that are inferred to make up the structural hingeline (Fig. 4.2). Both gas- and water-saturated coal seams are present in the Navajo Lake area. In this area, Fruitland coal rank increases from high volatile B bituminous at the south to medium volatile bituminous at the north (Scott and others, this volume, Fig. 9.3), and it contains more than 10 Bcf of methane/mi^2 (Ayers and others, this volume, Fig. 2.21). Fruitland coalbed gas is dry (C_1/C_{1-5} >95%), and it contains a high percentage of carbon dioxide (commonly 3–10%) (Scott and others, this volume, Fig. 9.10). Primary fractures (face cleats) in oriented cores from Blackwood and Nichols NEBU No. 403 trend northeastward, consistent with regional cleat trends in the southern part of the basin (Tremain and others, this volume, Fig. 5.1). Highly productive wells in the Navajo Lake area are reported to have fracture-enhanced permeability that may be predicted from lineament analysis. However, a recent study showed no significant relations between methane production and lineament attributes in the northern San Juan Basin (Baumgardner, this volume, Chapter 7). Geologic and hydrologic controls on producibility of coalbed methane in the Navajo Lake area are further discussed by Kaiser and Ayers (this volume, Chapter 10).

Summary and conclusions

In summary, we suggest both depositional and structural controls affect the occurrence and producibility of Fruitland coalbed methane in the Navajo Lake area. The distribution of thick coal seams was controlled by depositional setting, which in turn was structurally controlled; tectonically induced subsidence north of the hingeline temporarily confined the Pictured Cliffs shoreline to a narrow belt, and this

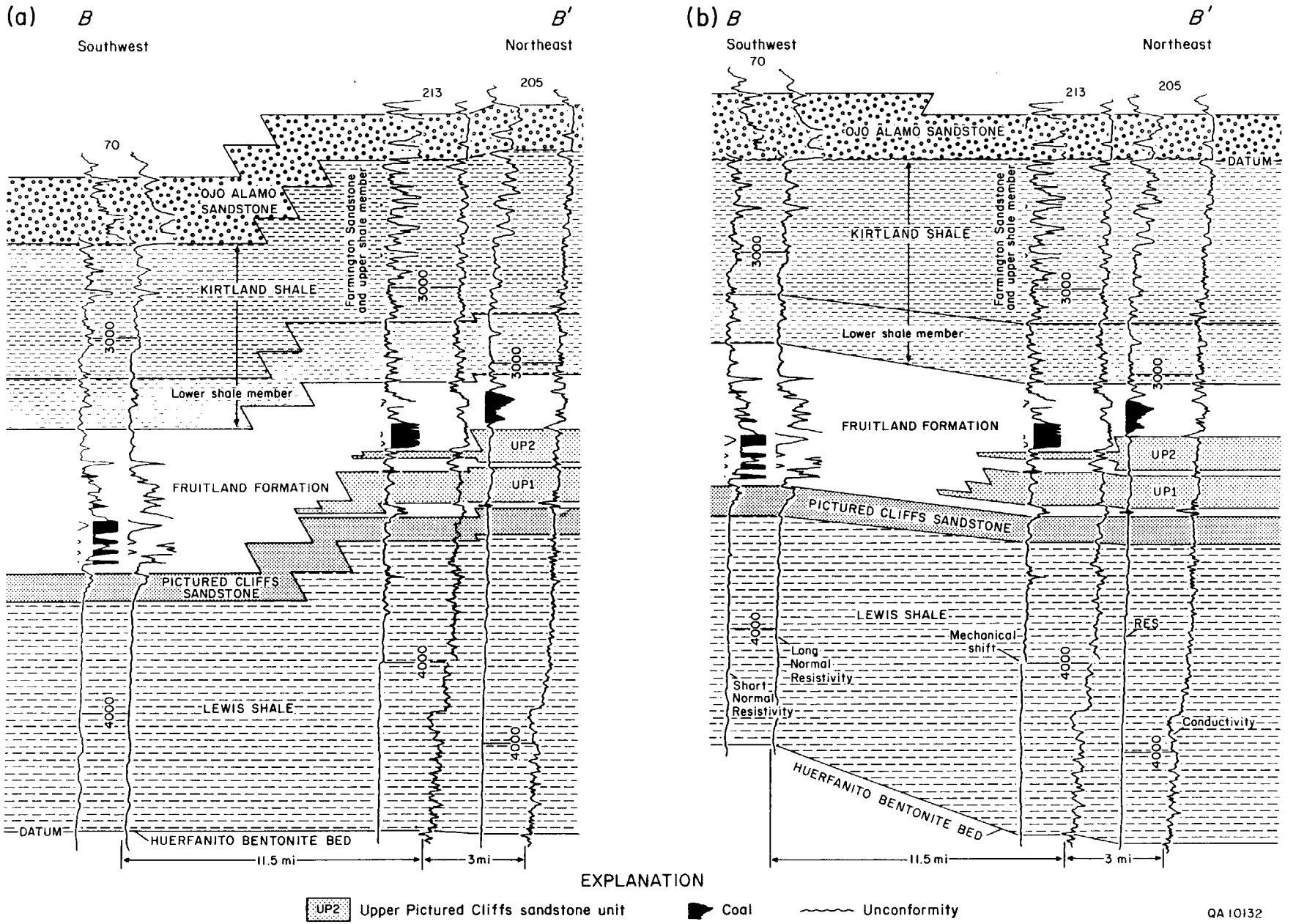

FIGURE 4.18—Cross section B–B'. (a) Datum is the Huerfanito Bentonite. Use of this datum suggests that coal seams terminate abruptly against Pictured Cliffs shoreline sandstones. (b) Datum is base of the Ojo Alamo Sandstone. Use of a datum above the Fruitland Formation suggests that swamp facies (coal seams) migrated over abandoned, foundered Pictured Cliffs shoreline sandstones. See Fig. 4.19 for location.

Chapter 55
Formation Fracturing

S.J. Martinez, U. of Tulsa *
R.E. Steanson, Dowell Schlumberger **
A.W. Coulter, Dowell Schlumberger **

Introduction

Fracturing techniques were developed in 1948 and the first commercial fracturing treatments were conducted in 1949. The process rapidly gained popularity because of its high success ratio, and within a very few years, thousands of wells per year were being stimulated by hydraulic fracturing treatments.

Early treatments consisted of pumping 1,000 to 3,000 gal of fracturing fluid, containing about 1 lbm of 20/40-mesh sand/gal, at rates of 1 to 2 bbl/min. Today, a single treatment can require several hundred thousand gallons of fluid and more than a million pounds of propping agent. Although injection rates have exceeded 300 bbl/min in some instances, rates of 20 to 60 bbl/min are about average. Materials, equipment, and techniques have become highly sophisticated. A bibliography is presented at the end of this chapter for those interested in a detailed discussion of particular technologies. This discussion is limited to a generalized description of fracturing theory, materials, techniques, equipment, and treatment planning and design.

Hydraulic Fracturing Theory

Oil and gas accumulations occur in the pore spaces or natural fractures of a subsurface rock where structural and/or stratigraphic features form a trap. When a well is drilled into an oil-bearing rock, the fluids must flow through the surrounding rock into the wellbore before they can be brought to the surface. If the pore spaces of the rock are interconnected so that channels exist through which the oil can flow, the rock is "permeable." The ease with which fluid can flow through a rock determines its degree of permeability. It has high permeability if oil, gas, or water can flow easily through existing channels and low permeability if the connecting channels are very small and fluid flow is restricted.

In the case of high permeability, drilling fluids may enter the flow channels and later impair flow into the wellbore. In the case of low permeability, the flow channels may not permit enough flow into the wellbore. In either case, the well may not be commercial because fluid cannot flow into the wellbore fast enough. It then becomes necessary to create an artificial channel that will increase the ability of the reservoir rock to conduct fluid into the wellbore. Such channels often can be created by hydraulic fracturing.

During hydraulic fracturing treatments, what actually happens when a rock ruptures, or fractures, can be explained by basic rock mechanics. All subsurface rocks are stressed in three directions because of the weight of overlying formations and their horizontal reactions. Whether one of the horizontal stresses or the vertical stress is the greatest will depend on the additional stresses imposed on the rock by prior folding, faulting, or other geological movement in the area. These tectonic stresses will control the direction of the fracture and determine whether the fracture plane will be horizontal, vertical, or inclined.

Every formation rock has some measure of strength depending on its structure, compaction, and cementation. It has tensile strength in both vertical and horizontal directions. The forces tending to hold the rock together are the stresses on the rock and the strength of the rock itself. When a wellbore is filled with fluid and pressure is applied at the surface, the pressure of the fluid in a perforation or even in the pore spaces of the rock will increase. This hydraulic pressure is applied equally in all directions. If the pressure is increased, the forces applied by the fluid pressure in the rock will become equal to the forces tending to hold the rock together. Any additional pressure applied will cause the rock to split or fracture. The fracture will extend as long as sufficient pressure is applied by injection of additional fluids.

*Deceased; this author also wrote the original chapter on this topic with coauthor P.E. Fitzgerald.
**Retired.

When the treatment is complete and flow is reversed to produce the well, pressure will gradually return (decline) to reservoir pressure. As this occurs, the forces tending to hold the rock together come into play again and the fracture will close or "heal." To prevent closure, some solid material must be placed in the fracture to hold it open. Such materials are called "propping agents." Since the permeability of these propping agents is much higher than that of the surrounding formation, the ability of the propped fracture to conduct fluids to the wellbore can result in good production increases. In fact, fracturing has made profitable production possible from many wells and fields that otherwise would not have been profitable.

Formations Fractured

Fracturing has been used successfully in all formations except those that are very soft. Fracturing has proved successful in sand, limestone, dolomitic limestone, dolomite, conglomerates, granite washes, hard or brittle shale, anhydrite, chert, and various silicates. The plastic nature of soft shales and clays makes them difficult to fracture.

Fracturing has helped wells producing from formations that have such a wide range of permeabilities that it is impossible to set upper and lower permeability limits of formations that might be helped by fracturing. Production increases have been obtained from zones having permeabilities ranging from less than 0.1 to as high as 900 md.

Fracture Planes

Analysis of pressures encountered on many thousands of fracturing treatments has shown that the bottomhole pressures (BHP) recorded during the injection of fracturing materials range from 0.40 to 1.80 psi/ft depth.[1] Only in a few treatments have fracturing pressure gradients been outside of this range. Those were almost all in shallow experimental treatments. The fracture gradient g_f is calculated from treatment data by Eq. 1:

$$g_f = \frac{p_h + p_s - p_f}{D}, \quad \ldots\ldots\ldots\ldots\ldots\ldots\ldots\ldots (1)$$

where

g_f = unit fracture gradient, psi/ft,
p_h = total hydrostatic pressure, psi,
p_s = total surface treating pressure, psi,
p_f = total friction loss, psi, and
D = depth of producing interval, ft.

Analysis of thousands of treatments plus experimental work in reservoirs with known fracture gradients indicate that horizontal fractures are produced in reservoirs having fracture gradients of 1.0 or higher. This is generally in shallow wells less than 2,000 ft deep. Vertical fractures are produced in reservoirs having fracture gradients of 0.7 or lower. Such gradients are normally encountered in wells deeper than 4,000 ft. Very few cases have been found where formations have gradients in the intermediate range between 0.7 and 1.0. Consequently, the use of fracture gradients to predict the general inclination of fractures should be useful in almost every case.

With few exceptions, wells in the same reservoir will have nearly identical fracture gradients. Thus, the gradient from one well generally will serve as a guide for the entire pool.

Fracture Area

In 1957, Howard and Fast[2] presented a mathematical equation to determine the surface area of a newly opened fracture. The equation, based on the quantity of fracturing materials used and the rate at which they are injected into the formation, takes into account the physical characterisitics of the fracturing fluids and the specific reservoir conditions. This equation is:

$$A_f = \frac{ib}{4\pi K^2}\left[e^{x^2}\cdot \mathrm{erfc}(x) + \frac{2x}{\sqrt{\pi}} - 1\right], \quad \ldots\ldots\ldots (2)$$

where

$$x = \frac{2K\sqrt{\pi t}}{b},$$

and

A_f = total area of one face of the fracture at any time during injection, sq ft,
i = constant injection rate during fracture extension, cu ft/min,
t = total pumping time, minutes,
b = fracture width (breadth), ft,
K = fluid coefficient, a constant that is a measure of the flow resistance of the fluid leaking off into the formation during fracture operations, and
$\mathrm{erfc}(x)$ = complementary error function of x.

Essentially, during a fracturing treatment, only the volume of fracturing fluid that remains within the wall of the fracture is effective. The fluid that leaks off into the pores of the rock is lost insofar as added fracture extension is concerned.

When the width of a fracture is known or assumed (fracture width is normally calculated using either Perkins and Kern[3] or Khristianovitch and Zheltov[4] models), the volume of the fracture can be calculated. With these data, it is possible to plot the controllable variables of a fluid volume and injection rate against the fracture area produced for any particular fluid coefficient. Examples of such graphs, for various injection rates, are shown in Figs. 55.1 through 55.5.

The rate of fluid leakoff into the formation, as expressed by the fluid coefficient, is controlled by three variables: the viscosity and compressibility of the reservoir fluid, the viscosity of the fracturing fluid, and the fluid-loss characteristics of the fracturing fluid.

Reservoir-Controlled Fluids

This group includes those fracturing fluids having low viscosity and high fluid-loss characteristics, in which the rate of leakoff is controlled by the compressibility and viscosity of the reservoir fluid.

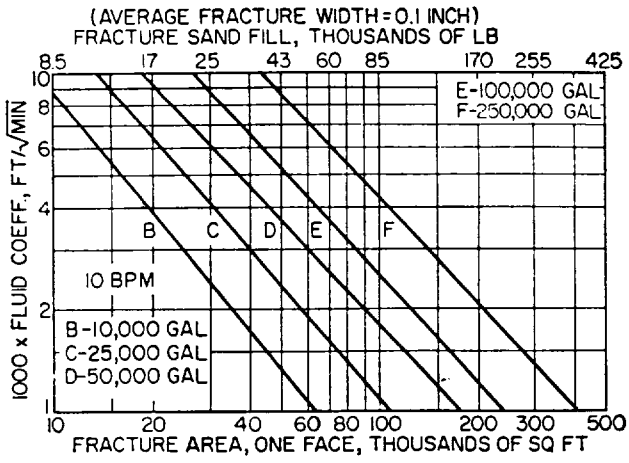

Fig. 55.1—Effect of fluid coefficient and volume on fracture area at constant injection rate of 10 bbl/min.

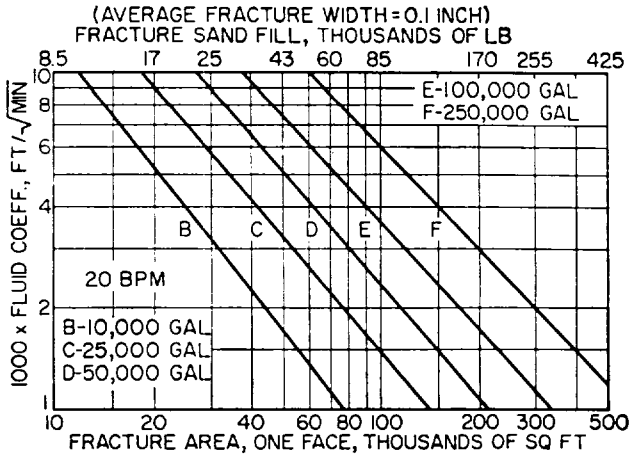

Fig. 55.2—Effect of fluid coefficient and volume on fracture area at constant injection rate of 20 bbl/min.

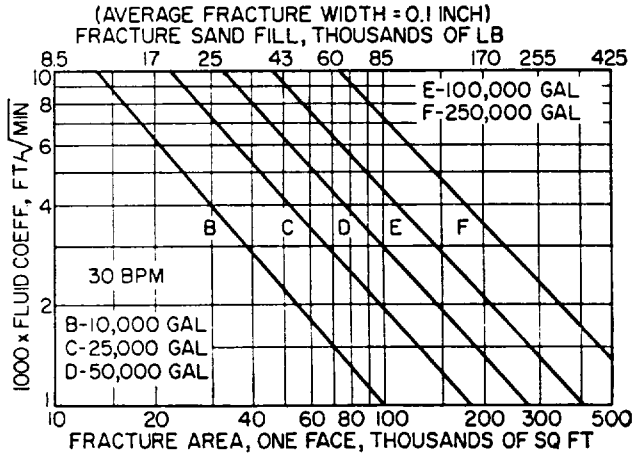

Fig. 55.3—Effect of fluid coefficient and volume on fracture area at constant injection rate of 30 bbl/min.

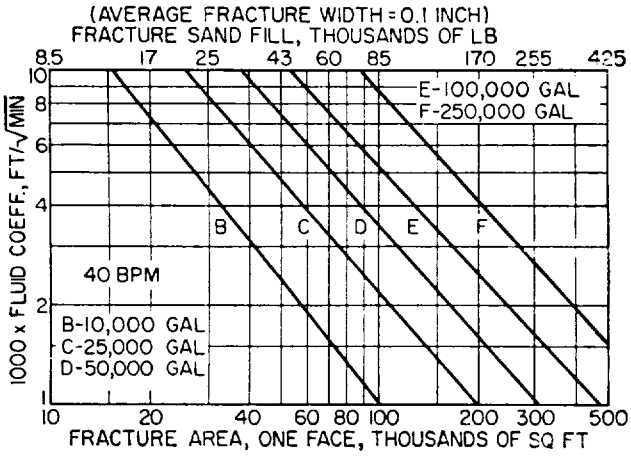

Fig. 55.4—Effect of fluid coefficient and volume on fracture area at constant injection rate of 40 bbl/min.

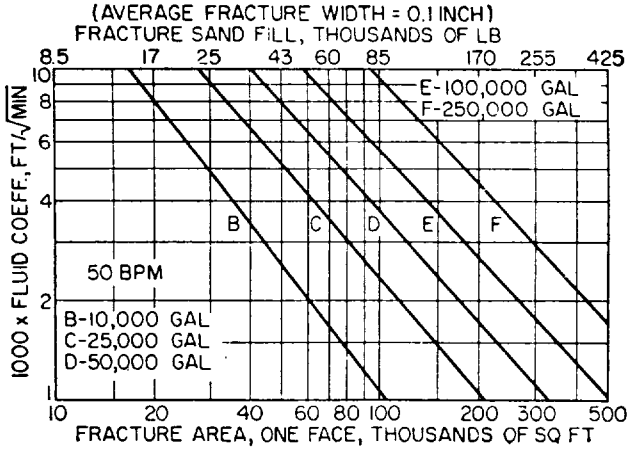

Fig. 55.5—Effect of fluid coefficient and volume on fracture area at constant injection rate of 50 bbl/min.

The coefficient for this type of fracturing fluid may be determined from Eq. 3.[2]

$$K_c = 0.0374\Delta p\sqrt{\frac{k_e \phi_e c_R}{\mu_R}}, \quad \ldots\ldots\ldots\ldots\ldots\ldots (3)$$

where

K_c = fluid coefficient (compressibility-viscosity controlled), ft/min$^{1/2}$,
Δp = differential pressure, across the face of the fracture, psi,
k_e = effective formation permeability, darcies,
ϕ_e = effective formation porosity, %,
c_R = isothermal coefficient of compressibility of the reservoir fluid, psi^{-1}, and
μ_R = reservoir fluid viscosity, cp.

Compressibility considerations are generally found to be most applicable in high-pressure, low-volume-factor wells that have high saturations.

Viscosity-Controlled Fluids

This group includes those fracturing fluids in which the rate of leakoff is controlled by the viscosity of the fluid itself. The coefficient for this type of fracturing fluid is expressed by Eq. 4.[2]

$$K_v = 0.0469\sqrt{\frac{k_e \Delta p \phi_e}{\mu_f}}, \quad \ldots\ldots\ldots\ldots\ldots\ldots (4)$$

where

K_v = fluid coefficient (viscosity controlled), ft/min$^{1/2}$,
k_e = effective formation permeability, darcies,
Δp = differential pressure across the face of the fracture, psi—this is the product of the fracture gradient and depth, minus normal reservoir pressure, $(g_f \times D) - p_R$,
ϕ_e = effective formation porosity, %, and
μ_f = fracturing fluid viscosity, cp.

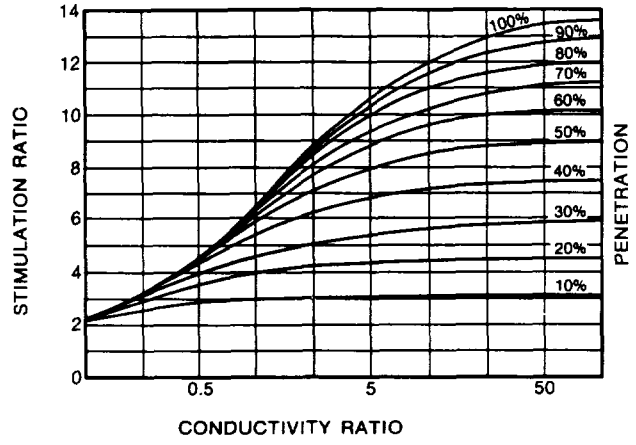

Fig. 55.6—Increased fracture penetration by containment of the fracture in the productive interval can provide much greater production increases.

The effective porosity represents the space in the matrix into which fracturing fluid will leak off. In figuring effective porosity, the effects of residual oil and water saturation should be considered. The permeability factor in the equation almost always will be the permeability of the water-wet formation, but it could be that of an oil-wet formation. The average md-ft of exposed section also is considered.

Fluid-Loss-Controlled Fluids

This group includes fracturing fluids containing special fluid-loss additives designed to reduce the loss of fluid taking place during a fracturing treatment.

The fluid coefficient for this type of fracturing fluid is based on Eq. 5[2]:

$$K_l = 0.0328\frac{m}{2A}, \quad \ldots\ldots\ldots\ldots\ldots\ldots (5)$$

where

K_l = fluid coefficient, wall building (fluid-loss additive), ft/min$^{1/2}$,
m = the slope of the fluid-loss curve, plotting cumulative filtrate volume vs. the square root of flow time, mL/min$^{1/2}$, and
A = cross-sectional area of test media through which flow takes place, cm^2.

In this case, the coefficient is obtained from an experimental test to determine the fluid loss resulting from the use of a particular fluid-loss additive in a particular fracturing fluid. The test must be performed at, or corrected to, bottomhole temperature (BHT) and pressure conditions. Spurt loss is the leakoff occurring while the fluid-retaining wall (filter cake) is being built up. It can be determined from this test by extrapolating the straight-line portion of the curve back to zero time on the ordinate. The value at this intercept is the spurt loss.

Stimulation Results

The increased production obtained following a fracturing treatment is the result of increased fracture penetration and conductivity. The greater penetration produces a larger drainage area from which reservoir fluids can be produced. Increased fracture conductivity results from the lowered resistance to flow through the fracture, permitting greater production of fluid under reservoir energy conditions.

Fig. 55.6[5] shows the relationship between fracture penetration, fracture conductivity ratio, and production increase. These curves represent fracture penetration as a decimal fraction of the drainage radius. If a good conductivity ratio can be achieved, then a fracture penetrating 100% of the drainage radius can provide as much as a 13-fold increase in the production.

Fracture conductivity is controlled largely by propping agent permeability, size, and placement. Strength of the propping agent is also very important. The effect of these properties on fracture conductivity will be discussed later.

Fracture penetration is related directly to fracture-fluid efficiency and containment of the fracture within the production zone. A good fracturing fluid should be relatively low in cost and have low fluid loss, low friction loss,

good proppant transport characteristics, temperature stability, ability to thin for good cleanup, and compatibility with reservoir rock and fluids. Containment of the fracture within the productive interval is a function not only of fluid properties but also of technique.

Fracturing Materials

Fracturing Fluids

Fracturing fluids may be divided into three broad divisions: oil based, water based, and mix based. Classification depends primarily on the main constituent of the fracturing fluid. The aqueous-based fluids are either water or acid, and the mix-based fluids are emulsions.

Oil-Based Fluids. In the past, refined oils, crude oils and soap-type gels of crude, kerosene, or diesel oil were quite common. Because of safety considerations, lack of temperature stability, and cost of tailoring these materials to be efficient fluids, they are seldom used today. A new thickened and crosslinked hydrocarbon gel, made from either light refined oils or crude oil, is used extensively in hydraulic fracturing of oil- and gas-condensate wells producing from reservoirs adversely affected by water or brine. These gels exhibit all the characteristics of an efficient fracturing fluid.

Water-Based Fluids. ***Gels.*** Water-based fluids are natural or synthetic polymer gels of water or hydrochloric acid. They may be either linear or crosslinked gels. The water-based fluids are used almost exclusively except in those extremely water-sensitive reservoirs previously mentioned. The popularity of aqueous fluids is based on many factors, including these four: (1) they are safe to handle, (2) their cost is low in comparison to oil-based fluids, (3) they are, or can be formulated to be, compatible with nearly all reservoir fluids and conditions, and (4) they can be tailored to meet almost any treating requirements. Rheological properties, friction pressure, fluid loss, and break time can be closely controlled to provide an efficient fracturing fluid over a wide range of well and reservoir conditions. The primary disadvantage of aqueous fluids is that they may not be applicable in formations that are adversely affected by water.

Waterfrac services use linear (uncrosslinked) gels of fresh water, salt water, or produced brine as efficient and economical fracturing fluids. Guar and hydroxypropyl guar thickening agents are available to satisfy the requirements of a wide range of reservoir properties. They can be used in either batch- or continuous-mix techniques. A cellulose derivative thickener is available for applications in which fluids with extremely low residue are required.

The viscosity of fluids used in waterfrac services is controlled by thickening-agent concentration.

High-viscosity fracturing fluids have been developed that contribute directly to wider, better-propped, and more-conductive fractures. Fracture width is increased by increasing the viscosity of the fracturing fluid. Wider fractures permit use of larger proppant, which has greater permeability. These viscous fluids also have the proppant-transport properties required to carry higher concentrations of proppant deeper into the fracture. They achieve their high viscosity at gel concentrations in the same range as the traditional waterfrac fluids by using special crosslinking systems and stabilizers. The high-viscosity gels are particularly useful in deep wells because of their temperature stability. They are able to create wide, deeply penetrating fractures at lower rates and can maintain their viscosity over the longer pumping times required in deeper wells. Fig. 55.7 shows the viscosity profile of one such fluid.

Two other characteristics of fracturing fluids normally are reported and are used in computer job design. These are the consistency index, I_c, and the behavior index, I_b. The power law model is used to calculate these characteristics. The consistency index is based on pipe flow geometry. The power law parameters are defined as follows:

I_b = behavior index; log slope of the shear stress vs. shear rate curve, dimensionless, and

I_c = consistency index; shear stress at 1 sec^{-1}, lbf-sec^{-1}/ft^2.

Apparent viscosity is related to the consistency index and behavior index as follows:

$$\mu_a = \frac{47{,}880 I_c}{\dot{\gamma}^{1-I_b}},$$

where

μ_a = apparent viscosity, cp, and

$\dot{\gamma}$ = shear rate, sec^{-1}

Since shear history (shear rate and time at shear) adversely affects the rheology of some crosslinked gels, test methods have been developed that more accurately describe the fluids at the time they enter the fracture. Table 55.1 compares data developed by the API test method and shear history method.[6] The data provided by the shear history method give more reliable prediction of friction losses while pumping. Such information is a requisite in job design to predict fracture geometry and reduce

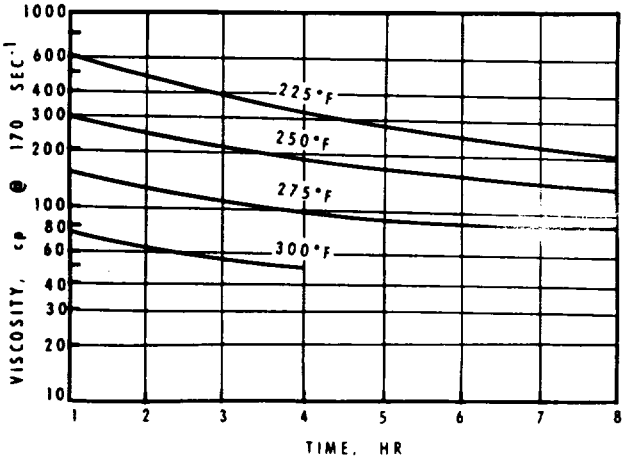

Fig. 55.7—Viscosity profile of high-viscosity, crosslinked, aqueous gel.

TABLE 55.1—COMPARISON OF RHEOLOGY DATA GENERATED BY API RP39M AND SHEAR HISTORY METHOD FOR CROSSLINKED AQUEOUS FLUID CONTAINING 30-lbm/1,000-gal THICKENER AND 10-lbm/100-gal STABILIZER

		RP39M-XL"A"			SHSM*-XL"A"		
Temperature (°F)	Time (hours)	l_b	l_c	cp at 170 sec^{-1}	l_b	l_c	cp at 170 sec^{-1}
225	0	—	—	—	0.7512	0.0017	23
	1	0.570	0.065	342	0.7709	0.0015	22
	2	0.588	0.045	259	0.7912	0.0013	20
	4	0.630	0.021	150	0.8309	0.0009	18
	6	0.672	0.011	98	0.8713	0.0007	17
	8	0.710	0.0058	63	0.9115	0.0005	15
250	0	—	—	—	0.7306	0.0021	25
	1	0.656	0.127	220	0.7743	0.0014	21
	2	0.674	0.019	170	0.8179	0.0009	17
	4	0.712	0.0095	103	0.9044	0.0004	11
	6	0.752	0.0046	62	0.9918	0.0002	7
	8	0.792	0.0024	39	—	—	—
275	0	—	—	—	0.7156	0.0020	22
	1	0.718	0.014	157	0.7371	0.0014	17
	4	0.740	0.010	126	0.7688	0.0009	13
	6	0.805	0.0048	84	—	—	—
	8	0.842	0.0037	79	—	—	—

*Shear history simulation method.

the possibility of premature screenout. Figs. 55.8 through 55.13 are examples of friction-loss data for various fluids.

In many of the high-viscosity fluids, shear history effects are minimized by using additives to delay crosslinking until the fluid reaches the bottom of the hole. This technique also reduces friction losses since high viscosity does not develop until after the fluid has passed through the tubulars.

Foams. During recent years, foams have become extremely popular as fracturing fluids. Normally classed as water-based fluid, foam is a dispersion of a gas, usually nitrogen, within a liquid. A surfactant is used as a foaming agent to initiate the dispersion. Stabilizers are used where high temperatures or long pumping time occur. The volumetric ratio of the gas to the total volume of the foam, under downhole conditions, is called the quality of the foam. Quality is expressed as a number equal to the percentage. A 75-quality foam is 75% gas by volume at downhole temperature and pressure. In fracturing, foam quality usually ranges from 65 to 85 (compositions containing less than 52% gas are not normally stable foams).

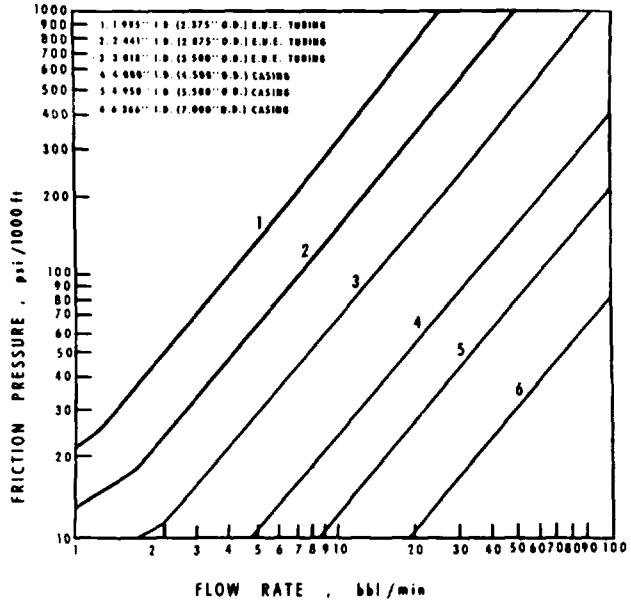

Fig. 55.8—Typical friction-loss curves for linear gel of fresh water or brine using guar or hydroxypropyl guar thickeners.

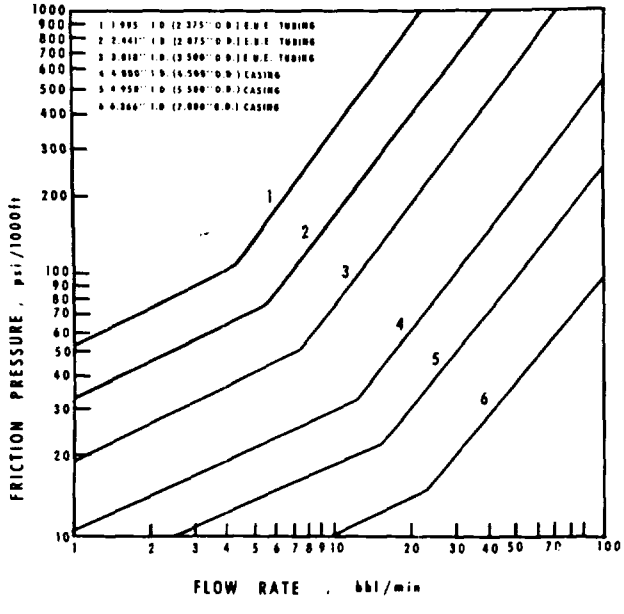

Fig. 55.9—Typical friction-loss curve of linear aqueous gel using cellulose thickener.

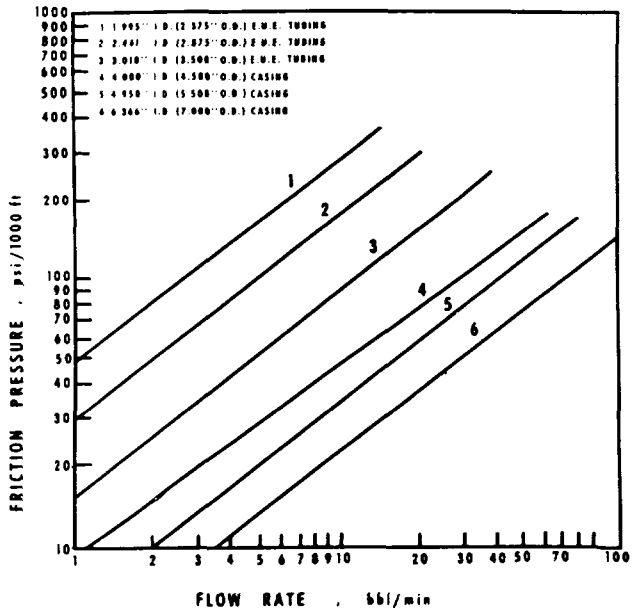

Fig. 55.10—Typical friction-loss curve for crosslinked aqueous gel using guar-based thickener.

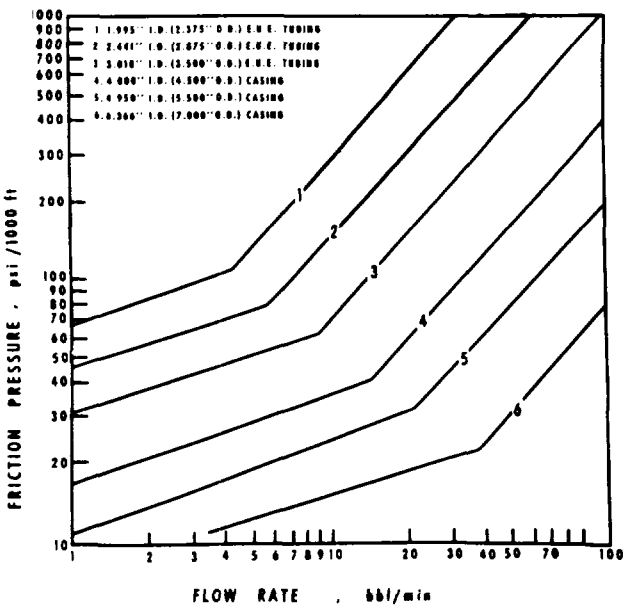

Fig. 55.11—Typical friction-loss curve for gelled oil fracturing fluid.

Foam is designed primarily for low-permeability or low-pressure gas wells. However, it may have equal advantages in low-pressure oil wells. In oil wells it may be necessary to use a different foaming agent that is compatible with reservoir fluids and reduces the possibility of emulsions.

Some advantages of foam are: (1) good proppant transport, (2) solids-free fluid-loss control, (3) low fluid loss, (4) minimum fluid retention owing to its low water content, (5) compatibility with reservoir fluids, and (6) low hydrostatic pressure of returned fluids, which gives rapid cleanup and allows quicker well evaluation (gas in foam helps return liquids to the wellbore).

Some disadvantages of foam are: (1) more surface pressure is required because of low hydrostatic head: and (2) there is the added expense of gas, especially under high pressure where volume is reduced.

Mix-Based Fluids. Mix-based fluids are oil-in-water dispersions or emulsions that serve as highly efficient water-based fracturing fluids.

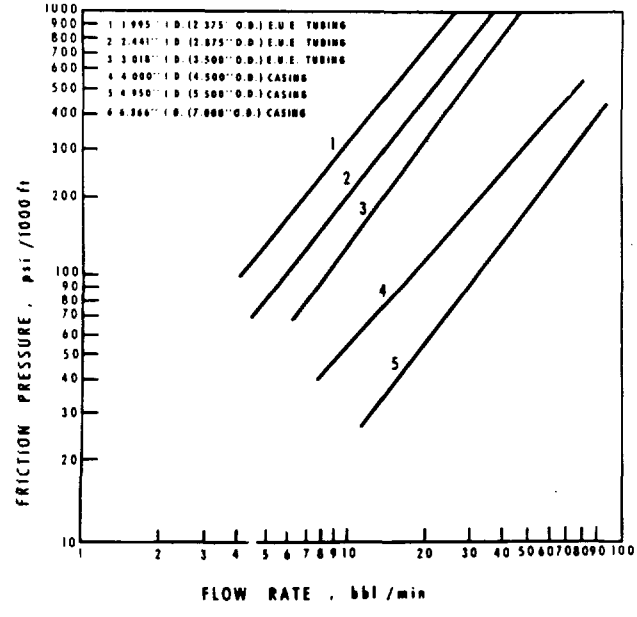

Fig. 55.12—Typical friction-loss curve for oil-in-water dispersion-type fracturing fluid.

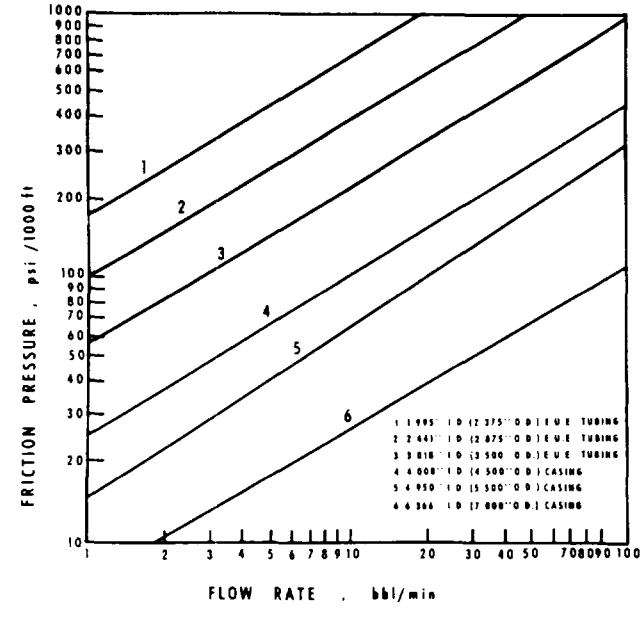

Fig. 55.13—Typical friction-loss curve for heavy oil-in-water emulsion-type fracturing fluid.

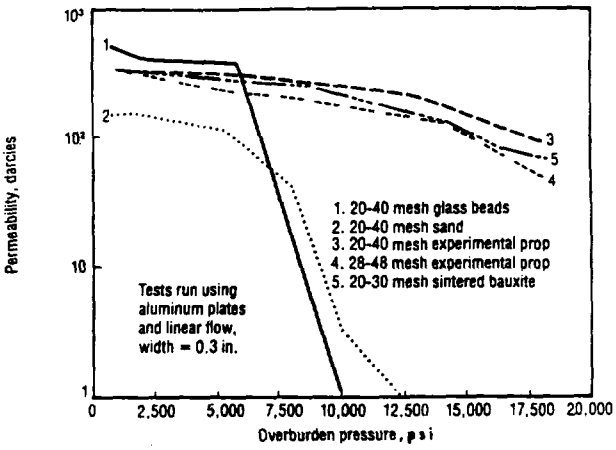

Fig. 55.14—Effect of closure stress on permeability of various propping agents.

The viscous emulsions are water-outside-phase emulsions containing two parts oil (crude or refined) and one part water or brine. These are commonly called "poly-emulsions" and are designed to provide high-viscosity fracturing fluids at temperatures up to 350°F. They are seldom used because of fire hazard and cost.

A crosslinked gel provides high viscosity in the water volume (95%), and a 5% oil phase is dispersed throughout the mixture to give excellent fluid-loss control properties without requiring the addition of solids. The leakoff control is the result of two-phase fluid flow that reduces the relative permeability of the formation more than conventional fracturing fluids do over a wide permeability range. The fluid is highly efficient even when compared to viscous-emulsion fracturing fluids. Normally, the 5% oil content is low enough to avoid significant effects on either friction pressure or hydrostatic head, even when used with the highly viscous water or brine gels.

Fracturing fluid composition is normally proprietary information of the service company supplying it. While competitive fluids are available from most of the service companies, rheological and friction-loss data will vary according to the fluid. Therefore, handbooks provided by the service companies should be used to obtain data for job design.

Propping Agents

Propping agents are used to maintain fracture-flow capacity after completion of a hydraulic fracturing treatment. The amount of proppant used, the manner in which it is placed in the fracture, and the properties of the material itself all play a vital role in maintaining productivity throughout the life of the well. The selection of the propping agent and scheduling of the proppant during the treatment are important parts of the overall completion and treatment design.

The six physical properties of propping agents that affect the resultant fracture conductivity are grain strength, grain size, grain size distribution, grain roundness factor, quality (amount of fines and impurities), and proppant density.

Grain Strength. While all these physical properties have a decided effect on fracture conductivity, quality standards have been established so that the main considerations are grain strength and grain size. If a proppant is not strong enough to withstand closure stress of the fracture, it will crush, and permeability will be reduced greatly. Also, as reservoir pressure is reduced by fluid production, the closure stress will increase. Therefore, it is important that proppant strength be selected for the stress that will be present during the later life of the well. Fig. 55.14 shows the effect of closure stress on permeability of various propping agents when the formation is a hard, competent rock. Sand is an acceptable propping agent at closure stresses up to 6,000 psi. At stresses greater than this, high-strength proppants such as sintered bauxite particles or plastic-coated sand grains should be used.

In soft formations, the proppant will tend to embed into the formation under closure stress and reduce fracture width. This, in turn, reduces fracture flow capacity. In the past, deformable proppants such as rounded walnut shells and aluminum pellets have been used in an attempt to overcome this problem. By deforming or spreading out, these proppants presented a larger surface area to the face of the fracture and resisted embedment. The low density and malleability of these proppants caused both pumping and placement problems, and they were never widely accepted. There was also a corrosion or oxidation of the aluminum that resulted in loss of pack permeability.

A better solution to embedment is a wide, packed fracture. In such a fracture, width reduction resulting from embedment is a small percentage of total fracture width, and adequate flow capacity is maintained even after embedment occurs.

Grain Size. A large proppant grain size provides a more permeable pack under low closure stress conditions and can be used in shallow wells. However, dirty formations or those subject to significant fines migration are poor candidates for large-size proppants. The fines tend to invade the proppant pack, causing partial plugging and rapid reduction in permeability. In these cases, smaller sizes of proppant that resist invasion of fines are better.

Larger grain sizes are generally not considered for deeper wells because of greater susceptibility to crushing.

Proppant Placement. The manner in which a propping agent is placed in a fracture is also important. As previously stated, soft or high-permeability formations need a wide, fully packed fracture. In very-low-permeability formations, only a thin fracture may be necessary. However, fracture length becomes important in such formations because the greater the surface area of formation exposed to the propped fracture, the greater the volume of oil or gas that can drain into the fracture. Since fluid enters the fracture along its entire length, long fractures must be wider at the wellbore than at the tip to accommodate the increasing amount of fluid as the fracture nears the wellbore. To accomplish this fracture geometry, the proppant must be scheduled so that its concentration in the fracture fluid increases steadily as the treatment progresses.

Fracturing Techniques

Although fracturing treatments usually are performed by pumping materials down the casing or tubing at rates as high as well limitations and economics will permit, spe-

cial techniques sometimes are used to help control vertical fracture growth. Such control is directly related to fracturing efficiency. In the case of massive zones, adequate fracture height to cover the entire zone is desirable. With narrow zones, containment of the fracture within the productive zone improves efficiency and penetration and prevents fracture growth into undesirable zones.

While vertical growth can be controlled to some extent by controlling injection rate, more sophisticated techniques are required for optimum efficiency.

A Limited Entry® technique involves designing the number and size of perforations to match an economically feasible pump rate so that all perforations are forced to accept fluid during the treatment.

Another specialty technique to limit downward growth of a vertical fracture involves building an artificial lower barrier. This is done by using low injection rates and fluids with poor proppant transport characteristics at the beginning of the treatment. Propping agent can create a proppant pack at the bottom of the fracture. A pressure drop will exist across this pack and will divert the fluid that follows outward and upward, thus slowing or even stopping downward fracture growth.

Similarly, a buoyant propping agent can create an artificial upper barrier by floating to the top of the fracture and bridging to form a proppant pack. In this case also, the pressure drop across the pack will force subsequent fluids outward to increase fracture length.

Multiple-Zone Fracturing

Where multiple zones are open to the wellbore, mechanical devices such as packers or bridge plugs can be used to isolate zones so that each can be treated individually. Where it is desirable to fracture more than one zone in a single treatment, sized particulate materials or perforation ball sealers can be used. The particulate materials usually are suspended in a viscous fluid and filter out at the fracture entrance. After treatment, they generally flow back with produced fluids. They also can break down through chemical reaction. Ball sealers seat in perforations and divert fluid flow. They are unseated by reverse flow and either fall to the bottom or are produced along with the returning fluids. When ball sealers are used, a mechanical device to catch the balls should be used at the surface to prevent the balls from plugging valves or other surface equipment.

Fracturing Equipment

Hydraulic fracturing equipment consists of pumps and blenders, high-pressure manifolds and treating line, remotely controlled master valves, and tree savers.

Pumping equipment is the conventional triplex pump, quintaplex pump, or a pressure-multiplier type of pump. The latter employs an entirely different pumping concept from the triplex pump. It operates by using a low-pressure working fluid to push a large piston. This large piston is directly connected to a smaller piston, or ram, which handles the treating fluid. Because of a slow cycle speed, the pressure multipliers are capable of long pumping times at high pressures. Both the triplex and pressure multiplier are capable of high-pressure operation. Above 12,000-psi treating pressure, however, the multiplier is preferred. These units are capable of operating at pressures slightly in excess of 20,000 psi.

Individual pumping units are powered by engines ranging from less than 100 to more than 1,300 hp. For high horsepower requirements, multiple units are used.

Fluids used in hydraulic fracturing are mixed in blenders. They are either batch mixed before a job and stored in tanks on location or continuously mixed during the job. Blenders are capable of metering both dry and liquid additives into a fluid, mixing the fluid and additives, and metering and mixing propping agent into the fluids. After mixing and blending, the slurries are supplied by the blender to the suction on the high-pressure pumps under pressure. Blending units capable of handling volumes in excess of 100 bbl/min are available.

Liquid nitrogen is the gas normally used for foam or energized fluid. Special transport and pumping equipment is required to handle the nitrogen, which generally is metered into the treating line on the downstream (high-pressure) side of the triplex or multiplier pumps.

Another piece of equipment recently added to fracturing fleets is the treatment monitoring vehicle. This vehicle gathers data, uses a computer to analyze them, and presents the results as they occur, or in "real time." The data are presented by a printer, plotter, and on a CRT screen. Real-time analysis and presentation of data allow positive control of a treatment. Ample warning of problems normally is available so that changes can be made to permit successful completion of the job. Also, the equipment can be used to monitor a minifrac job before the main treatment. Analysis of the minifrac can either verify job design or indicate needed design changes before the main treatment.

Treatment Planning and Design

Success of a hydraulic fracturing treatment depends on creating a deeply penetrating, highly conductive fracture in the producing zone. Research, engineering studies, and experience have provided reliable planning or treatment design guides. Job calculations with these guides are based on reservoir conditions, laboratory tests, theoretical data, well information, and experience in a given area. Most service companies and many oil-producing companies have job-design calculations computerized to aid in rapid and accurate design comparisons. Special computer programs are available also to calculate tubing expansion and contraction, bottomhole cool-down (fluid temperature at the wellbore and in the fracture), proppant scheduling to provide best propped fracture geometry, and anticipated productivity increase.

Evaluating and selecting optimal treating conditions for any individual well includes several steps. First, accurate reservoir and well-completion data must be accumulated to provide a sound basis for engineered treatment preplanning. Next, the fracture area and the extent of formation penetration necessary to provide the desired productivity increase are calculated. The fracture conductivity, as related to the permeability of the matrix, is determined also.

After this, the comparative efficiency of various fracturing fluids, based on specific well conditions, is determined, as well as the volumes and injection rates necessary to provide the desired fracture extension. Horsepower requirements for each type of treatment then can be calculated; and fracturing materials and techniques can be selected that, theoretically, will most efficiently and eco-

nomically produce the desired productivity increase. Only when all these factors are considered collectively can a well-integrated fracturing treatment be carried out.

Nomenclature

A = cross-sectional area of test media through which flow takes place, cm^2
A_f = total area of one face of the fracture at any time during injection, sq ft
b = fracture width (breadth), ft
c_R = isothermal coefficient of compressibility of the reservoir fluid, psi^{-1}
D = depth of producing interval, ft
$\text{erfc}(x)$ = complementary error function of x
g_f = unit fracture gradient, psi/ft
i = constant injection rate during fracture extension, cu ft/min
I_b = behavior index; log slope of the shear-stress vs. shear-rate curve, dimensionless
I_c = consistency index: shear stress at 1 sec^{-1}, $lbf\text{-}sec^{-1}/ft^2$
k_e = effective formation permeability, darcies
K = fluid coefficient, a constant that is a measure of the flow resistance of the fluid leaking off into the formation during fracture operations
K_c = fluid coefficient (compressibility-viscosity controlled), $ft/min^{1/2}$
K_l = fluid coefficient, wall building (fluid-loss additive), $ft/min^{1/2}$
K_v = fluid coefficient (viscosity controlled), $ft/min^{1/2}$
m = slope of fluid-loss curve, plotting cumulative filtrate volume vs. square root of flow time, $mL/min^{1/2}$
p_f = total friction loss, psi
p_h = total hydrostatic pressure, psi
p_R = normal reservoir pressure, psi
p_s = total surface treating pressure, psi
Δp = differential pressure across face of fracture, psi
t = total pumping time, minutes
γ = shear rate, sec^{-1}
μ_a = apparent viscosity, cp
μ_f = fracturing fluid viscosity, cp
μ_R = reservoir fluid viscosity, cp
ϕ_e = effective formation porosity, %

Key Equations in SI Metric Units

$$K_c = 1.9203 \times 10^{-4} \Delta p \sqrt{\frac{k_e \phi_e c_R}{\mu_R}}, \quad \ldots\ldots\ldots\ldots (3)$$

$$K_v = 2.41 \times 10^{-4} \sqrt{\frac{k_e \Delta p \phi_e}{\mu_f}}, \quad \ldots\ldots\ldots\ldots (4)$$

and

$$K_l = 0.001076 \frac{m}{2A}, \quad \ldots\ldots\ldots\ldots (5)$$

where
K_c, K_v, and K_l are in $m/s^{1/2}$,
Δp is in kPa,
k_e is in μm^2,
ϕ_e is in percent,
c_R is in kPa^{-1},
μ_R is in Pa·s,
m is in $mL/s^{1/2}$, and
A is in m^2.

References

1. Hurst, R.E., Franks, J.E., and Rollins, J.T.: "Horsepower Requirements for Well Stimulation," *Drill Bit* (Oct. 1958) **25**.
2. Howard, G.C. and Fast, C.R.: *Hydraulic Fracturing*, Monograph Series, SPE, Richardson, TX (1970) **2**.
3. Perkins, T.K. Jr. and Kern, L.R.: "Widths of Hydraulic Fractures," *J. Pet. Tech.* (Sept. 1961) 937-49; *Trans.*, AIME, **222**.
4. Khristianovitch, S.A. and Zheltov, Y.P.: "Formation of Vertical Fracture by Means of Highly Viscous Fluids," *Proc.*, Fourth World Pet. Cong., Rome (1955) **2**, 579.
5. McGuire, W.J. and Sikora, V.J.: "The Effect of Vertical Fractures on Well Productivity," *J. Pet. Tech.* (Oct. 1960) 72-74; *Trans.*, AIME, **219**.
6. Craigie, L.J.: "A New Method for Determining the Rheology of Crosslinked Fracturing Fluids Using Shear History Simulation," paper SPE 11635 presented at the 1983 SPE/DOE Low-Permeability Gas Reservoirs Symposium, Denver, March 14-16.

General References

Abou-Sayed, A.S.: "Laboratory Evaluation of In-Situ Stress Contrast in Deeply Buried Sediments," paper SPE 11069 presented at the 1982 SPE Annual Technical Conference and Exhibition, New Orleans, Sept. 26-29.

Abou-Sayed, A.S., Ahmed, U., and Jones, A.: "Systematic Approach to Massive Hydraulic Fracturing Treatment Design," paper SPE 9877 presented at the 1981 SPE/DOE Low-Permeability Gas Reservoirs Symposium, Denver, May 27-29.

Agarwal, R.G., Carter, R.D., and Pollock, C.B.: "Evaluation and Performance Prediction of Low-Permeability Gas Wells Stimulated by Massive Hydraulic Fracturing," *J. Pet. Tech.* (March 1979) 362-72.

Ahmed, U., Strawn, J., and Schatz, J.: "Effect of Stress Distribution on Hydraulic Fracture Geometry: A Laboratory Simulation Study in One-Meter Cubic Blocks," paper SPE 11637 presented at the 1983 SPE/DOE Low-Permeability Gas Reservoirs Symposium, Denver, March 14-16.

Ahmed, U. *et al.*: "State-of-the-Art Hydraulic Fracture Stimulation Treatment for a Western Tight Sand Reservoir," paper SPE 11184 presented at the 1982 SPE Annual Technical Conference and Exhibition, New Orleans, Sept. 26-29.

Ainley, B.R. and Charles, G.J.: "Fracturing Using a Stabilized Foam Pad," paper SPE 10825 presented at the 1982 SPE/DOE Unconventional Gas Recovery Symposium, Pittsburgh, May 16-18.

Almond, S.W.: "Factors Affecting Gelling-Agent Residue Under Low Temperature Conditions," paper SPE 10658 presented at the 1982 SPE Formation Damage Control Symposium, Lafayette, March 24-25.

Aron, J. and Murray, J.: "Formation Compressional and Shear Interval Transit-Time Logging by Means of Long Spacings and Digital Techniques," paper SPE 7446 presented at the 1978 SPE Annual Technical Conference and Exhibition, Houston, Oct. 1-4.

Baumgartner, S.A. *et al.*: "High-Efficiency Fracturing Fluids for High-Temperature, Low-Permeability Reservoirs," paper SPE 11615 presented at the 1983 SPE/DOE Low-Permeability Gas Reservoirs Symposium, Denver, March 14–16.

Bennett, C.O., Reynolds, A.C., and Raghavan, R.: "Analysis of Finite Conductivity Fractures Intercepting Multilayer Reservoirs," paper SPE 11030 presented at the 1982 SPE Annual Technical Conference and Exhibition, New Orleans, Sept. 26–29.

Bennett, C.O. *et al.*: "Performance of Finite Conductivity Vertically Fractured Wells in Single-Layer Reservoirs," paper SPE 11029 presented at the 1982 SPE Annual Technical Conference and Exhibition, New Orleans, Sept. 26–29.

Callahan, M.J., McDaniel, R.R., and Lewis, P.E.: "Application of a New Second-Generation High-Strength Proppant in Tight Gas Reservoirs," paper SPE 11633 presented at the 1983 SPE/DOE Low-Permeability Gas Reservoirs Symposium, Denver, March 14–16.

Cinco-Ley, H.: "Evaluation of Hydraulic Fracturing by Transient Pressure Analysis Methods," paper SPE 10043 presented at the 1982 SPE Intl. Petroleum Exhibition and Technical Symposium, Beijing, March 19–22.

Cinco-Ley, H. and Samaniego-V., F.: "Transient Pressure Analysis for Fractured Wells," *J. Pet. Tech.* (Sept. 1981) 1749–66.

Clark, J.A.: "The Prediction of Hydraulic Fracture Azimuth Through Geological, Core, and Analytical Studies," paper SPE 11611 presented at the 1983 SPE/DOE Low-Permeability Gas Reservoirs Symposium, Denver, March 14–16.

Clark, P.E. and Quadir, J.A.: "Proppant Transport in Hydraulic Fractures: A Critical Review of Particle Settling Velocity Equations," paper SPE 9866 presented at the 1981 SPE/DOE Low-Permeability Gas Reservoirs Symposium, Denver, May 27–29.

Clark, P.E. and Guler, N.: "Proppant Transport in Vertical Fractures: Settling Velocity Correlations," paper SPE 11636 presented at the 1983 SPE/DOE Low-Permeability Gas Reservoirs Symposium, Denver, March 14–16.

Cleary, M.B.: "Analysis of Mechanisms and Procedures for Producing Favorable Shapes of Hydraulic Fractures," paper SPE 9260 presented at the 1983 SPE Annual Technical Conference and Exhibition, Dallas, Sept. 21–24.

Cleary, M.P., Kavvadas, M., and Lam, K.Y.: "A Fully Three-Dimensional Hydraulic Fracture Simulator," paper SPE 11631 presented at the 1983 SPE/DOE Low-Permeability Gas Reservoirs Symposium, Denver, March 14–16.

Clifton, R.J. and Abou-Sayed, A.S.: "A Variational Approach to the Prediction of the Three-Dimensional Geometry of Hydraulic Fractures," paper SPE 9879 presented at the 1981 SPE/DOE Low-Permeability Gas Reservoirs Symposium, Denver, May 27–29.

Cloud, J.E. and Clark, P.E.: "Stimulation Fluid Rheology III. Alternatives to the Power Law Fluid Model for Crosslinked Gels," paper SPE 9332 presented at the 1980 SPE Annual Technical Conference and Exhibition, Dallas, Sept. 21–24.

Conway, M.W. and Harris, L.W.: "A Laboratory and Field Evaluation of a Technique for Hydraulic Fracturing Stimulation of Deep Wells," paper SPE 10964 presented at the 1982 SPE Annual Technical Conference and Exhibition, New Orleans, Sept. 26–29.

Cooke, C.E. Jr.: "Effect of Fracturing Fluid on Fracture Conductivity," *J. Pet. Tech.* (Oct. 1975) 1273–82.

Crawley, A.B., Northrup, D.A., and Sattler, A.R.: "The U.S. DOE Western Gas Sands Project Multiwell Experiment Updates," paper SPE 11183 presented at the 1982 SPE Annual Technical Conference and Exhibition, New Orleans, Sept. 26–29.

Cutler, R.A. *et al.*: "New Proppants for Deep Gas Well Stimulation," paper SPE 9869 presented at the 1981 SPE/DOE Low-Permeability Gas Reservoirs Symposium, Denver, May 27–29.

Cutler, R.A. *et al.*: "Comparison of the Fracture Conductivity of Commercially Available and Experimental Proppants at Intermediate and High Closure Stresses," *Soc. Pet. Eng. J.* (April 1985) 157–70.

Daneshy, A.A.: "On the Design of Vertical Hydraulic Fractures," *J. Pet. Tech.* (Jan. 1973) 83–97; *Trans.*, AIME, **255**.

Daneshy, A.A.: "Numerical Solution of Sand Transport in Hydraulic Fracturing," *J. Pet. Tech.* (Jan. 1978) 132–40.

Daneshy, A.A.: "Hydraulic Fracture Propagation in Layered Formations," *Soc. Pet. Eng. J.* (Feb. 1978) 33–41.

Daneshy, A.A. *et al.*: "Effect of Treatment Parameters on the Geometry of a Hydraulic Fracture," paper SPE 3507 presented at the 1971 SPE Annual Meeting, New Orleans, Oct. 3–6.

Dobkins, T.A.: "Improved Methods to Determine Hydraulic Fracture Height," *J. Pet. Tech.* (April 1981) 719–26.

Elkins, L.E.: "Western Tight Sands Major Research Requirements," paper presented at the 1980 Intl. Gas Research Conference, Chicago, June 9–12.

Fertl, W.H.: "Evaluation of Fractured Reservoir Rocks Using Geophysical Well Logs," paper SPE 8938 presented at the 1980 SPE/DOE Unconventional Gas Recovery Symposium, Pittsburgh, May 18–21.

Gardner, D.C. and Eikerts, J.V.: "The Effects of Shear and Proppant on the Viscosity of Crosslinked Fracturing Fluids," paper SPE 11066 presented at the 1982 SPE Annual Technical Conference and Exhibition, New Orleans, Sept. 26–29.

Geertsma, J. and de Klerk, F.: "A Rapid Method of Predicting Width and Extent of Hydraulically Induced Fractures," *J. Pet. Tech.* (Dec. 1969) 1571–81; *Trans.*, AIME, **246**.

Geertsma, J. and Haafkens, R.: "A Comparison of Theories for Predicting Width and Extent of Vertical Hydraulically Induced Fractures," *Trans.*, ASME (1979) **101**, 8–19.

Govier, G.W. and Aziz, K.: *The Flow of Complex Mixtures in Pipes*, Van Nostrand Reinhold Co., New York City (1972).

Guppy, K.H., Cinco-Ley, H., and Ramey, H.J. Jr.: "Pressure Build-up Analysis of Fractured Wells Producing at High Flow Rates," *J. Pet. Tech.* (Nov. 1982) 2656–66.

Hall, C.D. Jr. and Dollarhide, F.E.: "Performance of Fracturing Fluid Loss Agents Under Dynamic Conditions," *J. Pet. Tech.* (July 1968) 763–68; *Trans.*, AIME, **243**.

Hanson, J.M. and Owen, L.B.: "Fracture Orientation Analysis by the Solid Earth Tidal Strain Method," paper SPE 11070 presented at the 1982 SPE Annual Technical Conference and Exhibition, New Orleans, Sept. 26–29.

Hanson, M.E. *et al.*: "Some Effects of Stress, Friction, and Fluid Flow on Hydraulic Fracturing," *Soc. Pet. Eng. J.* (June 1982) 321–32.

Harrington, L.J., Hannah, R.R., and Beirute, R.: "Post-Fracturing Temperature Recovery and Its Implication for Stimulation Design," paper SPE 7560 presented at the 1978 SPE Annual Technical Conference and Exhibition, Houston, Oct. 1–4.

Harrington, L.J., Hannah, R.R., and Williams, D.: "Dynamic Experiments and Proppant Settling in Crosslinked Fracturing Fluids," paper SPE 8342 presented at the 1979 SPE Annual Technical Conference and Exhibition, Las Vegas, Sept. 23–26.

Harris, P.C.: "Dynamic Fluid-Loss Characteristics of Foam Fracturing Fluids," paper SPE 11065 presented at the 1982 SPE Annual Technical Conference and Exhibition, New Orleans, Sept. 26–29.

Hurst, R.E.: "An Engineered Method for the Evaluation and Control of Fracturing Treatments," *Drill & Prod. Prac.*, API (1959) 168–76.

King, G.E.: "Factors Affecting Dynamic Fluid Leakoff with Foam Fracturing Fluids," paper SPE 6817 presented at the 1977 SPE Annual Technical Conference and Exhibition, Denver, Oct. 9–12.

Lee, W.J. and Holditch, S.A.: "Fracture Evaluation with Pressure Transient Testing in Low-Permeability Gas Reservoirs," *J. Pet. Tech.* (Sept. 1981) 1776-92.

Lescarboura, J.A., Sifferman, T.R., and Wahl, H.A.: "Evaluation of Fracturing Fluid Stability Using a Heated Pressurized Flow Loop," *Soc. Pet. Eng. J.* (June 1984) 249-55.

McDaniel, R.R., Deysarker, A.K., and Callanan, M.J.: "An Improved Method for Measuring Fluid Loss at Simulated Fracture Conditions," *Soc. Pet. Eng. J.* (Aug. 1985) 482-90.

McLeod, H.O. Jr.: "A Simplified Approach to Design of Fracturing Treatments Using High-Viscosity Crosslinked Fluids," paper SPE 11614 presented at the 1983 SPE/DOE Low-Permeability Gas Reservoirs Symposium, Denver, March 14-16.

Neal, E.A., Parmley, J.L., and Colpoys, P.J.: "Oxide Ceramic Proppants for Treatment of Deep Well Fractures," paper SPE 6816 presented at the 1977 SPE Annual Technical Conference and Exhibition, Denver, 9-12.

Nolte, K.G.: "Determination of Fracturing Parameters from Fracturing Pressure Decline," paper SPE 8341 presented at the 1979 SPE Annual Technical Conference and Exhibition, Las Vegas, Sept. 23-26.

Nolte, K.G.: "Fracture Design Considerations Based on Pressure Analysis," paper SPE 10911 presented at the 1982 SPE Cotton Valley Symposium, Tyler, TX, May 20.

Nolte, K.G. and Smith, M.B.: "Interpretation of Fracturing Pressures," *J. Pet. Tech.* (Sept. 1981) 1767-75.

Nordgren, R.P.: "Propagation of a Vertical Hydraulic Fracture," *Soc. Pet. Eng. J.* (Aug. 1972) 306-14.

Palmer, I.D. and Carroll, H.B.: "Three-Dimensional Hydraulic Fracture Propagation in the Presence of Stress Variations," *Soc. Pet. Eng. J.* (Dec. 1983) 870-78.

Palmer, I.D. and Carroll, H.B.: "Numerical Solution for Height of Elongated Hydraulic Fractures with Leakoff," paper SPE 11627 presented at the 1983 SPE/DOE Low-Permeability Gas Reservoirs Symposium, Denver, March 14-16.

Penny, G.S.: "Nondamaging Fluid-Loss Additives for Use in Hydraulic Fracturing of Gas Wells," paper SPE 10659 presented at the 1982 SPE Formation Damage Control Symposium, Lafayette, March 24-25.

Rogers, R.E., Veatch, R.W., and Nolte, K.G.: "Pipe Viscometer Study of Fracturing Fluid Rheology," *Soc. Pet. Eng. J.* (Oct. 1984) 575-81.

Rosene, R.B. and Shumaker, E.G.: "Viscous Fluids Provide Improved Results from Hydraulic Fracturing Treatments," paper SPE 3347 presented at the 1971 SPE Rocky Mountain Regional Meeting, Billings, MT, June 2-4.

Rosepiler, M.H.: "Determination of Principle Stresses and the Confinement of Hydraulic Fractures in Cotton Valley," paper SPE 8405 presented at the 1979 SPE Annual Technical Conference and Exhibition, Las Vegas, Sept. 23-26.

Settari, A.: "Simulation of Hydraulic Fracturing Processes," *Soc. Pet. Eng. J.* (Dec. 1980) 487-500.

Settari, A.: "Quantitative Analysis of Factors Controlling Vertical Fracture Growth (Containment)," paper SPE 11629 presented at the 1983 SPE/DOE Low-Permeability Gas Reservoirs Symposium, Denver, March 14-16.

Settari, A.: "A New General Model of Fluid Loss in Hydraulic Fracturing," *Soc. Pet. Eng. J.* (Aug. 1985) 491-501.

Sinclair, A.R.: "Heat Transfer Effects in Deep Well Fracturing," *J. Pet. Tech.* (Dec. 1971) 1484-92; *Trans.*, AIME, **251**.

Sinclair, A.R. and Graham, J.W.: "A New Proppant for Hydraulic Fracturing," paper presented at the 1978 ASME Energy Technology Conference, Houston, Nov. 5-9.

Smith, M.B.: "Stimulation Design for Short, Precise Hydraulic Fractures—MHF," paper SPE 10313 presented at the the 1981 SPE Annual Technical Conference and Exhibition, San Antonio, Oct. 4-7.

Smith, M.B., Logan, J.M., and Wood, M.D.: "Fracture Azimuth—A Shallow Experiment," *Trans.*, ASME (June 1980) **102**, 99-105.

Smith, M.B., Rosenberg, R.J., and Bowen, J.F.: "Fracture Width: Design vs. Measurement," paper SPE 10965 presented at the 1982 SPE Annual Technical Conference and Exhibition, New Orleans, Sept. 26-29.

Thomas, R.L. and Elbel, J.L.: "The Use of Viscosity Stabilizers in High Temperature Fracturing," paper SPE 8344 presented at the 1979 SPE Annual Technical Conference and Exhibition, Las Vegas, Sept. 23-26.

Teufel, L.W.: "Determination of In-Situ Stresses from Anelastic Strain Recovery Measurements of Oriented Core: Applications to Hydraulic Fracturing Treatment Design," paper SPE 11649 presented at the 1983 SPE/DOE Low-Permeability Gas Reservoirs Symposium, Denver, March 14-16.

Teufel, L.W. and Clark, J.A.: "Hydraulic Fracture Propagation in Layered Rock: Experimental Studies of Fracture Containment," *Soc. Pet. Eng. J.* (Feb. 1984) 19-32.

Thiercelin, M. and Lemanczyk, R.: "The Effect of Stress Gradient on the Height of Vertical Hydraulic Fractures," paper SPE 11626 presented at the 1983 SPE/DOE Low-Permeability Gas Reservoirs Symposium, Denver, March 14-16.

Tinsley, J.M. *et al.*: "Vertical Fracture Height—Its Effect on Steady-State Production Increase," *J. Pet. Tech.* (May 1969) 633-38; *Trans.*, AIME, **246**.

van Poollen, H.K., Tinsley, J.M., and Saunders, C.D.: "Hydraulic Fracturing—Fracture Flow Capacity vs. Well Productivity," *J. Pet. Tech.* (May 1958) 91-95; *Trans.*, AIME, **213**.

Veatch, R.W. Jr. and Crowell, R.F.: "Joint Research/Operations Programs Accelerate Massive Hydraulic Fracturing Technology," *J. Pet. Tech.* (Dec. 1982) 2763-75.

Verbeek, C.M.J.: "Analysis of Production Tests of Hydraulically Fractured Wells in a Tight Solution Gas-Drive Reservoir," paper SPE 11084 presented at the 1982 SPE Annual Technical Conference and Exhibition, New Orleans, Sept. 26-29.

Warpinski, N.R. *et al.*: "Laboratory Investigation on the Effect of In-Situ Stresses on Hydraulic Fracture Containment," *Soc. Pet. Eng. J.* (June 1982) 333-40.

Waters, A.B.: "Hydraulic Fracturing—What Is It?" *J. Pet. Tech.* (Aug. 1981) 1416.

Wendorff, C.L.: "Frac Sand Quality Control—A Must for Good Frac Treatments," paper presented at the 1978 ASME Petroleum Div. Annual Meeting, Houston, Nov. 5-9.

Wheeler, J.A.: "Analytical Calculations of Heat Transfer from Fractures," paper SPE 2494 presented at the 1969 SPE Improved Oil Recovery Symposium, Tulsa, April 13-15.

White, J.L. and Daniel, E.F.: "Key Factors in MHF Design," *J. Pet. Tech.* (Aug. 1981) 1501-12.

Whitsitt, N.F. and Dysart, G.R.: "The Effect of Temperature on Stimulation Design," *J. Pet. Tech.* (April 1970) 493-502; *Trans.*, AIME, **249**.

Wood, M.D. *et al.*: "Fracture Proppant Mapping Using Surface Superconducting Magnetometers," paper SPE 11612 presented at the 1983 SPE/DOE Low-Permeability Gas Reservoirs Symposium, Denver, March 14-16.

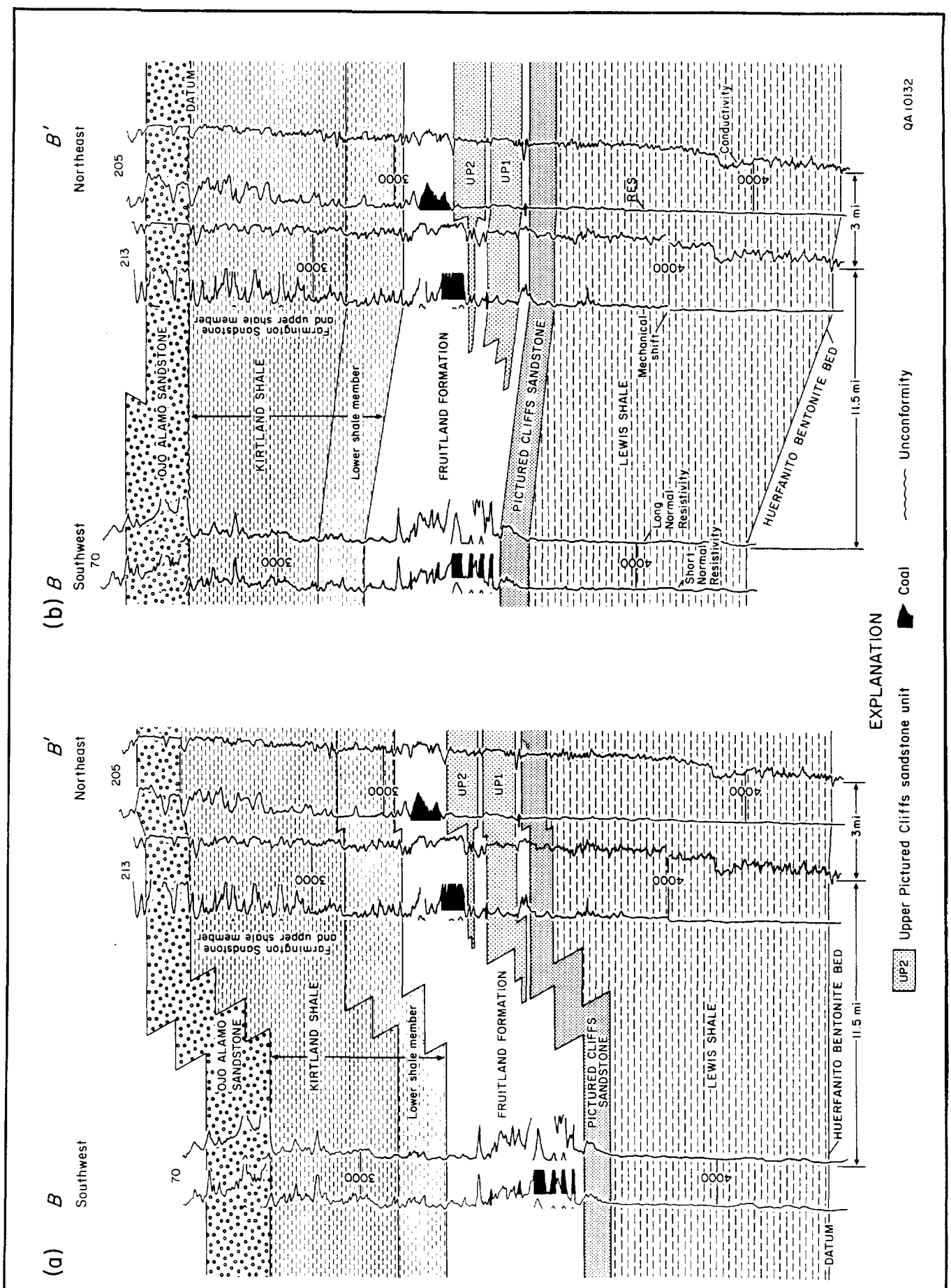

FIGURE 4.18—Cross section B–B′. (a) Datum is the Huerfanito Bentonite. Use of this datum suggests that coal seams terminate abruptly against Pictured Cliffs shoreline sandstones. (b) Datum is base of the Ojo Alamo Sandstone. Use of a datum above the Fruitland Formation suggests that swamp facies (coal seams) migrated over abandoned, foundered Pictured Cliffs shoreline sandstones. See Fig. 4.19 for location.

We suggest that structural activity contributed to relatively greater stratigraphic rise in this area and, indirectly, to the distribution of thick Fruitland coal seams (Ayers and others, this volume, Fig. 2.20). The Pictured Cliffs shoreline prograded rapidly basinward across the southern half of the basin. After the shoreline crossed the structural hingeline, sporadic structural activity began and the northern part of the basin subsided more rapidly to accommodate a greater thickness of sediment. The changing balance between sediment input and pulsatory subsidence north of the hingeline resulted in oscillation and aggradation of the shoreline, accounting for the most significant stratigraphic rise of the Pictured Cliffs in the basin and allowing time for thick peat accumulation landward of the oscillating shoreline. This model explains why the greatest net thickness of Fruitland coal is in the northern part of the basin, and why coal seams in the Fruitland Formation are thicker than those in subjacent continental strata. Further testing is needed to verify the existence of the structural hingeline; seismic studies would be especially useful. A regional map of structural elements that were identified in regional reflection seismic lines shows northwest-trending faults in the area of this hingeline (Huffman and Taylor, 1991).

Structural controls on producibility of coalbed methane

Earlier studies suggested that Fruitland coal seams have limited extent and that they are bounded on their basinward (northeast) margins by Pictured Cliffs shoreline sandstone and along paleostrike (northwest–southeast) by Fruitland fluvial sandstones (Fassett and Hinds, 1971; Fassett, 1986). However, as we have demonstrated, some Fruitland coal seams may be regionally continuous, overriding and thinning over upper Pictured Cliffs tongues (Figs. 4.16 and 4.18) in the paleodip direction. Updip pinch-out lines of upper Pictured Cliffs tongues may be areas where Fruitland coal seams drape over shoreline sandstones and have a higher fracture density because of compaction-induced fractures. The structural attitude of an upper Fruitland coal bed (Fig. 4.19) differs markedly from the structural attitude of other strata, such as the Huerfanito Bentonite (Fig. 4.2). Along paleostrike, coal seams split and interfinger with fluvial channel-fill sandstone complexes (Fig. 4.17), and many of these coal benches, rather than terminating against the channel sandstones, override or underlie them, forming zigzag splits similar to those described in coal-bearing strata in other basins (Britten and others, 1975; Ayers and Kaiser, 1984). Although these coal seams pinch and swell, they are laterally continuous, which contributes to their effectiveness as aquifers. Fractures related to compactional folding of coal beds are well documented (Donaldson, 1979; Houseknecht and Iannacchione, 1982; Tyler and others, 1991). If such fracture systems are sufficiently developed, areas of interbedded sandstones and coal seams would be good targets for coalbed methane exploration (Fig. 4.20).

This study has shown that Fruitland coal beds are more extensive and complex than previously inferred (Figs. 4.16–4.18). The significance of these findings is threefold. First, coalbed methane reservoirs are larger (more extensive) than previously thought. Second, compaction-induced fractures, and therefore enhanced coalbed permeability, may occur in areas where extensive coal seams drape over shoreline sandstones or form zigzag splits with channel-fill sandstone complexes. Finally, the greater lateral extent of coal seams, inferred from this research, is critical to the interpretation of ground-water flow and abnormal pressure in the Fruitland Formation (Kaiser and others, this volume, Chapter 8).

The viability of the hypothesis of increased fracture density where coal beds are folded is uncertain; additional subsurface and outcrop studies are required. However, given the abundance of folds and the potential for folding-induced fractures to contribute to enhanced coalbed methane production, such studies are warranted.

Coalbed methane activity and reservoir conditions

The Navajo Lake area has a long and noteworthy history of coalbed methane production. The Phillips No. 6–17 well (Figs. 4.2 and 4.3) is often referred to as the discovery well for coalbed methane in the San Juan Basin. This well, which is an open-hole completion in upper Fruitland coal beds and sandstones, is located on the northwest flank of a minor, north-plunging anticline. It has operated for more than 25 yrs with little decline in gas production (averaging 160 to 180 Mcf/d) or pressure (Hale and Firth, 1988). The well produces little or no water, indicating some element of structural and/or stratigraphic trapping. Although Hale and Firth (1988) discount structural trapping, their interpretation was based on a structure map of the Huerfanito Bentonite, which does not accurately reflect the structural attitude of Fruitland coal beds. Since 1985, Meridian Oil and Blackwood and Nichols have completed several coalbed methane wells in the Navajo Lake area, including the most productive coalbed methane wells in the United States. Some Meridian wells in this area (Figs. 4.2, 4.3, and 4.19) have produced at a rate of 300 to 15,000 Mcf/d (see Kaiser and Ayers, this volume, Chapter 10, for discussion of production). Meridian 400 wells are completed in lower Fruitland coal beds on the margin of a syncline and near the updip pinch-out of UP1 (Fig. 4.19).

In the Navajo Lake area, Fruitland coal beds are mostly in the area of regional overpressuring and highest Fruitland bottom-hole pressures; overpressuring is attributed to artesian conditions (Kaiser and others, this volume, Chapter 8). The boundary between overpressured and underpressured strata crosses the southern part of the area (Fig. 4.4); this boundary may be caused by southwestward pinch-out and/or offset of aquifer coal beds across faults that are inferred to make up the structural hingeline (Fig. 4.2). Both gas- and water-saturated coal seams are present in the Navajo Lake area. In this area, Fruitland coal rank increases from high volatile B bituminous at the south to medium volatile bituminous at the north (Scott and others, this volume, Fig. 9.3), and it contains more than 10 Bcf of methane/mi^2 (Ayers and others, this volume, Fig. 2.21). Fruitland coalbed gas is dry (C_1/C_{1-5} >95%), and it contains a high percentage of carbon dioxide (commonly 3–10%) (Scott and others, this volume, Fig. 9.10). Primary fractures (face cleats) in oriented cores from Blackwood and Nichols NEBU No. 403 trend northeastward, consistent with regional cleat trends in the southern part of the basin (Tremain and others, this volume, Fig. 5.1). Highly productive wells in the Navajo Lake area are reported to have fracture-enhanced permeability that may be predicted from lineament analysis. However, a recent study showed no significant relations between methane production and lineament attributes in the northern San Juan Basin (Baumgardner, this volume, Chapter 7). Geologic and hydrologic controls on producibility of coalbed methane in the Navajo Lake area are further discussed by Kaiser and Ayers (this volume, Chapter 10).

Summary and conclusions

In summary, we suggest both depositional and structural controls affect the occurrence and producibility of Fruitland coalbed methane in the Navajo Lake area. The distribution of thick coal seams was controlled by depositional setting, which in turn was structurally controlled; tectonically induced subsidence north of the hingeline temporarily confined the Pictured Cliffs shoreline to a narrow belt, and this

(Kaiser and others, this volume, Fig. 8.1) and, consequently, such areas are favorable for hydrocarbon accumulation (Tóth, 1980). Available chemical analyses show Na–Cl-type waters. Coal seams may be thicker than 10 ft (>3 m) and they occur primarily in northeast-trending belts (Ayers and others, this volume, Figs. 2.15 and 2.17). A northeast-trending, dip-elongate belt of thick coal extends almost to the southwestern margin of the basin (Ayers and others, this volume, Figs. 2.17 and 2.19) and coincides with a similar trending belt of high gas production (>100 Mcf/d) (Fig. 10.15). This belt includes productive wells (200 to 500 Mcf/d) in the Fulcher and WAW–Gallegos areas (Fig. 10.15) completed in coal seams of subbituminous and high volatile C bituminous rank (Scott and others, this volume, Fig. 9.3), and it flanks a major northeast-trending Fruitland channel-sandstone belt. Sandstone wells of the Aztec, Kutz, and Gallegos fields (Fig. 10.20) are completed in channel-sandstone belts (thin-coal areas) that flank northeast-trending belts of thick coal (Ayers and others, this volume, Fig. 2.15).

Northeast-trending coal seams may have served as pathways that allowed gas to migrate out of the north-central part of the basin, either entrained or dissolved in ground water, or by diffusion in response to the concentration gradient. Carbon dioxide appears to have migrated. Plumes of high carbon dioxide content gases extend updip (southwestward) from the overpressured area, coincident with northeast-trending coal belts (Scott and others, this volume, Fig. 9.10), and terminate at the San Juan River valley, a regional no-flow boundary (Kaiser and others, this volume, Figs. 8.1 and 8.24).

In the west-central part of the basin (area 2), the Fruitland Formation is mainly an aquitard, and gas is produced water free (Kaiser and others, this volume, Chapter 8). Water-free production in this regional discharge area is explained in terms of the low flow, hydrostratigraphy, trapping mechanism, and coal wettability. Limited flow in the basal Fruitland coal and Pictured Cliffs Sandstone accounts for water production from some wells completed in the basal coal. Conventional trapping and low gas permeability relative to water are also important factors. Stratigraphic trapping is postulated to be more important than structural trapping on the basis of gentle, northeast monoclinal dip and associated updip (southwestward) pinch-out of reservoir coal seams (Ayers and others, this volume, Fig. 2.2). Coal seams in the southern part of the basin are lower rank (subbituminous to high volatile C bituminous) and may be water wet; hence, in these low-permeability strata, water is less mobile than gas.

In the west-central, underpressured part of the basin, Fruitland coalbed wells have MAPs ranging from 30 to 300 Mcf/d, similar to productivities of many wells in the north-central, overpressured part of the basin (Ignacio Blanco field) in areas 1B and 1C (Fig. 10.19). Although coalbed methane production is highest from overpressured coal seams, economic production occurs over a wide pressure range. Cumulative production of some wells exceeds 1 Bcf in area 2 (for example, Clay 1, Gallegos area, >1 Bcf in 14 yrs). However, most wells in this area have cumulative productions of a few hundred million cubic feet, and some have produced oil at the rate of 2 or 3 bbls/d. Numerous Fruitland sandstone gas fields occur in the southwestern part of the basin (Fig. 10.20). Several of them, such as Aztec field, are associated with potentiometric mounds (Kaiser and others, this volume, Fig. 8.1). Analysis of production decline has shown that many wells identified as sandstone completions actually have coal-decline behavior and probably are producing coalbed methane indirectly from coal seams (Fig. 10.4). In some cases, sandstone volumetrics require gas production from the associated coal seams. Some wells are dually completed in Fruitland coal seams and Pictured Cliffs Sandstone or Mesaverde sandstones, and the production is commingled. Consequently, the contribution of Fruitland coalbed methane to total gas production in the west-central part of the basin is substantial but unquantifiable.

WAW–Gallegos area—Coalbed methane wells in the WAW–Gallegos area, which is located in area 2 in the southwestern corner of the basin (Figs. 10.15 and 10.20), produce at rates of 30 to more than 300 Mcf/d. Wells completed in 1990 average about 180 Mcf/d. Long-term productivity is demonstrated by the Clay 1 well (sec. 12 T26N R12W), which was completed as a coalbed well in 1976 and had an average production rate of 185 Mcf/d in 1989. The area is underpressured and lies mostly within the regional discharge area. Structural dip is homoclinal to the northeast at less than 1° (~80 ft/mi [~15 m/km]). Strike- and dip-elongate coal seams of subbituminous rank have maximum thicknesses of 10 to 20 ft (3 to 6 m) (Ayers and others, this volume, Fig. 2.17). Stratigraphic and hydrodynamic trapping may account for considerable gas volume beyond that adsorbed at reservoir pressures below or near hydrostatic pressure. Coal seams pinch out updip (southwestward), and ground water flows downdip (northward). Enhanced permeability is inferred for wells producing water from the basal Fruitland coal. Gas may in part come from the underlying Pictured Cliffs Sandstone. Thus, the presence of significant free gas and enhanced permeability are thought to combine to explain relatively high gas productivities in the WAW–Gallegos area.

Area 3: underpressured, eastern area

Little is known about the hydrogeology of the eastern part of the basin. Area 3 (Fig. 10.19) is regionally underpressured, and because of limited data, it appears to be hydrologically featureless. Widely spaced head contours suggest sluggish ground-water flow (Kaiser and others, this volume, Fig. 8.1). Fruitland-produced waters are Na–Cl type that resemble seawater. An area of thick coal, corresponding to coals of belt E (Ayers and others, this volume, Fig. 2.15), trends northwestward across Rio Arriba County, parallel to depositional strike. There are only a few producing Fruitland wells (coal and/or sandstone completions) in the area. After 1 or 2 yrs of production, these wells have average annual productions of less than 1 to 3 MMcf, accompanied by little or no water.

Conclusions

1. Coalbed methane production in the Fruitland Formation is lognormally distributed. Production histograms and probability and scatter plots suggest that coal beds having free gas may be common. Production from overpressured coal seams is greater than that from underpressured seams, although production rates from the two pressure regimes overlap. Initial gas potential is a predictor of long-term productivity. Highly productive wells produce both gas and water, reflecting superior permeability and artesian overpressure. Decline curves of coalbed and sandstone reservoirs differ. Coalbed wells have negative decline early in their production history, followed by exponential decline at less than 5%/yr late in their lives. Sandstone wells that exhibit coal-decline behavior probably are producing coalbed methane indirectly from adjoining coal seams.

2. Approximately 90% of the Fruitland coalbed methane production is from the Meridian 400 area and Cedar Hill and Ignacio Blanco fields in the overpressured part of the basin. Wells in the Meridian 400 area are the most productive (>1,000 Mcf/d), whereas those in Ignacio Blanco field are the least productive (~30 to 300 Mcf/d) and may still be dewatering. Coalbed wells in the west-central (underpres-

FLOW RATE CALCULATIONS
CHACO NO. 1

Perm	=	31 md
Net Pay	=	16.5 ft
Area	=	107 acres
Porosity	=	21.4 %
Water Saturation	=	34 %

<u>After Fracturing</u>

Average Gas Rate during 1st year	99 Mscf/d
Average Gas Rate after 2 years	13 Mscf/d
Cumulative Production after 2 years	47 MMscf

<u>With 30 ft Net Pay</u>

Average Gas Rate during 1st year	180 Mscf/d
Average Gas Rate after 2 years	25 Mscf/d
Cumulative Production after 2 years	85 MMscf

<u>With 320 acre Drainage</u>

Average Gas Rate during 1st year	140 Mscf/d
Average Gas Rate after 2 years	66 Mscf/d
Cumulative Production after 2 years	87 MMscf